TESIS DE LA UNIVERSIDAD DE ZARAGOZA
2025
114

María Josefa Cardiel García

Laponita para aplicación oftalmológica. Evaluación en modelos animales

Director/es
Rodrigo Sanjuán, María Jesús
Ramírez Gasca, María Teresa

ISSN 2254-7606

Prensas de la Universidad
Universidad Zaragoza

Universidad de Zaragoza
Servicio de Publicaciones

ISSN 2254-7606

Universidad Zaragoza
1542

Tesis Doctoral

LAPONITA PARA APLICACIÓN OFTALMOLÓGICA. EVALUACIÓN EN MODELOS ANIMALES

Autor

María Josefa Cardiel García

Director/es

Rodrigo Sanjuán, María Jesús
Ramírez Gasca, María Teresa

UNIVERSIDAD DE ZARAGOZA
Escuela de Doctorado

2025

Universidad Zaragoza
1542

Tesis Doctoral

LAPONITA PARA APLICACIÓN OFTALMOLÓGICA. EVALUACIÓN EN MODELOS ANIMALES

Autor

Mª José Cardiel García

Director/es

Mª Jesús Rodrigo Sanjuán

Mª Teresa Ramírez Gasca

Facultad de Medicina

Año 2024

Dª. MARÍA JESÚS RODRIGO SANJUÁN, Doctora en Medicina y Cirugía, facultativa especialista en Oftalmología del Hospital Miguel Servet de Zaragoza y profesora asociada de la Universidad de Zaragoza.

Certifica:

Que el trabajo de investigación titulado "LAPONITA PARA APLICACIÓN OFTALMOLÓGICA. EVALUACIÓN EN MODELOS ANIMALES" que presenta, Mª José Cardiel García, Licenciada en Medicina y Cirugía, para optar al GRADO DE DOCTORA, fue realizado bajo mi dirección, se ajusta al proyecto de tesis presentado con anterioridad y doy mi autorización para su defensa como tesis por compendio de publicaciones.

Y para que conste a los efectos oportunos, firmo el presente en Zaragoza, a 3 de junio de 2024.

Fdo. Dra. María Jesús Rodrigo Sanjuán

Dª. Mª TERESA RAMÍREZ GASCA, Doctora en Medicina y Cirugía, jefe del Servicio de Anatomía Patológica del Hospital Clínico Universitario Lozano Blesa de Zaragoza y profesor contratado doctor de la Universidad de Zaragoza.

Certifica:

Que el trabajo de investigación titulado "LAPONITA PARA APLICACIÓN OFTALMOLÓGICA. EVALUACIÓN EN MODELOS ANIMALES" que presenta, Mª José Cardiel García, Licenciada en Medicina y Cirugía, para optar al GRADO DE DOCTORA, fue realizado bajo mi dirección, se ajusta al proyecto de tesis presentado con anterioridad y doy mi autorización para su defensa como tesis por compendio de publicaciones.

Y para que conste a los efectos oportunos, firmo el presente en Zaragoza, a 3 de junio de 2024.

Fdo. Dra. Mª Teresa Ramírez Gasca

Agradecimientos

Quiero expresar mi más sincera gratitud al Grupo de Investigación e Innovación Miguel Servet Oftalmología (GIMSO) con el Dr. Luis E. Pablo al frente, por darme esta gran oportunidad de formar parte de este magnífico grupo y sin cuyo soporte, alcanzar esta meta que tenía pendiente, no hubiera sido posible.

De manera muy especial, quiero mostrar mi reconocimiento, admiración y profundo agradecimiento a Elena y Mª Jesús, por su total disposición y apoyo, por su profesionalidad y por todo lo que me han enseñado en esta singladura. Aquí me tenéis para lo que necesitéis.

Gracias a Teresa por ayudarme a cumplir este sueño y estar siempre pendiente de que se llevara a cabo. Seguiremos batallando cada día por conseguir la excelencia, que es nuestra meta común.

Por último, quisiera agradecer a mi familia su paciencia por todas las horas que les he escatimado para llegar aquí, especialmente a mis padres, que tanto me necesitan ahora y sin cuyo apoyo incondicional, sus sacrificios y su fe inquebrantable en mí desde mi infancia, nada habría sido posible.

Mil gracias a todos.

Contenido

ABREVIATURAS

ATP	Adenosina Trifosfato
AUC0-∞	Área bajo la curva de concentración-tiempo
BRI/LAP	Brimonidina/Laponita
BSS	Solución salina equilibrada (del inglés *balanced saline solution*)
CCG	Capa de células ganglionares
CFNR	Capa de fibras nerviosas de la retina
CGR	Células ganglionares de la retina
CIBA	Centro de Investigación Biomédica de Aragón
CL	Eliminación de la droga (del inglés *clearance*)
Cmax	Concentración máxima
CNE	Capa nuclear externa
CNI	Capa nuclear interna
CPE	Capa plexiforme externa
CPI	Capa plexiforme interna
CSF	Capa de segmentos de fotorreceptores
DAB	Diaminobencidina
DMAE	Degeneración macular asociada a la edad
DEX	Dexametasona
DEX/LAP	Dexametasona-Laponita
ERG	Electrorretinografía
EPR	Epitelio pigmentario de la retina
ESI	Ionización por electrospray (del inglés *electrospray ionization*)
GFAP	Proteína ácida fibrilar anti-glial (del inglés *glial fibrillary acidic protein*)
HRLC-MS	Cromatografía líquida acoplada a espectrometría de masas de alta resolución (del inglés *high resolution liquid chromatography-mass spectrometry*)
ICH	*International Council for Harmonisation of Technical Requirements for Pharmaceuticals for Human Use*
IF	Formulación intravítrea (del inglés *intravitreal formulation*)
IP	Intraperitoneal

IS	Estándar interno (del inglés *internal standard*)
ISQCH	Instituto de Síntesis Química y Catálisis Homogénea.
IV	Intravítrea
JCR	Informes de citas en revistas (del inglés *Jounal Citation Reports)*
KE	Constante de la tasa de eliminación
LAP	Laponita
µv	Microvoltios
ms	Milisegundos
Ms	Microesferas
MLE	Membrana limitante externa
MLI	Membrana limitante interna
OCT	Tomografía de coherencia óptica (del inglés *optical coherence tomography*)
OHT	Hipertensión ocular (del inglés *ocular hypertension*)
OMS	Organización mundial de la salud
OVCR	Oclusión de la vena central de la retina
PIO	Presión intraocular
PLGA	Ácido poliláctico-co-glicólico (del inglés *poly-lacticglycolic acid*)
PVC	Corteza vítrea posterior (del inglés *posterior vitreous cortex*)
RNF	Respuesta negativa fotópica (del inglés *PhNR: photopic negative response*)
SC	Supracoroideo
SCS	Espacio supracoroideo (del inglés *suprachoroidal space*)
SEM	Error estándar de la media (del inglés *standard error of mean*)
SIM	Monitoreo de iones únicos (del inglés s*elected ion monitoring*)
SNC	Sistema nervioso central
SPE	Extracción en fase sólida (del inglés *solid phase extraction*)
T½	Vida media de eliminación
Tmax	Tiempo hasta la concentración máxima

UHPLC-MS	Espectrómetro de masas de cromatografía líquida de ultra alta presión (del inglés u*ltra-performance liquid chromatography–mass spectrometry*)
VEGF	Factor de crecimiento vascular endotelial (del inglés *vascular endotelial growth factor*)
VIT	Vítreo

RESUMEN

La presente Tesis Doctoral se basa en el **estudio *in vivo* de la biocompatibilidad y eficacia de Laponita como portador de varios agentes farmacológicos** de diferentes características, concretamente un antiinflamatorio esteroideo de amplísima aplicación en patología oftalmológica como la dexametasona y un agente de baja solubilidad como la brimonidina. También se ha aprovechado para **comparar dos vías distintas de administración** (supracoroidea e intravítrea) y se ha trabajado con **modelos animales tanto sanos como enfermos**. Además, se ha desarrollado un sistema no invasivo de **monitorización de la formulación intravítrea mediante tomografía de coherencia óptica (OCT)**.

Las enfermedades del segmento posterior del ojo suponen un reto desde el punto de vista clínico, tanto por su frecuencia como por su grave afectación de la visión. La complejidad anatómica del ojo y la existencia de diversas barreras fisiológicas con función protectora hacen que las medidas terapéuticas disponibles en la actualidad sean frecuentemente insuficientes para mantener unos niveles del fármaco dentro del rango terapéutico. Las distintas vías de administración oftálmicas tienen en común la baja biodisponibilidad del fármaco en el lugar de acción y la necesidad de administraciones repetidas, lo que conlleva en el caso de las inyecciones oculares un riesgo no desdeñable de complicaciones graves. En los últimos años se han llevado a cabo investigaciones enfocadas en los sistemas de **nanopartículas** como biomateriales capaces de liberar fármacos de forma sostenida, lo cual permite de forma simultánea reducir la dosis y mantener la administración de forma prolongada a nivel del tejido diana. Entre los diversos nanomateriales que se están explorando, la Laponita, un silicato estratificado coloidal sintético, destaca como un biomaterial especialmente prometedor y emergente, el cual reúne una serie de características fisicoquímicas y biológicas que lo hacen especialmente atractivo para su aplicación ocular, como son el hecho de ser biocompatible, fácilmente inyectable y ópticamente transparente, con cualidades como la tixotropía, que facilita su inyección, y la capacidad para retener todo tipo de moléculas, así como para liberarlas de manera progresiva. Sin embargo, a pesar de sus prometedoras cualidades, existen pocos estudios realizados sobre aplicaciones del biomaterial Laponita en el ojo hasta la fecha, a pesar de existir numerosas pruebas científicas que sugieren que puede utilizarse de manera segura en los tejidos oculares.

Para avalar el desarrollo de los estudios que componen esta tesis, de manera previa nuestro grupo ya había realizado **estudios previos con Laponita**, tanto a nivel *in vitro* como *in vivo*. Inicialmente se creó y caracterizó, *in vitro*, una nueva formulación de dexametasona utilizando una matriz de Laponita como base (formulación DEX/LAP), la cual mostró una liberación sostenida del fármaco durante 24 semanas, testándose sobre soluciones que emulaban el humor vítreo. Este estudio puso de relieve la sencillez del método de preparación. Un estudio en paralelo demostró, *in vivo*, que la administración de Laponita en ojos sanos de conejo era segura y biocompatible, con persistencia intraocular tras inyección intravítrea y supracoroidea. No hubo diferencias significativas en la presión intraocular, no se observaron complicaciones oculares relevantes, ni cambios patológicos en el estudio histológico. Además, se observó una lenta degradación de Laponita durante 14 semanas.

A partir de ahí, el primer objetivo se centró en **evaluar *in vivo* el perfil farmacocinético y la seguridad ocular de la formulación DEX/LAP**. Para ello se seleccionó una cohorte de 30 conejos albinos hembra de Nueva Zelanda, dada la idoneidad de este modelo animal para los estudios farmacocinéticos, con un seguimiento de hasta 24 semanas. Se aprovechó la intervención para comparar dos rutas distintas de administración (intravítrea y supracoroidea). Los resultados demostraron que, tras una única inyección de la formulación, la liberación de dexametasona a partir de Laponita se mantiene hasta 6 meses en el cuerpo vítreo de ojos de conejo sanos. Además, ambas vías de administración fueron seguras, requiriendo menor dosis la supracoroidea.

Para demostrar el carácter generalizable del sistema de liberación, y al no existir en la actualidad ningún tratamiento intravítreo enfocado al control de la neuropatía glaucomatosa, para el siguiente estudio se seleccionó el fármaco brimonidina, en lugar de dexametasona (formulación BRI/LAP). Además, se aplicó sobre un modelo de enfermedad (glaucoma crónico inducido) para comprobar el efecto terapéutico mantenido durante un período prolongado y para confirmar la ausencia de efectos secundarios. La investigación se llevó a cabo con 91 ratas Long Evans (40% de machos, 60% de hembras). Este segundo estudio permitió **evaluar *in vivo* el efecto terapéutico de la formulación BRI/LAP** tras una única inyección intravítrea**.** Los resultados obtenidos mediante técnicas de evaluación de la eficacia y tolerancia (OCT, electrorretinografía, técnicas histológicas y estudios farmacocinéticos) mostraron que la formulación BRI-LAP produjo un efecto hipotensor y un efecto neuroprotector durante al menos 6 meses.

Los estudios realizados mediante OCT en este último estudio aportaron información no solo de la estructura y grosor neurorretinianos, sino también de la interfase vitreorretiniana, donde se observó la formulación en forma de agregados hiperreflectantes. A partir de estos hallazgos se realizó un nuevo estudio centrado en el desarrollo de un sistema para **monitorizar por OCT la formulación BRI/LAP** mediante una caracterización cualitativa y cuantitativa de dichos agregados basada en los cambios en la intensidad de la señal vítrea observada, respecto a la intensidad del epitelio pigmentario de la retina, expresado como ratio VIT/EPR. El análisis de los resultados obtenidos mostró que la intensidad relativa VIT/EPR es significativamente mayor en los ojos tratados con la formulación BRI/LAP que en los no tratados; que los valores de intensidad disminuyen con el tiempo y que los agregados pueden calcularse con un alto grado de reproducibilidad. Además, el área total agregada se correlaciona con la cantidad de brimonidina en todas las fases del estudio y muestra una curva de degradación similar. Por lo tanto, la intensidad relativa de VIT/EPR parece ser un biomarcador útil y objetivo para la monitorización de la formulación BRI/LAP, postulándose como un novedoso método de medición no invasivo.

Finalmente, como último trabajo de esta Tesis Doctoral, se realizó una **revisión de los estudios con Laponita** llevados a cabo en el ojo durante los últimos 10 años, así como de los estudios no realizados en el ojo pero que podrían ser potencialmente aplicables en oftalmología. La revisión mostró las numerosas evidencias científicas que sugieren que la Laponita puede utilizarse en todas las estructuras y tejidos oculares, desde la piel y los apéndices oculares hasta la retina y la órbita, a pesar de los pocos estudios realizados hasta la fecha sobre la aplicación del biomaterial Laponita en el ojo y/o tejido ocular. Entre sus ventajas destacan -en el caso de la oftalmología- la biocompatibilidad, la transparencia óptica, el grosor nanométrico y la tixotropía, que facilita la inyección, además de su

capacidad para retener todo tipo de moléculas, incluso en co-carga, y su habilidad para liberarlas progresivamente para tratar la célula diana tras su administración en forma de gel tópico o inyección cutánea, intravítrea o supracoroidea, o como andamiaje. También posee características bactericidas y regenerativas intrínsecas. La **translación a la práctica clínica del biomaterial Laponita como sistema de administración de fármacos** parece un hecho factible, sencillo y próximo. Sin embargo, su aplicación en el campo de la medicina regenerativa parece todavía lejano. Se concluyó con la idea de que la Laponita parece ser un biomaterial que merece un estudio más profundo en aplicaciones médicas, quirúrgicas y regenerativas en futuras investigaciones oftalmológicas.

ABSTRACT

The present Doctoral Thesis is based on the **in vivo study of the biocompatibility and efficacy of Laponite** as a carrier of several pharmacological agents with different properties, specifically a steroidal anti-inflammatory of very wide application in ophthalmologic pathology such as dexamethasone and an agent with low solubility such as brimonidine. It has also been used to **compare two different routes of administration** (suprachoroidal and intravitreal) and we have worked with both **healthy and diseased animal models**. In addition, a non-invasive system for **monitoring the intravitreal formulation using optical coherence tomography** (OCT) has been developed.

Diseases of the posterior segment of the eye are a clinical challenge, both because of their frequency and because of their severe visual impairment. The anatomical complexity of the eye and the existence of various physiological barriers with a protective function mean that currently available therapeutic measures are often insufficient to maintain drug levels within the therapeutic range. The different ophthalmic routes of administration have, in common, the low bioavailability of the drug at the site of action and the need for repeated administrations, which in the case of ocular injections entails a considerable risk of serious complications. In recent years, research has focused on **nanoparticle systems** as biomaterials capable of sustained drug release, which simultaneously reduces the dose and allows prolonged administration at the target tissue site. Among the various nanomaterials being explored, Laponite, a synthetic colloidal layered silicate, stands out as a particularly promising and emerging biomaterial, which brings together a series of physicochemical and biological characteristics that make it especially attractive for ocular application, such as being biocompatible, easily injectable and optically transparent, with qualities such as thixotropy, which facilitates its injection, and the ability to retain all types of molecules, as well as to release them progressively. However, despite its promising qualities, there have been few studies on applications of the biomaterial Laponite in the eye to date, even though there is ample scientific evidence to suggest that it can be used safely in ocular tissues.

To support the development of the studies that compose this Doctoral Thesis, our group had already conducted **previous studies with Laponite**, both in vitro and in vivo. Initially, a new formulation of dexamethasone was created and characterized in vitro using a Laponite matrix as a base (DEX/LAP formulation), which showed a sustained drug release for 24 weeks, tested on solutions emulating the vitreous humor. This study highlighted the simplicity of the preparation method. A parallel study demonstrated, in vivo, that Laponite administration in healthy rabbit eyes was safe and biocompatible, with intraocular persistence after intravitreal and suprachoroidal injection. There were no significant differences in intraocular pressure, neither relevant ocular complications, and no pathological changes were observed in the histological study. In addition, a slow degradation of Laponite was observed for 14 weeks.

Thereafter, the first objective focused on **evaluating the in vivo pharmacokinetic profile and ocular safety of the DEX/LAP formulation**. For this purpose, a cohort of 30 New Zealand female albino rabbits was selected, given the suitability of this animal model for pharmacokinetic studies, with a follow-up of up to 24 weeks. The intervention was used to compare two different routes of administration (intravitreal and suprachoroidal). The results demonstrated that, after a single injection of the formulation, dexamethasone release from Laponite was maintained for up to 6 months in the vitreous body of healthy rabbit eyes.

Furthermore, both routes of administration were safe, with the suprachoroidal route requiring lower dose.

To demonstrate the generalizability of the delivery system, and as there is currently no intravitreal treatment focused on the control of glaucomatous neuropathy, the drug brimonidine was selected for the following study (BRI/LAP formulation). In addition, it was applied on a disease model (chronic glaucoma induced) to test the therapeutic effect maintained over a prolonged period and to confirm the absence of side effects. The research was carried out on 91 Long Evans rats (40% male, 60% female). This second study made it possible to **evaluate in vivo the therapeutic effect of the BRI/LAP formulation** after a single intravitreal injection. The results obtained by efficacy and tolerance assessment techniques (OCT, electroretinography, histological techniques and pharmacokinetic studies) showed that the BRI-LAP formulation produced a hypotensive and a neuroprotective effect for at least 6 months.

The OCT studies performed in the latter study provided information not only on the neuroretinal structure and thickness, but also on the vitreoretinal interface, where the formulation was observed in the form of hyperreflective aggregates. Based on these findings, a new study focused on the development of a procedure to **monitor by OCT the BRI/LAP formulation** through a qualitative and quantitative characterization of these aggregates based on the changes in the intensity of the vitreous signal, with respect to the intensity of the retinal pigment epithelium, expressed as VIT/RPE ratio. Analysis of the results obtained showed that the relative VIT/RPE intensity is significantly higher in eyes treated with the BRI/LAP formulation than in untreated eyes; that the intensity values decrease with time; and that the aggregates can be calculated with a high degree of reproducibility. Furthermore, the total aggregate area correlates with the amount of brimonidine in all phases of the study and shows a similar degradation curve. Therefore, the relative intensity of VIT/RPE appears to be a useful and objective biomarker for monitoring the BRI/LAP formulation, postulating itself as a novel non-invasive measurement method.

Finally, as the last work of this Doctoral Thesis, **a review of the studies with Laponite** carried out in the eye during the last 10 years, as well as studies not carried out in the eye, but which could be potentially applicable in ophthalmology, was performed. The review showed the numerous scientific evidence suggesting that Laponite can be used in all ocular structures and tissues, from the skin and ocular appendages to the retina and orbit, despite the few studies performed to date on the application of the biomaterial Laponite in the eye and/or ocular tissue. Its advantages include - in the case of ophthalmology - biocompatibility, optical transparency, nanometric thickness and thixotropy, which facilitates injection, in addition to its capacity to retain all types of molecules, even in co-loading, and its ability to progressively release them to treat the target cell after administration in the form of a topical gel or cutaneous, intravitreal or suprachoroidal injection, or as a scaffold. It also shows intrinsic bactericidal and regenerative characteristics. The translation to clinical practice of the Laponite biomaterial as a drug delivery system seems a feasible, simple and near fact. However, its application in the field of regenerative medicine seems still far away. Laponite seems to be a biomaterial that deserves further study in medical, surgical and regenerative applications in future ophthalmological research.

RELACIÓN DE PUBLICACIONES QUE COMPONEN LA TESIS DOCTORAL

La presente Tesis Doctoral se estructura según la normativa para Tesis por compendio de publicaciones. Los artículos incluidos en la Tesis pertenecen a la misma línea de investigación, estando centrados en la Laponita como biomaterial oftalmológico evaluado en modelos animales y han sido publicados previamente en revistas indexadas en el Journal Citation Reports (Clarivate®) (JCR). Los tres primeros son artículos originales, mientras que el cuarto es una revisión. En el apartado APÉNDICE se incluye el factor de impacto, las áreas temáticas, la contribución del doctorando y las cartas de renuncia.

A continuación, se detallan los cuatro artículos que constituyen el cuerpo de la Tesis Doctoral.

1. Prieto E, **Cardiel MJ**, Vispe E, Idoipe M, Garcia-Martin E, Fraile JM, Polo V, Mayoral JA, Pablo LE, Rodrigo MJ. **Dexamethasone delivery to the ocular posterior segment by sustained-release Laponite formulation.** Biomed Mater. 2020 Nov 21;15(6):065021. doi: 10.1088/1748-605X/aba445 PMID: 32647098.

2. Rodrigo MJ, **Cardiel MJ**, Fraile JM, Mendez-Martinez S, Martinez-Rincon T, Subias M, Polo V, Ruberte J, Ramirez T, Vispe E, Luna C, Mayoral JA, Garcia-Martin E. **Brimonidine-LAPONITE® intravitreal formulation has an ocular hypotensive and neuroprotective effect throughout 6 months of follow-up in a glaucoma animal model".** Biomater Sci. 2020 Nov 21;8(22):6246-6260. doi: 10.1039/d0bm01013h PMID: 33016285.

3. Rodrigo MJ, Perez del Palomar A, Montolio A, Mendez-Martinez S, Subias M, **Cardiel MJ**, Martinez-Rincon T, Cegoñino J, Fraile JM, Vispe E, Mayoral JA, Polo V, Garcia-Martin E. **Monitoring new long-lasting intravitreal formulation for glaucoma with vitreous images using optical coherence tomography.** Pharmaceutics 2021 Feb 5;13(2):217. Doi: 10.3390/pharmaceutics13020217 PMID: 33562488.

4. Rodrigo MJ, **Cardiel MJ**, Fraile JM, Mayoral JA, Pablo LE, Garcia-Martin E. **Laponite for biomedical applications: An ophthalmological perspective.** Mater Today Bio. 2023 Dec 28;24:100935.doi: 10.1016/j.mtbio.2023.100935 PMID: 38239894. Erratum in: Mater Today Bio. 2024 Jan 27;25:100964.

INTRODUCCIÓN

1. Anatomía y fisiología del ojo

El ojo es uno de los órganos más complejos del cuerpo humano. En el ojo humano se pueden distinguir tres capas concéntricas (Figura 1):

a. **Capa externa (túnica fibrosa)**: está formada por la córnea y la esclerótica. La córnea se encuentra en la parte más anterior y es transparente debido a la disposición ordenada de los haces de colágeno y deshidratación. Esta cualidad permite el paso de luz hacia el interior del ojo. La esclera está en la parte posterior y tiene color blanquecino por la desorganización de los haces de colágeno e hidratación relativa. Estas capas protegen el interior del ojo de agentes externos. La parte visible de la esclerótica está cubierta por una membrana mucosa transparente, la conjuntiva, mientras que en su parte más interna está en contacto con la coroides. La córnea y la esclerótica están unidas por el limbo donde la córnea se encuentra con el tejido del iris en lo que se conoce como el ángulo irido-corneal. Dentro del tejido conectivo del ángulo se encuentra una red de canales revestidos de endotelio que es la malla trabecular, y profundo a la malla dentro del tejido conectivo de la esclerótica se encuentra el canal venoso de Schlem. Estas estructuras forman el sistema de drenaje del fluido intraocular para mantener la normotensión ocular.

b. **Capa intermedia o úvea (túnica vascular)**: se trata de una estructura muy vascularizada con elementos neuroepiteliales y tejido conjuntivo. Además, el tejido uveal contiene fibras musculares, nervios y melanocitos que le confieren un aspecto pigmentado. Está formada por tres estructuras anatómicas: el iris, el cuerpo ciliar y la coroides. El iris controla el tamaño de la pupila y la cantidad de luz que llega a la retina; el cuerpo ciliar controla la potencia y la forma del cristalino y produce el humor acuoso; y la coroides es la capa vascular que da oxígeno y nutrientes a las capas externas de la retina, extendiéndose desde la ora serrata hasta el nervio óptico.

c. **Capa interna (túnica nerviosa)**: está constituida por la retina, una compleja estructura en capas de neuronas que captan y procesan la luz. Recubre la superficie interna del ojo, rodeando la denominada cavidad vítrea. Como la corides, la retina se extiende desde la cabeza del nervio óptico hasta la ora serrata.

En el interior del globo ocular se encuentra el cristalino, un órgano encapsulado, de forma lenticular, transparente, biconvexo, formado por una serie de laminillas concéntricas y suspendido de los procesos ciliares por filamentos. Su ubicación establece la división entre el segmento anterior y el segmento posterior del ojo. A su vez el ojo se divide en tres cámaras: (1) **cámara anterior**, el espacio entre la córnea y el iris. (2) **cámara posterior**, el espacio entre la superficie posterior del iris y la superficie anterior del cristalino. (3) **cámara (o cavidad) vítrea**, el espacio entre la superficie posterior del cristalino y la retina. Las cámaras anterior y posterior contienen humor acuoso, que es un fluido acuoso producido por el cuerpo ciliar, mientras que la cámara vítrea contiene el cuerpo vítreo, una sustancia

gelatinosa constituida por fibras de colágeno de tipo II suspendidas dentro de un gel altamente hidratado de hialuronato, matriz extracelular y agua.

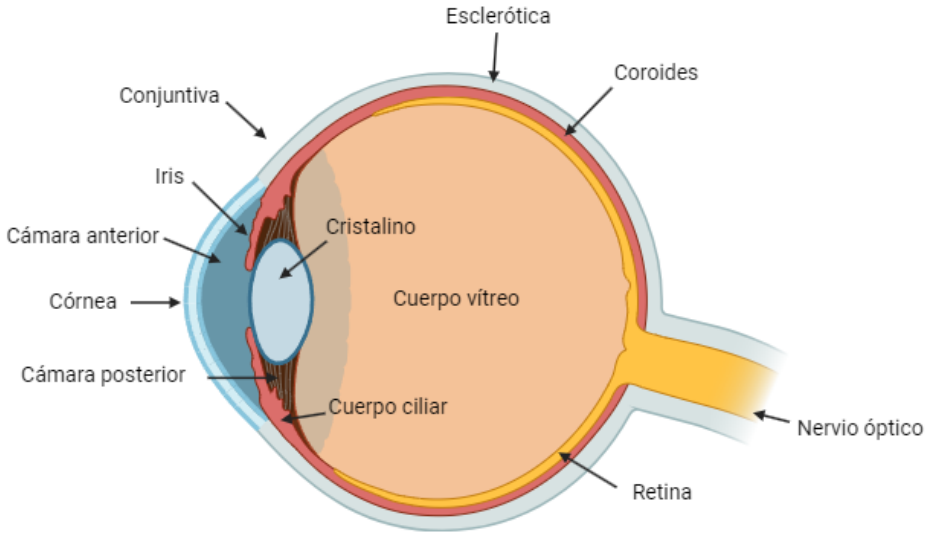

Figura 1. Ilustración esquemática de la estructura del ojo.

Centrándonos en aquellas estructuras anatómicas involucradas en el tema en estudio, se detallan los aspectos relevantes de la retina, la coroides y el cuerpo vítreo, ubicadas en el segmento posterior.

La retina se desarrolla a partir de la copa óptica durante la embriogénesis. Se forma por invaginación de la vesícula óptica, que es una excrecencia del cerebro anterior embrionario. La pared interna de la copa óptica (que rodea la cavidad vítrea) se convierte finalmente en la retina sensorial y la pared externa (rodeada por la coroides y la esclerótica) da lugar al epitelio pigmentario de la retina (EPR). Los distintos elementos que constituyen la retina son neuronas, tejido vascular y células gliales, que interactúan entre sí, dando lugar a un sistema neurovascular. El epitelio pigmentario mantiene la barrera hematorretiniana externa, mientras que los vasos sanguíneos de la retina mantienen la barrera hematorretiniana interna. La retina se organiza en diez estratos que, de dentro a fuera, son:

1) membrana limitante interna (MLI)

2) capa de fibras nerviosas de la retina (CFNR)

3) capa de células ganglionares (CCG)

4) capa plexiforme interna (CPI)

5) capa nuclear interna (CNI)

6) capa plexiforme externa (CPE)

7) capa nuclear externa (CNE)

8) membrana limitante externa (MLE)

9) capa de segmentos de fotorreceptores (CSF)

10) epitelio pigmentario de la retina (EPR)

La retina neural o sensorial consta de seis clases principales de neuronas: fotorreceptores, células bipolares, células horizontales, células amacrinas y células ganglionares, las cuales se encargan de captar y procesar las señales luminosas, y de la glía de Müller, que actúa como columna vertebradora y organizadora de la retina neural. Las células de la retina neural están dispuestas en capas paralelas (Figura 2). Los núcleos de las células fotorreceptoras forman la CNE. Los núcleos de las células gliales, las células bipolares, las células amacrinas y las células horizontales forman la CNI. La CNI tiene capas plexiformes a ambos lados. En la CPE, los fotorreceptores sinaptan con las células bipolares y horizontales, mientras que, en la CPI, las células bipolares y amacrinas hacen sinapsis con las células ganglionares. Los núcleos de las células ganglionares conforman la CCG y sus axones la CFNR. Los procesos de la glía de Müller se extienden por toda la retina. Las prolongaciones apicales forman la MLE mediante complejos de unión entre sí y con los fotorreceptores. Las prolongaciones terminales forman la MLI. Los procesos laterales de la glía entran en contacto con los vasos sanguíneos y las neuronas y forman sinapsis con las dendritas de las capas plexiformes y los axones de la CFNR.

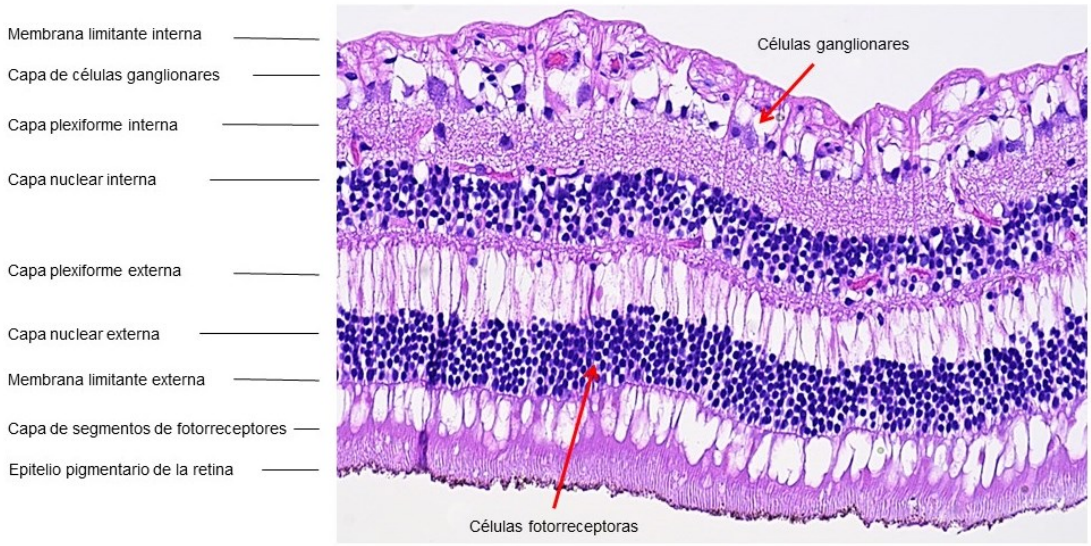

Figura 2. Imagen histológica de la retina teñida con hematoxilina-eosina (40X). Fuente: del autor.

El EPR es una monocapa de unos 3,5 millones de células epiteliales cuboidales dispuestas en un patrón hexagonal, con una densidad relativamente uniforme en toda la retina, entre la CSF y la coriocapilar, una capa de capilares adyacente a la capa más interna de la coroides. En el citoplasma apical de las células del EPR hay numerosos gránulos de pigmento (melanina y lipofuscina). Entre las funciones importantes del EPR se incluye el mantenimiento de la función fotorreceptora (fagocitosis de desechos de los fotorreceptores, regeneración y síntesis de pigmentos), adhesión retiniana, almacenamiento y metabolismo de la vitamina A, producción de factores de crecimiento y desempeña un papel importante en la función de barrera hemato-retiniana.

La retina recibe su suministro sanguíneo de dos sistemas circulatorios: los vasos sanguíneos retinianos y coroideos. La circulación retiniana suministra sangre a la retina interna, excepto a la zona foveal avascular. Las capas avasculares externas de la retina reciben sus nutrientes por difusión desde los vasos coroideos.

La coroides constituye la mayor parte de la región uveal. Se sitúa entre la esclerótica y la retina. Consta de vasos sanguíneos que le confieren su color parduzco y de tres capas bien definidas. La más próxima a la esclerótica se denomina supracoroides, la cual contiene melanocitos pigmentados; en la zona media se encuentra la capa coriocapilar y finalmente, se halla la membrana de Bruch, que es una membrana basal común compartida por las células endoteliales capilares y EPR. La coriocapilar está fenestrada, lo que permite la filtración de moléculas al EPR. Los sistemas de transporte especializados del EPR controlan el transporte de fluidos y nutrientes a los fotorreceptores.

El cuerpo vítreo es una masa transparente, incolora, de consistencia blanda, que ocupa el segmento posterior del globo ocular. Situado entre el cristalino, el cuerpo ciliar y la retina, constituye el volumen más amplio del ojo, representando aproximadamente el 80% del mismo. Mantiene la forma del globo ocular, permite la transmisión de la luz e interviene en el metabolismo del ojo (Holekamp, 2010) Carece de vasos, nutriéndose de los tejidos próximos: coroides, cuerpo ciliar y retina.

El ojo puede considerarse un sistema óptico compuesto concéntrico, ya que posee estructuras encargadas del correcto enfoque de los haces de luz que deben proyectarse sobre la retina con la mayor nitidez posible para una correcta visión. El ojo funciona como una cámara oscura cuyo objetivo es el conjunto de medios transparentes que, de fuera a dentro, son la lágrima, la córnea, el humor acuoso, el cristalino, el vítreo y la retina. La transparencia, curvatura e índice de refracción de los medios y la regularidad de las superficies limitantes, permiten la formación de la imagen al nivel de la capa sensible de la retina.

La retina es una unidad funcional del sistema nervioso central que convierte la señal luminosa en un impulso nervioso, estando físicamente conectada al cerebro a través de los axones del nervio óptico. Es considerada, por tanto, una extensión sensorial del sistema nervioso central. Ésta es una tarea de gran envergadura que requiere una ingente funcionalidad neuronal y tal es así que aproximadamente la mitad de la corteza cerebral humana se dedica al análisis del mundo visual (Bear et al., 2002). Es en la retina donde comienza el procesamiento de las señales que darán lugar a la visión. La luz incidente en la retina alcanza los segmentos externos de los fotorreceptores y asociado a ello, se desencadenan una serie de fenómenos químicos, conocidos como fototransducción, que transforman la energía lumínica en señales eléctricas o impulsos nerviosos. Estas señales se trasmiten a través de las neuronas hasta alcanzar finalmente los axones de las células ganglionares de la retina (CGRs), los cuales se encargan de conducir la información hacia el cerebro, donde finaliza el procesamiento visual (Bear et al., 1998) a través de sus axones, que forman el nervio óptico (Nelson & Connaughton, 1995). Aunque la visión parece ser responsabilidad exclusiva de las neuronas (elementos excitables) de la vía visual, es necesaria la presencia de otra clase de células no neuronales (elementos no excitables) en este proceso, las células gliales o neuroglia como son las células de Müller, los astrocitos y la microglía.

2. Patología oftálmica asociada a degeneración de la retina y del nervio óptico

La principal causa de ceguera irreversible se debe a la degeneración de neuronas retinianas específicas que tiene lugar en enfermedades oculares como el glaucoma, la degeneración macular asociada a la edad (DMAE), la retinopatía diabética y la retinosis pigmentaria (Jindal, 2015) (Ahmad et al., 2020). Y, en los países industrializados, las causas más frecuentes de ceguera son las enfermedades neuropatológicas oculares. La prevalencia y el agente causal varían con la edad; mientras que la DMAE y el glaucoma son causas más frecuentes en la vejez, las personas más jóvenes se ven afectadas con más frecuencia por la retinopatía diabética.

Dentro de las entidades asociadas a neurodegeneración retiniana, el **glaucoma** es, sin lugar a duda, la principal patología. Se considera la segunda causa principal de ceguera irreversible en el mundo y la primera en los países desarrollados, con más de 61 millones de personas afectadas según la Organización Mundial de la Salud (OMS). Es una neuropatía óptica multifactorial que se caracteriza por una pérdida progresiva e irreversible de la visión por la degeneración y muerte selectiva de las CGRs. Estas células son neuronas del sistema nervioso central (SNC) que tienen el cuerpo celular en la retina interna. Sus axones intraoculares no mielinizados forman la capa de fibras nerviosas de la retina (CFNR) que se mielinizan a su salida para formar el nervio óptico o segundo par craneal. El daño en la CFNR suele asociar posteriormente cambios estructurales en la cabeza del nervio óptico y defectos típicos en el campo visual (Weinreb et al., 2014), que pueden llegar finalmente a la ceguera. El principal factor de riesgo modificable es el aumento de la presión intraocular (PIO), que provoca la muerte progresiva de las CGR y la consiguiente pérdida irreversible de la visión (Jonas et al., 2017). Sin embargo, múltiples factores genéticos, celulares y ambientales influyen en el inicio y la progresión de la enfermedad. En este sentido, varios estudios han puesto de manifiesto una degeneración secundaria de las células de la retina debido al entorno citotóxico (especies reactivas de oxígeno, óxido nítrico, glutamato u otros radicales libres) producido por las neuronas circundantes (Almasieh et al., 2012). Además, hay que tener en cuenta que la disfunción y posterior muerte de las CGR también pueden ocurrir en un estado de normotensión ocular. Por otra parte, hay que considerar que otras enfermedades de la retina también pueden conducir a diversos tipos de glaucoma de forma secundaria. Las enfermedades isquémicas como la oclusión de la vena central de la retina (OVCR), las neoplasias malignas y la retinopatía diabética proliferativa están asociadas al glaucoma neovascular. Diversos tipos de uveítis, incluida la enfermedad de Behçet, la sarcoidosis, la sífilis, la iridociclitis de Fuchs y la artritis reumatoide juvenil son causas de glaucoma secundario.

Aunque las enfermedades que afectan al polo posterior son un problema creciente en las poblaciones que envejecen, no existen en muchos casos tratamientos eficaces para gran parte de los pacientes. Todo ello justifica la importancia de desarrollar modelos de experimentación animal tanto para reproducir la propia enfermedad como para abordar nuevas estrategias terapéuticas.

3. Estrategias en el abordaje terapéutico de la neurodegeneración retiniana

3.1. Vías de administración de los fármacos

El transporte de fluidos y solutos en el ojo está controlado por varias membranas y barreras fisiológicas, lo cual puede dificultar la administración de fármacos oculares tópicos (por ejemplo, colirios) y sistémicos (por vía oral o intravenosa). Las principales barreras fisiológicas son la película lagrimal, córnea, esclera y barreras hemato-oculares.

La película lagrimal es una fina capa líquida (3 μm) que recubre las superficies corneal y conjuntival. Tiene distintas funciones, entre las que destacan su acción lubricante, nutritiva y antibacteriana. Consta de tres capas: lipídica, acuosa y de mucina. La capa lipídica es la más externa y su principal función es disminuir la evaporación de la capa acuosa; la capa intermedia es la capa acuosa, que constituye alrededor del 90% del volumen total de la lágrima y, finalmente, la mucina es la capa más interna y está constituida por glucoproteínas que, debido a su hidrofilia, contribuyen a la adecuada humectación de la córnea y la conjuntiva. La lágrima es la barrera más importante para la absorción de fármacos administrados por vía tópica. Su drenaje a través del conducto nasolagrimal, la unión de sus proteínas con la molécula del fármaco y el recambio lacrimal continuo (1 ml/min) reducen drásticamente la concentración efectiva del fármaco en el lugar de acción. Los fármacos oculares tópicos, administrados principalmente en forma de colirio, son las formas de dosificación más utilizadas para el tratamiento de enfermedades oculares. La primera barrera que deben atravesar estos fármacos es la película lagrimal, que elimina rápidamente del ojo los compuestos instilados, lo que se traduce en una baja biodisponibilidad.

La córnea se compone de seis capas diferentes (epitelio, membrana de Bowman, estroma, capa de Dua, membrana de Descemet y endotelio). La vía corneal es la principal vía tópica ocular de administración de fármacos a la cámara anterior. Debido a la naturaleza de las diferentes capas, la absorción corneal de los fármacos va a estar fundamentalmente condicionada por su balance hidrofilia / lipofilia, peso molecular, carga y grado de ionización. Los fármacos lipófilos especialmente pequeños pueden atravesar fácilmente la córnea. La sección exterior limitará la absorción de sustancias hidrofílicas. La permeación de fármacos hidrófilos y macromoléculas a través del epitelio corneal está limitada por la presencia de uniones estrechas entre las células epiteliales superficiales externas adyacentes. A continuación, el estroma, formado por queratocitos y tejido conectivo, ocupa el 90% del espesor de la córnea y constituye el mayor reservorio para las sustancias hidrofílicas. La abundante presencia de colágeno hidratado en el estroma puede dificultar la difusión de agentes altamente lipofílicos. Y, por último, la sección más interna permite el paso de sustancias con relativa facilidad, incluso de aquellas proteínas con elevados pesos moleculares. El endotelio es más permeable y permite el paso de fármacos hidrófilos y macromoléculas entre el acuoso y el estroma debido a la presencia de uniones estrechas permeables llamadas desmosomas o mácula adherente. Tras atravesar la córnea, el fármaco difunde al humor acuoso y a la úvea anterior.

La conjuntiva tiene una rica vasculatura y una gran cantidad del fármaco administrado que la atraviesa es eliminado por la circulación sistémica. La vía conjuntival / escleral suele ser menos eficaz para la administración de fármacos, pero puede utilizarse para la administración de moléculas hidrófilas y de mayor tamaño, que no pueden difundirse

fácilmente a través del epitelio corneal. El fármaco penetra a través de la esclerótica, que es más permeable que la córnea, pero menos que la conjuntiva.

El paso de los fármacos de los segmentos anterior a posterior del ojo no es muy eficaz debido al recambio acuoso. Por lo tanto, los fármacos administrados en la superficie ocular no suelen alcanzar los segmentos posteriores del ojo (retina, vítreo, coroides) en concentraciones terapéuticas suficientes.

Las administraciones intravenosa e intravítrea (IV) parecen ser las principales estrategias para tratar las enfermedades del segmento posterior. Sin embargo, la administración intravenosa tiene un éxito limitado por la exclusión del ojo de la circulación sistémica. Las barreras hematooculares protegen al ojo de las sustancias circulantes en la sangre y, por tanto, impiden el acceso de muchos fármacos administrados por vía sistémica hacia el interior del ojo. Se distinguen dos tipos de barreras hematooculares: la barrera hematoacuosa, que está formada por el epitelio de los cuerpos ciliares y protege el segmento anterior, y la barrera hematorretiniana, que protege el segmento posterior y controla la entrada de los fármacos en la cavidad vítrea desde la circulación sistémica. A pesar de algunas similitudes, la BHR difiere de la barrera hematoencefálica por la presencia funcional de su barrera externa que está formada por el EPR. La barrera interna está formada por las células endoteliales de los vasos retinianos (Miller et al., 2005) (Barar et al., 2008) Urtti (2006). Ambas barreras presentan uniones estrechas restringidas, mediante las cuales se puede regular selectivamente la permeación/transferencia de sustancias hidrofílicas y macromoléculas hacia el interior y hacia el exterior de la retina. La permeabilidad pasiva transcelular es la principal vía de entrada/salida de moléculas pequeñas a través del BHR, mientras que la permeabilidad del EPR es bastante baja. Además, existe una correlación inversa entre el peso molecular y la permeabilidad.

Otras opciones de administración de drogas al segmento posterior del ojo son las rutas perioculares, debido a su capacidad de sortear la barrera conjuntivo-corneal y de proporcionar un espacio virtual desde donde liberar el fármaco de forma progresiva (S. H. Kim et al., 2007). Entre las diferentes modalidades de administración periocular, se encuentran las vías subtenoniana, subconjuntival, supracoroidal o transescleral (Figura 3).

La ruta **transescleral** permite superar la barrera del segmento anterior. El fármaco administrado a través de esta vía cuenta con las barreras de la esclera, el flujo sanguíneo coroideo y el epitelio pigmentario de la retina. La vía transescleral es menos invasiva, pero tiene una menor biodisponibilidad intraocular debido a que la vía de eliminación de la cámara vítrea se mueve hacia afuera, mientras que el fármaco se mueve hacia adentro (contra el flujo natural). Estas deficiencias pueden paliarse mediante modificaciones de formulación.

La administración vía **supracoroidea** (SC) representa una prometedora ruta emergente alternativa para el tratamiento de las enfermedades oculares del segmento posterior y se ha convertido en un foco de investigación de la administración de drogas (Gilger et al., 2014) (Rai et al., 2015) (Jung et al., 2019). El espacio supracoroideo (SCS) es un espacio virtual situado entre la esclerótica y la coroides que puede expandirse para dar cabida a las formulaciones de drogas (Chiang et al., 2017) (Chiang et al., 2018) (Emami-Naeini & Yiu, 2019). Proporciona mayores concentraciones de droga en la zona que abarca la unidad retina-epitelio pigmentario de la retina-coroides y el polo posterior, y minimiza la presencia de droga en las estructuras anteriores del ojo (Olsen et al., 2011) (Touchard et al., 2012) (Tyagi et al., 2012) (Chen et al., 2015) (Chiang et al., 2018) (Jung et al., 2018)

(Habot-Wilner et al., 2019). Sin embargo, la eficiencia de la droga varía entre las diferentes formulaciones debido a una alta tasa de eliminación en el SCS, las propiedades fisicoquímicas el tamaño o el radio molecular de la droga o las formulaciones viscosas o de partículas, entre otros (Olsen et al., 2011) (Gu et al., 2015); (Chen et al., 2015) (Rai et al., 2015) (Chiang, Venugopal, et al., 2016) (Chiang et al., 2017) (Y. Zhang et al., 2018) (Jung et al., 2018). La inyección SC se considera más eficaz que las rutas subconjuntival o subtenoniana, y más segura que la inyección intravítrea (Rai et al., 2015) (Chen et al., 2015) (Chiang et al., 2018) (Habot-Wilner et al., 2019).

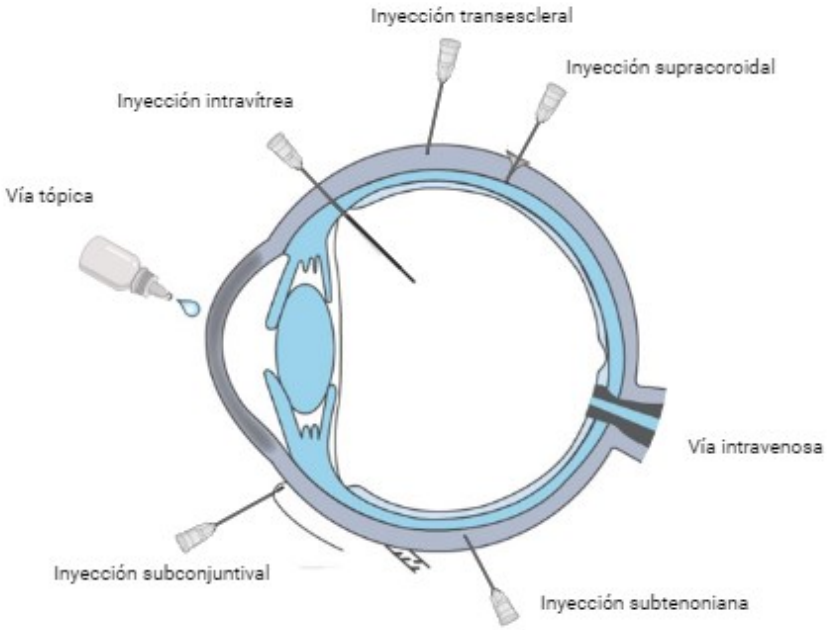

Figura 3. Rutas de administración de fármacos a nivel ocular.

La **inyección intravítrea** es la opción terapéutica de referencia para patologías del segmento posterior como la DMAE, la retinopatía diabética o las oclusiones vasculares. El interés de utilizar la administración intravítrea es saltarse las barreras oculares, evitar los eventos adversos sistémicos y mantener los niveles terapéuticos de la droga cerca del lugar de acción, actuando como reservorio (del Amo et al., 2017) (Bisht et al., 2018). Aunque, por otra parte, como es una vía invasiva, puede dar lugar a complicaciones locales como toxicidad o desprendimiento de la retina, lesiones del cristalino, infecciones o hemorragias intraoculares y elevación de la presión intraocular (Kwak & D'Amico, 1992) (Dossarps et al., 2015) (Kersey & Broadway, 2006).

3.2. Terapias intravítreas disponibles en la actualidad

La administración oftálmica de los fármacos es la ruta habitual para el tratamiento de patologías oculares frecuentes como el glaucoma, la DMAE, la retinopatía diabética, las infecciones y los trastornos autoinmunes. Tratamientos antiinflamatorios como los glucocorticosteroides (GC) se vienen utilizando de forma habitual en la práctica clínica para tratar las enfermedades oculares del segmento posterior como la uveítis posterior no

infecciosa, la retinopatía diabética, la oclusión venosa de la retina o la DMAE con edema macular (Chennamaneni et al., 2013) (Lowder et al., 2011) (Ciulla et al., 2014) (Haller et al., 2011) (Calvo et al., 2015). Los procesos del segmento posterior son difíciles de tratar por la poca permeabilidad de los tejidos, la existencia de barreras anatómicas y fisiológicas en el ojo y la baja biodisponibilidad del fármaco en el tejido diana (Ethier et al., 2004) (S. H. Kim et al., 2007) (Thakur et al., 2011) (Awwad et al., 2017). Las vías disponibles actualmente, en muchos casos, son insuficientes para mantener niveles terapéuticos adecuados del fármaco en la región posterior del ojo (Gaudana et al., 2010). Es por ello por lo que hay que recurrir a altas dosis y elevadas frecuencias de administración, lo que redunda en importantes efectos secundarios nocivos (Oray et al., 2016) (Caplan et al., 2017) y un elevado riesgo de complicaciones oculares graves (Dossarps et al., 2015) (Ganapathy et al., 2018).

A nivel clínico, los implantes son los únicos sistemas de liberación que han llegado a comercializarse para su administración intravítrea. Son pequeños dispositivos sólidos que se implantan quirúrgicamente o se inyectan en el humor vítreo (Gote et al., 2019). En la actualidad, en Europa existen implantes comercializados para prolongar la liberación de dexametasona (Ozurdex®), fluocinolona (Iluvien®) y ganciclovir (Vitrasert® 4,5 mg). Los implantes oculares buscan la liberación controlada de fármacos, al trabajar dosificaciones y cargas mayores de fármaco. Además, se presenta menor efecto secundario sistémico y mayor proximidad al segmento posterior del ojo. Se pueden emplear polímeros biodegradables o no biodegradables en los sistemas implantables oculares. Si bien los implantes biodegradables no necesitan ser removidos después de la inserción en el ojo, los no biodegradables requieren una intervención adicional para remover o rellenar los implantes, lo que conlleva costos adicionales y riesgos quirúrgicos intra o postoperatorios.

La administración intravítrea de fármacos se ha convertido en un método popular de tratamiento de la DMAE de tipo exudativo, en particular, desde la introducción de los medicamentos anti- factor de crecimiento del endotelio vascular (VEGF). Fármacos como bevacizumab (Avastin®), ranibizumab (Lucentis®), pegaptanib sódico (Macugen®), aflibercept (Eylea®) y acetónido de triamcinolona (Kenalog®) se utilizan ampliamente como inyecciones intravítreas para tratar esta y otras enfermedades de la retina. Por otro parte, hay que considerar que actualmente no existe ningún tratamiento intravítreo enfocado al control de la neuropatía glaucomatosa que simultáneamente disminuya la PIO y prevenga el daño neurorretiniano.

No obstante, hay que tener en cuenta que las inyecciones oculares repetidas pueden producir complicaciones como son: elevación de la PIO, inflamación intraocular, formación de cataratas, desprendimiento de retina o incluso endoftalmitis, con una incidencia del 0,02% por inyección en esta última (Pershing et al., 2013) (Kumar et al., 2012) (Dossarps et al., 2015). De ahí la necesidad de buscar un sistema mínimamente invasivo de administración sostenida de drogas el cual mantenga la concentración terapéutica durante períodos prolongados, mejorando la vida media y la biodisponibilidad del fármaco, lo que permitiría alargar los intervalos de administración (Urtti, 2006).

4. Biomateriales como sistemas de administración sostenida

Un biomaterial es un material destinado a interactuar con sistemas biológicos para evaluar, tratar, aumentar o sustituir cualquier tejido, órgano o función del cuerpo y, en el caso del ojo, para compensar la pérdida de visión que puede o no estar relacionada con la edad. Los biomateriales oftálmicos deben cumplir determinados requisitos (Ferraz, 2022). La compatibilidad y la capacidad de suministrar oxígeno a los tejidos es una cuestión fundamental. También se requiere un índice de refracción cercano al del agua, lo que significa que la mayoría de los materiales que se coloquen en el ojo deben ser transparentes, un prerrequisito exclusivo de los biomateriales oftálmicos. Así como combinar propiedades superficiales y mecánicas estables durante el periodo de aplicación.

La tecnología moderna de liberación sostenida de fármacos sólo tiene 60 años. La primera generación (1950-1980) sentó las bases de la liberación controlada y gestionó con éxito las propiedades físico - químicas de los sistemas de administración. La segunda generación desarrolló sistemas de administración inteligentes, pero tuvo problemas con las barreras biológicas. La tercera generación actual (desde 2010) comprende sistemas de administración modulados diseñados para superar tanto las barreras fisicoquímicas como las biológicas en el ojo con el objetivo de administrar niveles terapéuticos de fármaco con una intervención mínima (Yun et al., 2015).

Las formulaciones de liberación controlada permiten mantener las concentraciones intraoculares del fármaco dentro del índice terapéutico durante periodos prolongados, lo que posibilita intervalos de dosificación de varios meses. Pero el diseño de sistemas de liberación de fármacos a nivel intraocular presenta diversas dificultades. Por un lado, los sistemas deben tener un tamaño del orden de micrómetros o nanómetros, pero, a la vez, debe contener la dosis adecuada para obtener concentraciones efectivas durante largos períodos de tiempo. Por todo ello, a pesar de que numerosos sistemas de liberación de fármacos están en investigación, la mayoría de ellos están en fases muy tempranas y solo unos pocos han llegado a ser testados en ensayos clínicos. Entre los sistemas de liberación de fármacos en desarrollo destacan: hidrogeles, liposomas, micropartículas, nanopartículas, implantes y sistemas compuestos. En este sentido, los minerales de arcilla se postulan como una clase emergente de biomateriales, adecuados para una amplia gama de aplicaciones biomédicas. Tanto las arcillas sintéticas como las naturales ya han mostrado sus propiedades como moduladores de la administración de drogas, dada su capacidad de controlar o vectorizar la liberación de drogas y aumentar la biodisponibilidad (Rodrigues et al., 2013).

4.1. Laponita

La **Laponita (LAP),** cuyo nombre comercial es Laponite®, es una arcilla sintética, libres de impurezas y por tanto tienen una estructura y composición más uniformes. Fue desarrollada a principios de los años 60 (Shafran et al., 2020) como aditivo reológico para dispersiones de pigmentos (Neumann, 1965). Desde entonces, la LAP no sólo se ha empleado en diversas aplicaciones industriales, sino que también ha sido objeto de aplicaciones biomédicas (Das et al., 2019) (Tomás et al., 2018) (Samoylenko et al., 2022). La investigación traslacional realizada con la LAP se ha centrado principalmente en la cicatrización de heridas, en los sistemas de administración de fármacos (pequeñas moléculas y, más recientemente, liberación de proteínas) para tratar infecciones,

hemorragias o cáncer; y en la ingeniería de tejidos para andamiajes óseos (Kiaee et al., 2022) (C. Wang et al., 2023). Sin embargo, hay muy pocas publicaciones científicas relativas a aplicaciones oftalmológicas (Figura 4).

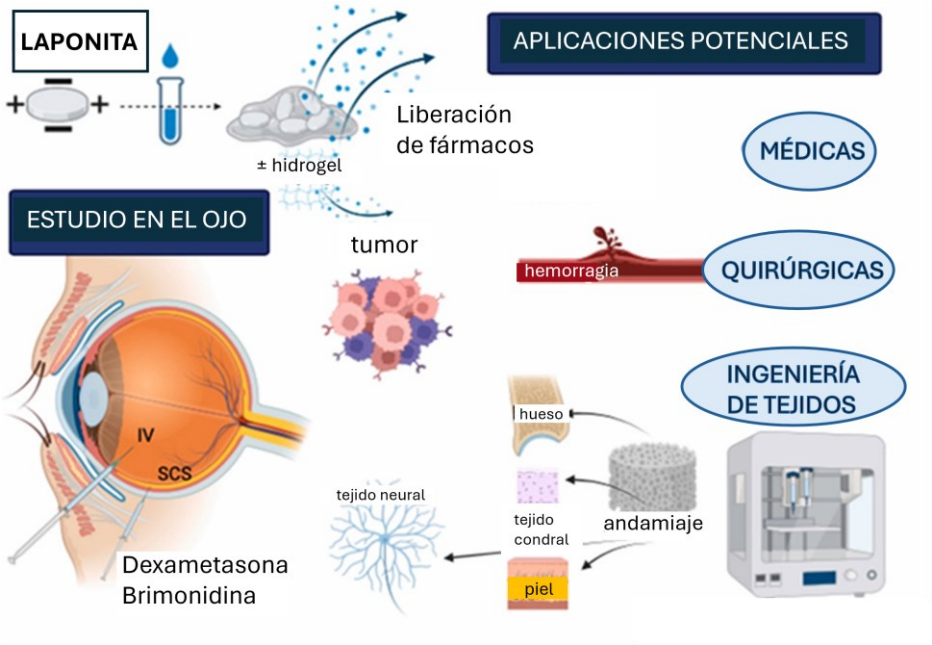

Figura 4. Aplicaciones potenciales de la laponita.

Desde un punto de vista fisicoquímico, la fórmula empírica de este nanosilicato sintético es $(Na^{+}_{0,7}[(Si_8Mg_{5.5}Li_{0,3})O_{20}(OH)_4])_{0.7}$ (Gaharwar et al., 2019). Como mineral arcilloso, su estructura básica consiste en la alternancia de una lámina octaédrica de AlO6 intercalada entre dos láminas tetraédicas de SiO4 (Pauling, 1930) (Murray, 1991). La LAP tiene una superficie de doble carga. Las superficies superior e inferior están cargadas negativamente debido al desequilibrio de carga causado por la sustitución del magnesio por el litio en la capa octaédrica, mientras que los bordes de las partículas pueden estar cargados positivamente por la protonación de los grupos hidroxilo (OH) terminales de las capas tetraédricas de silicato. Pueden apilarse varias capas unas sobre otras, principalmente por fuerza electrostática, pero también por enlaces de hidrógeno y por las fuerzas de Van der Waals. Las arcillas de silicato estratificado ofrecen una elevada superficie (más de 700 m^2/g) y permiten la interacción y retención de fármacos, polímeros, proteínas o vesículas extracelulares, formando así sistemas multifuncionales de administración de fármacos con un mejor rendimiento terapéutico. En forma seca, la LAP está formada por cristales bidimensionales en forma de disco (0,92 nm de altura, 25 nm de diámetro, 2,65x103g/cm^3 de densidad) (Lapasin et al., 2017). Al dispersarse en un medio acuoso, se convierte en partículas coloidales tridimensionales de gel incoloro, liberándose iones de sodio, lo que da lugar a una superficie de carga negativa débil y a una mayor absorción de agua, con el consiguiente aumento de volumen (Zhao et al., 2015). Forma una dispersión coloidal clara con características de gel tixotrópico, viscoelástico y transparente, apta para ser administrada por inyecciones (Lapasin et al., 2017). Las condiciones microambientales, como el pH o la concentración salina tienen un impacto significativo en

el tiempo de gelificación, el cual aumenta significativamente con la disminución de la concentración de sal. Sin embargo, con concentraciones de LAP superiores a 10 g/L la concentración de sal no influye en el tiempo de gelificación. Otros cambios ambientales, como la humedad local, pueden hacer que la arcilla absorba o pierda agua, dando lugar a un grado de hinchamiento variable. La permeabilidad al agua y la difusión de moléculas pequeñas depende de la orientación de las partículas de arcilla dentro del gel. Las partículas bien orientadas pueden servir de barrera a gases y líquidos, mientras que las partículas orientadas de forma aleatoria o desordenada pueden aumentar la permeabilidad (Wu et al., 2010). El hinchamiento puede evitarse mediante la formación de interacciones entre los polímeros y la Laponita, controlando así la liberación lenta (Takeno et al., 2017) (Tipa et al., 2022) (Yadav et al., 2022). La capacidad de interactuar con otras moléculas mediante mecanismos muy diversos le permite transportar compuestos que son insolubles en agua (Staniford et al., 2015). Puede actuar como portador de varios fármacos (Aguzzi et al., 2007), liberándolos de manera controlada según las condiciones del entorno, como el pH o la temperatura (Xiao et al., 2016) (G. Wang et al., 2014) (J. Wang et al., 2016).

La **biocompatibilidad** es clave para la traslación médica. Basándose en datos experimentales y modelizados, la Agencia de Protección Medioambiental de EE. UU. ha verificado que la LAP es un producto químico seguro y poco preocupante. Diversos estudios han demostrado la alta biocompatibilidad de LAP, así como su carácter biodegradable, permitiendo un amplio campo de aplicaciones biomédicas. No presenta toxicidad sistémica tras su administración oral, intramuscular u ocular (Lee et al., 2019) (L. Zhang et al., 2022) (Domeneguetti et al., 2023) tanto a bajas concentraciones (0,1-7% p/v) como con una concentración inhibitoria de 4 mg/mL (Gaharwar et al., 2012). Varios estudios afirman que los valores con concentración inhibitoria de la LAP varían considerablemente, oscilando entre 0,05 y 50 mg/mL (Veernala et al., 2019). Además, tras la administración intravenosa, un nanocompuesto basado en LAP no mostró actividad hemolítica *in vitro* ni alteraciones histopatológicas en los tejidos cerebral, cardíaco, hepático o renal de ratones *in vivo* (Singh et al., 2020). Sin embargo, no se recomienda la medicación oral prolongada debido al riesgo de formación de cálculos renales y la eliminación de enzimas y otros elementos nutritivos. Además, altas concentraciones de nanosilicatos pueden reducir la proliferación celular *in vitro* (Maisanaba et al., 2015). Por otro lado, se ha demostrado que las partículas de LAP se degradan de forma natural en aproximadamente 30 días de media. Un hidrogel con una vida de más de 30 días impidió que las partículas de Laponita escapen completamente del hidrogel, evitando así citotoxicidad adversa (Brokesh et al., 2022). La LAP, especialmente la forma comercial Laponita® XLG, se considera adecuada para aplicaciones biomédicas debido a su bajo contenido de metales pesados. Este nanosilicato hídrico contiene elementos como magnesio, zinc, litio y hierro que también se encuentran en el organismo y en el metabolismo cerebral, y sus productos de degradación no tóxicos [$Na+$, Mg^{2+}, $Si(OH)_4$, $Li+$] son fácilmente absorbidos por el organismo (Singh et al., 2020) (Thompson & Butterworth, 1992). La degradación de la LAP libera productos que tienen, por sí mismos, funciones biológicas. Reffit et al mostraron un aumento de la síntesis de colágeno tipo I debido al ácido ortosilícico [$Si(OH)_4$] (Reffitt et al., 2003). Los iones de magnesio también pueden desencadenar respuestas celulares, estabilizar los compuestos de polifosfato en las células, como el trifosfato de adenosina (ATP), o participar en la actividad enzimática y los procesos de señalización. Los cationes de sodio pueden interferir la generación de impulsos nerviosos y el equilibrio hidroelectrolítico y el litio puede afectar al comportamiento de las neuronas (Romani, 2011); (Williams et al., 2004).

A nivel oftalmológico, se ha demostrado *in vivo* la seguridad de LAP en la administración mediante inyección en conejos sanos, siendo un portador seguro y biocompatible para la administración sostenida de agentes bioactivos en el ojo con persistencia intraocular de larga duración después de la inyección SC e IV (Prieto et al., 2018). La LAP es un modificador reológico comúnmente utilizado para ajustar la viscosidad global de la formulación del fármaco y para controlar comportamientos no newtonianos como la deformación por cizalladura (X. Liu & Bhatia, 2015) (B. Liu et al., 2020). Esta propiedad tixotrópica de Laponita® (Barnes, 1997) facilita su inyección mediante agujas de pequeño calibre y preserva mejor el contenido del dispositivo inyectado en el momento de la cizalladura (Samimi Gharaie et al., 2018). Además, los nanosilicatos son ópticamente transparentes en medios acuosos. La LAP puede ser marcada con fluoróforos, luminiscencia y partículas paramagnéticas. Estas características pueden ser beneficiosas especialmente en aplicaciones oftálmicas, al facilitar su identificación y localización.

5. Modelos de experimentación en animales

La evaluación preclínica en animales es fundamental para el desarrollo de nuevos fármacos, de estrategias de administración de éstos, de tecnologías de diagnóstico oftálmico o para la simulación de enfermedades humanas en modelos animales. Los conejos son el modelo preclínico más utilizado para evaluar la farmacocinética ocular, mientras que los roedores se utilizan ampliamente para estudiar la respuesta ocular a los fármacos.

5.1. El conejo como modelo animal sano

La toma de muestras invasiva del ojo humano está muy limitada tanto desde el punto de vista ético como técnico. Los ojos humanos sólo contienen pequeñas cantidades de humor acuoso (unos 200 µl) y vítreo (unos 4,5 ml), por lo que es técnicamente difícil obtener cantidades suficientes de fluido ocular para medir la concentración del fármaco. Además, los métodos que se utilizan para obtener el líquido ocular, como la punción vítrea o la paracentesis de la cámara anterior, pueden dañar el tejido ocular y provocar complicaciones graves, como cataratas, endoftalmitis o desprendimiento de retina. Por consiguiente, la farmacocinética ocular ha de basarse en modelos animales.

La estimación del curso temporal de los efectos del fármaco en el segmento posterior del ojo solo puede llevarse a cabo con herramientas de modelización farmacocinética. El conejo es un modelo animal clínicamente predecible para la **farmacocinética** intravítrea, ya que tanto el volumen de distribución intravítrea como los valores de aclaramiento difieren sólo moderadamente entre el conejo y el ser humano (del Amo & Urtti, 2015). Los conejos, que son pequeños mamíferos del orden Lagomorpha de la familia Leporidae, se encuentran ampliamente disponibles y son animales fáciles de manejar. El tamaño de los ojos es similar al de los humanos y existe una gran base de datos de información para comparación (Figura 5). Como limitaciones a la hora de inferir resultados, hay que tener en cuenta el menor volumen de la cavidad vítrea (1,5 ml) y el menor compartimento sérico de los conejos. Además, en los seres humanos el vítreo se licua más y se vuelve menos homogéneo con el envejecimiento, lo que se asocia a un aumento del flujo convectivo en el vítreo. Por lo tanto, se ha sugerido que la licuefacción y la convección en el vítreo son diferencias farmacocinéticas importantes entre el conejo y el ser humano, las cuales deben tenerse muy

en cuenta a la hora de extrapolar las propiedades farmacocinéticas de los fármacos, obtenidas a partir de estudios en animales a los seres humanos (Ahn et al., 2016).

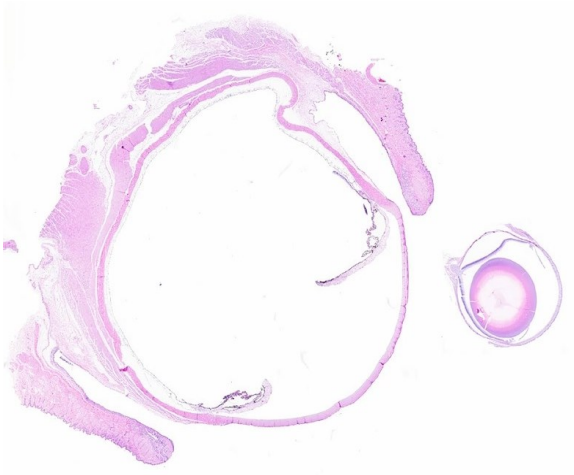

Figura 5. Cortes histológicos transversales de un ojo de conejo (izquierda) y un ojo de rata (derecha). Fuente: Wang et al., 2021.

5.2. Los roedores como modelo animal de patología

El desarrollo de modelos de inducción de glaucoma en roedores viene utilizándose desde hace más de dos décadas, habiendo contribuido a un mejor conocimiento de los mecanismos moleculares que sustentan la patofisiología de esta enfermedad neurodegenerativa multifactorial. La PIO puede ser inducida por diversos métodos: cauterización de la vena episcleral (Garcia-Valenzuela et al., 1995), inyección salina hipertónica en las vías de flujo del humor acuoso (Morrison et al., 1997), fotocoagulación del limbo con láser (WoldeMussie et al., 2001) (Levkovitch-Verbin et al., 2002) (Cuenca et al., 2010) o mediante inyecciones de microesferas (Ms) (Urcola et al., 2006) (Samsel et al., 2011). También se han desarrollado modelos de ratones transgénicos DBA/2J para el estudio de glaucoma (Vecino & Sharma, 2011). Descifrar los cambios anatómicos y funcionales de la retina de los roedores por la hipertensión ocular tiene un gran valor potencial. La retina de la rata, al igual que la de otros vertebrados, está formada por una capa pigmentaria y una capa neuronal, constituyendo ésta última en sentido estricto la retina (Ruberte et al., 2017).

En cuanto a los tipos celulares que encontramos en la retina de los roedores (Figura 6) existen 5 tipos de neuronas (fotorreceptores, células horizontales, células bipolares, células amacrinas y células ganglionares) y 3 tipos de células gliales (células de Müller, astrocitos y microglia). Las características de cada una de éstas son:

- Células ganglionares (CGR): tienen un gran núcleo vesiculoso con nucléolo prominente. En los roedores, la mayor densidad de CGR se localiza en la región temporal (>8.000 células/mm²), mientras que la menor densidad se da a nivel de la vertiente superior (<2.000 células/mm²). Los axones de las CGR forman la CFNR y convergen radialmente hacia el disco óptico donde constituyen el nervio óptico.
- Células bipolares: conectan los fotorreceptores y las CGR y son las células más abundantes en la CNI. Tienen un núcleo pequeño de morfología variable.

- Células horizontales: son similares en apariencia a las bipolares, aunque tienen más citoplasma.
- Células amacrinas: son de mayor tamaño que las células horizontales y tienen un núcleo con una indentación y un nucléolo prominente. Puede haber células amacrinas desplazadas a la CCG.
- Fotorreceptores: los bastones representan el 95% de los fotorreceptores. Los núcleos de los bastones tienen la cromatina más densa que los de los conos.
- Células de Müller: se extienden desde la cámara del vítreo, donde forman la MLI hasta el límite más externo de la CNE, donde constituyen la MLE. Los núcleos se localizan en la CPI. Estas células mantienen la integridad estructural de la retina.
- Astrocitos: están localizados preferentemente en la parte más interna de la retina, dentro de la CFNR y CCG.

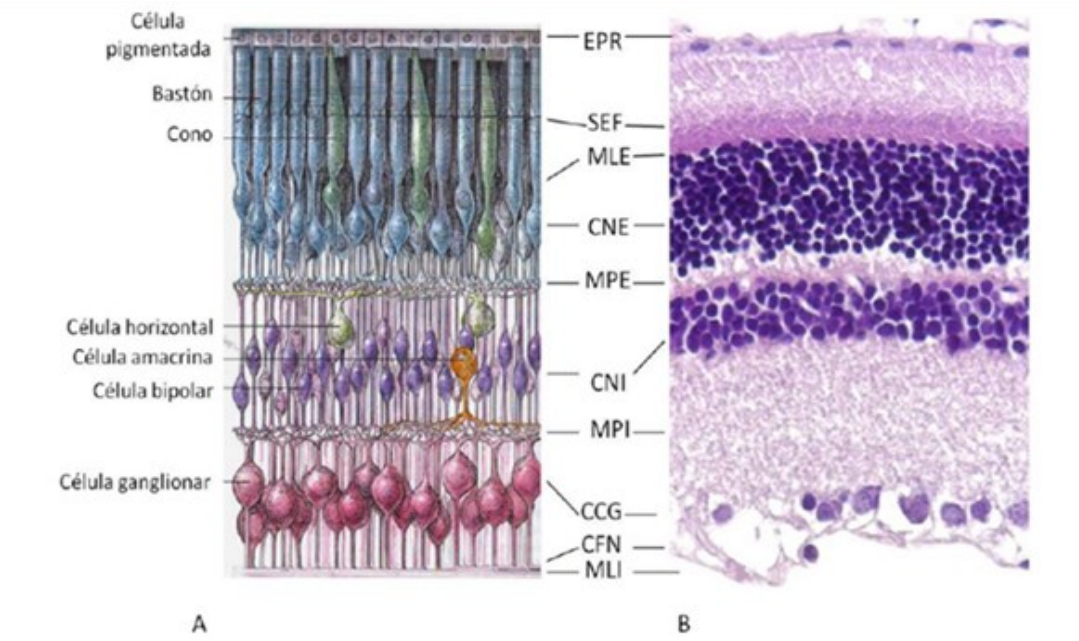

Figura 6. Corte sagital de retina de rata adulta. A: Esquema modificado de la retina con representación de los distintos tipos de células neuronales. B: Corte histológico teñido con hematoxilina-eosina (40X) (imagen extraída de Tesis Doctoral de Mayordomo, 2013). EPR: epitelio pigmentario de la retina; SEF: segmentos externos de fotorreceptores; MLE: membrana limitante externa; CNE: capa nuclear externa; MPE: membrana plexiforme externa; CNI: capa nuclear interna; MPI: membrana plexiforme interna; CCG: capa de células ganglionares; CFN: capa de fibras nerviosas; MLI: membrana limitante interna.

La población de CGR ha sido bien caracterizada anatómica y funcionalmente y puede estudiarse en secciones radiales o de forma íntegra si se disecciona y se extiende sobre un plano. Hay que tener en cuenta que en los roedores la CCG alberga una población de células amacrinas desplazadas de magnitud similar a la de las CGR; asimismo, también

hay un pequeño número de células horizontales desplazadas. Aunque las células amacrinas son más pequeñas que la mayoría de las CGR, hay una superposición de tamaño entre las células amacrinas más grandes y las CGR más pequeñas que hace que el tamaño celular no sea un criterio siempre válido para diferenciarlas. Esta característica anatómica de la CCG de los roedores ha hecho necesario el uso de técnicas alternativas para identificar de forma inequívoca las CGR, como es el uso de trazadores neuronales que dependen del transporte axonal funcional y/o la integridad anatómica del axón, o el uso de marcadores antigénicos y moleculares específicos para las CGR, más accesibles y de más fácil manejo (Vidal-Sanz et al., 2012).

6. Técnicas de evaluación de la tolerancia y eficacia terapéutica

Estas técnicas son fundamentales para predecir cómo un fármaco podría comportarse en humanos y son cruciales en las etapas iniciales del desarrollo de nuevas estrategias terapéuticas. La elección del tipo de técnica depende de los objetivos específicos del estudio y la etapa del desarrollo del fármaco. Las técnicas *in vivo* tienen un carácter más dinámico y son esenciales para monitorizar variables, mientras que las técnicas *ex vivo* permiten estudios específicos a nivel molecular / tisular, proporcionan un control más detallado de las condiciones experimentales y presentan la ventaja de la reproducibilidad.

6.1. Técnicas *in vivo*

6.1.1. Medición de la presión intraocular

Se realiza mediante el tonómetro. Es una técnica de fácil evaluación y plenamente implantada en la práctica clínica y en los modelos animales de glaucoma. Se aconseja realizar todas las mediciones en el mismo momento del día para evitar fluctuaciones circardianas y diarias. Se puede realizar sin y con sedación, en el caso de usar sedación debe ser inferior a 3 minutos para evitar hipotensiones.

6.1.2. Tomografía de coherencia óptica (OCT)

Desde hace años se utiliza ampliamente para estudiar la estructura neurorretiniana, tanto en la práctica clínica como en investigación, permitiendo cuantificar su espesor *in vivo*. La OCT es una tecnología de fácil manejo, económicamente rentable, no invasiva, inocua y objetiva que proporciona imágenes de corte transversal de alta resolución. Su funcionamiento está basado en la interferometría de baja coherencia, que utiliza fuentes de luz de banda ancha de baja energía y genera imágenes dependiendo del grado de reflectividad. Además, los dispositivos mejorados de OCT con fuente de barrido o de mejora de la imagen profunda han permitido estudiar también las características del vítreo en los últimos años (Uji & Yoshimura, 2016) (Keane et al., 2014) (Sreekantam et al., 2017).

6.1.3. Electrorretinografía

Para evaluar el daño desde el punto de vista funcional, la técnica más utilizada es la electrorretinografía (ERG), aunque suele presentar amplia variabilidad en sus respuestas. La electrorretinografía se basa en la estimulación de la retina con una luz de distintas intensidades, lo cual produce flujos iónicos (especialmente de sodio y potasio) que entran y salen de las células sensibles a la luz y genera un potencial eléctrico. El ERG representa gráficamente ese potencial eléctrico y nos permite medir la amplitud y la latencia de las

distintas ondas generadas, procedentes de los distintos tipos de células neurales de la retina. La amplitud se mide en microvoltios (μV) y la latencia en milisegundos (ms).

6.2. Técnicas *ex vivo*

Las técnicas más utilizadas hasta la fecha para evaluar desde el punto de vista morfológico la neurodegeneración retiniana inducida y el efecto de las terapias aplicadas en modelos animales son las técnicas histológicas. Por otro lado, la evaluación del comportamiento cinético y de la biodisponibilidad de los fármacos inyectados en el segmento posterior se realiza mediante los estudios farmacocinéticos.

6.2.1. Técnicas histológicas

Las técnicas histológicas permiten la observación directa de la estructura neurorretiniana, aunque requieren de la enucleación ocular. El sello distintivo de la neuropatía glaucomatosa es la progresiva y lenta degeneración de las CGR y sus axones. Por tanto, es en estas estructuras histológicas donde se centra el interés para evaluar los mecanismos fisiopatológicos de la enfermedad y los posibles beneficios farmacológicos. Entre los marcadores neuronales, el anticuerpo monoclonal frente al factor de transcripción **Brn3a** ha mostrado ser un marcador altamente específico de las CGR en ratas adultas, permitiendo no solo su identificación y cuantificación, sino también la evaluación de su estado funcional, dado que en los días siguientes a la destrucción axonal se observa una disminución en la expresión del anticuerpo. Los axones se pueden poner de manifiesto con anticuerpos anti-neurofilamentos; mientras que la población glial se puede visualizar con marcadores habituales de la glía como es el caso de la proteína ácida fibrilar glial (GFAP) (Vidal-Sanz et al., 2012).

6.2.2. Estudios farmacocinéticos

Comprender la farmacocinética de los fármacos intraoculares es importante para conocer la eficacia y seguridad de estos, determinar la dosis óptima y minimizar las complicaciones sistémicas y/o intraoculares. Los parámetros farmacocinéticos oculares primarios, como son el volumen de distribución y el aclaramiento, son la fuente de información más fiable para las comparaciones farmacocinéticas en función de la especie, la enfermedad, la edad, el fármaco y el sistema de administración. Los estudios farmacocinéticos se basan en la monitorización de las concentraciones de los fármacos inyectados. Para ello suele ser necesario que los animales sean sacrificados a diferentes intervalos de tiempo, extrayendo los ojos y analizando las muestras de humor vítreo para determinar las concentraciones de fármaco. El establecimiento de puntos temporales a intervalos adecuados es crucial para obtener perfiles farmacocinéticos fiables. Los valores obtenidos permiten mediante modelización estimar las concentraciones medias en estado de equilibrio, los perfiles de concentración, la vida media y la cantidad de fármaco en el ojo tras la administración de diferentes dosis o formas de dosificación (del Amo & Urtti, 2015).

ESTADO ACTUAL DEL TEMA

Las **enfermedades del segmento posterior del ojo** suponen un reto desde el punto de vista clínico, tanto por su frecuencia como por su grave afectación de la visión. La complejidad anatómica del ojo y la existencia de diversas barreras fisiológicas con función protectora dificultan el acceso de los tratamientos farmacológicos a su interior. Las diferentes vías de administración oftálmicas (tópica, intravítrea y periocular) tienen en común, en mayor o menor grado, la baja biodisponibilidad del fármaco en el lugar de acción y la necesidad de administraciones repetidas, lo que conlleva en el caso de las inyecciones oculares un riesgo no desdeñable de complicaciones graves. Por ello, sigue siendo necesario buscar nuevos sistemas y formulaciones de administración ocular que consigan que el fármaco esté disponible en el lugar adecuado, en una concentración suficiente, durante el tiempo preciso para lograr el efecto deseado y con un intervalo de administración lo más largo posible. Las **formulaciones de liberación sostenida** parecen ser la opción más adecuada en este contexto, especialmente si son biocompatibles y biodegradables, con sistemas de administración mínimamente invasivos y que permitan mantener las concentraciones intravítreas del fármaco dentro del índice terapéutico durante periodos prolongados (Patel et al., 2011) (Hartman & Kompella, 2018) (Emami-Naeini & Yiu, 2019).

Es, en este sentido, donde surgen los biomateriales, cuyo desarrollo en las últimas décadas ha permitido avanzar a la medicina en múltiples campos, incluida la oftalmología. Al seleccionar biomateriales oftalmológicos hay que considerar las peculiaridades del ojo humano frente a otras partes del organismo, lo que conlleva la exigencia de propiedades fisicoquímicas y biológicas adecuadas al contexto anatómico. Las arcillas, y muy especialmente las sintéticas como la **Laponita®**, se caracterizan por reunir los requisitos necesarios para ser potenciales candidatos en el diseño de sistemas de liberación prolongada de fármacos en el campo de las enfermedades oftalmológicas del segmento posterior. Sin embargo, a pesar de sus prometedoras cualidades, existen pocos estudios realizados sobre aplicaciones del biomaterial Laponita® en el ojo y/o tejido ocular hasta la fecha, a pesar de existir numerosas pruebas científicas que sugieren que puede utilizarse en todas las estructuras y tejidos oculares, desde la piel y los apéndices oculares hasta la retina y la órbita.

A la hora de plantearse la realización de nuevos estudios de investigación, es fundamental realizar un diseño bien estructurado y adecuado a los objetivos planteados. La fase experimental de los estudios sobre patología oftálmica del segmento posterior requiere una evaluación preclínica en modelos sanos, donde valorar la tolerancia, seguridad y estudios farmacocinéticos, y del desarrollo de modelos animales de enfermedad para evaluar la respuesta a la intervención terapéutica. Otro aspecto no menos importante es la selección adecuada del método y las técnicas de evaluación de los resultados. Estudios *ex vivo* como el examen histológico permiten la visión directa o el análisis de los tejidos, pero conllevan el sacrificio del animal. En la actualidad se apoya el desarrollo y aplicación de técnicas *in vivo* que posibilite el estudio monitorizado de forma no invasiva, además de suponer un menor coste y conllevar un fácil manejo.

HIPÓTESIS

Las formulaciones farmacológicas de liberación sostenida mínimamente invasivas, basadas en el uso de Laponita como vehículo, son seguras y eficaces en el tratamiento de enfermedades oculares del segmento posterior, siendo posible además monitorizar los cambios neuro-retinianos y los niveles de concentración de formulación intravítrea mediante técnicas no invasivas (tomografía de coherencia óptica).

OBJETIVOS

1) Estudiar *in vivo* la seguridad ocular y los parámetros farmacocinéticos de la formulación de liberación sostenida de Dexametasona-Laponita tras administración por inyección intravítrea y supracoroidea en ojos sanos de conejo.

2) Comparar el tiempo de permanencia de la dexametasona en el segmento posterior mediante la formulación de liberación sostenida de Dexametasona-Laponita respecto a la formulación convencional.

3) Demostrar la eficacia hipotensora y neuroprotectora de la formulación intravítrea de liberación sostenida de Brimonidina-Laponita en ratas con glaucoma inducido.

4) Comprobar si una única inyección intravítrea de la formulación Brimonidina-Laponita muestra una liberación sostenida y mantiene su efecto durante al menos 6 meses.

5) Analizar los cambios en la intensidad de la señal vítrea mediante tomografía de coherencia óptica (OCT) que genera la formulación intravítrea de Brimonidina-Laponita durante 24 semanas de seguimiento.

6) Evaluar si hay correlación entre los cambios en la intensidad de la señal vítrea de la formulación intravítrea de Brimonidina-Laponita mediante OCT con los niveles del fármaco brimonidina medidos mediante cromatografía líquida - espectrometría de masas, con el objetivo de monitorizar los niveles del fármaco de forma no invasiva.

7) Realizar una revisión sistemática de la evidencia científica actualmente disponible sobre el uso de Laponita en oftalmología.

8) Realizar una revisión bibliográfica de las potenciales aplicaciones biomédicas de la Laponita en patología ocular relativas a la administración de fármacos, prevención o tratamiento de hemorragias, e ingeniería de tejidos mediante medicina regenerativa.

METODOLOGÍA

1. Declaraciones éticas

La manipulación de los animales se realizó de acuerdo con la Política Española de Protección Animal RD1201/05, que cumple con la Directiva 86/609/CEE de la Unión Europea. Las prácticas y el cuidado de los animales cumplieron con la Declaración de la Asociación de Investigación en Visión y Oftalmología para el uso de animales en procedimientos experimentales y otros propósitos científicos.

Los procedimientos relativos al primer artículo se realizaron de acuerdo con la Licencia de Proyecto PI12/02285 aprobada por el Comité de Ética para Experimentos con Animales de la Universidad de Zaragoza (España) y los relativos al segundo y tercer artículo fue previamente aprobado con la Licencia de Proyecto PI34/17.

El trabajo con los animales se llevó a cabo en el servicio de cirugía experimental del Centro de Investigación Biomédica de Aragón (CIBA). Los animales fueron alojados individualmente en jaulas metabólicas estándar, en una habitación con luz controlada (12 h/12 h ciclo oscuro/luz) a 20±2º C con una humedad relativa del 40-70%. La dieta y el agua estaban disponibles ad libitum y se realizaban diariamente exámenes clínicos exhaustivos.

En relación con los animales concretos, en el primer artículo todos los experimentos se llevaron a cabo utilizando **30 conejos** albinos hembra de Nueva Zelanda con un peso de 2,5 a 4,0 kg (3,1±0,4 kg). En el segundo artículo, el estudio se llevó a cabo con **91 ratas** (40% de machos, 60% de hembras) Long Evans de 4 semanas de edad y con pesos que oscilaban entre 50 y 100 gramos al comienzo del estudio. El trabajo con animales se realizó en el seno del Grupo de Investigación de innovación Miguel Servet Oftalmología (GIMSO).

2. Formulaciones terapéuticas

Las formulaciones DEX/LAP y BRI/LAP fueron preparadas y caracterizadas por el Instituto de Síntesis Química y Catálisis Homogénea (ISQCH), grupo de investigación de la Universidad de Zaragoza. Después, este grupo realizó los estudios farmacocinéticos.

3. Estudio computacional de imagen

El grupo de Biomateriales del Instituto Universitario de Investigación en Ingeniería de la Universidad de Zaragoza, perteneciente al Departamento de Ingeniería Mecánica, realizó el estudio de procesamiento y análisis de imágenes sobre la monitorización de la formulación BRI/LAP a nivel vítreo mediante tomografía de coherencia óptica (OCT).

4. Metodología relativa al primer artículo

4.1. Formulación DEX/LAP

4.1.1. Química y reactivos

La dexametasona (DEX) era de Sigma-Aldrich (Madrid, España). Laponite®-RD (LAP) (densidad superficial 370 m^2/g, densidad aparente 1000 kg/m^3, composición química: SiO_2 59,5%, MgO 27,5%, Li_2O 0,8%, 2,8Na_2O %) fue comprada a Rockwood Additives (Widnes, Cheshire, Reino Unido). La solución de hialuronato sódico al 3% (Healon® EndoCoat OVD) y la solución salina equilibrada al 0,9% (9 mg/mL NaCl) (BSS) se obtuvieron de Abbott Medical Optics (Barcelona, España) y Fresenius Kabi (Barcelona, España), respectivamente. El etanol, la acetona y el acetonitrilo fueron de grado HPLC de Scharlab (Barcelona, España).

4.1.2. Preparación y caracterización de la formulación DEX/LAP

La concentración óptima de dexametasona (DEX) para cargar la Laponita ha sido determinada por nuestro grupo en estudios anteriores, en base a la naturaleza de la interacción fármaco-arcilla y el comportamiento *in vitro* del medio hasta la liberación del fármaco (Fraile et al., 2016). El fármaco se incorporó al polímero disolviéndolo en una dispersión acuosa de LAP: 10 mg-DEX se disolvieron en acetona (10 mL) y luego se añadieron 100 mg-LAP a esta solución. La lechada se agitó a temperatura ambiente durante 1 hora y luego se eliminó el disolvente en un evaporador rotativo. El sólido se secó a temperatura ambiente durante la noche al vacío sobre P2O5. El polvo dexametasona-Laponita (DEX/LAP) se almacenó en viales de un solo uso bien tapados y esterilizados con rayos gamma. Inmediatamente antes de la inyección, el polvo DEX/LAP se suspendió en 10 mL de BSS y se sometió a un suave vórtice durante 10 minutos, para obtener una suspensión transparente y homogénea (10 mg/mL; 1:10 p/p).

4.1.3. Determinación de los volúmenes de inyección

Se determinó un volumen de 50 µL y 100 µL de suspensión DEX/LAP para la administración intravítrea y supracoroidea, respectivamente. La dosis de DEX utilizada fue de 0,1 mg en 100 µL para la inyección IV y de 0,05 mg en 50 µL para la inyección SC, que es la concentración óptima de DEX para cargar a la arcilla LAP (10 mg/mL, 1:10 p/p) (Fraile et al., 2016). Se determinó que el volumen de suspensión utilizado para la inyección intravítrea y la inyección de SC era el volumen habitualmente utilizado para los estudios farmacocinéticos (PK) y que debía administrarse con seguridad sin riesgo de fugas, inducción de elevación de la presión intraocular o hemorragia coroidea (Ahn et al., 2016) (Chen et al., 2015) (Prieto et al., 2018)).

4.2. Diseño del estudio *in vivo*

4.2.1. Administración *in vivo*: procedimiento de inyección

Treinta animales se incluyeron en el estudio y se dividieron aleatoriamente en dos grupos. Quince animales recibieron una administración supracoroidea (grupo SC) y los otros quince animales una inyección intravítrea (grupo IV) de la formulación DEX/LAP. Sólo se administró en un ojo (ojo derecho) de cada animal. El otro ojo (ojo izquierdo) permaneció sin tratar.

Todas las inyecciones se realizaron bajo anestesia general y en condiciones asépticas. Para la inyección IV, se anestesió a los animales mediante la inyección intramuscular de clorhidrato de ketamina (25 mg/Kg) (Ketolar 50®, Pfizer, Madrid, España) y medetomidina (0,5 mg/Kg) (Domtor®, Esteve, Madrid, España). Para la administración vía SC, al ser un procedimiento más largo, se realizó una anestesia general inhalatoria con 2,5% de sevoflurano (Sevorane®, Abbott Laboratories, Madrid, España) en oxígeno por medio de una mascarilla, con control de los signos vitales. Se utilizó anestesia tópica con clorhidrato de tetracaína (1 mg/mL) y clorhidrato de oxibuprocaína (4 mg/mL) en gotas oftálmicas (Colircusí Anestésico Doble®, Alcon Cusí SA, Barcelona, España), y se aplicó solución de povidona yodada (5%) para la antisepsia de la superficie ocular antes y después de la inyección.

El mismo oftalmólogo realizó todas las inyecciones oculares, bajo la visión directa de un microscopio quirúrgico (Zeiss Opmi 6c/Osmi 99 Microscope, Carl Zeiss Meditec Inc, California, USA).

Después de los procedimientos quirúrgicos se permitió que los animales se recuperaran de la anestesia y se supervisó el estado de salud de la superficie ocular.

(a) Inyección supracoroidea

La administración SC se realizó en el cuadrante nasal superior del ojo mediante la técnica de la canulación del SCS (Olsen y otros, 2006). La esclerótica se expuso realizando una peritomía conjuntival con un corte radial paralelo al músculo recto superior. Se hizo una profunda incisión intraescleral de unos 9 mm más allá del limbo, cerca del meridiano del globo de las 2 en punto. Se utilizó una espátula roma para diseccionar la esclerótica y entrar en la SCS haciendo un pequeño bolsillo como depósito (Figura 7). La administración directa de la suspensión DEX/LAP se realizó mediante una inyección con una cánula de irrigación de calibre 25 (con un ángulo de 35º, 7,0 mm desde la curva hasta la punta, 19,0 mm de longitud total excluyendo el centro) unida a una jeringa de 1 mL, mientras que el bolsillo escleral se ocluyó con una microesponja quirúrgica y se mantuvo durante 1 minuto para evitar fugas en el lugar de la inyección. Finalmente, la conjuntiva fue restaurada por una sutura 8-0.

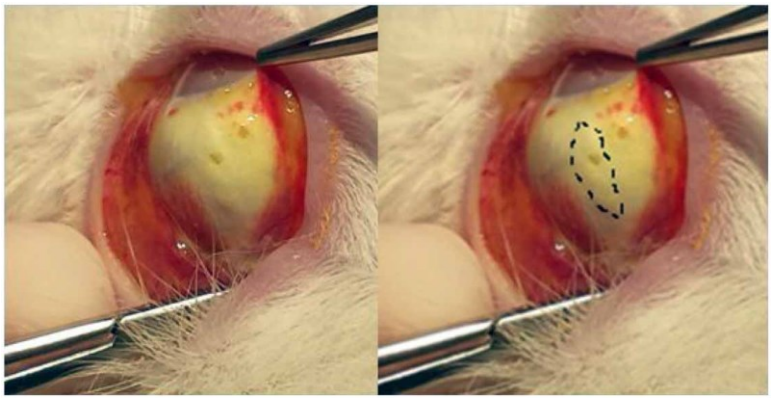

Figura 7. Colocación de la formulación DEX/LAP en el espacio subcoroideo.

(b) Inyección intravítrea

La inyección intravítrea se realizó con una aguja del calibre 25 en el cuadrante temporal superior, unos 3-5 mm posteriores al limbo, hacia el centro de la cavidad vítrea. Previamente, se realizó una paracentesis en la cámara anterior con una aguja hueca del calibre 30 con la eliminación del humor acuoso, para evitar una elevación de la presión intraocular. Después de la inyección, la ausencia de reflujo se verificó en todos los casos mediante la compresión suave del punto de inyección con un bastoncillo de algodón durante 30 segundos.

4.2.2. Análisis de seguridad de los ojos administrados con la suspensión DEX/LAP

Tras la administración ocular de la suspensión DEX/LAP en ambos grupos (SC y IV), los ojos fueron monitorizados mediante tonometría ocular, examen con lámpara de hendidura y oftalmoscopia indirecta, al día 1 y 1, 4, 12 y 24 semanas antes del sacrificio.

4.3. Estudio farmacocinético

Para la toma de muestras de tejidos oculares y posteriores estudios de farmacocinética ocular, se sacrificaron tres animales al día 1 y a las semanas 1, 4, 12 y 24 mediante una inyección intravenosa rápida de pentobarbital sódico (30 mg/kg) a través de la vena de la oreja. Inmediatamente después de la eutanasia, se enuclearon los ojos y se congelaron los globos a (-40ºC) para la posterior disección adecuada del cristalino, el vítreo, la unidad coroide-retina y la esclerótica. Las concentraciones de DEX en los tejidos oculares se determinaron utilizando un método sencillo y de fácil acceso mediante la cromatografía líquida acoplada a espectrometría de masas de alta resolución (HRLC-MS), de acuerdo con la metodología descrita por nuestro grupo (Prieto et al., 2017).

4.3.1. Método analítico

La determinación de DEX se realizó por el método HRLC-MS en un sistema Waters 2695 equipado con una columna Phenomenex Kinetex C18 (75 mm × 4,6 mm × 2,6 µm) acoplada a un detector PDA Waters 2995. La fase móvil era acetonitrilo/agua (35:65 v/v) bombeada a un flujo de 0,2 mL/min a 35ºC. Se utilizó la detección a 250 nm. La cantidad de DEX fue calculada por una curva de calibración de siete puntos contra 6-α-metilprednisolona como estándar interno. Se mezclaron alícuotas del medio de extracción (200 µL) con acetonitrilo (2 mL) y 100 µL de una solución estándar (20 ppm en acetonitrilo). A continuación, la solución se sometió a un vórtex durante 1 min y a una sonicación durante 5 min para asegurar la mezcla completa, y finalmente se centrifugó a 3000 rpm durante 5 min. El sobrenadante fue recogido y evaporado al vacío, y luego disuelto en 200 µL de acetonitrilo, filtrado a través de un filtro de jeringa de PTFE 0.22 µm y analizado.

4.3.2. Análisis farmacocinético

Se determinaron las concentraciones de DEX en los diferentes tejidos de los ojos inyectados y de control para realizar un análisis de PK. Los datos de PK se analizaron para determinar el mejor ajuste y, en consecuencia, se modelaron según modelos no compartimentados utilizando el "PK Solver Add-in" de Microsoft Excel (Albuquerque, NM, EE. UU.), en el que se utilizan ecuaciones que describen la concentración en función del tiempo. Se obtuvieron los siguientes parámetros PK: concentración máxima (Cmax), tiempo hasta la concentración máxima (Tmax), vida media de eliminación (T½), la constante de la

tasa de eliminación (Ke) que se deriva de la vida media de eliminación de la droga (Ke= 0,693/T1/2), eliminación de la droga (CL), y el área bajo la curva de concentración-tiempo (AUC0-∞).

Para describir el curso del tiempo-concentración de la DEX después de la administración se utilizó la siguiente ecuación, donde C es la concentración en el tejido, C0 es la concentración en el tiempo t0. El área bajo la curva de concentración-tiempo (AUC0-∞) fue estimada por el método lineal-trapezoidal a partir de las concentraciones tisulares experimentales, en el que el área desde el último punto de concentración (Tlast= 24 semanas) hasta el infinito (∞) se calculó como Clast/Ke.

4.4. Análisis estadístico

Los análisis estadísticos fueron realizados por SPSS versión 21.0 (SPSS Inc., Chicago, IL). Los datos de las concentraciones de DEX se expresaron como media ± desviación estándar. La prueba de Kolmogorov-Smirnov se utilizó para determinar la bondad del ajuste a la distribución normal de las variables continuas. La prueba t de Student se utilizó para comparar las concentraciones de tejido y los parámetros de farmacocinética entre los dos grupos. Otros resultados fueron medidas descriptivas y se utilizó la prueba de Chi cuadrado de Pearson para comparar los datos categóricos. La significación estadística fue aceptada a un nivel de $p< 0,05$.

5. Metodología relativa al segundo artículo

5.1. Formulación BRI/LAP

5.1.1. Productos químicos y reactivos

La brimonidina y la 2-bromoquinoxalina se obtuvieron de Sigma-Aldrich (Madrid, España). Laponita®-RD (LAP) (densidad superficial 370 m^2/g, densidad aparente 1000 kg/m^3, composición química: SiO_2 59,5%, MgO 27,5%, Li_2O 0,8%, Na_2O 2,8%) se ha obtenido de BYK Additives (Widnes, Cheshire, Reino Unido). La solución salina equilibrada al 0,9% (9 mg/mL NaCl) (BSS) se obtuvo de Fresenius Kabi (Barcelona, España). El etanol de grado HPLC, el acetonitrilo, el metanol, el formiato de amonio, el ácido fórmico, el amoníaco y el ácido fosfórico (85% p/p) se obtuvieron de Scharlab (Barcelona, España). La placa de elución de 96 pozos Oasis MCX Prime se obtuvo de Waters Chromatography (Barcelona, España).

5.1.2. Formulación de Brimonidina-Laponita

La brimonidina se cargó en la Laponita siguiendo la metodología descrita para la dexametasona (Fraile et al., 2016). Así pues, la Brimonidina/Laponita (BRI/LAP) se preparó añadiendo LAP (100 mg) a una solución de Brimonidina en etanol (10 mg/10 mL), agitándola a temperatura ambiente y evaporando el disolvente en vacío para obtener una buena dispersión de la Brimonidina en la superficie. El polvo de BRI/LAP se almacenó a -30ºC en viales de un solo uso bien tapados y esterilizados con rayos gamma.

La carga de droga en la LAP se determinó por el método del espectrómetro de masas de cromatografía líquida de ultra alta presión (UHPLC-MS) (ver abajo). La muestra en polvo (5 mg) se extrajo en 5 mL de acetonitrilo/etanol (1/1 v/v). Después de 1 h de agitación, la

muestra se centrifugó a 3000 rpm durante 10 min a temperatura ambiente y se analizó el sobrenadante, obteniéndose una carga total de 8,98 mg por 100 mg de sólido (98,8% de la cantidad inicial). Inmediatamente antes de la inyección, el polvo de BRI/LAP se suspendió en BSS (10 mg/mL) y se sometió a un suave vórtice durante 10 minutos para producir una dispersión coloidal amarilla.

5.2. Procesamiento de muestras para la determinación farmacocinética

El ojo de rata fue cortado con tijeras de disección, se añadió 1 mL de solución de ácido fórmico al 5% en acetonitrilo y la mezcla fue sonicada a 45W de potencia durante 10 min con un procesador de ultrasonidos Hierchler UP50H. A la mezcla se le añadió 1 mL de 200 mM de formiato de amonio en ácido fosfórico al 4%, y 100mL de 50 ppm de estándar interno (IS) de 2-bromoquinoxalina en ácido fórmico al 0,1% en acetonitrilo, y la mezcla fue sonicada durante 10 minutos adicionales. Luego la muestra se centrifugó a 3000 rpm durante 10 min. El sobrenadante fue recogido y limpiado por extracción en fase sólida (SPE) en una placa de elución Oasis MCX. Así, el sobrenadante se pasó a través del adsorbente bajo vacío, y la muestra adsorbida se enjuagó con 600 mL de metanol. Los Bri e IS adsorbidos fueron eluídos de la placa con 500 mL de una solución de amoníaco al 5% en metanol. El extracto recogido se evaporó al vacío y se disolvió en 200 mL de ácido fórmico al 0,1% en acetonitrilo. La solución fue analizada por UHPLC-MS. La recuperación del analito se determinó en muestras punzantes de ojo de rata en tres niveles de concentración (bajo, medio y alto). Se encontró que estaba entre el 92% (nivel de concentración más bajo) y el 98% (nivel de concentración más alto).

5.3. Método analítico

Las muestras fueron analizadas usando un instrumento UPLC de Aguas de Actitud acoplado a un espectrómetro de masas QDa de Aguas de Actitud. La separación cromatográfica se logró utilizando una columna de cortezas de agua T3 (1,6 mm, 2,1 x 75 mm) a 30ºC. La fase móvil comprendía una mezcla de acetonitrilo (0,1% de ácido fórmico) y agua (0,1% de ácido fórmico). Las muestras (10 mL) se eluyeron a un flujo de 0,5 mL/min.

El instrumento de MS funcionó en modo positivo de ionización por electrospray (ESI). Se utilizó el modo de exploración completa (150-500 Da) para identificar el analito (m/z = 293 (100%) y 295 para la Brimonidina) y el IS (m/z = 210 (100%) y 212 para la 2-bromoquinoxalina). La cuantificación se llevó a cabo en modo de monitoreo de iones únicos (SIM) (m/z = 293 para la brimonidina y 212 para la bromoquinoxalina). El método se validó de acuerdo con las directrices del International Council for Harmonisation of Technical Requirements for Pharmaceuticals for Human Use (ICH).

5.4. Inducción de hipertensión ocular (HTO) y procedimiento de inyección de drogas

Los 91 animales se dividieron en una cohorte control [no-BRI] y una cohorte con Laponita-Brimonidina [BRI-LAP]. La cohorte [no-BRI] estaba compuesta por 31 ratas. En esta cohorte, la HTO fue inducida en el ojo derecho y el ojo izquierdo se mantuvo sin intervención y sirvió como ojo de control. La cohorte [BRI-LAP] estaba compuesta por 60 ratas. En esta cohorte, la HTO fue inducida en ambos ojos, pero el ojo derecho recibió una inyección intravítrea con la formulación de Brimonidina-Laponita (FI BRI/LAP). El ojo

derecho sirvió como ojo hipertenso tratado y el ojo izquierdo como ojo hipertenso de control (Figura 8).

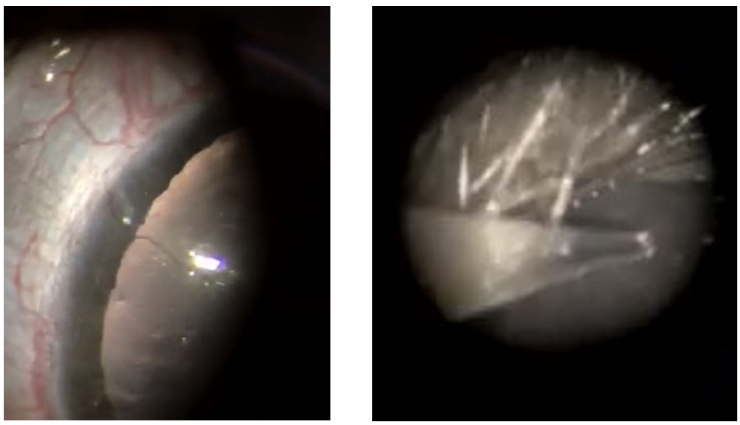

Figura 8. Imágenes bajo microscopio quirúrgico de un ojo de la cohorte [BRI-LAP]. En la imagen de la izquierda se observa la vena epiescleral esclerosada. En la imagen de la derecha se aprecia la formulación BRI/LAP.

La hipertensión ocular se generó con el modelo descrito por Morrison y otros por medio de la esclerosis de las venas epiesclerales (Morrison et al., 1997) con una solución hipertónica de 1,8M bajo gotas oculares tópicas (Anestésico doble Colircusi®, Alcon Cusí® SA, Barcelona, España) y anestesia general por inyección intraperitoneal (IP) (60 mg/Kg de Ketamina + 0,25mg/Kg de Dexmedetomidina). En ambas cohortes se reinyectaba a los animales cada dos semanas si las medidas de PIO eran inferiores a 20 mmHg para mantener la HTO. En el tiempo basal la cohorte [BRI-LAP] recibió 3 mL de la formulación BRI/LAP (10 mg BRI/LAP/mL, cantidad de Bri inyectada 2,69 mg). Esta concentración se determinó de acuerdo con las dosis usadas por otros autores en ratas (K. E. Kim et al., 2015), ratones (Lambert et al., 2015) y conejos (Chiang, Venugopal, et al., 2016), con su correspondiente corrección de escala. Los ojos derechos fueron inyectados intravítreos utilizando una jeringa Hamilton® medida en mL y una micropipeta de vidrio, lo que permitió la visualización de la formulación amarillenta que se estaba introduciendo. Después de la intervención, se dejó que los animales se recuperaran bajo control de temperatura con almohadillas calientes, por medio de una atmósfera de oxígeno enriquecido al 2,5% y un ungüento antibiótico lubricante en los ojos.

5.5. Examen clínico, funcional y estructural oftalmológico *in vivo*

Cada semana se evaluaron los signos clínicos oftalmológicos como el enrojecimiento, las cicatrices, la infección o la inflamación intraocular, así como las mediciones de la presión intraocular (PIO) registradas con el tonómetro de rebote Tonolab®. El valor de la PIO fue el promedio de tres mediciones consecutivas, que resultaron del promedio de 6 rebotes. Para ello, se sedó a las ratas durante menos de tres minutos con una mezcla de gas sevoflurano al 3% y oxígeno al 1,5% para evitar el posible efecto de la anestesia de gas, como se recomendó (Ding et al., 2011).

La funcionalidad de las estructuras neurorretinales se estudiaron con electrorretinografía (ERG) (Roland consult® RETIanimal ERG, Alemania) mediante los protocolos Flash escotópico ERG y Respuesta negativa fotópica (RNF) en el momento basal, a las 8, 12 y 24 semanas. Para probar el Flash escotópico ERG, los animales fueron previamente adaptados a la oscuridad durante 12 horas en una habitación oscura, anestesiados con inyección intraperitoneal y anestesia tópica y completamente dilatados con gotas oculares midriáticas (Tropicamida 10mg/ml, Fenilefrina 100mg/ml, Alcon Cusí® SA, Barcelona, España) y córnea lubricada (Hipromelosa 2%). Los electrodos de la córnea servían como electrodos activos, los electrodos de referencia se colocaban subcutáneamente a ambos lados y el electrodo de tierra cerca de su cola. La impedancia de los electrodos se aceptaba si había una diferencia <2kΩ entre los electrodos. Ambos ojos fueron probados simultáneamente por una esfera Ganzfeld Q450 SC con LEDs blancos que parpadean en busca de estímulos y se realizaron estos siete pasos con intensidad creciente de luminancia e intervalos (paso 1: 0,0003 cds/m^2, 0. 2Hz/s; paso 2: 0,003 cds/m^2, 0,125Hz/s; paso 3: 0,03 cds/m^2, 8,929Hz/s; paso 4: 0,03 cds/m^2, 0,111Hz/s; paso 5:0,3 cds/m^2, 0,077Hz/s; paso 6: 3,0 cds/m^2, 0,067Hz/s; y paso 7: 3,0 cds/m^2, 29,412Hz/s) (Umeya et al 2019). Luego se realizó el protocolo RNF después de la adaptación de la luz al fondo azul (470 nm, 25 cds/m^2) y se utilizó como estímulo el flash de LED rojo (625nm, 0,30 cds/m^2). Se estudiaron la latencia (en milisegundos) y la amplitud (en microvoltios) en las ondas a, b y RNF.

Las estructuras neurorretinianas se estudiaron con un dispositivo de tomografía de coherencia óptica de alta resolución (HR-OCT Spectralis, Heidelberg® Engineering, Alemania) al inicio, al tercer día y a las 2, 4, 6, 8, 12, 24 semanas después de la inyección de BRI/LAP. Se evaluaron protocolos como el polo posterior de la retina, la capa de fibra nerviosa de la retina (CFNR) y la capa de células ganglionares (CCG) con segmentación automática. Estos protocolos analizaron un área de 1, 2 y 3 mm alrededor del centro del disco óptico mediante 61 b-scans y los exámenes de seguimiento posteriores se adquirieron en este mismo lugar utilizando el software de seguimiento ocular y la aplicación de seguimiento. Para la adquisición de los escaneos, se anestesió a las ratas con inyección intraperitoneal y se adaptó una lente de contacto plano en su córnea para obtener imágenes de alta calidad.

Los exámenes sesgados se descartaban o se corregían manualmente por un técnico capacitado enmascarado si el algoritmo se había equivocado de forma obvia.

5.6. Inmunohistoquímica

Bajo anestesia general, los animales fueron sacrificados con una inyección intracardíaca de tiopenthal de sodio (25mg/ml). Los ojos se enuclearon inmediatamente, se fijaron en formalina tamponada neutra al 10% y se incluyeron en parafina. Se analizaron un total de 44 ojos pertenecientes a 22 ratas de la cohorte [BRI-LAP] (22 ojos derechos hipertensos inyectados con BRI/LAP y 22 ojos izquierdos hipertensos control). Los bloques de parafina fueron desbastados hasta llegar a la cabeza del nervio óptico. Posteriormente se realizaron secciones de 5 µm que fueron desparafinadas, rehidratadas y lavadas en H_2O_2 al 10% durante 5 minutos (enfriamiento) antes de proceder a la incubación con los siguientes anticuerpos primarios a 4ºC durante la noche: **Brn3a** de ratón (Santa Cruz Biotechnology, Inc, Heidelberg, Alemania) a una dilución de 1:50, y **proteína ácida fibrilar anti-glial** (GFAP) de conejo (DAKO, Bath, Reino Unido) a una dilución de 1:1000. Después de eso,

las secciones se incubaron durante 90 minutos a temperatura ambiente con anticuerpos secundarios específicos: anti-ratón biotinilado de caballo a 1:50 de dilución y anti-conejo biotinilado de cabra a 1:100 de dilución (Vector Laboratories, Burlingame, CA, USA). Luego se realizó la incubación con ABC-HRP (Thermo Fisher Scientific, Waltham Massachusetts, USA) en dilución 1:50 durante 90 minutos a temperatura ambiente. Las secciones se lavaron en solución salina tamponada con fosfato antes y después de cada incubación. Finalmente, las secciones se tiñeron con diaminobenzidina (DAB) durante 3 minutos y se tiñeron con hematoxilina de Harrys (Sigma-Aldrich Corp., St. Louis, MO, USA) durante 20 minutos a temperatura ambiente. Los controles inmunohistoquímicos de procedimiento se hicieron por omisión del anticuerpo primario en una sección secuencial de tejido. También se realizaron secciones oculares teñidas con hematoxilina/eosina para analizar la morfología general de la retina. Los portaobjetos se visualizaron en un microscopio óptico convencional (Figura 9).

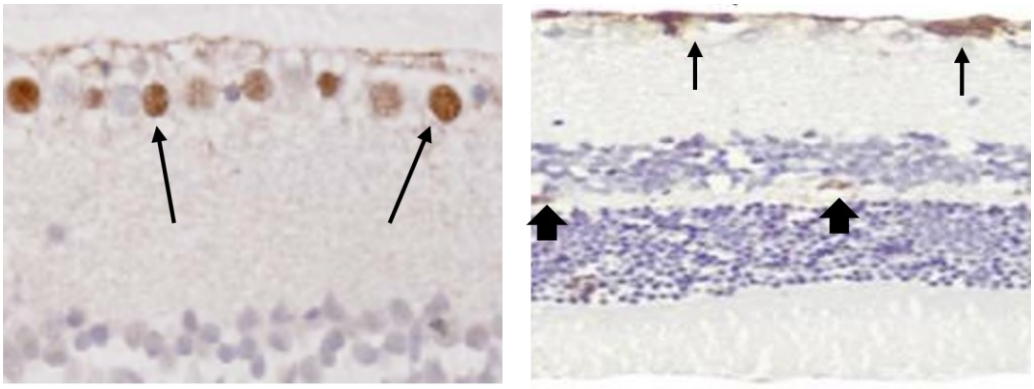

Figura 9. Imágenes microscópicas (40X) de cortes histológicos de retina normal teñidos con Brn3a (izquierda) y proteína glial fibrilar (GFAP) (derecha). El anticuerpo Brn3a tiñe las células ganglionares (flecha), mientras que GFAP muestra positividad débil lineal a nivel de la capa de fibras nerviosas (flecha delgada) y en células gliales aisladas de la capa nuclear interna (flecha gruesa).

5.7. Recuento de células ganglionares de la retina

Las células ganglionares de la retina fueron contadas sobre secciones radiales de la retina, a lo largo de 2 mm de una región lineal de la capa de células ganglionares, en cuatro áreas diferentes, dos a cada lado de la cabeza del nervio óptico. Las imágenes fueron analizadas por un operador ciego a los grupos de tratamiento.

5.8. Análisis estadístico

Todos los datos se registraron en una base de datos de Excel, y el análisis estadístico se realizó utilizando el software SPSS versión 20.0 (SPSS Inc., Chicago, IL). Se utilizó la prueba de Kolmogorov-Smirnov para evaluar la distribución de la muestra. Dada la distribución no paramétrica de la mayoría de los datos, las diferencias entre ambas cohortes se evaluaron utilizando la prueba de la U de Mann-Whitney y los cambios registrados en cada ojo durante el período de estudio de 24 semanas se compararon utilizando una prueba

de Wilcoxon emparejada. Todos los valores se expresaron como media ± desviaciones estándar. Se consideró que valores de p <0,05 eran estadísticamente significativos. Para evitar una alta tasa de falsos positivos, se calculó la corrección de Bonferroni para múltiples comparaciones. El nivel de significación de cada variable se estableció en base a los cálculos de Bonferroni. El análisis estadístico del número de células ganglionares se realizó en R (v. 3.6.0) utilizando una prueba t emparejada. Los resultados se muestran como error estándar de la media (SEM). Se consideró que los valores de p <0,05 eran estadísticamente significativos.

6. Metodología relativa al tercer artículo

6.1. Recopilación de datos

Las imágenes de tomografía de coherencia óptica (OCT) de los datos relativos a los niveles vítreos y de droga se obtuvieron a partir de los experimentos realizados en el estudio de intervención referido previamente (apartado 5.5). En ese estudio, el glaucoma crónico se indujo bilateralmente mediante inyecciones quincenales según el modelo bien establecido de Morrison (Morrison et al., 2015) y se realizó una única inyección de la formulación intravítrea brimonidina/Laponita (FI BRI/LAP) en el momento basal en los ojos derechos de ratas Long Evans, mientras que los ojos izquierdos sirvieron como hipertensos sin tratamiento. En este estudio se analizaron los exámenes de OCT en la línea de base y a las 1, 2, 4, 6, 8, 12, 24 semanas después de la inyección intravítrea de las ratas intervenidas para cuantificar la evolución de la FI BRI/LAP a lo largo de 6 meses. También se examinaron las ratas no intervenidas para compararse como controles.

6.2. Tomografía de coherencia óptica

Las imágenes se obtuvieron usando el dispositivo de OCT de alta resolución con una lente de contacto plana adaptada en la córnea de la rata para obtener imágenes de mayor calidad. La versión para roedores de este sistema adquiere imágenes de corte transversal mediante 61 b-scans de alrededor de 3 mm de longitud centrados en el nervio óptico. Explora con una resolución de 3 micras por píxel generado; y se analizaron un total de 1536 x 496 píxeles. Se utilizó el protocolo del polo posterior de la retina con segmentación automática, software de rastreo ocular y aplicación de seguimiento para asegurar que se volvieran a escanear los mismos puntos durante el estudio. El modo de "mejorar la imagen de profundidad" se desactivó en todos los casos.

6.3. Análisis de la formulación intravítrea mediante OCT

Los agregados de la FI BRI/LAP en el vítreo se estudiaron partir de los escaneos vítreos de la OCT. Estos agregados se definieron como puntos hiperreflectantes de mayor tamaño, irregulares o de mayor señal, dispersos en el humor vítreo o en la interfaz vítreo-retinal, que difieren del ruido de fondo (Figura 10).

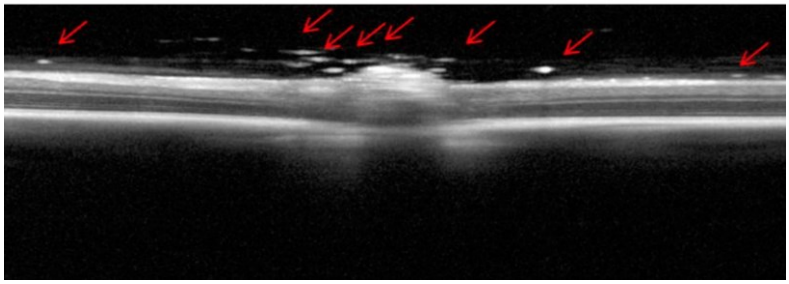

Figura 10. Imagen obtenida mediante tomografía de coherencia óptica en la que se observan los agregados hiperreflectantes (flechas rojas) de la formulación intravítrea de brimonidina-Laponita (BRI/LAP) detectados en la interfase vítreo-retiniana.

El contraste de la imagen no se ajustó en ningún momento en el sistema de la OCT. Las imágenes sin procesar fueron exportadas como videos AVI. Estos videos se analizaron por un programa personalizado implementado en Matlab (versión R218a, Mathworks Inc., Natick, MA). Con este código, podemos reconocer la membrana limitante interna (MLI), y la capa interna y externa del epitelio pigmentario de la retina (EPR) mediante conversión en escala de grises. De esta manera, el espacio vítreo y el espacio EPR se pueden delimitar en cada b-scan. El vítreo (VIT) se definió como el espacio entre la extensión superior del b-scan y el MLI, mientras que el EPR se definió como el espacio entre la capa interna y externa del EPR (Sreekantam et al., 2017) (Keane et al., 2014).

El valor de intensidad media de estos dos espacios se calculó como el promedio de la intensidad de todos los píxeles dentro de cada región, obteniendo la intensidad relativa de VIT/EPR en cada b-scan. Así, la intensidad relativa VIT/EPR de cada ojo es el promedio de los 61 b-scan. Además, como los agregados de BRI/LAP tienden a depositarse en la MLI-CFNR (capa de fibra nerviosa de la retina), se determinaron los límites internos y externos de la MLI-CFNR para obtener la evolución del espesor de la MLI-CFNR a lo largo de las 24 semanas de seguimiento.

El tamaño de los agregados en cada b-scan también se determinó calculando el número de píxeles que cada agregado contiene en la imagen. En los b-scans analizados, hay un total de 761856 píxeles y el área de la imagen es de 2.906 mm^2, por lo tanto, la proporción es de 3.815 μm^2/píxel. Para hacerlo correctamente, el ruido de fondo de la imagen fue eliminado primero usando un filtro de supresión de ruido que permitió distinguir entre los agregados y el ruido de fondo. Este filtro se implementó en nuestro código personalizado siguiendo la definición de los agregados como puntos más grandes cuya intensidad es mayor que la del fondo. Una vez calculado el tamaño de cada agregado, pudimos calcular el área promedio y el área total de FI BRI/LAP en cada ojo en diferentes momentos del seguimiento.

Los datos de las imágenes se estudiaron por un lector enmascarado para obtener información clínica y de niveles de drogas. Dos investigadores diferentes realizaron la segmentación de la OCT de forma enmascarada para comprobar la reproducibilidad.

6.4. Análisis estadístico

Todos los datos se registraron en una base de datos de Excel, y el análisis estadístico se realizó utilizando el software SPSS versión 20.0 (SPSS Inc., Chicago, IL). Para evaluar la distribución de la muestra se utilizó la prueba de Kolmogorov-Smirnov, pero dada la distribución no paramétrica de la mayoría de los datos, se utilizó la prueba de la U de Mann-Whitney para evaluar las diferencias entre ambas cohortes y una prueba de Wilcoxon emparejada para comparar los cambios registrados en cada ojo durante el período de estudio. Se consideró que los valores de $p < 0,05$ eran estadísticamente significativos.

7. Metodología relativa al cuarto artículo

Se llevó a cabo una búsqueda sistemática utilizando las guías Preferred Reporting Items for Systematic Reviews and Meta-Analyses (PRISMA) para revisiones estructuradas. La búsqueda bibliográfica se realizó en plataformas como Web of Science®, la base de datos Wiley, Scopus®, Google Scholar®, Pubmed, PubChem, Mendeley® y las bases de datos science.gov a fecha de agosto de 2023. Para la búsqueda bibliográfica, se emplearon diferentes combinaciones de palabras clave, como "minerales arcillosos", "Laponita", "aplicaciones biomédicas", "revisión" y "oftalmología". Se utilizaron los operadores booleanos para combinar los términos seleccionados ["Laponita" y "revisión"], ["Laponita" y "aplicaciones biomédicas"], ["Laponita" y "aplicaciones biomédicas" y "revisión"], y ["Laponita" y "oftalmología"] centrados más específicamente en la aplicación oftálmica de la Laponita.

Los estudios identificados, de más general a más específico, fueron los que contenían lo siguiente: el término general ["clay minerals"], que encontró 48521 coincidencias en Web of Science, 14400 en Google Scholar y cerca de 3000 tanto en Pubmed como en PubChem (desde 1915); el término específico ["Laponite"], que encontró más de 2700 coincidencias en Web of Science más de 2200 en Google Scholar y unos 700 resultados en Pubmed (desde 1969); y ["Laponite NM"], que arrojó un total de 187 resultados en Pubmed y 179 referencias consolidadas en PubChem (desde 2007).

Para la fase de cribado, se revisaron todos los títulos obtenidos de todas las búsquedas en bases de datos utilizando los operadores booleanos y las palabras clave ["Laponita" y "revisión"], ["Laponita" y "aplicaciones biomédicas"], ["Laponita" y "aplicaciones biomédicas" y "revisión"] y ["Laponita" y "oftalmología"]. Para las referencias que cumplían los criterios de exclusión y de inclusión, respectivamente, se leyó el resumen como criterio de elegibilidad.

Los criterios de exclusión fueron: (a) comunicaciones, resúmenes o estudios con escasa evidencia científica (es decir, no incluidos en el Journal Citation Reports [JCR®]) sobre arcillas minerales y que no mencionaran la Laponita, (b) referencias centradas únicamente en propiedades químicas, o aplicaciones industriales, (c) referencias en idiomas distintos del inglés.

Los criterios de inclusión fueron estudios o revisiones centradas en: (a) la arcilla Laponita en términos generales, (b) minerales arcillosos, incluida la Laponita, para aplicaciones biomédicas, (c) el uso de la Laponita en el ojo.

Si el artículo se consideró de especial interés para su aplicación y/o traslación oftalmológica, o por la perspectiva ofrecida, se leyó en detalle y se incorporó a esta revisión.

Para la etapa de inclusión, los estudios seleccionados se clasificaron según se realizaran en el ojo o no, pero cumpliendo los siguientes criterios: que los fármacos también se utilizaran en el ojo, que el tejido evaluado *in vitro* o *in vivo* estuviera presente en el ojo, que las patologías tratadas también se produjeran en el mismo y/o que los nuevos tratamientos fueran potencialmente aplicables.

RESULTADOS

1. Primer artículo

Prieto E, **Cardiel MJ,** Vispe E, Idoipe M, Garcia-Martin E, Fraile JM, Polo V, Mayoral JA, Pablo LE, Rodrigo MJ. **Dexamethasone delivery to the ocular posterior segment by sustained-release Laponite formulation.** Biomed Mater. 2020 Nov 21;15(6):065021. doi: 10.1088/1748-605X/aba445 PMID: 32647098.

IOP Publishing Biomed. Mater. 15 (2020) 065021 https://doi.org/10.1088/1748-605X/aba445

Biomedical Materials

PAPER

Dexamethasone delivery to the ocular posterior segment by sustained-release Laponite formulation

Esther Prieto[1,2], Maria Jose Cardiel[2,3], Eugenio Vispe[4], Miriam Idoipe[1,2], Elena Garcia-Martin[1,2,5], Jose Maria Fraile[6], Vicente Polo[1,2], Jose Antonio Mayoral[6], Luis Emilio Pablo[1,2] and Maria Jesus Rodrigo[1,2,5]

[1] Ophthalmology Department, Miguel Servet University Hospital, Paseo Isabel la Católica 1-3, E-50009, Zaragoza, Spain
[2] Aragon Institute for Health Research (IIS Aragon), GIMSO research group, University of Zaragoza (Spain), Avda. San Juan Bosco 13, Zaragoza E-50009, Spain
[3] Department of Pathology, Lozano Blesa University Hospital, Zaragoza, Spain
[4] Chromatography and Spectroscopy Laboratory, Institute for Chemical Synthesis and Homogeneous Catalysis (ISQCH), Faculty of Sciences, University of Zaragoza-CSIC, Pedro Cerbuna 12, E-50009, Zaragoza, Spain
[5] RETICS-Oftared: Thematic Networks for Co-operative Research in Health for Ocular Diseases, 28040, Madrid, Spain
[6] Institute for Chemical Synthesis and Homogeneous Catalysis (ISQCH), Faculty of Sciences, University of Zaragoza-CSIC, C/Pedro Cerbuna 12, E-50009, Zaragoza, Spain

E-mail: mariajesusrodrigo@hotmail.es

Keywords: intraocular drug delivery, Laponite, synthetic clays, dexamethasone, intravitreal injection, suprachoroidal administration, ocular pharmacokinetics

OPEN ACCESS

RECEIVED
19 March 2020

REVISED
15 June 2020

ACCEPTED FOR PUBLICATION
9 July 2020

PUBLISHED
20 November 2020

Abstract

This paper presents a novel nanoformulation for sustained-release delivery of dexamethasone (DEX) to the ocular posterior segment using a Laponite (LAP) carrier—DEX/LAP 1:10 w w^{-1} formulation; 10 mg ml^{-1}. *In vivo* ocular feasibility and pharmacokinetics after intravitreal (IV) and suprachoroidal (SC) administration in rabbit eyes are compared against IV administration of a DEX solution (1 mg ml^{-1}). Thirty rabbit eyes were injected with the DEX/LAP formulation (15 suprachoroid/15 intravitreous). Ophthalmological signs were monitored at day 1 and at weeks 1–4–12–24 post-administration. Three eyes per sample time point were used to quantify DEX concentration using high-performance liquid chromatography-mass spectrometry. The ocular tissues' pharmacokinetic parameters (lens, vitreous humour, choroid-retina unit and sclera) were studied. DEX/LAP was well tolerated under both administration methods. Peak intraocular DEX levels from the DEX/LAP were detected in the vitreous humour after both deliveries soon after administration. The vitreous area under the curve was significantly greater after both DEX/LAP deliveries (IV: 205 968.47; SC: 11 442.22 ng g^{-1} d^{-1}) than after IV administration of the DEX solution (317.17 ng g^{-1} d^{-1}). Intravitreal DEX/LAP delivery extended higher vitreous DEX levels up to week 24 (466.32 $\pm$ 311.15 ng g^{-1}). With SC delivery, DEX levels were detectable in the choroid-retina unit (12.04 $\pm$ 20.85 ng g^{-1}) and sclera (25.46 $\pm$ 44.09 ng g^{-1}) up to week 24. This study demonstrated the intraocular feasibility of both SC and IV administration of the DEX/LAP formulation. The LAP increased the intraocular retention time of DEX when compared with conventional solutions. DEX/LAP could be considered a biocompatible and useful sustained-release formulation for treating posterior-pole eye diseases.

1. Introduction

Glucocorticosteroids (GCs) have been widely used in clinical practice to treat posterior-segment eye diseases such as non-infectious posterior uveitis, diabetic retinopathy, retinal vein occlusion or age-related macular degeneration with macular oedema [1–5]. However, posterior segment processes are especially difficult to treat because of poor tissue permeability, anatomical and physiological barriers in the eye and low drug bioavailability in the target tissue [6–9]. The routes typically used [10] to administer GCs in ophthalmology are, in many cases, insufficient to deliver and maintain therapeutic drug levels in the posterior segment [11]. High and frequent doses by topical and systemic administration or by periocular and intravitreal (IV) injection are required, causing significant harmful side effects [12, 13] and heightened

risk of severe ocular complications [14, 15]. To overcome these limitations, alternative drug delivery systems and sustained-release formulations are being developed [16, 17].

IV administration of GCs by injection or by implantation of surgical devices have a powerful therapeutic effect on neuroretinal tissues by achieving high local drug concentrations in the vitreous humour near their site of action [3, 18]. This route acts as a reservoir and minimizes the systemic side effects. However, as it is an invasive route it could lead to local complications, such as retinal toxicity or detachment, lens injury, intraocular infections or haemorrhages, and elevated intraocular pressure (IOP) [14, 19, 20]. Periocular routes offer an alternative means of delivery to the posterior segment of the eye due to their ability to bypass the conjunctiva–cornea barrier, thereby enabling direct transscleral delivery [21]. Among the different forms of periocular administration, suprachoroidal (SC) injection is an emerging technique considered to be more effective than the subconjunctival or subtenon routes and to be safer than IV injection [22–25]. The suprachoroidal space (SCS) is a potential space located between the sclera and choroid that can expand to accommodate drug formulations [24, 26–28]. It delivers higher drug concentrations in the area spanning the retina–retinal pigment epithelium–choroidal unit and the posterior pole, and minimizes the presence of the drug in the anterior structures of the eye [23–25, 29–33]. However, drug efficacy varies among formulations due to the high rate of clearance in the SCS and to the differing physico-chemical properties and size or molecular radius of the drug, as well as depending on whether the formulation is viscous or particulate, among other aspects [22, 23, 26, 27, 29, 32, 34, 35]. SC administration represents a promising alternative route for treating posterior-segment eye diseases and has become a focus of drug delivery research [22, 36, 37].

Several GCs such as triamcinolone acetonide (TA), dexamethasone (DEX) and fluocinolone acetonide (FA), with which to treat posterior eye disease are now available [38]. TA is a potent selective GC agonist with low water solubility (21 $\mu g\ ml^{-1}$), which confers a sustained release in aqueous media [3, 23]. TA showed efficacy for diabetic macular oedema, retinal vein occlusion and non-infectious posterior uveitis in human and animal studies after IV or SC administration [25, 28, 39–42]. In contrast, DEX is more potent and has a lower risk of inducing ocular hypertension and cataracts after IV administration than TA [3], but it has a short half-life (3.5 h) [19] and higher water solubility (100 $\mu g\ ml^{-1}$), which reduces its clinical application when used in conventional formulations. Therefore, sustained-delivery systems (implants) are necessary to maintain long-lasting therapeutic effects and avoid re-injections. IV implants [43] require placement in the operating room, injection using larger gauge needles or even surgical extraction devices in the case of non-biodegradables (such as Retisert® and Iluvien® made of FA), and therefore conferring greater risk. Biodegradable IV DEX implants (Ozurdex®) are widely used in clinical care and their efficacy has been proved. However, IOP increases and cataracts are relatively frequent due to the passing of DEX to the anterior eye structures [44]. To reduce those side effects, SC administration may be more appropriate.

Nowadays, to create anti-inflammatory [45–49] treatments a wide variety of polymeric nanocarriers in the form of dendrimers, micelles, nanocapsules and vesicles, liposomes or nanoparticles and nanogels are being investigated [50]. These formulations are made of smart materials, which control drug release in response to exogenous or endogenous stimulations such as pH fluctuation, temperature or isquemic conditions. Gold nanoparticles loaded with DEX released the drug and induced apoptosis on a DEX sensitive lymphoma cell line [48]. A DEX-loaded lipid nanoemulsion with specific binding to endothelial cells via the P-selectin target reduced vascular inflammation *in vitro* and *in vivo*, after internalizing into the endothelial cell, reducing proinflammatory gene expression, and preventing monocyte adhesion and migration [47]. A combination of DEX and cholesteryl butyrate in solid-lipid nanoparticles relieved colon inflammation at doses lower than the required for each single drug [46]. And microplates made of poly(lactic-co-glycolic acid sustained release DEX for up to 60 d and decreased expression of the inflammatory cytokines IL-1β, IL-6 and TNF-α [49].

There is currently demand for biocompatible and biodegradable sustained-release formulations containing GCs for ocular administration by minimally invasive (IV or SC) injection in clinical practice [28, 51, 52]. DEX loaded oligo-cationic liposomes, by IV administration slowly released DEX for more than 20 d. And a polysaccharide-drug conjugate composed of hydrazine-DEX showed a very slow diffusivity and prolonged drug release in vitreous humour [49]. To the authors' knowledge, only one study featuring implantation of DEX in the SCS has been conducted. This paper demonstrated sustained DEX delivery from a polyurethane implant for 42 d and decreased inflammatory signs in uveitic rats [53].

Synthetic and natural clays have received great attention as drug delivery modulators in biomedical applications due to their ability to control or vectorize the release of drugs and increase bioavailability [54]. Laponite (LAP) is a synthetic colloidal layered silicate (Na0.7[(Si8Mg5.5Li0.3)O20(OH)4]0.7) used in various drug delivery applications in nanomedicine to treat skin, bones and cancer [55, 56]. Administration of LAP in rabbit eyes has also been shown to be safe and biocompatible, with long-lasting intraocular residence after SC and IV injection [57].

LAP has a high total surface area and offers cation exchange capacity, interchanging sodium counter ions in aqueous saline solution [58, 59], becoming a transparent thixotropic gel that allows administration by injection and providing good dispersibility and a stable structure [60]. In previous *in vitro* studies [61], we first demonstrated that DEX, despite being a neutral molecule, is retained on LAP due to weak non-ionic interactions (mainly hydrogen bonds). These findings were later corroborated by other authors [62]. DEX was also shown to be encapsulated in and uniformly distributed on the surface of LAP nanoplatelets, to possess pH-dependent properties and to have good *in vitro* cytocompatibility with MG63 cells [63]. The DEX/LAP formulation showed an initial burst release of DEX (of around 40% of the initial dose loaded on LAP, which is consistent with other drugs [64]) in saline or hyaluronate solutions, with subsequent progressive, sustained drug delivery [61, 62].

In this manuscript we describe the first *in vivo* application of the DEX/LAP formulation for sustained release of DEX. Specifically, it has been used in the ocular posterior segment and its ocular pharmacokinetics has been characterized over 6 months following IV and SC administration in healthy rabbit eyes.

2. Experimental procedures

2.1. DEX/LAP formulation

2.1.1. Chemical and reagents

DEX was obtained from Sigma-Aldrich (Madrid, Spain). Laponite®-RD (LAP) (surface density 370 $m^2\ g^{-1}$, bulk density 1000 kg m^{-3}, chemical composition: SiO2 59.5%, MgO 27.5%, Li2O 0.8%, Na2O 2.8%) was obtained from BYK Additives (Widnes, Cheshire, UK). The balanced 0.9% salt solution (9 mg ml^{-1} NaCl) (BSS) was obtained from Fresenius Kabi (Barcelona, Spain). The HPLC-grade ethanol and acetonitrile were obtained from Scharlab (Barcelona, Spain).

2.1.2. Preparation and characterization of the DEX/LAP formulation

The optimal loading of DEX on LAP was determined by our group in previous work based on the nature of the drug–clay interaction, where DEX was incorporated on the surface of the clay nanoplatelets and the *in vitro* behaviour of the medium in relation to the release of the drug was studied [61]. DEX/LAP was prepared by adding LAP (100 mg) to a solution of DEX in ethanol (10 mg/10 ml), stirring at r.t. and solvent evaporation under vacuum to get a good dispersion of DEX on the surface. The DEX/LAP powder was stored in tightly capped single-use vials that were gamma-ray sterilized.

Immediately before injection, the DEX/LAP powder was suspended in BSS (10 mg ml^{-1}) and gently vortexed for 10 min to yield a transparent colloidal dispersion.

2.2. *In vivo* study design

2.2.1. Ethics statement

All experiments were carried out using female New Zealand albino rabbits (obtained from the Animal Experimentation Service of the University of Zaragoza). Animal handling was in accordance with the Spanish Policy for Animal Protection (RD 1201/05), which meets European Council Directive 86/609/EEC. Animal care and practices complied with the ARVO Statement for the Use of Animals in Experimental Procedures and Other Scientific Purposes. All procedures were performed according to Project Licence PI12/02285 approved by the in-house Ethics Committee for Animal Experiments at the University of Zaragoza (Spain). The animals were singly housed in metabolic standard cages, in a light-controlled room (12 h/12 h dark/light cycle) at 20 ± 2 °C with a relative humidity of 40–70%. Diet and water were available ad libitum and thorough clinical examination was performed daily.

2.2.2. In vivo administration: injection procedure

Thirty animals weighing 2.5–4.0 kg (3.1 ± 0.4 kg) were included in the study and randomly divided into two groups. Fifteen animals received suprachoroidal administration (SC group) and the other 15 animals received an IV injection (IV group) of the DEX/LAP formulation (10 mg ml^{-1}, 1:10 w w^{-1}). Only one eye (right eye) of each animal was treated. The fellow eye (left eye) remained untreated and served as the comparative control. Data from 18 animals injected with DEX IV were also served as comparison [65].

All the injections were performed under general anaesthetic and aseptic conditions. For IV injection, the animals were anaesthetized by intramuscularly injecting ketamine hydrochloride (25 mg kg^{-1}) (Ketolar 50®, Pfizer, Madrid, Spain) and medetomidine (0.5 mg kg^{-1}) (Domtor®, Esteve, Madrid, Spain). As SC administration was a longer procedure, a general inhalation anaesthetic containing 2.5% sevoflurane (Sevorane®, Abbott Laboratories, Madrid, Spain) was administered in oxygen by mask and vital signs were monitored. A topical anaesthetic containing tetracaine chlorhydrate (1 mg ml^{-1}) and oxybuprocaine chlorhydrate (4 mg ml^{-1}) in the form of ophthalmic drops (Colircusí Anestésico Doble®, Alcon Cusí SA, Barcelona, Spain) was administered, and povidone-iodine solution (5%) was applied for ocular surface antisepsis before and after the injection.

The same ophthalmologist performed all the eye injections under the direct view of a surgical microscope (Zeiss Opmi 6 c/Osmi 99 Microscope, Carl Zeiss Meditec Inc. California, USA). Following administration, the animals were allowed to recover

from the anaesthetic, and the health state of the eye surface was monitored.

2.2.3. Determination of injection volumes

Volumes of 100 µl and 50 µl of DEX/LAP suspension were used for IV and SC administration, respectively. The DEX dose used was 0.1 mg in 100 µl for IV injection and 0.05 mg in 50 µl for SC injection. The volumes of formulation determined for IV and SC injection were the highest volumes that could be safely administered by either route without risk of leaking, elevating IOP or inducing choroidal haemorrhage [23, 57, 66].

2.2.4. SC injection

SC administration was carried out in the superior nasal quadrant of the eye by cannulation of the SCS [41]. The sclera was exposed by performing a conjunctival peritomy with a radial cut parallel to the superior rectus muscle. A deep intrascleral incision was made about 9 mm past the limbus, near the 2 o'clock meridian. A blunt spatula was used to dissect the sclera and enter the SCS, making a tiny pocket intended to serve as a reservoir. Direct administration of 50 µl of DEX/LAP suspension was performed by injection using a 25 gauge irrigating cannula (angled 35°, 7.0 mm from bend to tip, 19.0 mm overall length excluding hub) attached to a 1 ml syringe. The port of the pocket was occluded with surgical microsponges and maintained for 1 min to prevent as much leaking at the site of injection as possible, however a minimum leaking occurred and unfortunately the lost volume could not be quantified. Finally, the conjunctiva was repaired with an 8-0 suture.

2.2.5. IV injection

IV injection was performed using a 25 gauge needle in the superior temporal quadrant, about 3–5 mm posterior to the limbus and towards the centre of the vitreous cavity. Paracentesis had been performed beforehand in the anterior chamber using a 30 gauge hollow needle to remove aqueous humour so as to avoid elevating IOP. After the injection, the absence of reflux was verified in all cases by gentle compression of the injection point for 30 s with a cotton swab.

2.2.6. Clinical safety after ocular administration of the DEX/LAP formulation

After ocular administration of the DEX/LAP formulation in both groups (SC and IV), the eyes were monitored using ocular tonometry, slit-lamp examination and indirect ophthalmoscopy at day 1 and at weeks 1, 4, 12 and 24 before euthanasia, as described in our previous report [57].

2.3. Pharmacokinetic (PK) study

To determine eye-tissue drug concentrations and for subsequent ocular PK studies, three animals from each sampling time point (at day 1 and at weeks 1, 4, 12 and 24) were used. The animals were humanely euthanized using a rapid intravenous injection of sodium pentobarbital (30 mg kg^{-1}) through the ear vein. Immediately after euthanasia, the eyes were enucleated and the globes were snap-frozen (−40 °C) for posterior dissection of the lens, vitreous, choroid-retina unit and sclera. Each part was mixed with acetonitrile (2 ml), vortexed for 1 min, sonicated for 5 min to ensure thorough mixing, and finally centrifuged at 3000 rpm for 5 min. The supernatant was collected and evaporated under vacuum.

2.3.1. Analytical method

DEX concentrations in ocular tissue were determined using a simple and easily accessible method—high-performance liquid chromatography–mass spectrometry (HPLC-MS)—in a Waters 2695 system equipped with a Phenomenex Kinetex C18 column (75 mm × 4.6 mm × 2.6 µm) coupled to a Waters ZQ4000MS detector. A 35:65 mixture of acetonitrile and formic/formate buffer (2 mM ammonium formate buffer, adjusted to pH 3.5 with formic acid and doped with sodium formate 0.2 mM) was used as mobile phase. The dried samples obtained as described above were then dissolved in 200 µl of acetonitrile containing 6-α-methylprednisolone (20 ppm, internal standard), filtered through a 0.22 µm PTFE syringe filter and analysed. Analytical method validation was carried out according to ICH guidelines. Linearity was assessed by seven-point calibration curves in triplicate. The curves were constructed over a range between 50 and 100 000 ng g^{-1}. The limit of detection (LOD, 10 ng g^{-1}) and the lower limit of quantification (LLOQ, 45 ng g^{-1}) were determined by the method based on the standard deviation of the slope and response. Full details for this method have been published elsewhere [65].

2.3.2. PK analysis

DEX concentrations were determined in the different tissues of both injected and control eyes to perform PK analysis. PK data were analysed for best fit and were consequently modelled according to a non-compartmental model using Microsoft Excel's PK Solver Add-in (Albuquerque, NM, USA) in which equations describing concentration as a function of time are used. The following PK parameters were obtained: peak concentration (C_{max}), time to peak concentration (T_{max}), elimination half-life ($T_{1/2}$), elimination rate constant (K_e) as derived from the elimination half-life of the drug ($K_e = 0.693/T_{1/2}$), drug clearance (Cl), distribution volume (V_{ss}) and the area under the concentration–time curve ($AUC_{0\ \infty}$).

To describe the concentration–time of DEX after administration, the following equation was used: $C\_tissue = C\_0\text{^}*e\text{^}(-K\_e\ t)$, where C is the tissue concentration and C_0 is the concentration at

time T_0. The area under the concentration–time curve ($AUC_{0-\infty}$) was estimated using the linear–trapezoidal method taking the experimental tissue concentrations over 24 weeks, in which the area from the last concentration point (T_{last} = day 168) to infinity (∞) was calculated as C_{last}/K_e.

Finally, vitreous availability of DEX after LAP/-DEX administration was calculated and indicates the fraction of the administered drug that is absorbed and reaches the vitreous humour ($F = AUC_{0-\infty} * Cl/D$). The relative vitreous availability of DEX after SC injection was also calculated with respect to the IV route ($F_{sc/iv} = AUC_{sc} * D_{iv}/AUC_{iv} * D_{sc}$).

2.4. Statistical analysis

Statistical analyses were performed using SPSS version 21.0 (SPSS Inc. Chicago, IL). Data on DEX concentrations were expressed as mean ± standard deviation. The Shapiro–Wilk test was used to determine goodness of fit to the continuous variables' normal distribution. Student's *t*-test was used to compare PK parameters between the groups. Other results were assessed using descriptive measures, and Pearson's Chi-Square test was used to compare categorical data. Statistical significance was accepted at a level of $p < 0.005$.

3. Results

3.1. Clinical safety after ocular administration of the DEX/LAP formulation

The clinical ophthalmological signs in eyes after SC and IV administration of the DEX/LAP formulation are detailed in table 1.

Both SC and IV DEX/LAP injection were well tolerated. No case of infection, inflammation or ocular hypertension was detected (IOP ranged from 7 to 16 mmHg in both routes of administration under study). Variable grades of conjunctival hyperaemia and swelling were observed in both groups, although these were more intense in SC delivery and included haemorrhages located around the administration site up to week 1. Variable corneal epithelial defects were also observed, probably due to the surgical procedure. The IV group showed a higher rate of early cataract formation, in the form of focal opacity located in the posterior lens capsule, which did not interfere with the ophthalmoscope examination. This was also attributed to technical issues associated with rabbits' large lens. Using ophthalmoscopy, the DEX/LAP suspension could be observed in the vitreous as a transparent floater from 24 h up to 24 weeks after administration, and without any signs of inflammation of the retina or optic nerve.

3.2. Concentrations of DEX in posterior-segment eye tissue

Figure 1 shows the concentration–time curves in the ocular tissues (lens, vitreous, choroid-retina unit and sclera) over the course of the study following SC administration of DEX/LAP suspension. Concentration is expressed in nanograms of DEX per gram of the specific ocular tissue. The highest intraocular DEX levels after SC administration were observed in the vitreous humour (460.38 ± 93.79 ng g^{-1}) followed by the choroid-retina (275.54 ± 164.85 ng g^{-1}) at 1 week. Vitreous DEX levels experienced the most abrupt decrease (under the lowest limit of detection (LLD: 10 ng g^{-1}) at 12 weeks), contrasting with the other tissues, which experienced a gentler decrease. DEX levels in the sclera and choroid-retina unit plateaued from weeks 12 to 24 and maintained detectable concentrations in the sclera (25.46 ± 44.09 ng g^{-1}) and choroid-retina (12.04 ± 20.85 ng g^{-1}) up to the end of the study (week 24). These values were lower than expected, probably due to leaking in the administration procedure.

After IV administration, DEX was only detected in the vitreous humour. Levels in the other ocular tissues (lens, choroid-retina and sclera) were below the lowest limit of detection for the analytical method used. Peak DEX concentration (2258.00 ± 1610.32 ng g^{-1}) was observed on day 1 and then drastically decreased, plateauing (626.42 ± 251.31 to 466.32 ± 311.15 ng g^{-1}) from weeks 1 to 24 after administration (see figure 2).

DEX concentrations in the vitreous humour after SC and IV administration were compared (figure 2). Direct injection of DEX/LAP suspension into the vitreous humour showed 7 times higher DEX concentration at day 1—although the levels were roughly equal at week 1 (626.42 ± 251.31 vs 460.38 ± 93.79 ng g^{-1})—and concentration remained higher at week 24 (466.32 ± 311.15 ng g^{-1} vs non-detectable levels) than when DEX/LAP suspension was administered suprachoroidally. DEX levels were not detectable in contralateral eyes (in the vitreous humour or choroid-retina unit) after both SC and IV administration of the DEX/LAP formulation.

3.3. Ocular tissue pharmacokinetics

The experimental levels of DEX in ocular tissue over time after both SC and IV administration of DEX/LAP may be explained by a non-compartmental model. In the case of the SC route, there were not enough experimental points for compartmental modelling. Meanwhile, the IV route showed a good correlation between observed and predicted concentrations with this model ($R^2 = 0.9897$).

Following the SC route, the maximum concentrations (C_{max}) were found in the vitreous humour (460.38 ng g^{-1}), sclera (283.53 ng g^{-1}) and choroid-retina unit (275.54 ng g^{-1}). Times of maximum concentration (T_{max}) were achieved at day 7 after administration, with the exception of the sclera (day 1). The scleral tissue showed the highest area under the concentration–time curve value (AUC:

Table 1. Clinical evaluation of eyes administered DEX/LAP formulation after SC and IV delivery.

	24 h (n = 15 per group)		1 week (n = 12 per group)		4 weeks (n = 9 per group)		12 weeks (n = 6 per group)		24 weeks (n = 3 per group)	
	SC	IV	SC	IV	SC	IV	SC	IV	SC	IV
Conjunctival hyperaemia										
mild	1 (6.7%)	7 (46.7%)[b]	2 (16.7%)	4 (33.3%)	0	0	0	0	0	0
moderate	3 (20%)	5 (33.3%)	2 (16.7%)	0	0	0	0	0	0	0
severe	9 (60%)[a]	0	3 (25%)	0	0	0	0	0	0	0
Conjunctival swelling										
mild	2 (13.3%)	1 (6.7%)	3 (25%)	0	0	0	0	0	0	0
moderate	0	0	0	0	0	0	0	0	0	0
severe	0	0	0	0	0	0	0	0	0	0
Subconjunctival haemorrhage	4 (26.7%)	1 (6.7%)	1 (8.3%)	0	0	0	0	0	0	0
Eye discharge	8 (53.3%)[a]	4 (26.7%)	1 (8.3%)	2 (16.7%)	0	0	0	0	0	0
Corneal epithelial defect	6 (40%)	3 (20%)	0	0	0	0	0	0	0	0
Cataract	0	3 (20%)	0	5 (41.7%)[b]	0	1 (11.1%)	0	1 (16.7%)	0	1 (33.3%)
Vitreous clarity										
grade 1	0	0	0	0	0	0	0	0	0	0
grade 2	0	0	0	0	0	0	0	0	0	0
grade 3	0	0	0	0	0	0	0	0	0	0
Vitreous haemorrhage	0	0	0	0	0	0	0	0	0	0
Retinal haemorrhage	0	2 (13.3%)	0	1 (8.3%)	0	0	0	0	0	0
Retinal detachment	0	0	0	0	0	0	0	0	0	0
Intraocular pressure (range in mmHg)	8–13	8–13	8–14	8–12	7–12	10–16	9–13	10–13	9–11	7–13

n = number of animals, % = percentage.

[a]Indicates significant difference compared to IV injection ($p < 0.05$; Pearson's Chi-square test).

[b]Indicates significant difference compared to SC administration ($p < 0.05$; Pearson's Chi-square test).

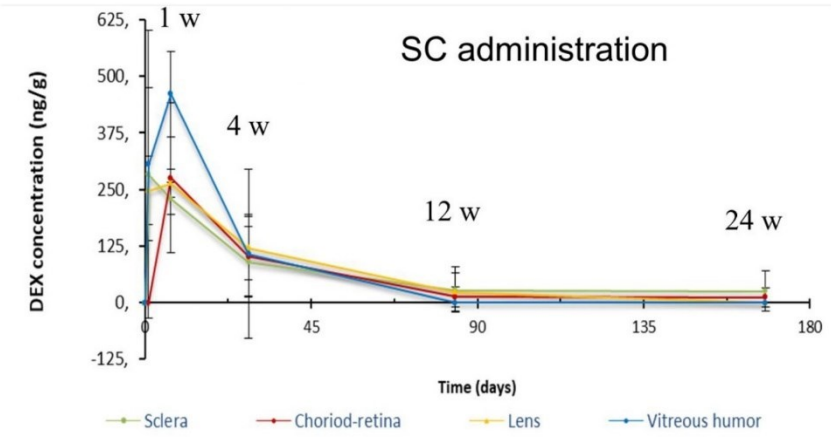

Figure 1. DEX concentrations in posterior segment tissues (lens, vitreous, choroid-retina unit and sclera) after SC administration of DEX/LAP (1:10 w w^{-1}) suspension (10 mg ml^{-1}). Data expressed as mean ± sd. n = 3 animals per sampling time point. Abbreviations: ng: nanograms; g: grams; w: week.

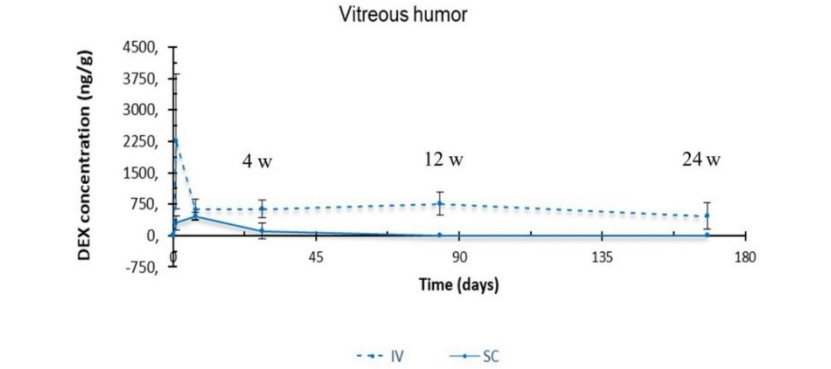

Figure 2. DEX concentrations in the vitreous humour after IV and SC administration of DEX/LAP (1:10 w w^{-1}) suspension (10 mg ml^{-1}). Data expressed as mean ± sd. n = 3 animals per sampling time point.

12 399.70 ng g^{-1} d^{-1}) after SC administration. Although the vitreous humour was the intraocular tissue that exhibited the lowest distribution volume (V_{ss}: 35.80 g), it nevertheless showed a large AUC (11 442.22 ng g^{-1} d^{-1}). The longest elimination half-life ($T_{1/2}$) was found in the sclera (48.05 d), followed by the choroid-retina unit (36.37 d). There were similar drug clearance (Cl) values in all ocular tissue: 4.724 g d^{-1} in the lens, 4.369 g d^{-1} in the vitreous, 5.118 g d^{-1} in the choroid-retina unit, and 4.032 g d^{-1} in the sclera. Table 2 shows the PK parameters of the DEX in the rabbits' ocular tissues after SC administration of DEX/LAP suspension.

PK parameters of the DEX in the rabbits' vitreous humour after IV administration of DEX/LAP suspension are shown in table 3. It compares the vitreous PK parameters of DEX versus SC and IV administration of DEX/LAP, and versus IV injection of DEX in solution (1 mg ml^{-1}) (data taken from our previous study [65]).

Following the IV route, the maximum concentration of DEX achieved in the vitreous humour after administration of DEX/LAP suspension was higher than that achieved with DEX solution (C_{max}: 2258.00 ng g^{-1} vs 112.27 ng g^{-1}). Even when the DEX/LAP suspension was administered suprachoroidally, vitreous levels were higher than after direct IV injection of DEX solution (460.38 ng g^{-1} vs 112.27 ng g^{-1}). The vitreous AUC was significantly larger ($p = 0.036$) after IV and SC administration of DEX/LAP suspension than following IV injection of DEX solution (205 968.47 and 11 442.22 ng g^{-1} d^{-1},

Table 2. Ocular tissue PK parameters after SC administration of DEX/LAP suspension.

PK parameters	Units	Lens	Vitreous humour	Choroid-retina unit	Sclera
K_e	d^{-1}	0.031	0.122	0.019	0.014
$T_{1/2}$[a]	d	22.65	5.68	36.37	48.05
V_{ss}	g	154.38	35.80	268.58	279.51
Cl	$g\ d^{-1}$	4.724	4.369	5.118	4.032
$AUC_{0-\infty}$	$ng\ g^{-1}\ d^{-1}$	10 584.36	11 442.22	9768.63	12 399.70
C_{max}	$ng\ g^{-1}$	263.34	460.38	275.54	283.53
T_{max}	d	7	7	7	1

[a]The $T^1/_2$ value was determined by calculating the lambda Z parameter (0.05 d-1).

Table 3. Vitreous PK comparison. Vitreous humour PK parameters following 50 µl SC and 100 µl IV administration of DEX/LAP (1:10 w w^{-1}) suspension (10 mg ml^{-1}) compared to IV injection of DEX in solution (1 mg ml^{-1}) [65]. A non-compartmental model was achievable for vitreous levels in the DEX/LAP administration groups—IV and SC. The monocompartmental model was a fit for vitreous levels in IV delivery of DEX in solution.

PK parameters	Units	SC DEX-LAP (1:10 w w^{-1}) (10 mg ml^{-1})	IV DEX-LAP (1:10 w w^{-1}) (10 mg ml^{-1})	IV DEX solution [65] (1 mg ml^{-1})
K_e	d^{-1}	0.122	0.005*	5.48
$T_{1/2}$[a]	d	5.68	134.75	0.13
V_{ss}	g	35.80	97.57*	57.55
Cl	$g\ d^{-1}$	4.369	0.486*	315.29
$AUC_{0-\infty}$	$ng\ g^{-1}\ d^{-1}$	11 442.22	205 968.47	317.17
C_{max}	$ng\ g^{-1}$	460.38	2258.00	112.27
T_{max}	d	7	1	0.5
F	%	99.98	100.10	100.00

[a]The $T^1/_2$ value was determined by calculating the lambda Z parameter (0.05 d^{-1}).

*Statistical difference at $p < 0.05$ compared with that of SC administration, calculated using Student's t- test.

respectively, vs 317.17 ng g^{-1} d^{-1}). SC administration of DEX/LAP suspension showed the lowest distribution volume (35.80 g), ($p = 0.022$).

DEX/LAP suspension, for both the SC and IV routes, showed a vitreous DEX elimination rate that was significantly lower ($p = 0.023$) than that found after IV administration of the DEX solution, with a clearance of 4.37, 0.49 vs 315.29 g day^{-1}, respectively. The half-life of DEX in the vitreous was extended from 0.13 d (IV DEX solution) to 5.68 d and 134.75 d (SC and IV DEX/LAP suspension, respectively) when the new LAP formulation was used.

Figure 3 shows the differences in DEX concentration–time profiles in the vitreous humour between the two IV formulations (DEX/LAP suspension and DEX solution) in order to observe the effect of the long-lasting release of DEX from the LAP carrier. In the vitreous humour, DEX levels remained detectable for up to 168 d after injection of the DEX/LAP formulation (figure 3(A)). In contrast, levels of DEX rapidly decreased within 24 h of administration of the solution (figure 3(B)).

4. Discussion

Treatment of chronic posterior segment pathologies with GCs requires sustained-release systems that maintain therapeutic levels of the drug near the site of action for long periods of time and with the least number of re-injections, since repeated injection has been shown to worsen patient compliance and increase the risk of possible severe ocular complications [67].

The vitreous is considered a natural ocular drug reservoir that extends therapeutic application near its site of action (the choroid-retina unit) [68]. However, part of the IV-administered dose is 'lost' through the anterior or posterior pathways, producing undesirable effects such as increased IOP or cataracts [69, 70] in addition to being greatly diluted due to the high water content of the vitreous humour [35] and having to pass through the retinal pigment epithelium (RPE) barrier, all of which reduces the bioavailability of the drug in the choroid-retina unit. SC administration maintains higher drug levels in the choroid-retina unit compared to IV delivery [31]. SC administration has the handicap of rapid clearance, as the choroid has the greatest vascular flow per unit of weight (62 ml h^{-1} in rabbits [71] and 1200 ml/100 g min^{-1} in humans [31]) and the choriocapillaris is fenestrated, which rapidly decreases the bioavailability of the drug administered in the SCS.

In order to overcome these limitations, research has been conducted in recent years into nanoparticle systems [72] capable of sustained release of drugs, thereby making it possible both to decrease the dose administered and to deliver them locally at the target site—the choroidal retinal tissue—in the posterior segment [25] over prolonged periods of time. Meanwhile, the high hydrosolubility of DEX means that in order to administer it intravitreally

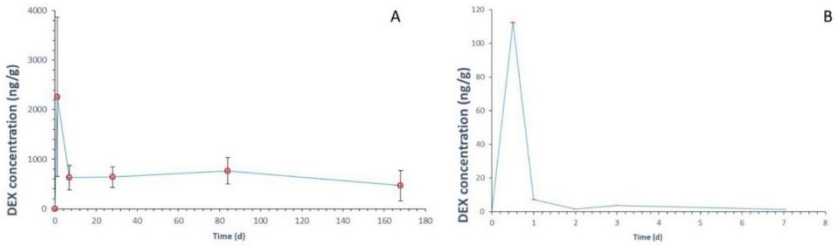

Figure 3. DEX concentrations in the vitreous humour after IV administration of DEX/LAP suspension (A) and DEX solution (B). Data expressed as mean ± sd. $n = 3$ animals per sampling time point.

or suprachoroidally it is necessary to develop systems that allow sustained long-term release of the drug.

In previous papers, our group created and characterized, *in vitro*, a new DEX formulation using a LAP matrix as the base (DEX/LAP formulation). DEX/LAP showed an initial burst release of less than 40% followed by sustained release of DEX from the carrier LAP for up to 24 weeks [61]. It also demonstrated the ocular feasibility and safety of IV and SC administration of LAP [57]. This study evaluates the ocular safety and PK profile of the new DEX/LAP formulation when administered in rabbit eyes after having demonstrated the suitability of this animal model in the form of a good pharmacokinetic correlation between the rabbits' vitreous humour and that of humans [71].

4.1. Analysis of IV administration

Currently, GCs are available that can be administered intravitreally either in suspension (TA) or in biodegradable (DEX) or non-biodegradable (FA) implants [70]. After IV administration, their ocular kinetics show an initial burst peak in the vitreous and then progressively and variably decrease until the levels stabilize, after which they fall further until they become non-detectable. IV TA (Kenalog®), DEX (Ozurdex®, Cortiject®, Posurdex®) and FA (Retisert®, Illuvien®) implants have different delivery mechanisms that contribute to the differing durations of their therapeutic effect (approximately 2 months, 4 months, and years, respectively). Studies in rabbits using IV TA showed high vitreous levels on day 1 followed by an exponential decrease up to week 4 and then a steady decline over the following months, with a C_{max} greater than 10 000 ng g^{-1}. However, IV FA implants (Retisert® or Illuvien®) show low and constant vitreous levels from 2 h up to more than 1 year, with a C_{max} of 1–20 ng g^{-1}. It has been hypothesized that GCs with a near zero-order burst maintain their efficacy for longer because, in contrast, a very high initial dose may make the cells dependent on high doses to maintain the same effect [70]. Furthermore, studies comparing dose efficacy showed that low doses (SC administration) can be just as effective as high IV doses in controlling acute inflammation [22]. Increasing the dose of steroids released does not necessarily result in a corresponding increase in efficacy [70]. We were unable to corroborate these findings in our study, however, as our animals were healthy. Regarding DEX (the GC chosen in this study), various trials have been conducted using sustained-release systems like Cortiject® (for DME), Posurdex (for DME and posterior uveitis), as well as the FDA-approved and commercially available surgically placed biodegradable PLGA (poly-lactic-glycolic acid) IV implant Ozurdex® that it is widely used in clinical practice. Ozurdex® maintains *in vitro* release of DEX for 6 months. Chang-Lin *et al* [73] demonstrated in male monkeys that vitreous DEX peaked at month 2. Levels then dropped progressively up to day 120 (4 months), were maintained up to day 180 (6 months) and became non-detectable beyond 6 months. However, in our case, IV administration of 0.1 mg of DEX in the form of a suspension (10 mg ml^{-1}) of DEX/LAP (1:10 w w^{-1}), in addition to presenting the advantage of being administered as a mild nanogel injected by 25 G needle [74], produced a short and early peak release of DEX at day 1 (2258.00 ± 1610.32 ng g^{-1}) followed by a drop at week 1 and a subsequent plateau DEX vitreous level for up to 6 months (466.32 ± 311.15 ng g^{-1}), even though the dose of DEX administered was lower than that of Ozurdex® (0.1 vs 0.7 mg). IV DEX/LAP decreased the time and minimized other ocular structures' exposure to high levels of DEX (at week 1) and, therefore, reduced the risk of developing cataracts, ocular hypertension or corticosteroid glaucoma. In our study, no animal developed these potential long-term complications following IV administration of DEX/LAP. In this regard, studies conducted with IV Illuvien® implants, with more posterior placement than Retisert®, decreased OHT events when compared with the latter. The fact that the DEX/LAP formulation is not an implantable insert and can be placed away from the ciliary body and iridocorneal angle may have helped to maintain ocular normotension.

The initial peak in DEX levels in the vitreous humour (matching that observed in *in vitro* studies [61]) may be due to the release of DEX from the surface of the LAP, with the entrapped DEX subsequently being released sustainedly [62]. Our findings showed that the use of LAP as a carrier extended the half-life of the DEX in the vitreous when compared with IV injection of the DEX in solution (134.75 vs 0.13 d). The LAP increased the viscosity of the formulation, which increased its residence time and bioavailability [26, 75]. In addition, highly cationic molecules such as LAP may find their mobility limited and so aggregate in the vitreous. In our study, we observed the DEX/LAP formulation as a single semi-transparent aggregate in the vitreous throughout the study.

However, the goal of IV administration is to achieve DEX levels in the choroid-retina unit, where the drug exerts its greatest effect. IV administration of 0.7 mg of Ozurdex® produces a peak in retinal DEX at day 60 (C_{max} 1110 ng g^{-1}) followed by a steep decline up to week 12 (0.0167 ng g^{-1} at day 210) and no detectable level after day 240.66. In our study, unfortunately, following IV administration of 0.1 mg of DEX in the form of a suspension (10 mg ml^{-1}) of DEX/LAP (1:10 w/w), DEX levels were below the detection limit.

4.2. Analysis of SC administration

SC administration presents several advantages over IV administration, among them lower risk of haemorrhage in the pars plana, not creating opacity in the visual axis (cataracts or floating bodies), better targeting of the choroid-retina unit and lower immune response. This higher potential is manifested in the number of SC administration patents registered, as well as in the growing number of publications in recent years in which this route is used [36].

Administration of 0.05 mg of DEX—in the form of a suspension (10 mg ml^{-1}) of DEX/LAP (1:10 w w^{-1})—in the SCS produced (despite of the non-quantified leaking at injection time) a peak in DEX in the choroid-retina unit at week 1 (C_{max} 275.54 ± 164.85 ng g^{-1}) followed by a progressive decline up to week 12 and plateauing up to week 24 (C_{max} 12.04 ± 20.85 ng g^{-1}). SC administration of DEX/LAP increased DEX availability in the choroid-retina compared with IV injection of Ozurdex® (AUC 9786 vs 47 200 ng g^{-1} d^{-1}) and was also maintained more consistently and prolongedly until the end of the study [70, 73]. This could prevent overdosing, fluctuations and side effects, as no animal in the study showed increases in IOP, cataracts or infection after SC administration of DEX/LAP. The presence of DEX levels in the choroid-retina unit at the end of the study can be explained by retention of the formulation as a macro-aggregate at the injection site (SCS), acting as a reservoir from where DEX is slowly released over time. The pore size of the choriocapillaris vessels is estimated at 6 nm, meaning that during biodegradation of the gel small subcomponents of it could pass through the pores and thus produce progressive release. In this regard, Chiang *et al* [27] showed how non-rigid molecules (DEX or even DEX/LAP nano-aggregates in our case) can adapt and pass through the fenestrations (which would coincide with the initial burst). Polystyrene particles of between 20 nm and 10 μm, however, were still retained in the SCS 2 months after injection [76]. In our study, the DEX/LAP aggregate was retained in the SCS for up to 6 months, enabling prolonged release of the drug.

Olsen *et al* [29] asserted that the sustained release of small molecules may indicate an ideal candidate for SC administration, as they clear quickly by themselves (2 d) [27]. The distribution of small molecules in the posterior segment, after SC administration, was studied using fluorescein as a model. As DEX has a slightly lower molecular mass than fluorescein (332 vs 392.46 Daltons), we consider the latter's behaviour to be extrapolatable to the GC in our study. Small molecules spread rapidly throughout the posterior segment [22], meaning that the DEX released in the initial burst could be widely distributed. Previous studies show an approximate asymmetrical circumferential distribution of 50%, which is limited in the equatorial area by the vascular barriers of the long posterior ciliary arteries (LPCAs) in rabbits or the short ones in humans [27, 51]. In our study, the SC injection site selected was 9 mm from the limbus in order to avoid possible ectasia, due to the increased scleral thinning in the pre-equatorial region [41], and to overcome the LCPA barriers and so achieve wider potential distribution of our formulation in the posterior segment.

In contrast, agents with LAP-like viscous and hydrophilic properties, such as carboxymethylcellulose (CMC), expand and increase their area at the SC injection site for up to 2 d after administration [27]. In addition, the use of hydrogels has shown an increase in particle distribution secondary to an osmotic push [33], although it is generally located at the injection site, since the more viscous a formulation is the less it is distributed [51]. Low-viscosity formulations expand with a constant thickness. However, if the viscosity of the formulation is increased, the thickness of the SCS likewise increases [27] (to more than 30 microns under normal conditions) [22] until reaching a maximum thickness after gelatine injection of 250 microns [77], at which point the viscosity matches the biomechanical resistance exerted by the tissues. This makes it possible to place the formulation at a specific site away from the ciliary body so as to prevent ocular hypertension or to treat specific sites/targets. The nanogel DEX/LAP formulation remained at the injection site and could be observed and delimited macroscopically at the moment of injection (figure 4). Thus, although in

our study we do not evaluate the placement or distribution of the DEX/LAP formulation, based on histological studies or imaging tests using fluorescent markers or stains the above evidence suggests that DEX/LAP may behave in a similar way.

The LAP swells in an aqueous medium and facilitates −OH−H + exchange of the drug (in our case, DEX). This may be what caused higher and earlier levels (initial burst) of DEX to be detected in the most hydrated tissues. Our study showed that the highest concentration of DEX, following SC administration of DEX/LAP, was detected in the vitreous humour, followed by the sclera. Chiang *et al* [27] found that after initial leaking, the main clearance route for small molecules was transscleral diffusion. The sclera shows increased permeability to small molecules (such as DEX) and decreased permeability to macromolecules (LAP aggregate), thus retaining them. As the LAP was not cleared by the transscleral route, the DEX could be released sustainedly to the choroid-retina unit (12.04 ± 20.85 ng g^{-1}) and sclera (25.46 ± 44.09 ng g^{-1}) (greater in the sclera as it is a more hydrated tissue) through to the end of the study.

The DEX's hydrophilia was also considered responsible for the greater early loss rate in the tissues with the greatest water component: the vitreous, followed by the choroid-retina unit (even when the formulation is injected directly there), the sclera and the crystalline cone. The high concentration of DEX in the vitreous after SC injection was noteworthy because the RPE-choroid has thin bonds that, under normal conditions, restrict the passage of hydrosoluble or polar molecules, such as DEX, to the retina. Thus, these unexpectedly high concentrations in the vitreous suggest a possible disruption of the Bruch membrane in the rabbits in this study. In this regard, disruption of the RPE may occur with application of certain injection and/or cannulation techniques in the SCS, as we used in this study [10]. The use of standardized microneedles (as Clearside®) for SC administration seems important, as gauge, length and injection force, as well as type of formulation, influence placement of the formulation in the SCS. And probably, the use of these standardized microneedles would avoid the undesirable initial leaking. Viscous gels may require long needles or extended injection times, although there are cases in which gel-type formulations have been injected using 30 G needles and the LAP's thixotropic property would facilitate this [78]. Using microneedles 1 mm long appears to be advisable so as to avoid puncturing the choroidal vasculature [52].

Most studies of SC administration of GCs have been conducted with TA due to its intrinsic sustained release capability. Animal and human studies showed an increase in TA levels in the choroid-retina unit and sclera up to 6 months after administration, with levels decreasing in anterior structures and less need for re-injection when compared with IV administration [23, 40, 42].

To our knowledge, there has only been one study of administering DEX in the SCS [53]. This study demonstrated the safety and efficacy of controlling inflammation in rats with uveitis following the surgical placement of a slow-degradation polyurethane/-DEX implant with a semi-crystalline structure. However, it did not analyse *in vivo* pharmacokinetics. The *in vitro* release study shows that the DEX release profile of the implant exhibited a higher initial burst than that observed with our DEX/LAP formulation (55% vs 40%), as was the case in our study in week 1, as well as subsequent sustained release of shorter duration (42 d vs 6 months) [61]. However, it uses much higher doses of DEX (6, 18.8 and 29 mg) than used in our DEX/LAP SC delivery study (0.05 mg of DEX in the form of a suspension (10 mg ml^{-1}) of DEX/LAP (1:10 w w^{-1})) [53].

4.3. Comparison between IV and SC route for DEX/LAP formulation

Both routes of administration were safe and the combination with LAP allowed sustained and longer ocular levels of DEX compared to a conventional injection. Our results suggest a greater benefit of the SC route of DEX/LAP compared to the IV route. Although the SC route led to increased hyperemia and epithelial defects, these inconveniences were attributed to the surgical intervention of the cannulation process. It could be minimized with the use of injections such as Clearside®. The SC route produced reversible and time-limited side effects on the ocular surface. However, iatrogenesis by IV injection was permanent (cataract) and generated a vision of floater with potential visual alteration until the end of the study. It did not occur with the SC route.

The SC route maintained sustained levels of DEX in ocular tissues with a lower amount of drug injected into the eye (0.1 IV vs. 0.05 mg SC). The IV route exhibited higher dilution and greater initial burst. Therefore, to maintain prolonged eye levels it is necessary to administer a greater amount of DEX, which carries a potential greater risk of side effects such as cataracts or ocular hypertension (although no animal developed these complications).

Nowadays, it would be convenient to carry out further studies on SC administration to facilitate the wide use of this route in daily practice. The extensive experience obtained with IV injections in clinical practice makes the IV route also have to be considered. The authors recommend evaluating the suitability of using one route or another depending on the individual characteristics of each patient. IV administration could be more suitable to treat pathologies (1) of inner neuroretina, or 2) with intraocular inflammation of the posterior pole, (3) requiring wider diffusion of the drug, (4) with necessity of an attack dose and subsequent control of immunity, (5) and in

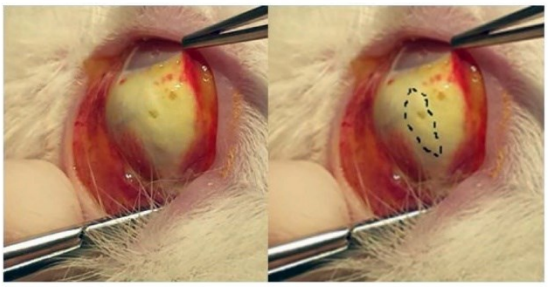

Figure 4. Placement of the DEX/LAP formulation in the SC space.

which visual quality is not the first handicap to solve at that stage. However, the SC route seems ideal to treat pathologies (1) of outer retina (2) that require a targeted location and (3) in need of preserving the available visual quality of the patient at that time.

4.4. Limitations and objectives for future studies

The analytical medium used in this study to quantify the DEX was only able to detect DEX levels in the vitreous, not in the other tissues analysed, so unfortunately comparison of DEX in retina-choroid between the two administration routes could not be made. No blood tests were performed to determine DEX levels, (further studies for quantification of plasma DEX concentration would be interesting to further validate the ocular PK data) nor were histological studies conducted to confirm the correct placement of the DEX/LAP formulation in the SCS, its distribution area, its degradation over time and its effect on the near tissue.

The PK behaviour of a substance can be modified by the presence of disease, which causes tissue-specific bonds to form faster. Future studies using models of inflammatory ocular disease will allow for better understanding of the pharmacodynamics and comparison with those of other formulations or devices. Development of formulations that modulate the release of DEX from the LAP carrier based on pH or temperature is also considered of interest, as in the presence of disease the medium becomes more acidotic and its temperature rises due to the increase in flow and cell activity. In these situations, there could potentially be greater degradation of the DEX/LAP formulation and, therefore, greater release of DEX, positioning it as a shock treatment. Subsequently, with the improvement in the hyperkinetic pathology, the degradation of the DEX/LAP would decrease while maintaining low-level sustained DEX release, allowing a form of control or maintenance.

5. Conclusions

The DEX/LAP formulation was administered by minimally invasive IV injection and by safe SC administration in healthy rabbits. A single IV or SC administration of the DEX/LAP formulation produced the progressive release of DEX and extended the residence time in the vitreous humour and choroid-retina unit by up to 6 months when compared with conventional formulations. DEX/LAP could therefore be considered as a biocompatible sustained-release formulation to treat ocular posterior segment diseases.

Acknowledgments

The authors would like to acknowledge the contribution of the staff at the Centro de Investigación Biomédica de Aragón (CIBA) as regards animal supply, care, feeding and maintenance services and access to the Servicio General de Apoyo a la Investigación-SAI, Universidad de Zaragoza.

Funding

This paper was supported by the Carlos III Health Institute (Programme Grant PI12/02285), by Rio Hortega Research Grant M17/00213, PI17/01726, PI17/01946 (Carlos III Health Institute), by MAT2017-83858-C2-2 MINECO/AEI/FEDER, EU, and by the Regional Government of Aragon (E37_17R group, co-financed under FEDER 2014–2020 'Construyendo Europa desde Aragón'). The funders had no role in study design, data collection and analysis, decision to publish or preparation of the manuscript.

Conflicts of interest

There are no conflicts to declare.

ORCID iDs

Eugenio Vispe https://orcid.org/0000-0002-4921-4734

Maria Jesus Rodrigo https://orcid.org/0000-0002-4009-3075

References

[1] Chennamaneni S R, Mamalis C, Archer B, Oakey Z and Ambati B K 2013 Development of a novel bioerodible dexamethasone implant for uveitis and postoperative cataract inflammation *J. Control. Release* **167** 53–59

[2] Lowder C, Belfort R, Lightman S, Foster C S, Robinson M R, Schiffman R M, Li X Y, Cui H and Whitcup S M 2011 Dexamethasone intravitreal implant for noninfectious intermediate or posterior uveitis *Arch. Ophthalmol.* **129** 545–53

[3] Ciulla T A, Harris A, McIntyre N and Jonescu-Cuypers C 2014 Treatment of diabetic macular edema with sustained-release glucocorticoids: intravitreal triamcinolone acetonide, dexamethasone implant, and fluocinolone acetonide implant *Expert Opin. Pharmacotherapy* **15** 953–9

[4] Haller J A *et al* 2011 Dexamethasone intravitreal implant in patients with macular edema related to branch or central retinal vein occlusion: twelve-month study results *Ophthalmology* **118** 2453–60

[5] Calvo P, Abadia B, Ferreras A, Ruiz-Moreno O, Verdes G and Pablo L E 2015 Diabetic macular edema: options for adjunct therapy *Drugs* **75** 1461–9

[6] Ethier C R, Johnson M and Ruberti J 2004 Ocular biomechanics and biotransport *Annu. Rev. Biomed. Eng.* **6** 249–73

[7] Kim S H, Lutz R J, Wang N S and Robinson M R 2007 Transport barriers in transscleral drug delivery for retinal diseases *Ophthalmic Res.* **39** 244–54

[8] Thakur A, Kadam R S and Kompella U B 2011 *Drug. Metab. Dispos.* **39** 771–81

[9] Lockwood A C, Awwad S, Mohamed Ahmed A H A, Sharma G, Heng J S, Khaw P T, Brocchini S and Lockwood A 2017 Principles of pharmacology in the eye *Br. J. Pharmacol.* **174** 4205

[10] Yamada N and Olsen T W 2015 Routes for drug delivery to the retina: topical, transscleral, suprachoroidal and intravitreal gas phase delivery *Dev. Ophthalmol.* **55** 71–83

[11] Gaudana R, Ananthula H K, Parenky A and Mitra A K 2010 Ocular drug delivery *Aaps J.* **12** 348–60

[12] Oray M, Abu Samra K, Ebrahimiadib N, Meese H and Foster C S 2016 Long-term side effects of glucocorticoids *Expert Opin. Drug Saf.* **15** 457–65

[13] Caplan A, Fett N, Rosenbach M, Werth V P and Micheletti R G 2017 Prevention and management of glucocorticoid-induced side effects: a comprehensive review: ocular, cardiovascular, muscular, and psychiatric side effects and issues unique to pediatric patients *J. Am. Acad. Dermatol.* **76** 201–7

[14] Dossarps D *et al* 2015 Endophthalmitis after intravitreal injections: incidence, presentation, management, and visual outcome *Am. J. Ophthalmol.* **160** 17–25.e1

[15] Ganapathy P S, Lowder C Y, Arepalli S, Baynes K, Li M, Bena J and Srivastava S K 2018 Treatment duration and side effect profile of long-term use of intravitreal preservative-free triamcinolone acetonide in uveitis *Am. J. Ophthalmol.* **194** 63–71

[16] Patel A, Cholkar K, Agrahari V and Mitra A K 2013 Ocular drug delivery systems: an overview *World J. Pharmacol.* **2** 47–64

[17] Behar-Cohen F 2018 Towards an optimized use of ocular corticosteroids: EURETINA award lecture 2017 *Ophthalmologica* **240** 111–9

[18] Da Silva G R, Ayres E, Orefice R L, Moura S A L, Cara D C and Da Silva Cunha A 2009 Controlled release of dexamethasone acetate from biodegradable and biocompatible polyurethane and polyurethane nanocomposite *J. Drug Target* **17** 374–83

[19] Kwak H W and D'amico D J 1992 Evaluation of the retinal toxicity and pharmacokinetics of dexamethasone after intravitreal injection *Arch. Ophthalmol.* **110** 259–66

[20] Kersey J P and Broadway D C 2006 Corticosteroid-induced glaucoma: a review of the literature *Eye* **20** 407–16

[21] Kim S H, Galbán C J, Lutz R J, Dedrick R L, Csaky K G, Lizak M J, Wang N S, Tansey G and Robinson M R 2007 Assessment of subconjunctival and intrascleral drug delivery to the posterior segment using dynamic contrast-enhanced magnetic resonance imaging *Investigative Ophthalmol. Vis. Sci.* **48** 808–14

[22] Rai U D J P, Young S A, Thrimawithana T R, Abdelkader H, Alani A W G, Pierscionek B and Alany R G 2015 The suprachoroidal pathway: A new drug delivery route to the back of the eye *Drug Discovery Today* **20** 491–5

[23] Chen M, Li X, Liu J, Han Y and Cheng L 2015 Safety and pharmacodynamics of suprachoroidal injection of triamcinolone acetonide as a controlled ocular drug release model *J. Control. Release* **203** 109–17

[24] Chiang B, Jung J H and Prausnitz M R 2018 The suprachoroidal space as a route of administration to the posterior segment of the eye *Adv. Drug Deliv. Rev.* **126** 58–66

[25] Habot-Wilner Z, Noronha G and Wykoff C C 2019 Suprachoroidally injected pharmacological agents for the treatment of chorio-retinal diseases: a targeted approach *Acta Ophthalmol.* **97** 460–72

[26] Gu B, Liu J, Li X, Ma Q K, Shen M and Cheng L 2015 Real-time monitoring of suprachoroidal space (SCS) following SCS injection using ultra-high resolution optical coherence tomography in guinea pig eyes *Investigative Ophthalmol. Vis. Sci.* **56** 3623–34

[27] Chiang B, Venugopal N, Edelhauser H F and Prausnitz M R 2016 Distribution of particles, small molecules and polymeric formulation excipients in the suprachoroidal space after microneedle injection *Exp. Eye Res.* **153** 101–9

[28] Emami-Naeini P and Yiu G 2019 Medical and surgical applications for the suprachoroidal space *Int. Ophthalmol. Clin.* **59** 195–207

[29] Olsen T W, Feng X, Wabner K, Csaky K, Pambuccian S and Cameron J D 2011 Pharmacokinetics of pars plana intravitreal injections versus microcannula suprachoroidal injections of bevacizumab in a porcine model *Investigative Ophthalmol. Vis. Sci.* **52** 4749–56

[30] Touchard E, Berdugo M, Bigey P, El Sanharawi M, Savoldelli M, Naud M C, Jeanny J C and Behar-Cohen F 2012 Suprachoroidal electrotransfer: a nonviral gene delivery method to transfect the choroid and the retina without detaching the retina *Mol. Ther.* **20** 1559–70

[31] Tyagi P, Kadam R S and Kompella U B 2012 Comparison of suprachoroidal drug delivery with subconjunctival and intravitreal routes using noninvasive fluorophotometry *PLoS One* **7** 1–9

[32] Jung J H, Chiang B, Grossniklaus H E and Prausnitz M R 2018 Ocular drug delivery targeted by iontophoresis in the suprachoroidal space using a microneedle *J. Control. Release* **277** 14–22

[33] Jung J H, Desit P and Prausnitz M R 2018 Targeted drug delivery in the suprachoroidal space by swollen hydrogel pushing *Investigative Ophthalmol. Vis. Sci.* **59** 2069–79

[34] Chiang B, Wang K, Ethier C R and Prausnitz M R 2017 Clearance kinetics and clearance routes of molecules from the suprachoroidal space after microneedle injection *Investigative Ophthalmol. Vis. Sci.* **58** 545–54

[35] Zhang Y, Bazzazi H, e Silva R L, Pandey N B, Green J J, Campochiaro P A and Popel A S 2018 Three-dimensional transport model for intravitreal and suprachoroidal drug injection *Investigative Ophthalmol. Vis. Sci.* **59** 5266–76

[36] Gilger B, Mandal A, Shah S and Mitra A 2014 Episcleral, intrascleral, and suprachoroidal routes of ocular drug delivery - recent research advances and patents *Recent Pat. Drug Deliv. Formulation* **8** 81–91

[37] Jung J H, Chae J J and Prausnitz M R 2019 Targeting drug delivery within the suprachoroidal space *Drug Discovery Today* **24** 1654–9

[38] Edelman J L 2010 Differentiating intraocular glucocorticoids *Ophthalmologica* **224** 25–30

[39] Willoughby A S, Vuong V S, Cunefare D, Farsiu S, Noronha G, Danis R P and Yiu G 2018 Choroidal changes

after suprachoroidal injection of triamcinolone in eyes with macular edema secondary to retinal vein occlusion *Am. J. Ophthalmol.* **186** 144–51
[40] Tetz M, Rizzo S and Augustin A J 2012 Safety of submacular suprachoroidal drug administration via a microcatheter: retrospective analysis of European treatment results *Ophthalmologica* **227** 183–9
[41] Olsen T W, Feng X, Wabner K, Conston S R, Sierra D H, Folden D V, Smith M E and Cameron J D 2006 Cannulation of the suprachoroidal space: a novel drug delivery methodology to the posterior segment *Am. J. Ophthalmol.* **142** 777–787.e2
[42] Goldstein D A, Do D, Noronha G, Kissner J M, Srivastava S K and Nguyen Q D 2016 Suprachoroidal corticosteroid administration: a novel route for local treatment of noninfectious uveitis *Transl. Vis. Sci. Technol.* **5** 4–11
[43] Barar J, Aghanejad A, Fathi M and Omidi Y 2016 Advanced drug delivery and targeting technologies for the ocular diseases *BioImpacts* **6** 49–67
[44] Allergan, Ozurdex Prescribing Information (www.allergan.com/assets/pdf/ozurdex_pi.pdf)
[45] Fratoddi I *et al* 2019 Effects of topical methotrexate loaded gold nanoparticle in cutaneous inflammatory mouse model *Nanomed. Nanotechnol. Biol. Med.* **17** 276–86
[46] Dianzani C, Foglietta F, Ferrara B, Rosa A C, Muntoni E, Della Pepa C, Canaparo R, Serpe L and Gasco P 2017 Solid lipid nanoparticles delivering anti-inflammatory drugs to treat inflammatory bowel disease: effects in an in vivo model basic study *World J. Gastroenterol.* **23** 4200–10
[47] Simion V, Constantinescu C A, Stan D, Deleanu M, Tucureanu M M, Butoi E, Manduteanu I, Simionescu M and Calin M 2016 P-selectin targeted dexamethasone-loaded lipid nanoemulsions: a novel therapy to reduce vascular inflammation *Mediators Inflamm.* **2016** 1625149
[48] Rossi A, Donati S, Fontana L, Porcaro F, Battocchio C, Proietti E, Venditti I, Bracci L and Fratoddi I 2016 Negatively charged gold nanoparticles as a dexamethasone carrier: stability in biological media and bioactivity assessment: in vitro *RSC Adv.* **6** 99016–22
[49] Caliceti P and Matricardi P 2019 Advances in drug delivery and biomaterials: facts and vision *Pharmaceutics* **11** 48
[50] Venditti I 2019 Morphologies and functionalities of polymeric nanocarriers as chemical tools for drug delivery: a review *J. King Saud Univ. Sci.* **31** 398–411
[51] Patel S R, Lin A S P, Edelhauser H F and Prausnitz M R 2011 suprachoroidal drug delivery to the back of the eye using hollow microneedles *Pharm. Res.* **28** 166–76
[52] Hartman R R and Kompella U B 2018 Intravitreal, subretinal, and suprachoroidal injections: evolution of microneedles for drug delivery *J. Ocul. Pharmacol. Ther.* **34** 141–53
[53] Saliba J B *et al* 2016 Anti-inflammatory effect of dexamethasone controlled released from anterior suprachoroidal polyurethane implants on endotoxin-induced uveitis in rats *Investigative Ophthalmol. Vis. Sci.* **57** 1671–9
[54] de Sousa Rodrigues L A, Figueiras A, Veiga F, de Freitas R M, Nunes L C C, da Silva Filho E C and da Silva Leite C M 2013 The systems containing clays and clay minerals from modified drug release: a review *Colloids Surf.* B **103** 642–51
[55] Tomás H, Alves C S and Rodrigues J 2018 Laponite®: a key nanoplatform for biomedical applications? *Nanomed. Nanotechnol. Biol. Med.* **14** 2407–20
[56] Peña-Parás L, Sánchez-Fernández J A and Vidaltamayo R 2018 Nanoclays for biomedical applications *Handbook of Ecomaterials* ed L Martínez, O Kharissova and B Kharisov (Berlin: Springer) pp 1–19
[57] Prieto E, Vispe E, De Martino A, Idoipe M, Rodrigo M J, Garcia-Martin E, Fraile J M, Polo-Llorens V and Mayoral J A 2018 Safety study of intravitreal and suprachoroidal Laponite clay in rabbit eyes *Graefe's Arch. Clin. Exp. Ophthalmol.* **256** 535–46
[58] Mohanty R P and Joshi Y M 2016 Chemical stability phase diagram of aqueous Laponite dispersions *Appl. Clay Sci.* **119** 243–8
[59] Gaharwar A K, Peak C W, Gold K, Carrow J K, Brokesh A, Engineering B and Singh K-A 2019 Two-dimensional nanoclay for biomedical applications: regenerative medicine, therapeutic delivery, and additive manufacturing *Adv. Mater.* **31** 1900332
[60] Lapasin R, Abrami M, Grassi M and Šebenik U 2017 Rheology of Laponite-scleroglucan hydrogels *Carbohydr. Polym.* **168** 290–300
[61] Fraile J M, Garcia-Martin E, Gil C, Mayoral J A, Pablo L E, Polo V, Prieto E and Vispe E 2016 Laponite as carrier for controlled in vitro delivery of dexamethasone in vitreous humor models *Eur. J. Pharm. Biopharm.* **108** 83–90
[62] Roozbahani M, Kharaziha M and Emadi R 2017 pH sensitive dexamethasone encapsulated laponite nanoplatelets: release mechanism and cytotoxicity *Int. J. Pharm.* **518** 312–9
[63] Roozbahani M and Kharaziha M 2019 Dexamethasone loaded Laponite®/porous calcium phosphate cement for treatment of bone defects *Biomed. Mater.* **14** 055008
[64] Ghadiri M, Chrzanowski W and Rohanizadeh R 2015 Biomedical applications of cationic clay minerals *RSC Adv.* **5** 29467–81
[65] Prieto E, Vispe E, Otín-Mallada S, Garcia-Martin E, Polo-Llorens V, Fraile J M, Pablo L E and Mayoral J A 2017 Determination of three corticosteroids in the biologic matrix of vitreous humor by HPLC–tandem mass spectrometry: method development and validation *Curr. Eye Res.* **42** 244–51
[66] Ahn S J, Hong H K, Na Y M, Park S J, Ahn J J, Oh J, Chung J Y, Park K H and Woo S J 2016 Use of rabbit eyes in pharmacokinetic studies of intraocular drugs *J. Vis. Exp.* **113** 53878
[67] Kaji H, Nagai N, Nishizawa M and Abe T 2018 Drug delivery devices for retinal diseases *Adv. Drug Deliv. Rev.* **128** 148–57
[68] Duvvuri S, Majumdar S and Mitra A K 2003 Drug delivery to the retina: challenges and opportunities *Expert Opin. Biol. Ther.* **3** 45–56
[69] Käsdorf B T, Arends F and Lieleg O 2015 Diffusion regulation in the vitreous humor *Biophys. J.* **109** 2171–81
[70] Yang Y, Bailey C, Loewenstein A and Massin P 2015 Intravitreal corticosteroids in diabetic macular edema pharmacokinetic considerations *Retina* **35** 2440–9
[71] Del Amo E M and Urtti A 2015 Rabbit as an animal model for intravitreal pharmacokinetics: clinical predictability and quality of the published data *Exp. Eye Res.* **137** 111–24
[72] Lynch C, Kondiah P P D, Choonara Y E, du Toit L C, Ally N and Pillay V 2019 Advances in biodegradable nano-sized polymer-based ocular drug delivery *Polymers* **11** 1371
[73] Chang-Lin J E, Attar M, Acheampong A A, Robinson M R, Whitcup S M, Kuppermann B D and Welty D 2011 Pharmacokinetics and pharmacodynamics of a sustained-release dexamethasone intravitreal implant *Investigative Ophthalmol. Vis. Sci.* **52** 80–86
[74] Soni K S, Desale S S and Bronich T K 2016 Nanogels: an overview of properties, biomedical applications and obstacles to clinical translation *J. Control. Release* **240** 109–26
[75] Morrison P W and Khutoryanskiy V V 2014 Advances in ophthalmic drug delivery *Ther. Deliv.* **5** 1297–315
[76] Patel S R, Berezovsky D E, McCarey B E, Zarnitsyn V, Edelhauser H F and Prausnitz M R 2012 Targeted administration into the suprachoroidal space using a microneedle for drug delivery to the posterior segment of the eye *Investigative Ophthalmol. Vis. Sci.* **53** 4433–41
[77] Krohn J and Bertelsen T 1998 Light microscopy of uveoscleral drainage routes after gelatine injections into the suprachoroidal space *Acta Ophthalmol. Scand.* **76** 521–7
[78] Tyagi P, Barros M, Stansbury J W and Kompella U B 2013 Light activated, in situ forming gel for sustained suprachoroidal delivery of bevacizumab *Mol. Pharm.* **10** 2858–67

2. Segundo artículo

Rodrigo MJ, **Cardiel MJ**, Fraile JM, Mendez-Martinez S, Martinez-Rincon T, Subias M, Polo V, Ruberte J, Ramirez T, Vispe E, Luna C, Mayoral JA, Garcia-Martin E. **Brimonidine-LAPONITE® intravitreal formulation has an ocular hypotensive and neuroprotective effect throughout 6 months of follow-up in a glaucoma animal model".** Biomater Sci. 2020 Nov 21;8(22):6246-6260. doi: 10.1039/d0bm01013h PMID: 33016285.

Biomaterials Science

ROYAL SOCIETY OF CHEMISTRY

PAPER

View Article Online
View Journal

Check for updates

Cite this: DOI: 10.1039/d0bm01013h

Brimonidine-LAPONITE® intravitreal formulation has an ocular hypotensive and neuroprotective effect throughout 6 months of follow-up in a glaucoma animal model†

M. J. Rodrigo, *[a,b,c,d] M. J. Cardiel, [c,e] J. M. Fraile, [f] S. Mendez-Martinez, [a,b,c] T. Martinez-Rincon,[a,b,c] M. Subias, [a,b,c] V. Polo,[a,b,c] J. Ruberte,[d,g,h,i] T. Ramirez,[c,e] E. Vispe,[j] C. Luna,[c,j] J. A. Mayoral[f] and E. Garcia-Martin[a,b,c,d]

Received 19th June 2020,
Accepted 15th September 2020

DOI: 10.1039/d0bm01013h

rsc.li/biomaterials-science

Intravitreal administration is widely used in ophthalmological practice to maintain therapeutic drug levels near the neuroretina and because drug delivery systems are necessary to avoid reinjections and sight-threatening side effects. However, currently there is no intravitreal treatment for glaucoma. The brimonidine-LAPONITE® formulation was created with the aim of treating glaucoma for extended periods with a single intravitreal injection. Glaucoma was induced by producing ocular hypertension in two rat cohorts: [BRI-LAP] and [non-bri], with and without treatment, respectively. Eyes treated with brimonidine-LAPONITE® showed lower ocular pressure levels up to week 8 ($p < 0.001$), functional neuroprotection explored by scotopic and photopic negative response electroretinography ($p = 0.042$), and structural protection of the retina, retinal nerve fibre layer and ganglion cell layer ($p = 0.038$), especially on the superior-inferior axis explored by optical coherence tomography, which was corroborated by a higher retinal ganglion cell count ($p = 0.040$) using immunohistochemistry (Brn3a antibody) up to the end of the study (week 24). Furthermore, delayed neuroprotection was detected in the contralateral eye. Brimonidine was detected in treated rat eyes for up to 6 months. Brimonidine-LAPONITE® seems to be a potential sustained-delivery intravitreal drug for glaucoma treatment.

1. Introduction

Glaucoma is the second-biggest cause of irreversible blindness worldwide and the leading cause in developed countries. According to the World Health Organization, it affects over 61 million people. The main modifiable risk factor is intraocular pressure (IOP) increase, which leads to progressive retinal ganglion cell (RGC) death and subsequent irreversible vision loss.[1] However, RGC dysfunction and death can also occur in ocular normotensive subjects. Although not fully explored yet, several studies have shown secondary degeneration of retinal cells due to the cytotoxic environment (reactive oxygen species, nitric oxide, glutamate or other free radicals) produced by surrounding affected neurons.[2]

Brimonidine is a highly selective alpha-2 adrenergic pan-agonist lipophilic drug.[3] It has been used in ophthalmological care to produce ocular hypotension since 1974.[4] The 20–30% reduction in IOP[5] is due to its effect on alpha$_{2A,C}$ adrenergic receptors in the ciliary epithelium,[6,7] which inhibit aqueous humour inflow and lead to an increase in uveoscleral

[a]Department of Ophthalmology, Miguel Servet University Hospital, Zaragoza, Spain. E-mail: mariajesusrodrigo@hotmail.es
[b]Aragon Institute for Health Research (IIS Aragon), GIMSO Research Group, University of Zaragoza (Spain), Avda. San Juan Bosco 13, E-50009 Zaragoza, Spain
[c]Miguel Servet Ophthalmology Research Group (GIMSO), Aragon Health Research Institute (IIS Aragon), University of Zaragoza, Spain
[d]RETICS: Thematic Networks for Co-operative Research in Health for Ocular Diseases, Spain
[e]Department of Pathology, Lozano Blesa University Hospital, Zaragoza, Spain
[f]Institute for Chemical Synthesis and Homogeneous Catalysis (ISQCH), Faculty of Sciences, University of Zaragoza-CSIC, C/Pedro Cerbuna 12, E-50009 Zaragoza, Spain
[g]Centre for Animal Biotechnology and Gene Therapy (CBATEG), Universitat Autònoma de Barcelona, Bellaterra, Spain
[h]CIBER for Diabetes and Associated Metabolic Diseases (CIBERDEM), Madrid, Spain
[i]Department of Animal Health and Anatomy, School of Veterinary Medicine, Universitat Autònoma de Barcelona, Bellaterra, Spain
[j]Chromatography and Spectroscopy Laboratory, Institute for Chemical Synthesis and Homogeneous Catalysis (ISQCH), Faculty of Sciences, University of Zaragoza-CSIC, Pedro Cerbuna 12, E-50009 Zaragoza, Spain
†Electronic supplementary information (ESI) available. See DOI: 10.1039/d0bm01013h

outflow.[8,9] The peak occurs within 2–3 hours and lasts until 10–14 hours after instillation.[10] Therefore, to decrease IOP to optimal therapeutic levels, topical eye drops must be administered twice a day by the patient. This can have several disadvantages, such as therapeutic oversights, loss of drug efficacy when crossing the anterior eye structures, and a remarkable 12.7% incidence of ocular and periocular allergic reactions,[11–13] or even intraocular inflammation.[14] These drawbacks worsen patient quality of life and decrease the compliance rate, which lead to progression of the disease.[15] Meanwhile, the neuroprotective effect of brimonidine has been described by many research groups since the four criteria used to evaluate the potential role of a neuroprotective agent are widely proven:[16] (1) brimonidine has targets (alfa-$_{2A,B,C}$ adrenergic receptors for RGCs, glial cells and photoreceptors) in the retina,[7,17] (2) the neuroprotective effect was demonstrated in cell and animal studies,[18–20] mainly in the RGC body and axons, but also in bipolar cells[21] and photoreceptors,[22] (3) it reaches neuroprotection concentration on the posterior segment where the drug interacts with retinal cells,[23,24] and finally (4) it showed neuroprotective characteristics in recent clinical trials in patients with diabetes[25] and age-related macular degeneration.[26]

LAPONITE® $Na^{+0.7}$ $[(Si_8Mg_{5.5}Li_{0.3})O_{20}(OH)_4]^{-0.7}$ is a biocompatible and biodegradable synthetic clay that in recent years has been used in a wide range of biomedical and biomaterial applications, particularly in nanomedicine, regenerative medicine and tissue engineering.[27] LAPONITE® is composed of two-dimensional nanoscale disk-shaped crystals (0.92 nm height, 25 nm diameter, 2.65×10^3 g cm^{-3} density) comprising an octahedral magnesia sheet sandwiched between two tetrahedral silica sheets.[28] When dispersed in aqueous media, a three-dimensional house-of-cards structure is formed. Sodium ions are released, leading to a weak negative-charge surface and further water absorption, resulting in an increase in the clay's volume.[29,30] It forms a clear colloidal dispersion with thixotropic, viscoelastic and transparent gel characteristics, suitable for administration by injection.[28] Since it is able to interact with other molecules by ion-exchange, van de Waals forces, hydrogen bonding, cation/water bridging, protonation or ligand exchange, LAPONITE® is even able to bring into solution compounds that are water insoluble.[31] It can act as a carrier for several drugs,[32] and can also release drugs in a controlled manner depending on surrounding conditions such as pH or temperature.[33–35] Degradation of LAPONITE® releases products that have, by themselves, biological roles; Reffitt *et al.*, showed an increase in collagen type I synthesis because of orthosilicic acid $[Si(OH)_4]$;[36] magnesium ions may also trigger cell responses, stabilize polyphosphate compounds in cells such as adenosine triphosphate (ATP), or be involved in enzymatic activity and signalling processes; sodium cations interfere with the generation of nerve impulses and the hydroelectrolyte balance, and lithium affects the behaviour of neurons.[37,38] Previous animal studies demonstrated LAPONITE®'s safety[39] and analysed the pharmacokinetics and pharmacodynamics up to 24 weeks of intravitreal injection of dexamethasone-LAPONITE® formulation in the vitreous humour of rabbit eyes.[40]

Intravitreal injection is the gold standard therapeutic option for posterior segment pathologies such as age-related macular degeneration, diabetic retinopathy or vascular occlusions. It has long been used in ophthalmological treatment[41] because it maintains therapeutic drug levels at the target site while avoiding ocular barriers.[42] Thus, repeated ocular injections are needed, threatening complications such as IOP elevation, intraocular inflammation, cataract formation, retinal detachment or even endophthalmitis, with a 0.02% incidence per injection in the latter.[43–45] Minimally invasive sustained drug delivery maintains therapeutic concentration for prolonged periods, enhancing the half-life and bioavailability of the drug and preventing the need for frequent administration.[46]

There is currently no intravitreal treatment focused on control of glaucomatous neuropathy that simultaneously decreases the IOP and prevents neuroretinal damage.

To our knowledge, this is the first study demonstrating that a sustained-release brimonidine-LAPONITE® formulation, administered in a single intravitreal injection, exerts a functional and structural ocular hypotensive and neuroprotective effect lasting at least 6 months in a glaucoma animal model.

2. Materials and methods

Chemicals and reagents

Brimonidine and 2-bromoquinoxaline were obtained from Sigma-Aldrich (Madrid, Spain). LAPONITE®-RD (LAP) (surface density 370 m^2 g^{-1}, bulk density 1000 kg m^{-3}, chemical composition: SiO_2 59.5%, MgO 27.5%, Li_2O 0.8%, Na_2O 2.8%) was obtained from BYK Additives (Widnes, Cheshire, UK). Balanced 0.9% salt solution (9 mg ml^{-1} NaCl) (BSS) was obtained from Fresenius Kabi (Barcelona, Spain). HPLC-grade ethanol, acetonitrile, methanol, ammonium formate, formic acid, ammonia and phosphoric acid (85% w/w) were obtained from Scharlab (Barcelona, Spain). Oasis MCX Prime 96-well μElution plates were obtained from Waters Chromatography (Barcelona, Spain).

Brimonidine-LAPONITE® formulation

Brimonidine (BRI) was loaded on LAPONITE® (LAP) following the previously described methodology for dexamethasone.[40,47] Thus, BRI/LAP was prepared by adding LAP (100 mg) to a solution of brimonidine in ethanol (10 mg per 10 ml), stirring at r. t. with solvent evaporation under vacuum to get a good dispersion of brimonidine on the surface. The BRI/LAP powder was stored at −30 °C in tightly capped single-use vials that were gamma-ray sterilized.

Drug load on the LAP was determined using the ultra-high-pressure liquid chromatography mass spectrometry (UHPLC-MS) method (see below). Sample powder (5 mg) was extracted in 5 ml of acetonitrile/ethanol (1/1 v/v). After 1 h of stirring, the sample was centrifuged at 3000 rpm for 10 min at

r.t. and the supernatant was analysed, yielding a total load of 8.98 mg per 100 mg of solid (98.8% of the initial amount).

Immediately before injection, the brimonidine/LAP powder was suspended in BSS (10 mg ml^{-1}) and gently vortexed for 10 min to yield a yellow colloidal dispersion.

Sample processing for pharmacokinetic determination

Each rat eye was cut with dissecting scissors, 1 ml of 5% formic acid solution in acetonitrile was added and the mixture was sonicated at 45 W power for 10 min with a Hielscher UP50H ultrasound processor. Next, 1 ml of 200 mM ammonium formate in 4% phosphoric acid, and 100 μλ of 50 ppm 2-bromoquinoxaline internal standard (IS) in 0.1% formic acid in acetonitrile were added to the purée and the mixture was sonicated for 10 additional minutes. The sample was then centrifuged at 3000 rpm for 10 min. The supernatant was collected and cleaned up by solid phase extraction (SPE) in an Oasis MCX μElution plate. Thus, the supernatant was passed through the adsorbent under vacuum, and the adsorbed sample was rinsed with 600 μl of methanol. The adsorbed BRI and IS were eluted from the plate with 500 μl of 5% ammonia solution in methanol. The collected extract was evaporated under vacuum and dissolved in 200 μl of 0.1% formic acid in acetonitrile. The solution was analysed by UHPLC-MS. Recovery of the analyte was determined on spiked samples of rat eye at three concentration levels (low, medium and high) and was found to be between 92% (lowest concentration level) and 98% (highest concentration level).

Analytical method

Samples were analysed using a Waters Acquity UPLC instrument coupled to a Waters Acquity QDa mass spectrometer. The chromatographic separation was achieved using a Waters Cortecs T3 column (1.6 μm, 2.1 × 75 mm) at 30 °C. The mobile phase comprised a mixture of 0.1% formic acid in water (solvent A) and 0.1% formic acid in acetonitrile (solvent B). Samples (10 μl) were eluted in gradient mode (t = 0 min, 75% A; t = 3 min, 50% A, t = 4 min, 75% A) at a flow rate of 0.5 ml min^{-1}.

The MS instrument was operated in electrospray ionization (ESI) positive mode. Full scan mode (150–500 Da) was used to identify the analytes (m/z = 292 (100%) and 294 for brimonidine and m/z = 209 (100%) and 211 (92.8%) for 2-bromoquinoxaline as the IS). Quantization was carried out in single ion monitoring (SIM) mode (m/z = 292 and 209 for brimonidine and 2-bromoquinoxaline, respectively).

The method was validated according to the ICH guidelines. Selectivity was assessed by analyzing blank samples from non-treated rat eyes, and no interferences were found. Calibration curves for brimonidine were constructed in the range 1–0.025 μg mL^{-1} by plotting the brimonidine/IS peak area ratio vs brimonidine nominal concentration. A weighted ($1/X^2$) linear regression model was applied to fit the data ($r^2 > 0.999$). The measured concentration of the standard samples was found to be within 10% of the nominal concentration, showing the accuracy of the method. The limit of detection (LOD) was found to be 0.005 μg mL^{-1}, calculated by the standard error of the intercept method. The LOD was assessed with a sample of nominal concentration obtained by the method of signal-to-noise ratio of at least 10. The limit of quantization (LOQ) was determined by the standard error of the intercept method and was found to be 0.017 μg mL^{-1}.

Animals

The study was carried out on 91 4 week old Long–Evans rats (40% males, 60% females) weighing from 50–100 grams at the beginning of the study. The animals were housed in standard cages with water and food *ad libitum* in rooms kept at a controlled temperature (22 °C) and relative humidity (55%) with 12-hour dark/light cycles. The work with animals was carried out in the experimental surgery service department of the Aragon Biomedical Research Centre (CIBA). The experiment was previously approved by the Ethics Committee for Animal Research (PI34/17) and was carried out in strict accordance with the Association for Research in Vision and Ophthalmology's Statement for the Use of Animals.

Ocular hypertension (OHT) induction and drug injection procedure

The animals were divided in two cohorts: [non-bri] and [BRI-LAP]. The [non-bri] cohort comprised 31 rats. In this cohort, OHT was induced in the right eye (RE) and the left eye (LE) was untreated and served as the control eye. The [BRI-LAP] cohort comprised 60 rats. In this cohort, OHT was induced in both eyes but the RE received an intravitreal injection with the brimonidine-LAPONITE® (Bri-Lap) formulation. The RE served as the treated hypertensive eye and the LE served as the hypertensive control eye.

Ocular hypertension was generated using the model described by Morrison *et al.* by means of sclerosis of episcleral veins[48] with a hypertonic 1.8 M solution in topical eye drops (*Anestesico doble* Colircusi®, Alcon Cusí® SA, Barcelona, Spain) and general anaesthesia by intraperitoneal (IP) injection (60 mg kg^{-1} of ketamine + 0.25 mg kg^{-1} of dexmedetomidine). To maintain OHT, animals in both cohorts were re-injected every two weeks if IOP measurements were less than 20 mmHg. At the baseline, the [BRI-LAP] cohort received 3 μl[49] of the Bri-Lap formulation (10 mg Bri-Lap per ml; amount of brimonidine injected: 2.69 μg, 0.13 mg ml^{-1} of vitreous humour, considering a rat vitreous volume of 20 μl[50]). Determination of this concentration, applying the corresponding scale correction, was based on the doses given by other authors to rats (8.8 mg of brimonidine in nanoparticles, 0.44 mg ml^{-1} of vitreous, induces neuroprotection),[51] mice (1.07 mg of Bri-tartrate in nanosponges, 0.14 mg Bri per ml of vitreous, induces ocular hypopressure)[52] and rabbits (lower dose of 0.45 mg of Bri-tartrate in microspheres, 0.20 mg ml^{-1} of vitreous, induces ocular hypopressure).[53] REs were intravitreally injected using a Hamilton® syringe (measured in μl) and a glass micropipette, which allowed visualization of the yellowish formulation being administered. After intervention, animals were left to recover at a temperature controlled by

r.t. and the supernatant was analysed, yielding a total load of 8.98 mg per 100 mg of solid (98.8% of the initial amount).

Immediately before injection, the brimonidine/LAP powder was suspended in BSS (10 mg ml^{-1}) and gently vortexed for 10 min to yield a yellow colloidal dispersion.

Sample processing for pharmacokinetic determination

Each rat eye was cut with dissecting scissors, 1 ml of 5% formic acid solution in acetonitrile was added and the mixture was sonicated at 45 W power for 10 min with a Hielscher UP50H ultrasound processor. Next, 1 ml of 200 mM ammonium formate in 4% phosphoric acid, and 100 μλ of 50 ppm 2-bromoquinoxaline internal standard (IS) in 0.1% formic acid in acetonitrile were added to the purée and the mixture was sonicated for 10 additional minutes. The sample was then centrifuged at 3000 rpm for 10 min. The supernatant was collected and cleaned up by solid phase extraction (SPE) in an Oasis MCX μElution plate. Thus, the supernatant was passed through the adsorbent under vacuum, and the adsorbed sample was rinsed with 600 μl of methanol. The adsorbed BRI and IS were eluted from the plate with 500 μl of 5% ammonia solution in methanol. The collected extract was evaporated under vacuum and dissolved in 200 μl of 0.1% formic acid in acetonitrile. The solution was analysed by UHPLC-MS. Recovery of the analyte was determined on spiked samples of rat eye at three concentration levels (low, medium and high) and was found to be between 92% (lowest concentration level) and 98% (highest concentration level).

Analytical method

Samples were analysed using a Waters Acquity UPLC instrument coupled to a Waters Acquity QDa mass spectrometer. The chromatographic separation was achieved using a Waters Cortecs T3 column (1.6 μm, 2.1 × 75 mm) at 30 °C. The mobile phase comprised a mixture of 0.1% formic acid in water (solvent A) and 0.1% formic acid in acetonitrile (solvent B). Samples (10 μl) were eluted in gradient mode (t = 0 min, 75% A; t = 3 min, 50% A, t = 4 min, 75% A) at a flow rate of 0.5 ml min^{-1}.

The MS instrument was operated in electrospray ionization (ESI) positive mode. Full scan mode (150–500 Da) was used to identify the analytes (m/z = 292 (100%) and 294 for brimonidine and m/z = 209 (100%) and 211 (92.8%) for 2-bromoquinoxaline as the IS). Quantization was carried out in single ion monitoring (SIM) mode (m/z = 292 and 209 for brimonidine and 2-bromoquinoxaline, respectively).

The method was validated according to the ICH guidelines. Selectivity was assessed by analyzing blank samples from non-treated rat eyes, and no interferences were found. Calibration curves for brimonidine were constructed in the range 1–0.025 μg mL^{-1} by plotting the brimonidine/IS peak area ratio vs brimonidine nominal concentration. A weighted ($1/X^2$) linear regression model was applied to fit the data ($r^2 > 0.999$). The measured concentration of the standard samples was found to be within 10% of the nominal concentration, showing the accuracy of the method. The limit of detection (LOD) was found to be 0.005 μg mL^{-1}, calculated by the standard error of the intercept method. The LOD was assessed with a sample of nominal concentration obtained by the method of signal-to-noise ratio of at least 10. The limit of quantization (LOQ) was determined by the standard error of the intercept method and was found to be 0.017 μg mL^{-1}.

Animals

The study was carried out on 91 4 week old Long–Evans rats (40% males, 60% females) weighing from 50–100 grams at the beginning of the study. The animals were housed in standard cages with water and food *ad libitum* in rooms kept at a controlled temperature (22 °C) and relative humidity (55%) with 12-hour dark/light cycles. The work with animals was carried out in the experimental surgery service department of the Aragon Biomedical Research Centre (CIBA). The experiment was previously approved by the Ethics Committee for Animal Research (PI34/17) and was carried out in strict accordance with the Association for Research in Vision and Ophthalmology's Statement for the Use of Animals.

Ocular hypertension (OHT) induction and drug injection procedure

The animals were divided in two cohorts: [non-bri] and [BRI-LAP]. The [non-bri] cohort comprised 31 rats. In this cohort, OHT was induced in the right eye (RE) and the left eye (LE) was untreated and served as the control eye. The [BRI-LAP] cohort comprised 60 rats. In this cohort, OHT was induced in both eyes but the RE received an intravitreal injection with the brimonidine-LAPONITE® (Bri-Lap) formulation. The RE served as the treated hypertensive eye and the LE served as the hypertensive control eye.

Ocular hypertension was generated using the model described by Morrison *et al.* by means of sclerosis of episcleral veins[48] with a hypertonic 1.8 M solution in topical eye drops (*Anestesico doble* Colircusi®, Alcon Cusí® SA, Barcelona, Spain) and general anaesthesia by intraperitoneal (IP) injection (60 mg kg^{-1} of ketamine + 0.25 mg kg^{-1} of dexmedetomidine). To maintain OHT, animals in both cohorts were re-injected every two weeks if IOP measurements were less than 20 mmHg. At the baseline, the [BRI-LAP] cohort received 3 μl[49] of the Bri-Lap formulation (10 mg Bri-Lap per ml; amount of brimonidine injected: 2.69 μg, 0.13 mg ml^{-1} of vitreous humour, considering a rat vitreous volume of 20 μl[50]). Determination of this concentration, applying the corresponding scale correction, was based on the doses given by other authors to rats (8.8 mg of brimonidine in nanoparticles, 0.44 mg ml^{-1} of vitreous, induces neuroprotection),[51] mice (1.07 mg of Bri-tartrate in nanosponges, 0.14 mg Bri per ml of vitreous, induces ocular hypopressure)[52] and rabbits (lower dose of 0.45 mg of Bri-tartrate in microspheres, 0.20 mg ml^{-1} of vitreous, induces ocular hypopressure).[53] REs were intravitreally injected using a Hamilton® syringe (measured in μl) and a glass micropipette, which allowed visualization of the yellowish formulation being administered. After intervention, animals were left to recover at a temperature controlled by

3. Results

Intraocular pressure and clinical signs

In the [non-bri] cohort, an IOP increase of >20 mmHg was found in the RE between weeks 1 and 10, peaking at week 7 (29.92 ± 7.39 mmHg). Between week 11 and the end of the study (week 24) IOP remained stable at 17.38 ± 2.87 to 23.66 ± 5.45 mmHg (Fig. 1a).

In the [BRI-LAP] cohort, REs showed normotensive levels (IOP < 20 mmHg) until week 3, after which IOP increased, ranging between 17.36 ± 4.10 and 23.99 ± 4.04 mmHg until the end of the study. LEs also showed progressive increases in IOP throughout follow-up. REs, however, showed statistically significant higher levels of IOP than LEs (Fig. 1b).

When REs from the [non-bri] and [BRI-LAP] cohorts were compared, the eyes treated with Bri-Lap always exhibited statistically lower IOP levels from weeks 1 to 10, and even Bonferroni correction for multiple comparisons (marked with **) was exceeded from weeks 1 to 8 ($p < 0.001$). However, this trend inverted from week 12 and no statistical differences were found after that (Fig. 1a).

The percentage of eyes with OHT (>20 mmHg) in both cohorts was studied and analysis revealed a lower percentage of hypertensive eyes when treated with Bri-Lap up to week 8. This was especially remarkable during the first month (0% *vs.* 72% at week 1, 4.8% *vs.* 88% at week 2, and 28.1% *vs.* 91.7% at week 4, respectively) both in the injected RE but also in the untreated LE. Nevertheless, a higher percentage of hypertensive eyes treated with Bri-Lap intravitreal formulation from the [BRI-LAP] cohort, as compared with the LEs used as hypertensive controls, was found throughout the study (Fig. 1c).

There were no cases of allergic reaction, infection, intraocular inflammation or retinal detachment. Two animals developed cataracts during the episcleral vein sclerosis procedure, though these reverted spontaneously in the subsequent weeks.[56] One case of cataract formation after the intravitreal injection developed, probably due to surgical issues as rats have thick lenses. This animal was thus only used for histological studies. As a remarkable adverse event, fifteen early and unexpected animal deaths occurred without any obvious cause: four rats died at week 2, four rats died at week 4, six rats died at week 8 and one rat died at week 12.

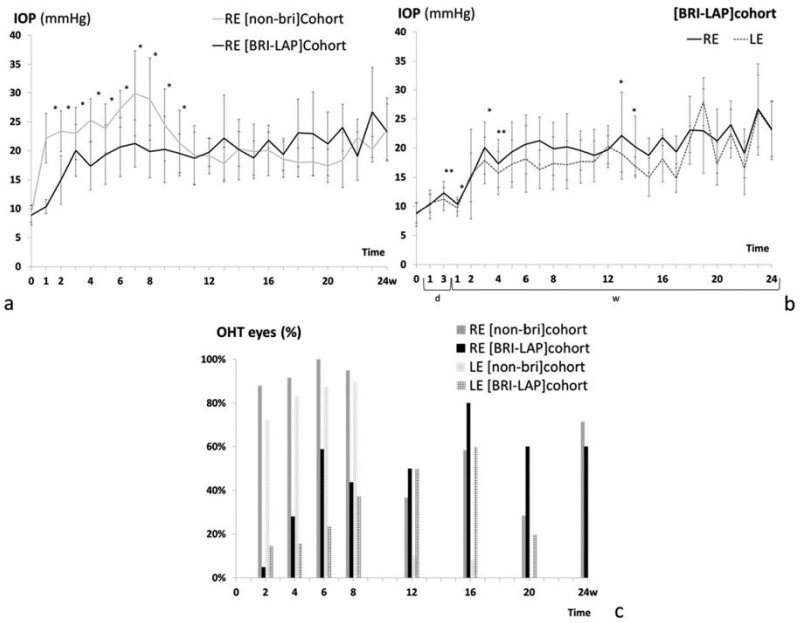

Fig. 1 Intraocular pressure curves. (a) Right eye comparison between the [non-bri] cohort (rats with ocular hypertension in the right eye) and the [BRI-LAP] cohort (rats with ocular hypertension in both eyes and an intravitreal injection of brimonidine-LAPONITE® formulation in the right eye). (b) Comparison between right and left eyes in the [BRI-LAP] cohort. (c) Percentage of ocular hypertensive eyes (>20 mmHg) in the [non-bri] cohort and the [BRI-LAP] cohort during follow-up. Abbreviations: IOP: intraocular pressure; RE: right eye; LE: left eye; w: week; d: day; *$p < 0.05$: statistical differences, **$p < 0.001$: statistical differences with Bonferroni's correction. REs from the [non-bri] cohort received an ocular hypertensive injection by sclerosing the episcleral veins. LEs from the [non-bri] cohort did not receive any treatment. REs from the [BRI-LAP] cohort received an ocular hypertensive injection by sclerosing the episcleral veins plus an intravitreal injection with brimonidine-LAPONITE® formulation. LEs from the [BRI-LAP] cohort received an ocular hypertensive injection by sclerosing the episcleral veins.

Electroretinography

REs from the [non-bri] cohort showed a decreasing tendency in amplitude in *a* (13.25 ± 16.78 *vs.* 67.53 ± 138.31 μV), *b* (44.64 ± 28.20 *vs.* 56.54 ± 53.34 μV) and *PhNR* (18.68 ± 24.77 *vs.* 25.52 ± 26.79 μV) waves when explored using the PhNR protocol at week 24 with respect to week 12, although no statistical differences were found.

The [BRI-LAP] cohort did not exhibit statistical differences in latency between REs and LEs when explored using the scotopic flash ERG protocol, but statistically significant higher amplitudes in *a* and *b* waves were found in the REs injected with Bri-Lap formulation as compared with LEs, mainly with lower intensity stimulus, at 8, 12 and 24 weeks. Similar results were obtained with the PhNR protocol, in which no statistical differences in latency were found between eyes, although a tendency to maintain this value was observed over 24 weeks. Statistically significant higher amplitudes in REs *vs.* LEs were also obtained in *a*, *b* and *PhNR* waves at 8, 12 and 24 weeks. Furthermore, a progressively increasing trend in *PhNR* wave amplitude was found in REs from weeks 8 to 12 (Fig. 2a and b).

When REs from the [non-bri] and [BRI-LAP] cohorts were compared, no statistically significant differences in latency were found using any protocol. The scotopic ERG test at week 24 showed worse statistically significant results in the amplitude and latency parameters in the [BRI-LAP] cohort, but the PhNR protocol revealed statistically significant higher amplitudes in the *PhNR* wave at week 12 and in the *a* and *PhNR* waves at week 24 in eyes treated with the Bri-Lap formulation (Fig. 2c and d).

Optical coherence tomography

In the [non-bri] cohort, REs showed a progressive loss in R, RNFL and GCL thickness measured by OCT over 24 weeks of follow-up.

In the [BRI-LAP] cohort, REs showed a trend towards greater R thickness and lower percentage loss (mainly in the inner sectors at early stages; $p < 0.05$) when compared with untreated contralateral hypertensive LEs (Fig. 3a). Higher RNFL thickness and, consequently, lower percentage loss were found in REs over follow-up with statistically significant differences in the early stages (Fig. 3a). A striking increase in thickness in most sectors was also found at day 3. When analysing the GCL protocol, LEs exhibited greater thickness ($p < 0.05$) in outer sectors in the early stages (outer nasal and outer temporal sectors at weeks 2 and 4, respectively). However, a lower percentage loss trend was observed in REs throughout the rest of the follow-up (ESI Table 1†).

With the aim of finding out the total effect exerted by the Bri-Lap formulation, REs from the [non-bri] and [BRI-LAP] cohorts were compared. Retina scans from the [BRI-LAP] cohort showed a tendency towards greater thickness in the early stages (statistically significant sectors are detailed in Fig. 3b). Analysing the RNFL protocol, a tendency to greater thickness in eyes injected with Bri-Lap formulation was observed from early/intermediate stages through to the end of the study, and the glaucomatous superior/inferior axis showed higher statistical significance (Fig. 3b). According to GCL examinations in the [BRI-LAP] cohort, all sectors (except the temporal sector) exhibited greater thicknesses with statistical significance in the superior/inferior axis at earlier stages (Fig. 3b); at the end of the study (week 24) every single sector from the group injected with Bri-Lap formulation had greater thicknesses, reaching statistically significant differences in the inner inferior and outer temporal sectors (ESI Table 2†).

To evaluate if the Bri-Lap formulation could exert an effect on the contralateral eye, LEs from the [non-bri] cohort (control eye without any treatment, but with contralateral OHT eye) *vs.* LEs from the [BRI-LAP] cohort (OHT eye without treatment but with Bri-Lap injection in the contralateral OHT eye) were compared. No statistical differences were found in most sectors at any of the stages analysed, except at week 24, when greater RNFL thickness was measured in the [BRI-LAP] cohort explored using the RNFL protocol in the nasal superior sector (18.57 ± 6.24 *vs.* 34.60 ± 10.55 μm, $p = 0.023$), and in GCL thickness explored using the GCL protocol in total volume (0.14 ± 0.01 *vs.* 0.15 ± 0.01 μm, $p = 0.030$) and in the inner inferior sector (21.71 ± 1.60 *vs.* 26.20 ± 1.09 μm, $p = 0.004$). LEs from both cohorts were >20 mmHg at week 24. However, by that stage LEs from the [BRI-LAP] cohort had statistically higher axonal and ganglion thickness than LEs from the [non-bri] cohort.

Images from vitreous scans showed hyperreflective aggregates of Bri-Lap formulation dispersed in the vitreous body as floaters, with a tendency to move to the vitreoretinal interface. A progressive decrease in the number and size of Bri-Lap aggregates was also detected over time (ESI Video 1†).

Immunohistochemistry

In experimental glaucoma, accurate measures of the number of RGCs are essential to evaluating the efficacy of novel therapeutic agents.[57] However, because there are around 30 different types of RGCs with different morphologies, gene expression and physiological properties,[58] it is necessary in experimental glaucoma to use a marker that identifies all the different types of RGCs. In this study, we have used an antibody against transcription factor Brn3a that is considered the most reliable pan-marker of RGCs in retinal sections.[59]

As expected,[60] simple visual examination revealed that the central areas of the retina showed greater density of RGCs marked with anti-Brn3a than the peripheral areas (Fig. 4a). Furthermore, the count of positive Brn3a cells along 2 mm of the retina showed that the mean number of RGCs was significantly higher in hypertensive eyes injected with the Bri-Lap formulation than in untreated contralateral hypertensive eyes (REs 23 ± 0.39 *vs.* LEs 20.66 ± 0.98; mean number of RGCs per linear mm of retina, $p = 0.040$) (Fig. 4b and c), confirming the neuroprotective effect of brimonidine during glaucoma.

Although it is generally accepted that glaucomatous damage is a consequence of axonal degeneration that leads to RGC death, glial activation is also present in glaucoma.[61]

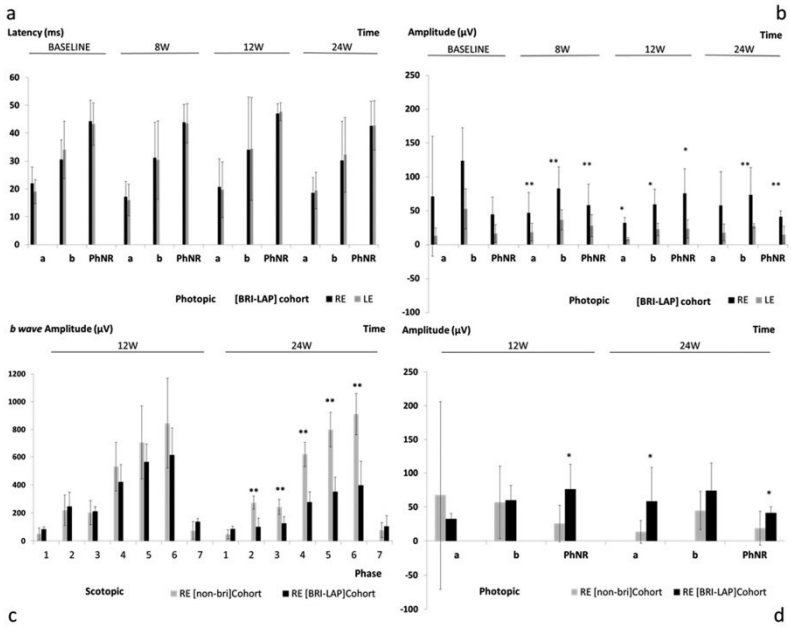

Fig. 2 Functional examinations using electroretinography (ERG). (a) PhNR (photopic negative response) latency from the [BRI-LAP] cohort (rats with ocular hypertension in both eyes and an intravitreal injection of brimonidine-LAPONITE® formulation in the right eye), maintained over 24 weeks. (b) PhNR amplitude, (*a*, *b* and *PhNR* waves) increased and was statistically significantly higher in eyes treated with the Bri-Lap formulation in comparison with contralateral left eyes. (c) The scotopic ERG test showed lower (*b* wave) amplitude at 24 weeks in eyes treated with the Bri-Lap formulation. (d) PhNR amplitude (*a* and *PhNR* waves) was statistically significantly higher in eyes treated with the Bri-Lap formulation in comparison with hypertensive and untreated eyes in the [non-bri] cohort. Abbreviations: RE: right eye; LE: left eye; *a* wave: signal from photoreceptors; *b* wave: signal from intermediate cells; *PhNR* wave: signal from retinal ganglion cells; Phases 1 to 7: multistep procedure with increasing intensity of luminance and different intervals from 0.0003 cds m^{-2} to 3.0 cds m^{-2}; w: week; ms: milliseconds; μV: microvolts; $*p < 0.05$: statistical differences, $**p < 0.001$: statistical differences with Bonferroni's correction.

Experimental IOP triggers GFAP upregulation in astrocytes and Müller cells.[62] To test if the hypotensive effect of brimonidine had any effect on GFAP expression in hypertensive eyes, GFAP immunohistochemistry was performed in the radial eye sections of the [BRI-LAP] cohort. The results obtained showed increased GFAP expression in the ganglion cell layer of the central retina two weeks after injection of a hypertonic solution into the episcleral veins (Fig. 5). In contrast, there was not an obvious increase in GFAP expression in the optic nerve head of glaucomatous eyes (Fig. 5). No differences in GFAP expression were observed between the glaucomatous eyes injected with Bri-Lap (REs) and untreated control eyes (LEs) (Fig. 5), suggesting that the Bri-Lap formulation does not have a beneficial effect on the gliosis produced by the increased IOP.

Concentration of brimonidine in rat eyes

In contrast to our previous study using dexamethasone release in rabbits,[40] this study on rats precluded analysis of the brimonidine content in the different ocular tissues, and total content in the rat eyes was determined after appropriate homogenization and subsequent fractionation by SPE. Fig. 6 shows the brimonidine concentration curves *vs.* time over the course of the study following IV administration of the Bri-Lap formulation. Concentration is expressed in nanograms of brimonidine per ml of the final solution.

Brimonidine concentration remains nearly constant in the first week after IV administration (121.0 ± 25.6 ng ml^{-1}), showing a steady decrease until a plateau was reached at 6 weeks and achieving a value of 62.8 ± 9.0 ng ml^{-1} 24 weeks after administration. Brimonidine levels in contralateral eyes were always below the detection limit.

4. Discussion

In our previous paper, we showed that the release of dexamethasone from LAPONITE® was sustained for up to 6 months in the vitreous body of healthy rabbit eyes.[40] In this

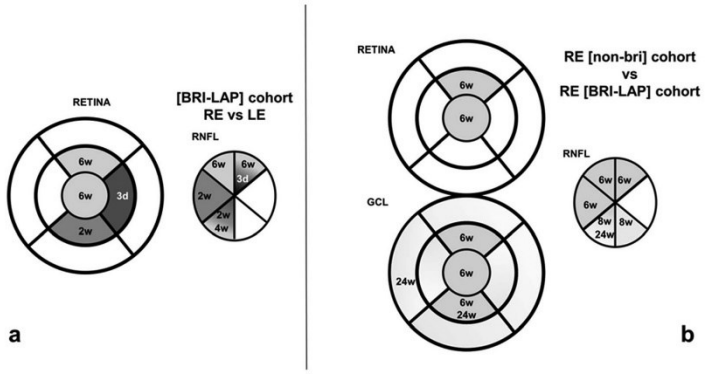

Fig. 3 Neuroretinal analysis using OCT. (a) OCT sectors with increased thickness in right eyes injected with Bri-Lap formulation as compared with untreated left eyes. (b) OCT sectors with statistically significant increases in thickness in right eyes from the [BRI-LAP] cohort as compared with right eyes from the [non-bri] cohort. Dark to light greyish sectors indicate OCT neuroretinal sectors exhibiting greater thicknesses with statistical significance, from earlier to later stages, respectively. Abbreviations: GCL: ganglion cell layer; RNFL: retinal nerve fibre layer; RE: right eye; LE: left eye; w: week; d: day; *$p < 0.05$: statistical differences. REs from the [non-bri] cohort received an ocular hypertensive injection by sclerosing the episcleral veins. LEs from the [non-bri] cohort did not receive any treatment. REs from the [BRI-LAP] cohort received an ocular hypertensive injection by sclerosing the episcleral veins plus an intravitreal injection with brimonidine-LAPONITE® formulation. LEs from the [BRI-LAP] cohort received an ocular hypertensive injection by sclerosing the episcleral veins.

study, we decided to make three important changes: (1) use of brimonidine, a different drug, to demonstrate the generality of the release method; (2) tests in another animal (rats), required before translational trials; and (3) application in a disease model (chronic glaucoma) in order to confirm not only the absence of side effects but also the therapeutic effect over an extended period, the goal being to use the treatment in future glaucomatous patients.

At present, there is no effective intravitreal hypotensive and neuroprotective treatment for glaucoma or other optic neuropathies in daily ophthalmology practice. The results of this study show that a single intravitreal injection of the Bri-Lap formulation, producing sustained release of brimonidine from the LAPONITE® carrier clay for at least 6 months, had a functional and structural hypotensive and neuroprotective effect. As it is administered intravitreally, this formulation would ensure treatment compliance and satisfactory control of the disease over extended periods of time, with administration being necessary perhaps twice yearly.

This paper shows that the Bri-Lap formulation has a net hypotensive effect (decrease of approximately 9 mmHg) when injected into an eye with ocular hypertension (compared to an untreated hypertensive cohort [non-bri]) lasting for 8 weeks. This is twice the time described when using intravitreal nanosponges.[52] The greatest hypotensive effect was observed in the early stages and coincided with the greatest release of brimonidine (approximately 120–80 ng ml^{-1}). It disappeared in later stages when the release of brimonidine plateaued (approximately 60 ng ml^{-1}).

Meanwhile, the fact that in the eye injected intravitreally with the Bri-Lap formulation IOP did not increase until week 3 of the study suggesting that the volume (3 microlitres) did not cause hypertensive iatrogenesis and that the greatest hypotensive effect (14.96 ± 4.16 *vs.* 23.34 ± 3.53 mmHg) occurs within the first two weeks of administration. However, from week 3 onwards the REs injected with Bri-Lap showed higher IOP than the contralateral hypertensive left eyes ($p < 0.05$). This finding may be because of both the variability described for the Morrison technique[56] for hypertensive induction (although all injections were administered by the same experienced ophthalmologist) and the intrinsic characteristics of the clay. LAPONITE® becomes hydrated and expands in volume in aqueous media.[29] However, the brimonidine deposited on the surface produces a hydrophobic effect, which gradually dissipates as release occurs, which would delay hydration and expansion until the surface of the LAPONITE® recovers its hydrophilic characteristics, which appears to occur from week 3 or 4 onwards.

Neuroretinal examinations using OCT technology showed that Bri-Lap formulation enhanced structural protection in axonal (up to week 6) and ganglion structures in intermediate (weeks 6 and 8) and late (weeks 12 and 24) stages. These results support the previous ones, in which the greater hypotensive effect observed in the early stages of the study protected the axons from IOP-dependent damage while the subsequently inferior concentrations of brimonidine (in the order of nanograms) detected in the plateau stage later provided neuroretinal protection by interacting with the retina's adrenergic receptors.[7,17]

Our findings also showed a protective functional effect, as explored with the PhNR ERG and mainly applicable to the RGCs (greater amplitude at week 12) and the axons (main-

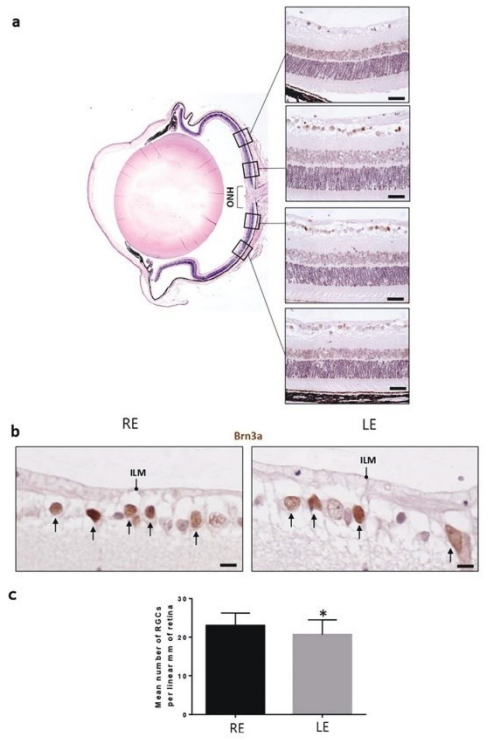

Fig. 4 Retinal ganglion cell analysis in glaucomatous eyes. (a) Retinal ganglion cells were counted in radial sections of the eye along 2 mm of a linear region of the retina, corresponding to four areas, two on each side of the optic nerve head (ONH). (b) Two representative images of the ganglion cell layer marked with anti-Brn3a corresponding to a right eye (RE) and a left eye (LE) of the same animal. Arrows mark the positive nuclei to Brn3a. (c) The mean number of retinal ganglion cells per linear mm of retina was significantly higher in hypertensive eyes injected with Bri-Lap formulation than in the untreated contralateral hypertensive eyes (RE 23.00 ± 0.39 *vs.* LE 20.66 ± 0.98, $p = 0.040$). Abbreviations: RE: right eye; LE: left eye; ILM: internal limiting membrane. Scale bars: (a) 22.72 μm, (b) 5.8 μm.

tained latency). This suggests that the Bri-Lap formulation has a mainly protective effect on the soma of the RGCs, which was corroborated in the histological studies' finding of a higher RGC count using the specific Ac Brn3a. Kim *et al.*,[51] also reported a neuroprotective effect after intravitreal injection of brimonidine-loaded nanoparticles that improved RGC survival in an optic nerve crush model, though this did not last longer than 14 days. The axonal protection provided by intravitreal brimonidine, associated with better anterograde and retrograde transport, has also been demonstrated by other groups.[63,64]

The Bri-Lap intravitreal formulation also has a protective structural and functional effect on the retina in the early stages of treatment (up to week 8; $p < 0.05$). This was maintained in photoreceptors under photopic stimulation (but not under scotopic stimulation) in the later stages (week 24) (see Fig. 3d). Similar results were reported by Ortín-Martínez *et al.*,[22] where topical brimonidine had a protective effect on the cones, and by Yukita *et al.*,[63] who observed conservation of RGC function under photopic conditions but without effect on the *a* and *b* waves of the scotopic ERG. Intraocular injection of brimonidine has also been shown to preserve outer nuclear layer thickness as measured by OCT[65] and even to reduce geographic atrophy secondary to age-related macular degeneration in a phase 2 study with a brimonidine drug delivery system.[26]

The difference found between the protective functional effect on RGCs (observed throughout the study) relative to photoreceptors with photopic stimulus (found at a later stage) may be due to the time required for the formulation to pass through the different layers of the retina and approach the photoreceptors. For instance, week 12 was the earliest that intraretinal Bri-Lap formulation was observed using OCT imaging.

OCT studies of GCL thickness detected a smaller percentage loss of thickness in the REs of the [BRI-LAP] cohort from week 4 onwards (*vs.* LE). However, a higher number of RGCs were counted from the start of the study, indicating that BRI-LAP also had an early neuroprotective effect on the injected eye. This finding seems to suggest underestimation of the neuroprotective effect on the GCL as measured by OCT. Before week 4, the left eyes of the [BRI-LAP] cohort exhibited greater GCL thickness (as measured by OCT) but nonetheless showed a lower number of RGCs (histological studies). This may be due to the increase in the size of the soma prior to ganglion death[66] because, as in the case of other authors who used the same glaucoma model,[48,67,68] RGC death was observed in the early stages of the study (before week 4). Another thickness confusion factor may have been glial infiltration and activation.[69] This was ruled out, however, as glial activation with no statistically significant differences between REs and LEs was detected in the [BRI-LAP] cohort (with induced bilateral glaucoma). Another fact to consider is that the astrocyte and Müller cell reaction (detected using GFAP) occurred at a very early stage of the study (from week 2 onwards) in both OHT-induced eyes, even when IOP was on average less than 20 mmHg. This shows that an upward fluctuation in IOP (albeit in a range considered normotensive: <20 mmHg) triggered a premature immune response resulting in consequent cell death, as also described in ref. 70 and 71.

These analyses seem to suggest a possible error or deviation with regard to considering—in the early stages of the disease—greater GCL thickness, as measured by OCT, as indicative of better condition or protection, and lesser thickness as neurodegeneration. This long-term longitudinal study has demonstrated the dynamism, and therefore change in thickness, that can be quantified by OCT. The authors of this study consider that the results measured by OCT in the early stages should be

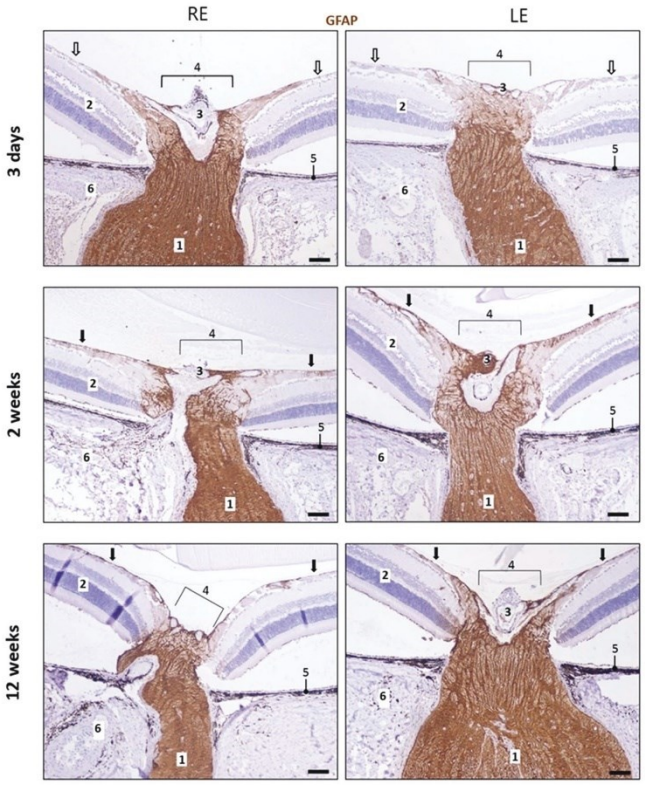

Fig. 5 Increased GFAP expression was observed in the ganglion cell layer of the central retina two weeks after injection of a hypertonic solution into the episcleral veins (black arrows). The Bri-Lap formulation does not induce any obvious change in GFAP expression in the retina or in the optic nerve head in glaucomatous eyes. 1: Optic nerve; 2: Central retina; 3: Central vessel of the retina; 4: Optic nerve head; 5: Retinal pigment epithelium; 6: Sclera; Arrows: central retina without overexpression of GFAP. Scale bars: 82.2 μm.

considered as a whole and not from the simplistic assumption of greater thickness/protection and lesser thickness/damage, as other authors have shown in other inflammatory neurodegenerative diseases.[72]

Interestingly, starting treatment with the Bri-Lap formulation in one eye could also control IOP in the contralateral eye, even though brimonidine levels were below the detection limit. In this regard, it was observed that when LEs from the [BRI-LAP] cohort were compared with LEs from the [non-bri] cohort the percentage of eyes with OHT was lower in the [BRI-LAP] cohort. Even in the later stages of the study (week 24) OCT detected greater thicknesses in the untreated hypertensive LE in the [BRI-LAP] cohort when compared with a healthy normotensive eye (left eye of the [non-bri] cohort) that undergoes the physiological process of ganglion death and is affected by the harmful agents in its OHT-induced contralateral eye.[73] These optimal results may have been a consequence of retrograde and anterograde contralateral substance dissemination *via* the visual pathway[74–76] and of improvement of axonal transport by brimonidine.[77] In addition, brimonidine may spread through the blood vessels. Communication and propagation of molecules to the opposite eye affecting the retina has also been suggested.[78] As brimonidine in the blood was not quantified in this study, neither of these routes can be ruled out.

It is a remarkable hallmark that intravitreal injection of Bri-Lap produces neuroprotection, even with higher IOP ($p < 0.05$), in the treated eye very soon after injection and over a period of six months. Furthermore, to the best of our knowledge, this paper is the first to demonstrate a neuroprotective effect on the eye contralateral to the one treated, which even shows an improvement in degeneration over time.

Brimonidine concentration in the vitreous of treated patients stands at 185 nM.[79] The amounts analysed in the rats

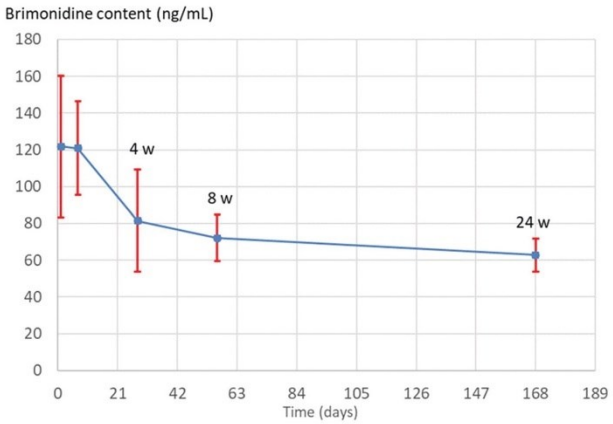

Fig. 6 Mean brimonidine concentrations in rat eyes after intravitreal administration of the Bri-Lap formulation.

in our study reveal an apparent concentration (considering a vitreous volume of 20 µl) ranging from 4.1 µM (week 1) to 2.0 µM (week 24). The decrease in drug levels in the eye throughout the study coincided with the degradation (smaller aggregates over time) of the Bri-Lap formulation observed using OCT (unpublished data). It is an order of magnitude greater than the concentration observed in patients and three orders of magnitude greater than that required for receptor activation, since only 2 nM of alpha-2 agonists are required for maximum receptor activation.[16] This suggests that formulations with lower doses could also be effective while incurring lower risk of side effects.

Brimonidine, in neutral form, shows very low solubility in the aqueous phase. This is one of the reasons why it is usually administered in cationic form (as tartrate). The slow release of Bri-Lap can therefore be explained by two factors: the low solubility of brimonidine and the retention ability of LAPONITE® due to hydrogen bonds and van der Waals interactions, as we previously observed with dexamethasone.[40,47] All brimonidine content (associated or not associated with LAPONITE®) was measured in the eye over the study. As mentioned in the introduction, brimonidine has a short half-life (12 hours) and rapid clearance in the eye.[10] It is probable that at 6 months (60 ng ml^{-1}) most of the analysed brimonidine is associated with LAPONITE®. The very low (unknown) quantity of non-associated brimonidine would not control IOP efficiently in the final stages of the study. This observation concurs with previous authors, showing an initially higher ocular hypopressure effect[52] that decreases later (up to 4 weeks).[53] Drug resistance cannot therefore be ruled out. However, up to the end of the study it showed a neuroprotective effect (as found when using nanoparticles[51]). In addition, the basicity of the Bri-Lap formulation could counteract the acidosis of glaucoma[80,81] and enhance the benefits.

This study demonstrates that using LAPONITE® as a drug carrier for intraocular delivery has several advantages. From a chemical perspective, the Bri-Lap formulation is easy and simple to prepare and drug release is not associated with carrier degradation, unlike other drug delivery systems (DDS).[82] From a clinical perspective, the clear, thixotropic and nanoscale gel formulation allows it to be injected into the vitreous body through smaller-gauge needles, in contrast to Brimo DDS®—which requires applicators[26]—or other devices and implants.[83] To the authors' knowledge, this is the first *in vivo* study of a brimonidine DDS that shows longer sustained reduction of IOP[53,84] and a neuroprotective effect, even in a disease model in which degradation is assumed to occur more rapidly.

Limitations and future studies

It should be mentioned that there was a striking and unexpected level of early death among the rats. This may have resulted from both repetition of intraperitoneal anaesthesia with dexmedetomidine (deaths decreased drastically or disappeared in the later stages when anaesthetic interventions were less frequent), and by the depressant effects of brimonidine on the central nervous system. It may also have been due to potentiation of the effects of both alpha-2 agonists simultaneously.[3] Brimonidine is able to cross the blood–brain barrier,[4] and can cause sedation, bradycardia, hypotension and subsequent death.

Based on all the above, the authors consider that blood analysis and future pharmacodynamic adjustment and scaling studies would be advisable and necessary before exploring potential transferability to clinical practice. It would also be interesting to co-insert[85] different agents in the clay carrier to combat various neurodegenerative pathways using microcapsule systems as described by Arranz-Romera *et al.*[86] Prieto

et al.[40] demonstrated sustained release and tolerance of intraocular dexamethasone with LAPONITE®; this powerful anti-inflammatory drug could combat gliosis and even improve the results achieved in this study, as it appears that the Bri-Lap formulation has no effect on gliosis as there are no differences between eyes or cohorts with respect to GFAP.

5. Conclusions

This paper presents, for the first time, a study in which intraocular administration in a rat eye of a brimonidine-LAPONITE® formulation was well tolerated and had an early functional and structural hypotensive and neuroprotective effect. It acted mainly on retinal ganglion cells and the sustained-release mechanism enabled a single intravitreal injection to last for at least 6 months. The study presents a formulation with potential for transfer to clinical treatment of glaucoma[79] and other optic neuropathies.

Funding

This paper was supported by the Rio Hortega Research Grant M17/00213, PI17/01726, PI17/01946 (Instituto de Salud Carlos III), and by MAT2017-83858-C2-2 MINECO/AEI/ERDF, EU. The funders had no role in the study design, data collection and analysis, decision to publish or preparation of the manuscript.

Conflicts of interest

There are no conflicts to declare.

Acknowledgements

The authors would like to acknowledge the contribution of the staff at the Centro de Investigación Biomédica de Aragón (CIBA) with regard to animal supply, care, feeding and maintenance services and access to the Servicio General de Apoyo a la Investigación-SAI, Universidad de Zaragoza.

References

1 J. B. Jonas, T. Aung, R. R. Bourne, A. M. Bron, R. Ritch and S. Panda-Jonas, Glaucoma, *Lancet*, 2017, **390**(10108), 2183–2193, DOI: 10.1016/S0140-6736(17)31469-1.
2 M. Almasieh, A. M. Wilson, B. Morquette, J. L. Cueva Vargas and A. Di Polo, The molecular basis of retinal ganglion cell death in glaucoma, *Prog. Retinal Eye Res.*, 2012, **31**(2), 152–181, DOI: 10.1016/j.preteyeres.2011.11.002.
3 K. Gyires, Z. S. Zádori, T. Török and P. Mátyus, α2-Adrenoceptor subtypes-mediated physiological, pharmacological actions, *Neurochem. Int.*, 2009, **55**(7), 447–453, DOI: 10.1016/j.neuint.2009.05.014.
4 A. L. Robin and Y. Burnstein, Selectivity of site of action and systemic effects of topical alpha agonists, *Curr. Opin. Ophthalmol.*, 1998, **9**(2), 30–33, DOI: 10.1097/00055735-199804000-00006.
5 R. J. Derick, A. L. Robin, T. R. Walters, *et al.*, Brimonidine tartrate: A one-month dose response study, *Ophthalmology*, 1997, **104**(1), 131–136, DOI: 10.1016/S0161-6420(97)30349-2.
6 D. B. Bylund, Characterization of alpha2 adrenergic receptor subtypes in human ocular tissue homogenates, *Invest. Ophthalmol. Visual Sci.*, 1999, **40**(10), 2299–2306.
7 E. Woldemussie, M. Wijono and D. Pow, Localization of alpha 2 receptors in ocular tissues, *Vis. Neurosci.*, 2007, **24**(5), 745–756, DOI: 10.1017/S0952523807070605.
8 R. Schadlu, T. L. Maus, C. B. Nau and R. F. Brubaker, Comparison of the efficacy of apraclonidine and brimonidine as aqueous suppressants in humans, *Arch. Ophthalmol.*, 1998, **116**(11), 1441–1444, DOI: 10.1001/archopht.116.11.1441.
9 C. B. Toris, M. L. Gleason, C. B. Camras and M. E. Yablonski, Effects of Brimonidine on Aqueous Humor Dynamics in Human Eyes, *Arch. Ophthalmol.*, 1995, **113**(12), 1514–1517, DOI: 10.1001/archopht.1995.01100120044006.
10 T. R. Walters, Development and use of brimonidine in treating acute and chronic elevations of intraocular pressure: A review of safety, efficacy, dose response, and dosing studies, *Surv. Ophthalmol.*, 1996, **41**(Suppl. 1), DOI: 10.1016/s0039-6257(96)82028-5.
11 ★ Vademecum.es -. https://www.vademecum.es/. Published 2013. Accessed May 12, 2020.
12 A. A. Shah, Y. Modi, B. Thomas, S. R. Wellik and A. Galor, Brimonidine allergy presenting as vernal-like keratoconjunctivitis, *J. Glaucoma*, 2015, **24**(1), 89–91, DOI: 10.1097/IJG.0b013e3182953aef.
13 P. K. Sodhi, L. Verma and J. Ratan, Dermatological side effects of brimonidine: A report of three cases, *J. Dermatol.*, 2003, **30**(9), 697–700, DOI: 10.1111/j.1346-8138.2003.tb00461.x.
14 H. I. Becker, R. C. Walton, J. I. Diamant and M. E. Zegans, Anterior uveitis and concurrent allergic conjunctivitis associated with long-term use of topical 0.2% brimonidine tartrate, *Arch. Ophthalmol.*, 2004, **122**(7), 1063–1066, DOI: 10.1001/archopht.122.7.1063.
15 G. A. Alessandro and R. Teresa, Ocular Surface Alterations and Topical Antiglaucomatous Therapy: A Review, *Open Ophthalmol. J.*, 2014, **8**(1), 67–72, DOI: 10.2174/1874364101408010067.
16 L. Wheeler, E. WoldeMussie and R. Lai, Role of alpha-2 agonists in neuroprotection, *Surv. Ophthalmol.*, 2003, **48**(2 Suppl. 1), DOI: 10.1016/S0039-6257(03)00004-3.
17 F. B. Kalapesi, M. T. Coroneo and M. A. Hill, Human ganglion cells express the alpha-2 adrenergic receptor: Relevance to neuroprotection, *Br. J. Ophthalmol.*, 2005, **89**(6), 758–763, DOI: 10.1136/bjo.2004.053025.

18 D. Lee, K. Y. Kim, Y. H. Noh, *et al.*, Brimonidine Blocks Glutamate Excitotoxicity-Induced Oxidative Stress and Preserves Mitochondrial Transcription Factor A in Ischemic Retinal Injury, *PLoS One*, 2012, **7**(10), e47098, DOI: 10.1371/journal.pone.0047098.

19 V. Prokosch, L. Panagis, G. F. Volk, C. Dermon and S. Thanos, α2-adrenergic receptors and their core involvement in the process of axonal growth in retinal explants, *Invest. Ophthalmol. Visual Sci.*, 2010, **51**(12), 6688–6699, DOI: 10.1167/iovs.09-4835.

20 M. P. Lafuente, M. P. Villegas-Pérez, S. Mayor, M. E. Aguilera, J. Miralles de Imperial and M. Vidal-Sanz, Neuroprotective effects of brimonidine against transient ischemia-induced retinal ganglion cell death: A dose response in vivo study, *Exp. Eye Res.*, 2002, **74**(2), 181–189, DOI: 10.1006/exer.2001.1122.

21 C. J. Dong, Y. Guo, Y. Ye and W. A. Hare, Presynaptic inhibition by α2 receptor/adenylate cyclase/PDE4 complex at retinal rod bipolar synapse, *J. Neurosci.*, 2014, **34**(28), 9432–9440, DOI: 10.1523/JNEUROSCI.0766-14.2014.

22 A. Ortín-Martínez, F. J. Valiente-Soriano, D. García-Ayuso, *et al.*, A novel in vivo model of focal light emitting diode-induced cone-photoreceptor phototoxicity: Neuroprotection afforded by brimonidine, BDNF, PEDF or bFGF, *PLoS One*, 2014, **9**(12), 1–30, DOI: 10.1371/journal.pone.0113798.

23 A. R. Kent, J. D. Nussdorf, R. David, F. Tyson, D. Small and D. Fellows, Vitreous concentration of topically applied brimonidine tartrate 0.2%, *Ophthalmology*, 2001, **108**(4), 784–787, DOI: 10.1016/S0161-6420(00)00654-0.

24 Y. Takamura, T. Tomomatsu, T. Matsumura, *et al.*, Vitreous and aqueous concentrations of brimonidine following topical application of brimonidine tartrate 0.1% ophthalmic solution in humans, *J. Ocul. Pharmacol. Ther.*, 2015, **31**(5), 282–285, DOI: 10.1089/jop.2015.0003.

25 R. Simó, C. Hernández, M. Porta, *et al.*, Effects of topically administered neuroprotective drugs in early stages of diabetic retinopathy: Results of the EUROCONDOR clinical trial, *Diabetes*, 2019, **68**(2), 457–463, DOI: 10.2337/db18-0682.

26 B. D. Kuppermann, S. S. Patel, D. S. Boyer, *et al.*, Phase 2 study of the safety and efficacy of brimonidine drug delivery system (brimo DDS) generation 1 in patients with geographic atrophy secondary to age-related macular degeneration, *Retina*, 2020, DOI: 10.1097/IAE.0000000000002789.

27 H. Tomás, C. S. Alves and J. Rodrigues, Laponite®: A key nanoplatform for biomedical applications? *Nanomedicine Nanotechnology, Biol. Med.*, 2018, **14**(7), 2407–2420, DOI: 10.1016/j.nano.2017.04.016.

28 R. Lapasin, M. Abrami, M. Grassi and U. Šebenik, Rheology of Laponite-scleroglucan hydrogels, *Carbohydr. Polym.*, 2017, **168**, 290–300, DOI: 10.1016/j.carbpol.2017.03.068.

29 R. P. Mohanty and Y. M. Joshi, *Chemical stability phase diagram of aqueous Laponite dispersions*, 2015, DOI: 10.1016/j.clay.2015.10.021.

30 L. Z. Zhao, C. H. Zhou, J. Wang, D. S. Tong, W. H. Yu and H. Wang, Recent advances in clay mineral-containing nanocomposite hydrogels, *Soft Matter*, 2015, **11**(48), 9229–9246, DOI: 10.1039/c5sm01277e.

31 M. C. Staniford, M. M. Lezhnina, M. Gruener, *et al.*, Photophysical efficiency-boost of aqueous aluminium phthalocyanine by hybrid formation with nano-clays, *Chem. Commun.*, 2015, **51**(70), 13534–13537, DOI: 10.1039/c5cc05352h.

32 C. Aguzzi, P. Cerezo, C. Viseras and C. Caramella, Use of clays as drug delivery systems: Possibilities and limitations, *Appl. Clay Sci.*, 2007, **36**(1-3), 22–36, DOI: 10.1016/j.clay.2006.06.015.

33 S. Xiao, R. Castro, D. Maciel, *et al.*, Fine tuning of the pH-sensitivity of laponite-doxorubicin nanohybrids by polyelectrolyte multilayer coating, *Mater. Sci. Eng., C*, 2016, **60**, 348–356, DOI: 10.1016/j.msec.2015.11.051.

34 G. Wang, D. Maciel, Y. Wu, *et al.*, Amphiphilic polymer-mediated formation of laponite-based nanohybrids with robust stability and pH sensitivity for anticancer drug delivery, *ACS Appl. Mater. Interfaces*, 2014, **6**(19), 16687–16695, DOI: 10.1021/am5032874.

35 J. Wang, G. Wang, Y. Sun, *et al.*, In Situ formation of pH-/thermo-sensitive nanohybrids via friendly-assembly of poly (N -vinylpyrrolidone) onto LAPONITE®, *RSC Adv.*, 2016, **6**(38), 31816–31823, DOI: 10.1039/c5ra25628c.

36 D. M. Reffitt, N. Ogston, R. Jugdaohsingh, *et al.*, Orthosilicic acid stimulates collagen type 1 synthesis and osteoblastic differentiation in human osteoblast-like cells in vitro, *Bone*, 2003, **32**(2), 127–135, DOI: 10.1016/S8756-3282(02)00950-X.

37 A. M. P. Romani, *Cellular Magnesium Homeostasis*, 2011. DOI: 10.1016/j.abb.2011.05.010.

38 R. Williams, W. J. Ryves and E. C. Dalton, *et al.*, *A molecular cell biology of lithium*, in *Biochemical Society Transactions*, Biochem Soc Trans, 2004, vol. 32, pp. 799–802. DOI: 10.1042/BST0320799.

39 E. Prieto, E. Vispe, A. De Martino, *et al.*, Safety study of intravitreal and suprachoroidal Laponite clay in rabbit eyes, *Graefe's Arch. Clin. Exp. Ophthalmol.*, 2018, **256**(3), 535–546, DOI: 10.1007/s00417-017-3893-5.

40 E. Prieto, M. J. Cardiel, E. Vispe, *et al.*, Dexamethasone delivery to the ocular posterior segment by sustained-release Laponite formulation, *Biomed. Mater.*, 2020, DOI: 10.1088/1748-605X/aba445.

41 R. Bisht, A. Mandal, J. K. Jaiswal and I. D. Rupenthal, Nanocarrier mediated retinal drug delivery: overcoming ocular barriers to treat posterior eye diseases, *Wiley Interdiscip. Rev.: Nanomed. Nanobiotechnol.*, 2018, **10**(2), 1–21, DOI: 10.1002/wnan.1473.

42 P. M. Hughes, O. Olejnik, J. E. Chang-Lin and C. G. Wilson, Topical and systemic drug delivery to the posterior segments, *Adv. Drug Delivery Rev.*, 2005, **57**(14 Spec. Iss.), 2010–2032, DOI: 10.1016/j.addr.2005.09.004.

43 S. Pershing, S. J. Bakri and D. M. Moshfeghi, Ocular hypertension and intraocular pressure asymmetry after intra-

vitreal injection of anti-vascular endothelial growth factor agents, *Ophthalmic Surg. Lasers Imaging Retina*, 2013, **44**(5), 460–464, DOI: 10.3928/23258160-20130909-07.

44 A. Kumar, S. V. Sehra, M. B. Thirumalesh and V. Gogia, Secondary rhegmatogenous retinal detachment following intravitreal bevacizumab in patients with vitreous hemorrhage or tractional retinal detachment secondary to Eales' disease, *Graefe's Arch. Clin. Exp. Ophthalmol.*, 2012, **250**(5), 685–690, DOI: 10.1007/s00417-011-1890-7.

45 D. Dossarps, A. M. Bron, P. Koehrer, *et al.*, Endophthalmitis after intravitreal injections: Incidence, presentation, management, and visual outcome, *Am. J. Ophthalmol.*, 2015, **160**(1), 17–25.e1, DOI: 10.1016/j.ajo.2015.04.013.

46 A. Urtti, Challenges and obstacles of ocular pharmacokinetics and drug delivery, *Adv. Drug Delivery Rev.*, 2006, **58**(11), 1131–1135, DOI: 10.1016/j.addr.2006.07.027.

47 J. M. Fraile, E. Garcia-Martin, C. Gil, *et al.*, Laponite as carrier for controlled in vitro delivery of dexamethasone in vitreous humor models, *Eur. J. Pharm. Biopharm.*, 2016, **108**, 83–90, DOI: 10.1016/j.ejpb.2016.08.015.

48 J. C. Morrison, C. G. Moore, L. M. H. Deppmeier, B. G. Gold, C. K. Meshul and E. C. Johnson, A rat model of chronic pressure-induced optic nerve damage, *Exp. Eye Res.*, 1997, **64**(1), 85–96, DOI: 10.1006/exer.1996.0184.

49 P. Dureau, S. Bonnel, M. Menasche, J. L. Dufier and M. Abitbol, Quantitative analysis of intravitreal injections in the rat, *Curr. Eye Res.*, 2001, **22**(1), 74–77, DOI: 10.1076/ceyr.22.1.74.6974.

50 Determination of Injectable Intravitreous Volumes in Rats | IOVS | ARVO Journals, https://iovs.arvojournals.org/article.aspx?articleid=2354793. Accessed September 1, 2020.

51 K. E. Kim, I. Jang, H. Moon, *et al.*, Neuroprotective effects of human serum albumin nanoparticles loaded with brimonidine on retinal ganglion cells in optic nerve crush model, *Invest. Ophthalmol. Visual Sci.*, 2015, **56**(9), 5641–5649, DOI: 10.1167/iovs.15-16538.

52 W. S. Lambert, B. J. Carlson, A. E. Van der Ende, *et al.*, Nanosponge-mediated drug delivery lowers intraocular pressure, *Transl. Vis. Sci. Technol.*, 2015, **4**(1), 1–16, DOI: 10.1167/tvst.4.1.1.

53 B. Chiang, Y. C. Kim, A. C. Doty, H. E. Grossniklaus, S. P. Schwendeman and M. R. Prausnitz, Sustained reduction of intraocular pressure by supraciliary delivery of brimonidine-loaded poly(lactic acid) microspheres for the treatment of glaucoma, *J. Controlled Release*, 2016, **228**, 48–57, DOI: 10.1016/j.jconrel.2016.02.041.

54 C. Ding, P. Wang and N. Tian, Effect of general anesthetics on IOP in elevated IOP mouse model, *Exp. Eye Res.*, 2011, **92**(6), 512–520, DOI: 10.1016/j.exer.2011.03.016.

55 N. Umeya, Y. Yoshizawa, K. Fukuda, K. Ikeda, M. Kamada and I. Miyawaki, Availability of multistep light stimulus method for evaluation of visual dysfunctions, *J. Pharmacol. Toxicol. Methods*, 2019, **96**, 27–33, DOI: 10.1016/j.vascn.2018.12.005.

56 J. C. Morrison, W. O. Cepurna and E. C. Johnson, Modeling glaucoma in rats by sclerosing aqueous outflow pathways to elevate intraocular pressure, *Exp. Eye Res.*, 2015, **141**, 23–32, DOI: 10.1016/j.exer.2015.05.012.

57 H. A. Quigley, Neuronal death in glaucoma, *Prog. Retinal Eye Res.*, 1999, **18**(1), 39–57, DOI: 10.1016/S1350-9462(98)00014-7.

58 J. R. Sanes and R. H. Masland, The Types of Retinal Ganglion Cells: Current Status and Implications for Neuronal Classification, *Annu. Rev. Neurosci.*, 2015, **38**(1), 221–246, DOI: 10.1146/annurev-neuro-071714-034120.

59 B. Mead, A. Thompson, B. A. Scheven, A. Logan, M. Berry and W. Leadbeater, Comparative evaluation of methods for estimating retinal ganglion cell loss in retinal sections and wholemounts, *PLoS One*, 2014, **9**(10), e110612, DOI: 10.1371/journal.pone.0110612.

60 U. O. J. Dräger, Ganglion cell distribution in the retina of the mouse, *Invest. Ophthalmol. Visual Sci.*, 1981, **20**(3), 285–293.

61 M. R. Hernandez, H. Miao and T. Lukas, Astrocytes in glaucomatous optic neuropathy, *Prog. Brain Res.*, 2008, **173**, 353–373, DOI: 10.1016/S0079-6123(08)01125-4.

62 E. C. Johnson, J. C. Morrison and K. C. Swan, Friend or Foe? Resolving the Impact of Glial Responses in Glaucoma, *J. Glaucoma*, 2009, **18**(5), 341–353, DOI: 10.1097/IJG.0b013e31818c6ef6.

63 M. Yukita, K. Omodaka, S. Machida, *et al.*, Brimonidine Enhances the Electrophysiological Response of Retinal Ganglion Cells through the Trk-MAPK/ERK and PI3K Pathways in Axotomized Eyes, *Curr. Eye Res.*, 2017, **42**(1), 125–133, DOI: 10.3109/02713683.2016.1153112.

64 Y. Kitaoka, K. Kojima, Y. Munemasa, K. Sase and H. Takagi, Axonal protection by brimonidine with modulation of p62 expression in TNF-induced optic nerve degeneration, *Graefe's Arch. Clin. Exp. Ophthalmol.*, 2015, **253**(8), 1291–1296, DOI: 10.1007/s00417-015-3005-3.

65 L. Rajagopalan, C. Ghosn, M. Tamhane, A. Kulkarni and L.-A. Christie, Francisco López MECyto-/neuro-protective effects of brimonidine drug delivery system (DDS) in a non-human primate progressive retinal degeneration model of geographic atrophy (GA) secondary to age-related macular degeneration (AMD) | IOVS | ARVO Journals, *Invest. Ophthalmol. Visual Sci.*, 2019, **60**(9), 2993.

66 G. Kalesnykas, E. N. Oglesby, D. J. Zack, *et al.*, Retinal ganglion cell morphology after optic nerve crush and experimental glaucoma, *Invest. Ophthalmol. Visual Sci.*, 2012, **53**(7), 3847–3857, DOI: 10.1167/iovs.12-9712.

67 A. L. Georgiou, L. Guo, M. Francesca Cordeiro and T. E. Salt, Electroretinogram and visual-evoked potential assessment of retinal and central visual function in a rat ocular hypertension model of glaucoma, *Curr. Eye Res.*, 2014, **39**(5), 472–486, DOI: 10.3109/02713683.2013.848902.

68 B. M. Davis, L. Guo, J. Brenton, L. Langley, E. M. Normando and M. F. Cordeiro, Automatic quantitative analysis of experimental primary and secondary retinal neurodegeneration: implications for optic neuropathies,

Cell Death Discovery, 2016, **2**, 16031, DOI: 10.1038/cddiscovery.2016.31 eCollection 2016.

69 A. I. Ramirez, R. de Hoz, E. Salobrar-Garcia, *et al.*, The role of microglia in retinal neurodegeneration: Alzheimer's disease, Parkinson, and glaucoma, *Front. Aging Neurosci.*, 2017, **9**(Jul), 1–21, DOI: 10.3389/fnagi.2017.00214.

70 O. W. Gramlich, J. Teister, M. Neumann, *et al.*, Immune response after intermittent minimally invasive intraocular pressure elevations in an experimental animal model of glaucoma, *J. Neuroinflammation*, 2016, **13**, 82, DOI: 10.1186/s12974-016-0542-6.

71 H. Chen, K. S. Cho, T. H. K. Vu, *et al.*, Commensal microflora-induced T cell responses mediate progressive neurodegeneration in glaucoma, *Nat. Commun.*, 2018, **9**(1), 3209, DOI: 10.1038/s41467-018-05681-9.

72 A. Petzold, L. J. Balcer, P. A. Calabresi, *et al.*, Retinal layer segmentation in multiple sclerosis: a systematic review and meta-analysis, *Lancet Neurol.*, 2017, **16**(10), 797–812, DOI: 10.1016/S1474-4422(17)30278-8.

73 A. Sapienza, A.-L. Raveu, E. Reboussin, *et al.*, Bilateral neuroinflammatory processes in visual pathways induced by unilateral ocular hypertension in the rat, *J. Neuroinflammation*, 2016, **13**(1), 44, DOI: 10.1186/s12974-016-0509-7.

74 B. M. Davis, L. Crawley, M. Pahlitzsch, F. Javaid and M. F. Cordeiro, Glaucoma: the retina and beyond, *Acta Neuropathol.*, 2016, **132**(6), 807–826, DOI: 10.1007/s00401-016-1609-2.

75 M. Lawlor, H. Danesh-Meyer, L. A. Levin, I. Davagnanam, E. De Vita and G. T. Plant, Glaucoma and the brain: Trans-synaptic degeneration, structural change, and implications for neuroprotection, *Surv. Ophthalmol.*, 2018, **63**(3), 296–306, DOI: 10.1016/j.survophthal.2017.09.010.

76 K. Evangelho, M. Mogilevskaya, M. Losada-Barragan and J. K. Vargas-Sanchez, Pathophysiology of primary open-angle glaucoma from a neuroinflammatory and neurotoxicity perspective: a review of the literature, *Int. Ophthalmol.*, 2019, **39**(1), 259–271, DOI: 10.1007/s10792-017-0795-9.

77 W. S. Lambert, L. Ruiz, S. D. Crish, L. A. Wheeler and D. J. Calkins, Brimonidine prevents axonal and somatic degeneration of retinal ganglion cell neurons, *Mol. Neurodegener.*, 2011, **6**(1), 4, DOI: 10.1186/1750-1326-6-4.

78 A. Pronin, D. Pham, W. An, *et al.*, Inflammasome Activation Induces Pyroptosis in the Retina Exposed to Ocular Hypertension Injury, *Front. Mol. Neurosci.*, 2019, **12**, 36, DOI: 10.3389/fnmol.2019.00036.

79 M. Q. Rahman, K. Ramaesh and D. M. Montgomery, Brimonidine for glaucoma, *Expert Opin. Drug Saf.*, 2010, **9**(3), 483–491, DOI: 10.1517/14740331003709736.

80 A. Gala, Observations on the hydrogen ion concentration in the vitreous body of the eye with reference to glaucoma, *Br. J. Ophthalmol.*, 1925, **9**(10), 516–519, DOI: 10.1136/bjo.9.10.516.

81 D. W. Lu, C. J. Chang and J. N. Wu, The changes of vitreous pH values in an acute glaucoma rabbit model, *J. Ocul. Pharmacol. Ther.*, 2001, **17**(4), 343–350, DOI: 10.1089/108076801753162753.

82 J. Sun, Y. Lei, Z. Dai, *et al.*, Sustained Release of Brimonidine from a New Composite Drug Delivery System for Treatment of Glaucoma, *ACS Appl. Mater. Interfaces*, 2017, **9**(9), 7990–7999, DOI: 10.1021/acsami.6b16509.

83 S. P. Deokule, J. Z. Baffi, H. Guo, M. Nazzaro and H. Kaneko, Evaluation of extended release brimonidine intravitreal device in normotensive rabbit eyes, *Acta Ophthalmol.*, 2012, **90**(5), e344–e348, DOI: 10.1111/j.1755-3768.2012.02418.x.

84 Y. S. Pek, H. Wu, S. T. Mohamed and J. Y. Ying, Long-Term Subconjunctival Delivery of Brimonidine Tartrate for Glaucoma Treatment Using a Microspheres/Carrier System, *Adv. Healthcare Mater.*, 2016, **5**(21), 2823–2831, DOI: 10.1002/adhm.201600780.

85 A. Arranz-Romera, S. Esteban-Pérez, D. Garcia-Herranz, A. Aragón-Navas, I. Bravo-Osuna and R. Herrero-Vanrell, Combination therapy and co-delivery strategies to optimize treatment of posterior segment neurodegenerative diseases, *Drug Discovery Today*, 2019, **24**(8), 1644–1653, DOI: 10.1016/j.drudis.2019.03.022.

86 A. Arranz-Romera, B. M. Davis, I. Bravo-Osuna, *et al.*, Simultaneous co-delivery of neuroprotective drugs from multi-loaded PLGA microspheres for the treatment of glaucoma, *J. Controlled Release*, 2019, **297**, 26–38, DOI: 10.1016/j.jconrel.2019.01.012.

3. Tercer artículo

Rodrigo MJ, Perez del Palomar A, Montolio A, Mendez-Martinez S, Subias M, **Cardiel MJ**, Martinez-Rincon T, Cegoñino J, Fraile JM, Vispe E, Mayoral JA, Polo V, Garcia-Martin E. **Monitoring new long-lasting intravitreal formulation for glaucoma with vitreous images using optical coherence tomography.** Pharmaceutics 2021 Feb 5;13(2):217. Doi: 10.3390/pharmaceutics13020217 PMID: 33562488.

pharmaceutics

MDPI

Article

Monitoring New Long-Lasting Intravitreal Formulation for Glaucoma with Vitreous Images Using Optical Coherence Tomography

Maria Jesus Rodrigo [1,2,3,*], Amaya Pérez del Palomar [4,5], Alberto Montolío [4,5], Silvia Mendez-Martinez [1,2], Manuel Subias [1,2], Maria Jose Cardiel [6], Teresa Martinez-Rincon [1,2], José Cegoñino [4,5], José Maria Fraile [7], Eugenio Vispe [8], José Antonio Mayoral [7], Vicente Polo [1,2] and Elena Garcia-Martin [1,2,3]

1 Department of Ophthalmology, Miguel Servet University Hospital, 50009 Zaragoza, Spain; silviamendezmartinez@hotmail.com (S.M.-M.); manusubias@gmail.com (M.S.); teresamrincon@gmail.com (T.M.-R.); vpolo@unizar.es (V.P.); egmvivax@yahoo.com (E.G.-M.)
2 Miguel Servet Ophthalmology Research Group (GIMSO), Aragon Health Research Institute (IIS Aragon), University of Zaragoza, 50009 Zaragoza, Spain
3 RETICS: Thematic Networks for Co-Operative Research in Health for Ocular Diseases, 28040 Madrid, Spain
4 Biomaterials Group, Aragon Institute of Engineering Research (I3A), University of Zaragoza, 50018 Zaragoza, Spain; amaya@unizar.es (A.P.d.P.); amontolio@unizar.es (A.M.); jcegoni@unizar.es (J.C.)
5 Department of Mechanical Engineering, University of Zaragoza, 50018 Zaragoza, Spain
6 Department of Pathology, Lozano Blesa University Hospital, 50009 Zaragoza, Spain; mjcardielgarcia@gmail.com
7 Institute for Chemical Synthesis and Homogeneous Catalysis (ISQCH), Faculty of Sciences, University of Zaragoza-CSIC, C/Pedro Cerbuna 12, 50009 Zaragoza, Spain; jmfraile@unizar.es (J.M.F.); mayoral@unizar.es (J.A.M.)
8 Chromatography and Spectroscopy Laboratory, Institute for Chemical Synthesis and Homogeneous Catalysis (ISQCH), Faculty of Sciences, University of Zaragoza-CSIC, Pedro Cerbuna 12, 50009 Zaragoza, Spain; evp@unizar.es
* Correspondence: mariajesusrodrigo@hotmail.es; Tel.: +34-619788942 or +34-976765558; Fax: +34-976566234

check for updates

Citation: Rodrigo, M.J.; Palomar, A.P.d.; Montolío, A.; Mendez-Martinez, S.; Subias, M.; Cardiel, M.J.; Martinez-Rincon, T.; Cegoñino, J.; Fraile, J.M.; Vispe, E.; et al. Monitoring New Long-Lasting Intravitreal Formulation for Glaucoma with Vitreous Images Using Optical Coherence Tomography. *Pharmaceutics* **2021**, *13*, 217. https://doi.org/10.3390/pharmaceutics13020217

Academic Editor: Anuj Chauhan
Received: 30 November 2020
Accepted: 2 February 2021
Published: 5 February 2021

Publisher's Note: MDPI stays neutral with regard to jurisdictional claims in published maps and institutional affiliations.

Abstract: Intravitreal injection is the gold standard therapeutic option for posterior segment pathologies, and long-lasting release is necessary to avoid reinjections. There is no effective intravitreal treatment for glaucoma or other optic neuropathies in daily practice, nor is there a non-invasive method to monitor drug levels in the vitreous. Here we show that a glaucoma treatment combining a hypotensive and neuroprotective intravitreal formulation (IF) of brimonidine–Laponite (BRI/LAP) can be monitored non-invasively using vitreoretinal interface imaging captured with optical coherence tomography (OCT) over 24 weeks of follow-up. Qualitative and quantitative characterisation was achieved by analysing the changes in vitreous (VIT) signal intensity, expressed as a ratio of retinal pigment epithelium (RPE) intensity. Vitreous hyperreflective aggregates mixed in the vitreous and tended to settle on the retinal surface. Relative intensity and aggregate size progressively decreased over 24 weeks in treated rat eyes as the BRI/LAP IF degraded. VIT/RPE relative intensity and total aggregate area correlated with brimonidine levels measured in the eye. The OCT-derived VIT/RPE relative intensity may be a useful and objective marker for non-invasive monitoring of BRI/LAP IF.

Keywords: brimonidine; Laponite; drug delivery; glaucoma; nanomedicine; monitoring; optical coherence tomography; vitreous; intravitreal

1. Introduction

Brimonidine is an ocular hypotension drug widely used in ophthalmological clinical care. For adequate therapeutic control, topical administration is recommended twice a day because of its short half-life (approximately 12 h) [1]. Recently, brimonidine also exhibited a neuroprotective effect in retinal ganglion cells (RGCs), photoreceptors and other retinal

cells [2] in animal and human studies [3] and with both topical and intravitreal administration [4]. The short half-life of brimonidine means that periodic intravitreal administration is needed to achieve therapeutic efficacy. However, repeated injection could lead to complications [5]. Therefore, development of sustained drug delivery systems is necessary. Laponite® $Na^{+0.7}[(Si_8Mg_{5.5}Li_{0.3})O_{20}(OH)_4]^{-0.7}$ is a biocompatible and biodegradable clay used in biomedicine [6]. Its safety in intravitreal injection has been demonstrated in animal studies [7–9]. Laponite® forms a transparent gel when dispersed in an aqueous medium. It is able to interact with other molecules, acting as a carrier and releasing the drug in a controlled manner [10]. In this regard, our research group recently demonstrated that an intravitreal formulation (IF) containing brimonidine–Laponite (BRI/LAP) produced a hypotensive and neuroprotective effect in a chronic glaucoma animal model over 6 months of follow-up [9].

The vitreous humour is a 3-D structure mainly composed of water, collagen fibres and hyaluronan that occupies 80% of eye volume. It allows light transmission and intervenes in eye metabolism [11]. A vitreous sample biopsy is a useful means of diagnosing inflammatory, infectious or oncological ocular diseases as well as of carrying out toxicological post-mortem analysis [12,13]. Furthermore, the vitreous humour is becoming increasingly important in clinical practice as it acts as a therapeutic target for posterior pole pathologies involving macular oedema, such as diabetic retinopathy, vascular occlusions or aged-related macular degeneration. However, as an intravitreal treatment for glaucoma is not yet available in clinical practice, many researchers are working to resolve this limitation within a medium-term horizon. The potential interest in using intravitreal administration is to circumvent ocular barriers while avoiding systemic adverse events and, by acting as a reservoir, maintaining therapeutic drug levels near the site of action [14].

Optical coherence tomography (OCT) is an easy-to-handle, cost-efficient, and objective technology that provides high-resolution cross-sectional images. It has long been widely used in clinical practice and research to study neuroretinal structure. Improved OCT devices with swept-source or enhanced vitreous imaging have made it possible to study the vitreous in normal and inflamed states and to study changes to it after treatment [15–17]. However, it has never been used to monitor drug levels in IFs. Currently, loss in IF therapeutic efficacy is evaluated on the basis of changes in neuroretinal structure or decreases in subjective visual acuity measurements, which indicate an increase in disease activity. It would be beneficial, however, to find an objective vitreous monitoring marker with which to quantify the degradation of the injected molecule and which could even anticipate the loss of therapeutic effect before structural retinal changes are detected by OCT, especially as compared with other more expensive or invasive techniques used in research, such as positron emission tomography or magnetic resonance imaging [18,19].

In previous OCT-based studies by this group, BRI/LAP IF was visualised in the vitreous cavity as hyperreflective aggregates [9]. Expanding on this finding, this study uses OCT to analyse changes in the hyperreflectivity signal from the BRI/LAP IF in the vitreous humour in rat eyes over a 24-week period. This paper describes a monitoring marker for the IF, correlates the OCT vitreous signal to drug levels and discusses the therapeutic effect of BRI/LAP IF [9]. It proposes serial OCT as a more affordable and simpler method for monitoring BRI/LAP IF in vivo in animal research.

2. Materials and Methods

2.1. Data Collection

OCT images of the vitreoretinal interface and drug level data were obtained from the experiments carried out in a previous interventional study conducted by the authors [9] (CC BY 4.0 license). In that study, chronic glaucoma was bilaterally induced by biweekly injections of hypertonic solution into the episcleral veins, according to the well-established Morrison model [20], which led to episcleral vein sclerosis and therefore ocular hypertension (OHT). Thereafter, a single 3-µL BRI/LAP IF injection (10 mg BRI/LAP/mL) into the vitreous cavity of right eye (RE) of Long–Evans rats was performed at baseline. Left

eyes (LEs) served as non-treated hypertensive controls. Intraocular pressure was measured with a rebound tonometer (Tonolab® iCare, Helsinki, Finland) for rodent research. The material and methods used for the study were deeply detailed in [9]. In this study, OCT examinations of the 43 treated rats at baseline and at weeks 1, 2, 4, 6, 8, 12, 24 after intravitreal injection were analysed to quantify BRI/LAP IF evolution over 6 months. Another 23 non-treated healthy rats were examined for comparison as non-hypertensive controls. The experiment was approved beforehand by the Ethics Committee for Animal Research of Zaragoza University (PI34/17, 27th June 2017) and was carried out in strict accordance with the Association for Research in Vision and Ophthalmology's Statement for the Use of Animals.

2.2. Optical Coherence Tomography

Images were acquired using a high-resolution OCT device (HR-OCT Spectralis, Heidelberg® Engineering, Heidelberg, Germany) with a plane power polymethylmethacrylate (PMMA) contact lens of 270 µm thickness and 5.2 mm diameter (Cantor+Nissel®, Northamptonshire, UK) adapted to the rats' cornea to obtain higher quality images. The rodent version of this system acquires cross-sectional images by means of 61 b-scans measuring around 3 mm in length and centred on the optic nerve. It has a resolution of 3 microns per pixel generated. A total of 1536 × 496 pixels per image were analysed. The retinal posterior pole protocol with automatic segmentation, eye-tracking software and follow-up application were used to ensure that the same points were re-scanned throughout the study. The "enhance depth imaging" mode was disabled in all cases.

2.3. Brimonidine–Laponite (BRI/LAP) Formulation and Analysis

BRI/LAP was prepared [9] by addition of Laponite (100 mg) to a solution of Brimonidine (10 mg) in ethanol (10 mL) with stirring and then solvent evaporation under a vacuum, to obtain the BRI/LAP formulation in powder form, which was gamma-ray sterilised. BRI/LAP was injected in the form of a yellow colloidal dispersion in balanced saline solution (BSS) (10 mg/mL).

The brimonidine content in the rat eyes was analysed [8,9] using an ultra-high-pressure liquid chromatography mass spectrometer (UHPLC-MS, Waters, Milford, MA, USA). The eyes were first cut into pieces, sonicated with a solution of formic acid in acetonitrile, then with ammonium formate in phosphoric acid and internal standard (2-bromoquinoxaline), centrifuged and the supernatant was cleaned up by solid phase extraction.

2.4. In Vitro Release of BRI from BRI/LAP Formulation

Release was studied in a model of vitreous humour made up of 0.5% sodium hyaluronate in saline solution (pH 7.1–7.4). The release tests were performed by dispersing BRI/LAP (5 mg, weight ratio 1/10, brimonidine amount 454.5 µg) in the extraction medium (0.5 g of the vitreous model) under stirring at 120 rpm at 37 °C. After 24 h the dispersion was centrifuged at 14,000 rpm for 20 min. The liquid phase was separated and the solid was re-dispersed in fresh extraction medium for a new cycle. The liquid phase was diluted with acetonitrile (0.5 mL) containing the internal standard, centrifuged again and analysed by HPLC as described above.

2.5. Analysis of the Intravitreal Formulation Using OCT

The BRI/LAP IF aggregates present in the OCT scans of the vitreoretinal interface were studied. This technique focuses on the analysis of opacities in the vitreoretinal interface by OCT, which does not require a correction factor for its histological correlation [21] and ensures a characterisation of the actual aggregate. These aggregates were defined as being dots dispersed in the vitreous humour or vitreoretinal interface whose larger size, irregularity or greater signal hyperreflectivity differentiated them from background speckle noise.

OCT image contrast was not adjusted at any time. OCT raw images were exported as Audio Video Interleave (AVI) videos. These videos were analysed using a custom program implemented in Matlab (version R218a, Mathworks Inc., Natick, MA, USA). This code allows us to find the inner limiting membrane (ILM) and the inner and outer layers of the retinal pigment epithelium (RPE) by grayscale conversion. This makes it possible to delimit vitreous space and RPE space in each b-scan (Figure 1). The vitreous was defined as the space between the uppermost extent of the b-scan and the ILM, whereas the RPE was defined as the space between the inner and outer layer of the RPE [16,17]. The mean intensity value of these two spaces was calculated as the average of the intensity of all the pixels within each region, obtaining the VIT/RPE relative intensity in each b-scan. Thus, the VIT/RPE relative intensity of each eye is the average of the 61 b-scans. Furthermore, as the BRI/LAP aggregates tend to be deposited on the ILM–retinal nerve fibre layer (RNFL), the inner and outer limits of the ILM–RNFL were determined to obtain the evolution of ILM–RNFL thickness throughout the 24 weeks of follow-up.

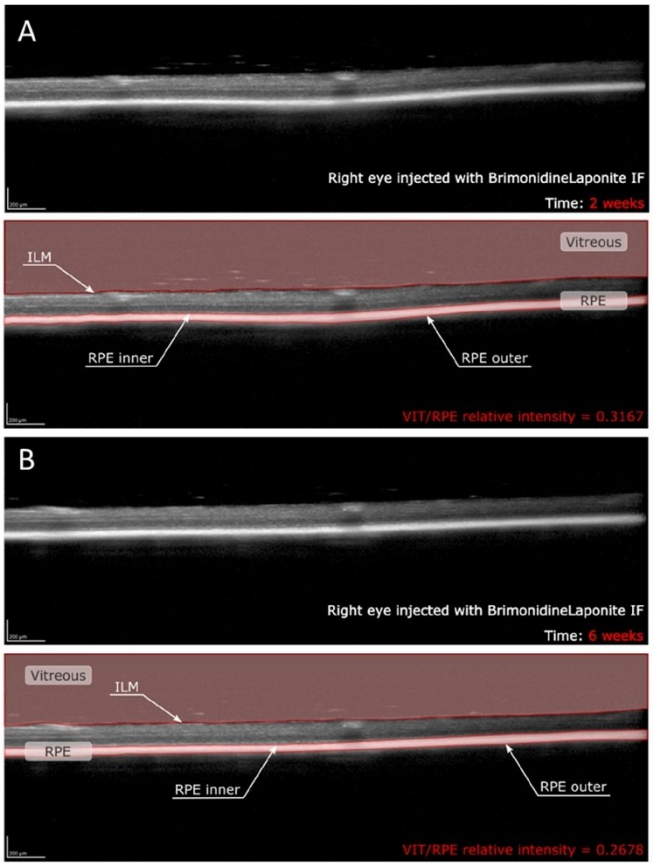

Figure 1. Quantitative assessment of VIT/RPE relative intensity in the same right eye of a rat at (**A**) two weeks and (**B**) six weeks post-injection with brimonidine–Laponite intravitreal formulation. Abbreviations: IF: intravitreal formulation; VIT: vitreous; RPE: retinal pigment epithelium; ILM: inner limiting membrane.

The size of the aggregates in each b-scan was also determined by calculating the number of pixels that each aggregate contains in the image. In the analysed b-scans, there are a total of 761,856 pixels and the image area is 2906 mm^2. Therefore, the ratio is 3815 μm^2/pixel. To calculate that correctly, the background speckle noise of the image was deleted using a denoising filter, which made it possible to distinguish between aggregates and background noise. This filter was implemented in our custom code following the definition of aggregates as larger dots whose intensity is greater than the background intensity. In order to ensure that we only quantify the aggregates produced by the BRI/LAP IF, a minimum limit was established, so that the possible noise [22] due to the physiological components of the eye were not taken into account. This minimum limit was set at 500 μm^2 per aggregate. Once we had calculated the size of each aggregate, we could compute the average area and total area of the BRI/LAP IF in each eye at different stages during the follow-up.

The imaging data were analysed for clinical and drug level information by a masked reader. OCT segmentation was performed by two different researchers, likewise masked, to verify reproducibility.

2.6. Statistical Analysis

All data were recorded in an Excel database, and statistical analysis was performed using SPSS software version 20.0 (SPSS Inc., Chicago, IL, USA). To assess sample distribution, the Kolmogorov–Smirnov test was used. However, given the non-parametric distribution of most of the data, the Mann–Whitney U test was employed to evaluate the differences between both cohorts, and a paired Wilcoxon test was used to compare the changes recorded in each eye over the study period. p values < 0.05 were considered to indicate statistical significance.

3. Results

A total of 186 OCT videos from 43 treated rats (43 hypertensive REs treated with BRI/LAP IF and 29 non-treated hypertensive LEs) and 23 non-treated healthy rats (23 REs/23 LEs) were analysed. The REs injected with the BRI/LAP IF showed hyperreflective dots/aggregates mixing uniformly in the vitreous gel and dispersed as floaters, with a tendency to move toward the vitreoretinal interface during the 24-week follow-up [9]. There was also OCT-guided evidence of the hyperreflective dots crossing the vitreoretinal interface and embedding deeply in the retinal tissue. Particular qualitative characteristics of the behaviour of the BRI/LAP IF observed in several animals are shown in Figure 2.

OCT also detected a progressive decrease over time in the number and size of BRI/LAP aggregates (Figure 3). Figure 4 shows the temporal change in aggregate size. Figure 4A shows that total aggregate area decreased with time over the 24 weeks of follow-up. This drop was very marked during the first 4–6 weeks, after which the change was more gradual. Moreover, total aggregate area increased two weeks after injection. Although a similar trend was observed (aggregate size increased at 2 weeks), this seems to be at the expense of an increase in mean aggregate size. A considerable decrease was then detected around 8 weeks, and from 12 weeks onwards mean aggregate size remained practically constant (Figure 4B).

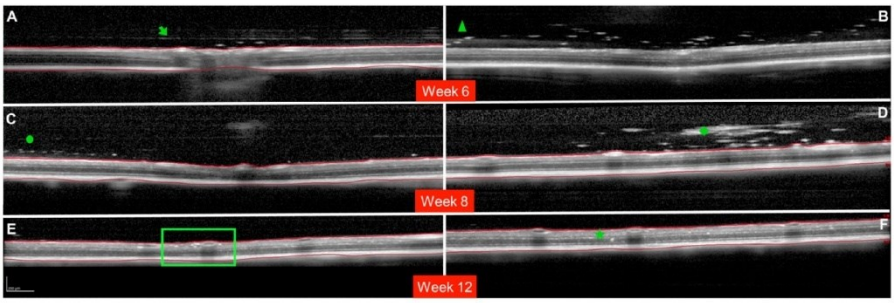

Figure 2. Milestones in the evolution of the brimonidine–Laponite intravitreal formulation (BRI/LAP IF) analysed using optical coherence tomography. (**A**): Cross-sectional image of the optic nerve showing hyper-reflective IF aggregates after crossing the posterior vitreous cortex (PVC). The green arrow points to the posterior vitreous cortex. Three hyper-reflective dots are found in the space between the PVC and the inner limiting membrane (ILM). (**B**): Hyper-reflective aggregates (green triangle) at the moment of crossing the posterior vitreous cortex. (**C**): Hyper-reflective aggregates (green circle) arranged one-by-one in a row. (**D**): Large BRI/LAP IF aggregate (green rhombus) in the vitreous humour. A light optical shadow can be observed (indicating potential perception of floaters) similar to the shadow that retinal vessels produce. (**E**,**F**): Hyper-reflective aggregates penetrating the retinal layers. Deposits in the inner nuclear layer or perivascular (green square). Deposits in the outer nuclear layer (green star). Red lines indicate the ILM and retinal pigment epithelium (RPE) boundaries. (**B**) Shows an example without boundaries (red lines) so as to permit measurement. (**A**,**B**) Show images obtained at 6 weeks of follow-up. (**C**,**D**) Show images obtained at 8 weeks of follow-up. (**E**,**F**) Show images obtained at 12 weeks of follow-up. Representative images are extracted from different animals.

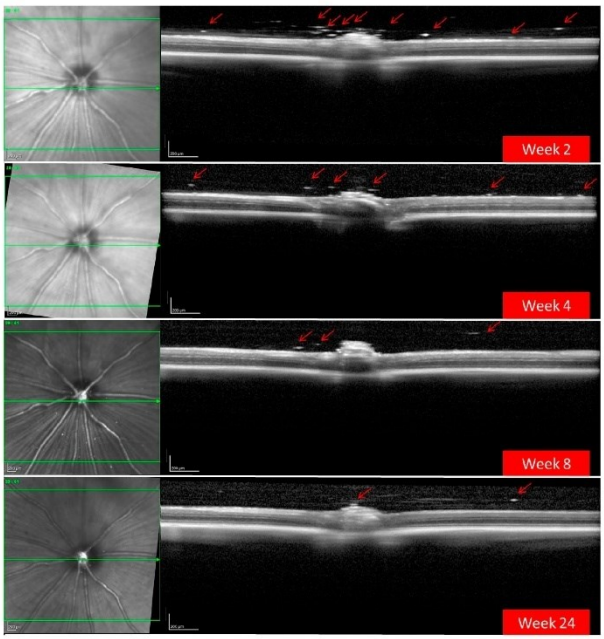

Figure 3. Progressive decrease in hyper-reflective aggregates (red arrows) of the brimonidine–Laponite intravitreal formulation (BRI/LAP IF) detected in the vitreous–retinal interface using optical coherence tomography over 24 weeks of follow-up.

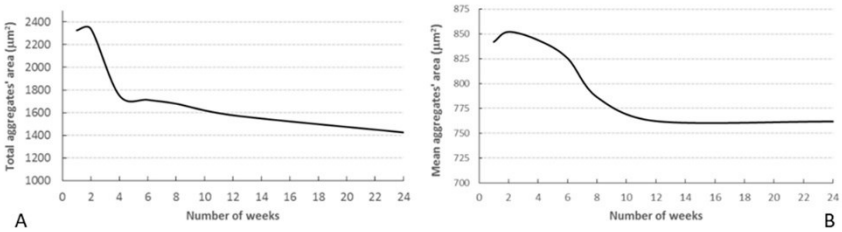

Figure 4. Temporal change in aggregate area. (**A**) Total area of the aggregates located in the vitreous; (**B**) mean area of the aggregates.

OCT analysis revealed the decreasing intensity of the hyperreflective IF aggregates in the vitreous over 24 weeks of follow-up (Figure 5A). The figure shows that the intensity peaked at the end of the second week and then decreased until it stabilised around week 12. It should be noted that the intensity index rose slightly from weeks 4 to 6 and that this coincided with a decrease in total aggregate area (Figure 4A) and a slight increase in mean aggregate area (Figure 4B). Comparison of the intensity indices for REs (treated with BRI/LAP IF) and LEs (non-treated) (Figure 5A) shows that the intensity is very much lower in the LEs (0.30 vs., 0.25; $p < 0.001$). As can be seen, VIT/RPE relative intensity in eyes with glaucoma treated with BRI/LAP IF is higher than in eyes with non-treated glaucoma due to the presence of BRI/LAP IF. Interestingly, the index similarly increased over the first two weeks. This effect could be produced by the induction of glaucoma. Furthermore, the intensity index for non-treated eyes (right and left control eyes; the grey lines in Figure 5A) was also computed. In this case, the intensity value remained constant (0.17). Here, the difference observed in the intensity index between eyes with glaucoma and healthy controls is produced by glaucoma induction. Finally, we observed that the aggregates were initially distributed throughout the vitreous but as time went by (6 to 8 weeks) they settled on top of the ILM–RNFL. It was not possible to distinguish between the aggregates and the ILM–RNFL because the intensity values are very similar. Therefore, this co-layer was segmented in order to measure the deposited aggregates. Figure 5B shows how RE ILM–RNFL thickness increased until it plateaued at week 12. This increase in thickness is directly related to the aggregates' distribution on top of the retina. In the same plot, LE (untreated) ILM–RNFL thickness remained unaltered or decreased slightly during the follow-up if no aggregates were present. Furthermore, we previously not only ruled out that the thickness increase in the treated eye was a consequence of neurodegeneration or cystoid oedema, but also observed functional neuroprotection and a higher RGC count [9].

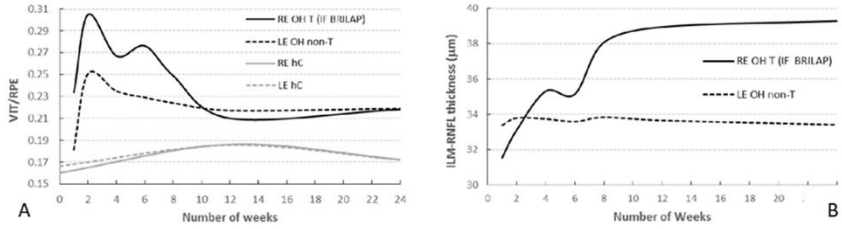

Figure 5. (**A**) Mean VIT/RPE relative intensity in rats with induced bilateral glaucoma (RE treated with brimonidine–Laponite) and healthy controls over 24 weeks of follow-up. (**B**) Segmentation of the ILM–RNFL in rats with induced bilateral glaucoma (RE treated with brimonidine–Laponite) over 24 weeks of follow-up. Abbreviations: RE: right eye; LE: left eye; OH: ocular hypertension; T: treated; BRI/LAP IF: Brimonidine–Laponite intravitreal formulation; non-T: non-treated; hC: healthy control; ILM: inner limiting membrane; RNFL: retinal nerve fibre layer.

Finally, a 3-D reconstruction of the 61 b-scans from a specific rat was performed in order to assess the qualitative decrease in aggregates with time. Figure 6 shows the same eye at 2 weeks of follow-up and then 6 weeks later (8 weeks of follow-up). It clearly shows that the aggregates are widely dispersed 2 weeks post-injection, and that 6 weeks later the aggregates are fewer and smaller and have practically disappeared from the vitreous humour.

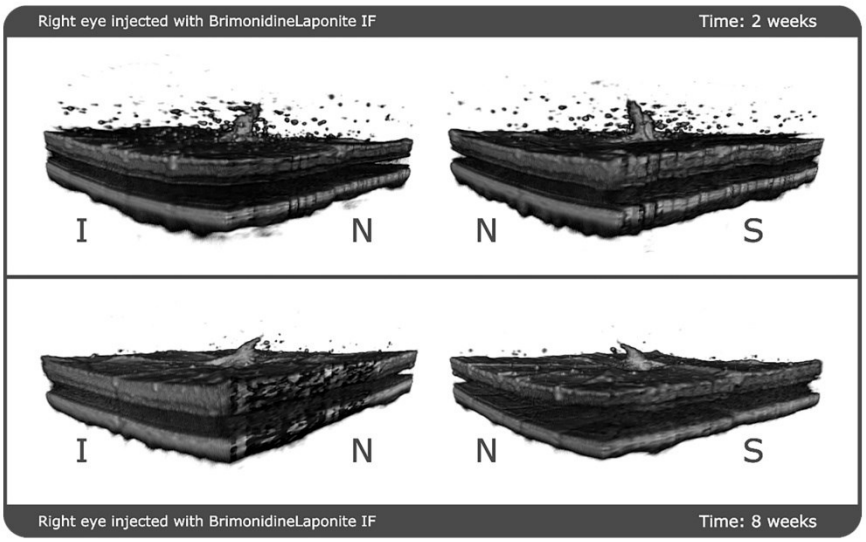

Figure 6. 3-D reconstruction of the evolution of the aggregates at 2 weeks and 8 weeks of follow-up. The reconstruction is shown from two different perspectives at each point in time. Abbreviations: N: nasal; I: inferior; S: superior; IF: intravitreal formulation.

In order to investigate if the vitreous OCT data could serve as an objective marker for non-invasive monitoring of the IF, the curve of the brimonidine levels extracted from our previous study [9] (CC BY 4.0 license) was correlated with the VIT/RPE relative intensities and with the curve of the total aggregate area (as an expression of the total amount of IF injected) obtained using OCT at weeks 1, 4, 8, and 24 after intravitreal injection. Both the brimonidine levels and the VIT/RPE relative intensity curves showed a negative linear tendency with a direct correlation ($y = -0.0003x + 0.1016$ $R^2 = 0.5616$ vs. $y = -0.0002x + 0.2543$ $R^2 = 0.4301$, respectively). Moreover, the logarithmic curves of the brimonidine levels and the total aggregate area were very similar (Figure 7).

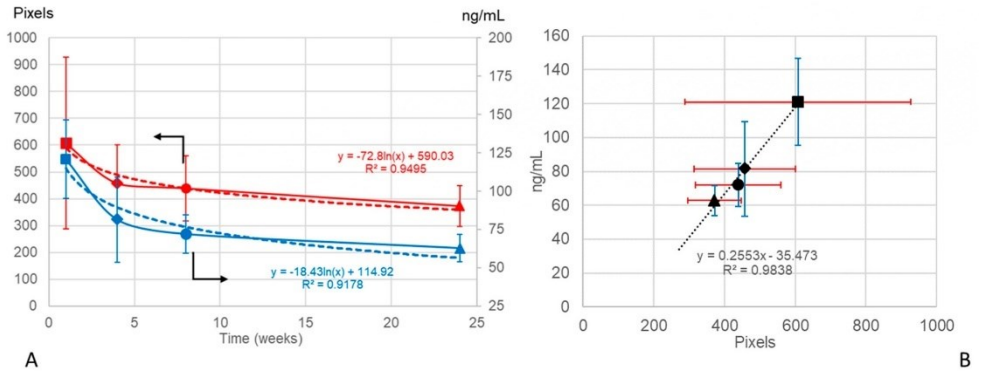

Figure 7. (**A**) Decreasing brimonidine level curves in rat eyes expressed in ng/mL (mean ± standard deviation; n = 3 eyes in each study time) (data from [9] (CC BY 4.0 license)) (in blue) and total aggregate area in the rat eye vitreous expressed in pixels (mean ± standard deviation; n = 9 eyes at week 1, n = 21 eyes at week 4, n = 8 eyes at week 8 and n = 5 eyes at week 24), obtained using optical coherence tomography (in red) over 24 weeks of follow-up. Logarithmic curves in dashes. (**B**) Positive linear correlation between drug levels and total aggregate area. Data are expressed as means ± standard deviation; optical coherence tomography (OCT) data in red; brimonidine data in blue; ■: 1 week; ♦: 4 weeks; ●: 8 weeks; ▲: 24 weeks.

A short in vitro study was performed to compare with the results obtained in the in vivo study. A model for vitreous humour (VHM) formed by sodium hialuronate in saline solution was chosen as medium for release, and the procedure was analogous to our precedent study with the DEX/LAP system [23], with equilibration of the BRI/LAP formulation in the VHM for 24 h, centrifugation to separate the liquid phase with the released BRI for analysis and re-suspension of the solid in a new batch of VHM. As can be seen in Figure 8, the released amount was higher in the first extractions, indicating the presence of a fraction of BRI loosely bound to LAP, whereas the released amount in the successive extractions is much lower, corresponding to the BRI fraction more tightly bound to LAP. In any case, the total amount released after eight extractions is lower than the 22% of the total BRI present in BRI/LAP, confirming in this way the ability of this formulation for a sustained release for a long time period.

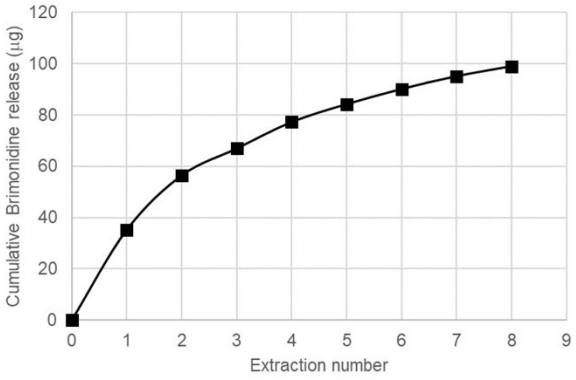

Figure 8. Cumulative release of BRI from BRI/LAP to the model of vitreous humour.

4. Discussion

This paper describes use of OCT to perform non-invasive monitoring of an intravitreal formulation (BRI/LAP) used to treat glaucoma.

Qualitative study made it possible to observe the behaviour of BRI/LAP IF in the vitreous and retina over a 24-week period [9]. In the early stages of the study the BRI/LAP IF was mixed in the vitreous, remaining in suspension in small microaggregates that later showed a tendency to approach and attach to the retina, possibly due to brimonidine tropism towards the alpha-adrenergic receptors present in the ganglion cell layer, inner nuclear layer and outer nuclear layer [24], melanin, the RPE and the choroid. In animal studies, brimonidine has been shown to have both a functional and a structural neuroprotective effect. Intravitreal administration of brimonidine-loaded nanoparticles has shown a neuroprotective effect over 14 days of monitoring [4], a hypotensive and neuroprotective effect lasting 4 weeks in an acute glaucoma model [25] and, recently, our group [9] demonstrated a functional and structural hypotensive and neuroprotective effect lasting 6 months with BRI/LAP IF in a chronic glaucoma model. This was proved not only by analysing the neuroretinal thickness with OCT and the functionally with electroretinography, but also by analysing images of the vitreoretinal interface obtained with OCT, which is a novel measurement method that could provide a non-invasive, objective and reliable means of monitoring the pharmacodynamics of the IF. In addition, brimonidine has been shown to be effective in clinical trials with human patients when administered topically to treat diabetic retinopathy [3] and intravitreally with a brimonidine drug delivery system (Brimo DDS Allergan®, Irvine, CA, USA) in geographic atrophy from age-related macular degeneration [26]. The administration of Brimo DDS® requires an applicator and therefore larger gauge needles, as well as re-implantation every 3 months. A potential sustained-release intravitreal injection-based therapy such as BRI/LAP IF could be effective and useful in these patients as it offers advantages such as injection with smaller micrometric needles, nanoscale formulation and longer therapeutic effects lasting up to 6 months [9].

Repeated intravitreal injections can increase intraocular pressure (IOP) and alter the structure of the optic nerve [27], which can hinder or skew diagnosis and follow-up based on OCT measurements, which are very important in assessing progression in glaucoma. Hence, the use of sustained release systems is necessary in order to reduce re-injection and risk to patients. In this regard, Laponite produced sustained release of drugs for at least 6 months [7–9] and improved the solubility of hydrophobic substances such as brimonidine, thereby facilitating their administration and diffusion within the vitreous.

For the formulation injected into the vitreous to reach the retinal cells (and exert its effect), it must pass through the posterior vitreous cortex (PVC) as well as the ILM, which has pores measuring 10–20 nm. OCT showed hyperreflective aggregates capable of traversing the PVC and ILM and reaching the intraretinal space, possibly by diffusion (Figure 2) due to the small size of the Laponite platelets (1 nm high, 30 nm diameter) [6] and the lipophilicity of brimonidine. In this regard, various authors also found internalisation of drug delivery systems in the retina. Koo et al. [28] described the passage of intravitreal nanoparticles through the retina by both diffusion and endocytosis by the Müller cells, and Xu et al. [29] found that cationic amphiphilic intravitreal polymers reached RPE cells. The space between the ILM and the PVC houses an interdigitate extracellular matrix [15]. In this space, the authors observed that the BRI/LAP IF arranged itself in a row with the aggregates ordered one after the other at different heights, concentrically (see Figure 2A,C and Figure 6). This arrangement is similar to that proposed in the formation of Laponite film, [30] exhibiting a side-by-side arrangement of the Laponite platelets and subsequent stacking of them in different layers. This arrangement is favoured by several film-forming methods, including the Langmuir–Blodgett method, in a liquid–solid interface similar to the vitreous–retina interface, and even more so in the case of hybrid films with organic molecules and macromolecules [31].

OCT was fundamental to demonstrate in vivo degradation of the amount of BRI/LAP IF injected (based on total aggregate area) and morphological and dynamic aggregation of

the Laponite molecules (based on mean aggregate area). Acidosis [32] and inflammatory proteins [33] have been detected in the vitreous of glaucoma patients. In both situations, Laponite degradation increases. In our in vivo study (coinciding with the in vitro study), the highest rate of BRI/LAP IF degradation with brimonidine release occurred in the early stages (the largest decrease in total aggregate area occurred in the first 2–6 weeks (Figure 4A)). However, between the middle of the study and the end (at 24 weeks) degradation happened very slowly and the size of the aggregates remained stable. In our previous paper [9], we demonstrated that the BRI/LAP IF produced an early hypotensive effect until 6–8 weeks (peaking at 2 weeks) (see Table 1) that coincided with higher levels of brimonidine in the eye, with the greatest aggregates' area (Figure 4B) and relative intensities of VIT/RPE (Figure 5A), as well as a neuroprotective effect mainly occurring in the later stages (with sustainedly low levels of brimonidine), quantified in the form of reduced retinal RGC death. This reduced RGC death, which brimonidine achieves by blocking the excitotoxicity of the glutamate [34], is probably why the vitreous acidosis was maintained or did not increase and, consequently, why the BRI/LAP IF degradation rate was slower in the later stages. In addition, Laponite aggregates in situations in which pH is very low (acidosis) [35]. Greatest aggregation observed using OCT (measured as an increase in the area of the aggregate) was found in the early stages, coinciding with the onset of the damage induced by ocular hypertension and, therefore, increased acidosis. However, at later stages the aggregates were much smaller, suggesting less acidosis. Both OCT analyses of the aggregates (degradation based on total aggregate area, and aggregation based on mean aggregate area) support the idea of lower cell death due to neuroprotection in the later stages. This suggests a possible correlation/association between analysis of the vitreous using OCT with BRI/LAP IF and the results of structural analysis using OCT and retinal histology [9].

Table 1. Effect of BRI/LAP IF on intraocular pressure.

TIME	OHT (>20 mmHg) EYES (in %)		Intraocular Pressure (X ± sd)		
	Non-Treated	Treated	Non-Treated	Treated	*p*
BASELINE	0	0	9.12 ± 1.48	8.86 ± 1.69	0.476
2 w	88	4.8	23.34 ± 3.53	14.96 ± 4.16	<0.001
4 w (1 m)	91.7	28.1	25.26 ± 3.69	17.36 ± 4.10	<0.001
6 w	100	58.8	27.22 ± 3.15	20.64 ± 5.04	<0.001
8 w (2 m)	95	43.8	28.93 ± 7.11	19.85 ± 4.51	<0.001
12 w (3 m)	36.8	50	19.10 ± 3.07	19.70 ± 2.39	0.423
16 w (4 m)	58.3	80	20.05 ± 4.35	21.79 ± 1.42	0.364
20 w (5 m)	28.6	60	17.38 ± 2.87	21.19 ± 5.49	0.166
24 w (6 m)	71.4	60	23.66 ± 5.45	23.26 ± 4.82	0.684

Abbreviations: BRI/LAP IF. Brimonidine/laponite intravitreal formulation; OHT: ocular hypertension; w. week; m: month; $p < 0.05$: statistical significance; %: percentage; X ± sd: media ± standard deviation. Data from [9] (CC BY 4.0 license).

The OCT study of the vitreoretinal interface was also helpful in understanding a phenomenon that was unresponsive in our previous study [9]. We found that although BRI/LAP IF generally exerted a hypotensive effect on the eye treated, a peak in IOP was detected in week 3 compared to the non-treated LE. Laponite swells in aqueous media, so we hypothesised that an increase in the size of the aggregate was responsible for the IOP increase. In this study based on OCT monitoring of aggregates, as expected, an increase in size of the BRI/LAP IF was measured in the early stages (2–3 weeks), confirming our hypothesis.

Studying pharmacokinetics or tracing in relation to an IF in the visual pathway is not simple [14] as it requires invasive biopsies or tests that are either very expensive or only accessible to researchers [18]. OCT is a non-invasive technology capable of offering almost histological images depending on the light transmitted or reflected as light passes through different structures with differing densities. Those areas that light finds it harder to pass

through have higher optical densities (e.g., lipid or calcium membranes), and different optical density ratios have been found according to pathology [36]. The increase in signal offered by BRI/LAP IF may be a consequence of the lipophilicity of the brimonidine and the silicon and magnesium components of the Laponite.

As OCT is a light-scattering imaging technique, higher VIT/RPE relative intensity would indicate greater light scattering, with risk of perception of floaters. In this regard, the size of the aggregates was in the order of microns (from 850 to 760 microns) (Figure 4B), much smaller than the commercially available Ozurdex® implant measuring 0.46 × 6 mm (22G needle) or Brimo DDS® (25G needle) [26]. Larger aggregates potentially perceivable as floaters (Figure 2D) were nevertheless observed occasionally. It was only in the largest and least frequently occurring sizes that a posterior shadow was detected. In most aggregates no shadow was detected, suggesting that potential floater perception would be minimal or non-existent. This was reinforced by the fact that the animals did not exhibit any abnormal behaviour.

Two previous studies involving intravitreal administration of Laponite and using indirect ophthalmoscopy [7,8] describe the IF as a single floccule/lump floating in the vitreous. However, in this study observations of large floccules were incidental/isolated. Laponite has thixotropic characteristics that facilitate IF injection fluidity by using smaller-gauge needles (such as the Hamilton μLSyringes® used in this study) [9]. Likewise, the injection force or speed and the needle gauge used have been shown to influence turbulence and mixing after injection of aqueous and viscous solutions into the vitreous gel [37]. This study suggests that BRI/LAP IF administration using smaller-gauge needles would, in addition to causing less patient discomfort, prevent the formation of large floccules.

In this paper, OCT analysis of the vitreous shows that VIT/RPE relative intensity is (1) significantly higher in eyes treated with IF than in non-treated eyes; (2) that intensity values decrease over time; (3) that scores can be calculated with a high degree of reproducibility; and (4) that the total aggregate area correlates with the amount of brimonidine at all stages of the study and shows a similar degradation curve. Therefore, VIT/RPE relative intensity would be an objective marker. The advantage of this OCT-guided analysis of IF persistence in the vitreous would be the possibility of acquiring simple measurements in repeatable explorations at any stage of disease development. This would help detect or predict a loss of treatment efficacy, avoiding detection of the absence of therapeutic effect only after retinal structural damage occurs, in other words as the disease progresses, as is currently the case with glaucoma. Moreover, it also makes it possible to evaluate the rate of IF degradation individually per patient, thereby making precision medicine more personalised [38]. In addition, guided OCT evaluation can reduce sample size as well as cost both in animal studies and in future clinical trials with patients.

VIT/RPE relative intensity has been used because in previous studies it proved, as a marker of inflammation, to be a repeatable measure with a high degree of reproducibility and sensitivity [16]. Furthermore, Sreekantam et al. [17] mentioned that the RPE signal may be slightly attenuated in the case of macular oedema, resulting in lower VIT/RPE relative intensity. However, glaucoma does not present with oedema, so presumably the utility would be maintained in this pathology, perhaps with even greater reliability.

Limitations of the Study

The depth of the vitreous analysed using OCT is partial and limited to a maximum of 1.9 mm. The authors consider that the analysis performed on the vitreoretinal interface using a follow-up protocol (which involves studying the exact same location in serial scans) presents a representative sample of the complete vitreous gel. This view is shared by other researchers who demonstrated the use of vitreoretinal interface analysis as a non-invasive measure correlated with eye inflammation in animal and human studies [21,39]. The high correlation shown in the results (OCT signal intensity vs. brimonidine concentration in the eye) demonstrates applicability in rats and, presented as a logarithmic scale, suggests that study of the whole vitreous body would not be necessary. However, these animals

have a huge lens and therefore a very small vitreous volume compared to humans. In further studies full analysis of the vitreous body would be recommended to corroborate the applicability of this monitoring in animals with a similar organisational structure to humans, such as pigs or dogs. For that purpose, swept-source OCT would help to enhance visualisation of the vitreous cavity. Moreover, as noted above, the increased signal obtained with IF may be a consequence of lipolicity of brimonidine inserted between the silica and magnesium components of the Laponite. This technique seems to be suitable for hyperreflective IF, in contrast to previous therapies injected into the vitreous humour. In this study, blank Laponite was not used because it was previously shown to have an intraocular durability of up to 6 months [7–9]. We are now focusing on IF monitoring for therapeutic application of glaucoma over a long period of time. However, it would be desirable to conduct further studies with only Laponite evaluated with OCT. This study was conducted without enhanced vitreous imaging technology, which could have helped reveal more subtle diffusion characteristics that were not found with the technology used. This research was performed using a commercially available OCT device employed in animal study and a protocol customised specifically for OCT image analysis. Automated analysis of the type that already exists for the study of the neuroretina and that would allow for graduation of signal intensity loss or its rate at the time of acquisition would be beneficial and would facilitate real-time clinical decision-making.

Another limitation could be that some of the hyperreflective dots were due to latent inflammation [16] secondary to the induction of glaucoma and alteration or increase in signal intensity. Eye infection and severe vitritis were discarded in rat eyes injected with BRI/LAP IF in our previous study [9], (CC BY 4.0 license). In this regard, the vitreous cells, hyalocytes, can be exacerbated in inflamed eyes [40] and vitreous changes are early markers of retinal damage [41]. Several studies have demonstrated the capability of monitoring acute and obvious ocular inflammation in vitreous by OCT and correlated it with retinal disease progression [16,17,21,39,42]. However, this first study opens a window to the possibility of also evaluating subclinical inflammation by vitreous imaging. To our knowledge, this is the first OCT-based study to detect an alteration in the vitreous of eyes with glaucoma (higher signal intensity) when compared with healthy eyes. As both eyes were injected to induce OHT, the increased signal intensity found in the RE is considered a consequence of BRI/LAP IF.

Considering translation to clinical settings, one issue to take into consideration would be the vitreous opacities that are normally present in older humans, which are the primary target population for this formulation. However, in general, floaters are usually kept in a stable range, and the monitoring method presented in this study is conducted with a relative signal (VIT/RPE). Therefore, the change of signal in the successive re-scans (monitoring) would be the consequence of a change in the formulation. Furthermore, in the case of pathology, the metabolism of the drugs is altered. Recently, an increase in vitreous signal VIT/RPE has been described in pathologies such as diabetic retinopathy [39], meaning future studies would be necessary to shed light on these doubts. Nevertheless, this study presents a non-invasive, cost-efficient and customisable monitoring method that would facilitate precision medicine [38].

5. Conclusions

This longitudinal study describes for the first time a qualitative and quantitative method of using OCT to analyse the signal generated in the vitreous by the BRI/LAP IF for glaucoma treatment. It enables initial monitoring of a therapeutic intravitreal formulation based on objective measurement of changes in the vitreous using OCT and demonstrates an adequate correlation with brimonidine drug levels. These results are a preliminary step in the validation of this potential biomarker identified with OCT for use in therapeutic monitoring, IF monitoring or tracing and could also be useful for conducting more accurate clinical trials based on early critical points of loss of efficacy. They could also

potentially be transferred to clinical settings employing new OCT devices that offer higher image resolution.

6. Patents

J.M.F., J.A.M., V.P. and E.G.M. are inventors on a pending European patent application (No. 20 382 021.2) related to this technology. The terms of this arrangement are being managed by the Aragon Health Research Institute (IIS Aragon) and Zaragoza University in accordance with its conflict of interest policies.

Author Contributions: Conceptualisation, M.J.R. and A.P.d.P.; formal analysis, A.P.d.P., A.M. and E.V.; investigation, J.C. and J.A.M.; methodology, M.J.R., A.P.d.P., A.M., S.M.-M., M.S., M.J.C., T.M.-R. and J.M.F.; resources, V.P.; software, A.M., M.S. and T.M.-R.; validation, M.J.R.; visualisation, A.M., J.M.F., J.A.M. and E.G.-M.; writing—original draft, M.J.R., A.P.d.P., A.M., S.M.-M., J.M.F. and E.G.-M.; writing—review and editing, M.J.R., A.P.d.P. and E.G.-M. All authors have read and agreed to the published version of the manuscript.

Funding: This study was supported by Carlos III Health Institute, (grants numbers: M17/00213, PI17/01726, PI17/01946), and by MINECO/AEI/ERDF, EU (grants numbers: MAT2017-83858-C2-2).

Institutional Review Board Statement: This study was approved beforehand by the Ethics Committee for Animal Research of Zaragoza University (PI34/17, 27 June 2017) and was carried out in strict accordance with the Association for Research in Vision and Ophthalmology's Statement for the Use of Animals.

Informed Consent Statement: Not applicable.

Data Availability Statement: The data presented in this study are available on request from the corresponding author.

Conflicts of Interest: J.M.F., J.A.M., V.P. and E.G.M., are inventors on a pending European patent application (No. 20 382 021.2) related to this technology. The terms of this arrangement are being managed by the Aragon Health Research Institute (IIS Aragon) and Zaragoza University in accordance with its conflict of interest policies. The funders had no role in the design of the study; in the collection, analyses, or interpretation of data; in the writing of the manuscript, or in the decision to publish the results.

References

1. Walters, T.R. Development and use of brimonidine in treating acute and chronic elevations of intraocular pressure: A review of safety, efficacy, dose response, and dosing studies. *Surv. Ophthalmol.* **1996**, *41*, S19–S26. [CrossRef]
2. Nizari, S.; Guo, L.; Davis, B.M.; Normando, E.M.; Galvao, J.; Turner, L.; Bizrah, M.; Dehabadi, M.; Tian, K.; Cordeiro, M.F. Non-amyloidogenic effects of α2 adrenergic agonists: Implications for brimonidine-mediated neuroprotection. *Cell Death Dis.* **2016**, *7*, e2514. [CrossRef]
3. Simó, R.; Hernández, C.; Porta, M.; Bandello, F.; Grauslund, J.; Harding, S.P.; Aldington, S.J.; Egan, C.; Frydkjaer-Olsen, U.; García-Arumí, J.; et al. Effects of Topically Administered Neuroprotective Drugs in Early Stages of Diabetic Retinopathy: Results of the EUROCONDOR Clinical Trial. *Diabetes* **2019**, *68*, 457–463. [CrossRef] [PubMed]
4. Kim, K.E.; Jang, I.; Moon, H.; Kim, Y.J.; Jeoung, J.W.; Park, K.H.; Kim, H. Neuroprotective Effects of Human Serum Albumin Nanoparticles Loaded With Brimonidine on Retinal Ganglion Cells in Optic Nerve Crush Model. *Investig. Opthalmol. Vis. Sci.* **2015**, *56*, 5641. [CrossRef]
5. Dossarps, D.; Bron, A.M.; Koehrer, P.; Aho-Glélé, L.S.; Creuzot-Garcher, C.; Berthon, L.; Maftouhi, Q.-E.; Bakhti, A.; Conrath, J.; Le Mer, Y.; et al. Endophthalmitis After Intravitreal Injections: Incidence, Presentation, Management, and Visual Outcome. *Am. J. Ophthalmol.* **2015**, *160*, 17–25.e1. [CrossRef]
6. Tomás, H.; Alves, C.S.; Rodrigues, J. Laponite®: A key nanoplatform for biomedical applications? *Nanomed. Nanotechnol. Biol. Med.* **2018**, *14*, 2407–2420. [CrossRef]
7. Prieto, E.; Vispe, E.; De Martino, A.; Idoipe, M.; Rodrigo, M.J.; Garcia-Martin, E.; Fraile, J.M.; Polo-Llorens, V.; Mayoral, J.A. Safety study of intravitreal and suprachoroidal Laponite clay in rabbit eyes. *Graefe's Arch. Clin. Exp. Ophthalmol.* **2018**, *256*, 535–546. [CrossRef]
8. Prieto, E.; Cardiel, M.J.; Vispe, E.; Idoipe, M.; Garcia-Martin, E.; Fraile, J.M.; Polo, V.; Mayoral, J.A.; Pablo, L.E.; Rodrigo, M.J. Dexamethasone delivery to the ocular posterior segment by sustained-release Laponite formulation. *Biomed. Mater.* **2020**, *15*, 065021. [CrossRef] [PubMed]

9. Rodrigo, M.J.; Cardiel, M.J.; Fraile, J.M.; Mendez-Martinez, S.; Martinez-Rincon, T.; Subías, M.; Polo, V.; Ruberte, J.; Ramirez, T.; Vispe, E.; et al. Brimonidine-LAPONITE® intravitreal formulation has an ocular hypotensive and neuroprotective effect throughout 6 months of follow-up in a glaucoma animal model. *Biomater. Sci.* **2020**, *8*, 6246–6260. [CrossRef] [PubMed]
10. Lapasin, R.; Abrami, M.; Grassi, G.; Šebenik, U. Rheology of Laponite-scleroglucan hydrogels. *Carbohydr. Polym.* **2017**, *168*, 290–300. [CrossRef] [PubMed]
11. Holekamp, N.M. The Vitreous Gel: More than Meets the Eye. *Am. J. Ophthalmol.* **2010**, *149*, 32–36. [CrossRef]
12. Margolis, R. Diagnostic vitrectomy for the diagnosis and management of posterior uveitis of unknown etiology. *Curr. Opin. Ophthalmol.* **2008**, *19*, 218–224. [CrossRef]
13. Bévalot, F.; Cartiser, N.; Bottinelli, C.; Fanton, L.; Guitton, J. Vitreous humor analysis for the detection of xenobiotics in forensic toxicology: A review. *Forensic Toxicol.* **2016**, *34*, 12–40. [CrossRef]
14. Del Amo, E.M.; Rimpelä, A.-K.; Heikkinen, E.; Kari, O.K.; Ramsay, E.; Lajunen, T.; Schmitt, M.; Pelkonen, L.; Bhattacharya, M.; Richardson, D.; et al. Pharmacokinetic aspects of retinal drug delivery. *Prog. Retin. Eye Res.* **2017**, *57*, 134–185. [CrossRef]
15. Uji, A.; Yoshimura, N. Microarchitecture of the Vitreous Body: A High-Resolution Optical Coherence Tomography Study. *Am. J. Ophthalmol.* **2016**, *168*, 24–30. [CrossRef] [PubMed]
16. Keane, P.A.; Karampelas, M.; Sim, D.A.; Sadda, S.R.; Tufail, A.; Sen, H.N.; Nussenblatt, R.B.; Dick, A.D.; Lee, R.W.; Murray, P.I.; et al. Objective Measurement of Vitreous Inflammation Using Optical Coherence Tomography. *Ophthalmology* **2014**, *121*, 1706–1714. [CrossRef] [PubMed]
17. Sreekantam, S.; Macdonald, T.; Keane, P.; Sim, D.; Murray, P.; Denniston, A.K. Quantitative analysis of vitreous inflammation using optical coherence tomography in patients receiving sub-Tenon's triamcinolone acetonide for uveitic cystoid macular oedema. *Br. J. Ophthalmol.* **2016**, *101*, 175–179. [CrossRef] [PubMed]
18. Fernández-Ferreiro, A.; Luaces-Rodríguez, A.; Aguiar, P.; Pardo-Montero, J.; González-Barcia, M.; García-Varela, L.; Herranz, M.; Silva-Rodríguez, J.; Gil-Martínez, M.; Bermudez, M.; et al. Preclinical PET Study of Intravitreal Injections. *Investig. Ophthalmol. Vis. Sci.* **2017**, *58*, 2843–2851.
19. Li, S.K.; Lizak, M.J.; Jeong, E.-K. MRI in ocular drug delivery. *NMR Biomed.* **2008**, *21*, 941–956. [CrossRef]
20. Morrison, J.C.; Cepurna, W.O.; Johnson, E.C. Modeling glaucoma in rats by sclerosing aqueous outflow pathways to elevate intraocular pressure. *Exp. Eye Res.* **2015**, *141*, 23–32. [CrossRef]
21. Chu, C.J.; Herrmann, P.; Carvalho, L.S.; Liyanage, S.E.; Bainbridge, J.W.B.; Ali, R.R.; Dick, A.D.; Luhmann, U.F. Assessment and In Vivo Scoring of Murine Experimental Autoimmune Uveoretinitis Using Optical Coherence Tomography. *PLoS ONE* **2013**, *8*, e63002. [CrossRef]
22. Liba, O.; Lew, M.D.; SoRelle, E.D.; Dutta, R.; Sen, D.; Moshfeghi, D.M.; Chu, S.; De La Zerda, A. Speckle-modulating optical coherence tomography in living mice and humans. *Nat. Commun.* **2017**, *8*, 15845. [CrossRef]
23. Fraile, J.M.; Garcia-Martin, E.; Gil, C.; Mayoral, J.A.; Pablo, L.; Polo-Llorens, V.; Prieto, E.; Vispe, E. Laponite as carrier for controlled in vitro delivery of dexamethasone in vitreous humor models. *Eur. J. Pharm. Biopharm.* **2016**, *108*, 83–90. [CrossRef]
24. Kalapesi, F.B.; Coroneo, M.T.; Hill, M.A. Human ganglion cells express the alpha-2 adrenergic receptor: Relevance to neuroprotection. *Br. J. Ophthalmol.* **2005**, *89*, 758–763. [CrossRef]
25. Lambert, W.S.; Carlson, B.J.; Van Der Ende, A.E.; Shih, G.; Dobish, J.N.; Calkins, D.J.; Harth, E. Nanosponge-Mediated Drug Delivery Lowers Intraocular Pressure. *Transl. Vis. Sci. Technol.* **2015**, *4*, 1. [CrossRef]
26. Kuppermann, B.D.; Patel, S.S.; Boyer, D.S.; Augustin, A.J.; Freeman, W.R.; Kerr, K.J.; Guo, Q.; Schneider, S.; López, F.J. Phase 2 Study of the Safety and Efficacy of Brimonidine Drug Delivery System (Brimo Dds) Generation 1 in Patients with Geographic Atrophy Secondary to Age-Related Macular Degeneration. *Retina* **2021**, *41*, 144–155. [CrossRef] [PubMed]
27. Gómez-Mariscal, M.; Puerto, B.; Muñoz-Negrete, F.J.; De Juan, V.; Rebolleda, G. Acute and chronic optic nerve head biomechanics and intraocular pressure changes in patients receiving multiple intravitreal injections of anti-VEGF. *Graefe's Arch. Clin. Exp. Ophthalmol.* **2019**, *257*, 2221–2231. [CrossRef] [PubMed]
28. Koo, H.; Moon, H.; Han, H.; Na, J.H.; Huh, M.S.; Park, J.H.; Woo, S.J.; Park, K.H.; Kwon, I.C.; Kim, K.; et al. The movement of self-assembled amphiphilic polymeric nanoparticles in the vitreous and retina after intravitreal injection. *Biomaterials* **2012**, *33*, 3485–3493. [CrossRef] [PubMed]
29. Xu, X.; Xu, Z.; Liu, J.; Zhang, Z.; Chen, H.; Li, X.; Shi, S. Visual tracing of diffusion and biodistribution for amphiphilic cationic nanoparticles using photoacoustic imaging after ex vivo intravitreal injections. *Int. J. Nanomed.* **2016**, *11*, 5079–5086. [CrossRef] [PubMed]
30. Le Luyer, C.; Lou, L.; Bovier, C.; Plenet, J.; Dumas, J.; Mugnier, J. A thick sol–gel inorganic layer for optical planar waveguide applications. *Opt. Mater.* **2001**, *18*, 211–217. [CrossRef]
31. Schoonheydt, R.A. Functional hybrid clay mineral films. *Appl. Clay Sci.* **2014**, *96*, 9–21. [CrossRef]
32. Gala, A. Observations on the Hydrogen Ion Concentration in the Vitreous Body of the Eye with Reference to Glaucoma. *Br. J. Ophthalmol.* **1925**, *9*, 516–519. [CrossRef]
33. Mirzaei, M.; Gupta, V.B.; Chick, J.M.; Greco, T.M.; Wu, Y.; Chitranshi, N.; Wall, R.V.; Hone, E.; Deng, L.; Dheer, Y.; et al. Age-related neurodegenerative disease associated pathways identified in retinal and vitreous proteome from human glaucoma eyes. *Sci. Rep.* **2017**, *7*, 1–16. [CrossRef]

34. Lee, D.; Kim, K.-Y.; Noh, Y.H.; Chai, S.; Lindsey, J.D.; Ellisman, M.H.; Weinreb, R.N.; Ju, W.-K. Brimonidine Blocks Glutamate Excitotoxicity-Induced Oxidative Stress and Preserves Mitochondrial Transcription Factor A in Ischemic Retinal Injury. *PLoS ONE* **2012**, *7*, e47098. [CrossRef]
35. Tawari, S.L.; Koch, D.L.; Cohen, C. Electrical Double-Layer Effects on the Brownian Diffusivity and Aggregation Rate of Laponite Clay Particles. *J. Colloid Interface Sci.* **2001**, *240*, 54–66. [CrossRef] [PubMed]
36. Fujimoto, J.G. Optical coherence tomography for ultrahigh resolution in vivo imaging. *Nat. Biotechnol.* **2003**, *21*, 1361–1367. [CrossRef] [PubMed]
37. Hartman, R.R.; Kompella, U.B. Intravitreal, Subretinal, and Suprachoroidal Injections: Evolution of Microneedles for Drug Delivery. *J. Ocul. Pharmacol. Ther.* **2018**, *34*, 141–153. [CrossRef] [PubMed]
38. Moroi, S.E.; Reed, D.M.; Sanders, D.S.; AlMazroa, A.; Kagemann, L.; Shah, N.; Shekhawat, N.; Richards, J.E. Precision medicine to prevent glaucoma-related blindness. *Curr. Opin. Ophthalmol.* **2019**, *30*, 187–198. [CrossRef] [PubMed]
39. Korot, E.; Comer, G.M.; Steffens, T.; Antonetti, D.A. Algorithm for the Measure of Vitreous Hyperreflective Foci in Optical Coherence Tomographic Scans of Patients with Diabetic Macular Edema. *JAMA Ophthalmol.* **2016**, *134*, 15–20. [CrossRef]
40. Sakamoto, T.; Ishibashi, T. Hyalocytes: Essential cells of the vitreous cavity in vitreoretinal pathophysiology? *Retina* **2011**, *31*, 222–228. [CrossRef]
41. Vagaja, N.N.; Chinnery, H.R.; Binz, N.; Kezic, J.M.; Rakoczy, E.P.; McMenamin, P.G. Changes in Murine Hyalocytes Are Valuable Early Indicators of Ocular Disease. *Investig. Ophthalmol. Vis. Sci.* **2012**, *53*, 1445–1451. [CrossRef] [PubMed]
42. Liu, X.; Hui, B.T.; Way, C.; Beese, S.; Adriano, A.; Keane, P.; Moore, D.J.; Denniston, A.K. Noninvasive Instrument-based Tests for Detecting and Measuring Vitreous Inflammation in Uveitis: A Systematic Review. *Ocul. Immunol. Inflamm.* **2020**, 1–12. [CrossRef] [PubMed]

4. Cuarto artículo

Rodrigo MJ, **Cardiel MJ**, Fraile JM, Mayoral JA, Pablo LE, Garcia-Martin E. **Laponite for biomedical applications: An ophthalmological perspective.** Mater Today Bio. 2023 Dec 28;24:100935.doi: 10.1016/j.mtbio.2023.100935 PMID: 38239894. Erratum in: Mater Today Bio. 2024 Jan 27;25:100964.

Materials Today Bio 24 (2024) 100935

Contents lists available at ScienceDirect

Materials Today Bio

journal homepage: www.journals.elsevier.com/materials-today-bio

Laponite for biomedical applications: An ophthalmological perspective

Maria J. Rodrigo [a,b], Maria J. Cardiel [b,c], Jose M. Fraile [d], Jose A. Mayoral [d], Luis E. Pablo [a,b,e], Elena Garcia-Martin [a,b,*]

[a] Department of Ophthalmology, Miguel Servet University Hospital, Zaragoza, Spain
[b] Aragon Institute for Health Research (IIS Aragon), GIMSO Research Group, University of Zaragoza (Spain), Avda. San Juan Bosco 13, E 50009 Zaragoza, Spain
[c] Department of Pathology, Lozano Blesa University Hospital, Zaragoza, Spain
[d] Institute for Chemical Synthesis and Homogeneous Catalysis (ISQCH), Faculty of Sciences, University of Zaragoza–CSIC, C/Pedro Cerbuna 12, 50009 Zaragoza, Spain
[e] Biotech Vision SLP (spin-off Company), University of Zaragoza, Spain

ARTICLE INFO

Keywords:
Laponite
Clay
Biomedical application
Review
Ophthalmology

ABSTRACT

Clay minerals have been applied in biomedicine for thousands of years. Laponite is a nanostructured synthetic clay with the capacity to retain and progressively release drugs. In recent years there has been a resurgence of interest in Laponite application in various biomedical areas. This is the first paper to review the potential biomedical applications of Laponite in ophthalmology. The introduction briefly covers the physical, chemical, rheological, and biocompatibility features of different routes of administration. After that, emphasis is placed on 1) drug delivery for antibiotics, anti-inflammatories, growth factors, other proteins, and cancer treatment; 2) bleeding prevention or treatment; and 3) tissue engineering through regenerative medicine using scaffolds in intraocular and extraocular tissue. Although most scientific research is not performed on the eye, both the findings and the new treatments resulting from that research are potentially applicable in ophthalmology since many of the drugs used are the same, the tissue evaluated in vitro or in vivo is also present in the eye, and the pathologies treated also occur in the eye. Finally, future prospects for this emerging field are discussed.

1. Introduction

Clay minerals' biocompatibility and nanoscale make them an emerging class of biomaterials suitable for a wide range of biomedical applications. To date (2023), the terms "clays" and "biomedical applications" have been referenced in more than a thousand publications. Clay minerals, however, are not new [1]. Their powerful colloidal properties have been known since 2500 BCE and they have long been used to prevent and treat bleeding [2], skin wounds [3], and gastrointestinal diseases, as well as in cosmetics and personal care products. Several types of mineral clay are currently used in biomedical applications. Natural clays, such as montmorillonite, kaolinite, and halloysite, among others, are abundant in nature and easily obtained, although in general they contain different types of impurities, such as non-clay-mineral particles like quartz and calcite [4]. Synthetic clays like Laponite, meanwhile, are free of impurities and therefore have a more uniform structure and composition. A search for "Laponite" in the PubMed database revealed an increase between 2007 and 2023 in the number of published papers containing this term, demonstrating that Laponite's unique characteristics have made it an attractive biomaterial in recent years. Other emerging materials also have potential biomedical applications. Layered double hydroxides are quite similar to synthetic clays as regards the preparation method. They differ, however, in their greater compositional variability, layered structure, and possible non-covalent interaction with drugs [5]. Their particle size is also usually larger than Laponite's, which has rheological consequences when forming gels. Likewise, their layer charge is positive, in contrast to Laponite's negative charge, leading to different types of electrostatic interaction with drugs and the ionic medium. While hexagonal boron nitride is another promising nanomaterial, preparing it in a form suitable to produce stable colloidal suspensions is challenging [6]. Molybdenum sulfide (MoS_2) nanoparticles are also emerging as materials with potential for different biomedical applications, including drug delivery [7]. However, this delivery is usually linked to near-infrared laser irradiation which, combined with the black color of MoS_2 and the doubts about its biocompatibility, makes it difficult to envisage an ophthalmic application for this material.

Laponite® (trademark of the company BYK Additives Ltd) is a

* Corresponding author. C/ Padre Arrupe. Servicio de Oftalmología, Edificio de consultas externas, planta 1, 50009, Zaragoza, Spain.
E-mail address: egmvivax@yahoo.com (E. Garcia-Martin).

https://doi.org/10.1016/j.mtbio.2023.100935
Received 25 October 2023; Received in revised form 20 December 2023; Accepted 27 December 2023
Available online 28 December 2023

synthetic clay developed in the early 1960s [8] as a rheological additive for pigment dispersions [9]. It was prepared by the co-precipitation method using Mg and Li sources ($MgSO_4$ and LiF in the first reports [10]), together with a silicon source (sodium silicate) in a basic medium. Improvements to this method allowed preparation to take place in the absence of fluorine, producing different hydrophilicity/hydrophobicity and rheological behavior [11]. Since then, Laponite has not only been used in a variety of industrial applications but has also been subject to extensive research in relation to biomedical applications [12–14]. The translational research performed with Laponite has mainly centered on wound healing; drug delivery systems (small molecules and, more recently, protein delivery) to treat infections, bleeding, or cancer; and tissue engineering for bone scaffolds [15,16]. Very few references to ophthalmological applications for Laponite are found in the scientific literature.

From a physical–chemical point of view, the empirical formula of this synthetic nanosilicate is $(Na^{+}_{0.7}[(Si_8Mg_{5.5}Li_{0.3})O_{20}(OH)_4]^{-}_{0.7}$ [17]. As a clay mineral, its basic building blocks consist of alternating tetrahedral SiO_4 and octahedral AlO_6 sheets in a 2:1 ratio [4,18]. This means it comprises two tetrahedral silica sheets positioned on either side of an octahedral sheet bound through shared oxygens [19], thus forming a layered structure. Laponite has a dual-charged surface. The faces (upper and lower surfaces) are negatively charged due to the charge imbalance caused by magnesium substitution by lithium in the octahedral layer, while particle edges can be positively charged by protonation of the terminal hydroxyl (OH) groups of the tetrahedral silicate layers. Several layers may be stacked one on top of the other, mainly by electrostatic force, but also hydrogen bonding and Van der Waals force, and joined in clay crystallites with interlayer cations [20]. Layered silicate clays offer a high surface area (more than 700 m^2/g) and allow drug, polymer, protein, or extracellular vesicle interaction and retention to occur, thus forming multifunctional drug delivery systems for better pharmaceutical performance.

In dry form, Laponite has a two-dimensional (2D) disc-shaped geometry (diameter 20–50 nm and thickness approximately 1–2 nm). However, in water this becomes three-dimensional (3D) colloidal particles of colorless gel (the 'house of cards' structure or 'T configuration') [9]. Microenvironmental conditions such as pH or salt concentration have a significant impact on gelation time. The charge on the edges of the Laponite is pH-dependent because of protonation of exposed hydroxyl groups. Gelation time is found to increase significantly with decreasing salt and Laponite concentration. Conversely, an increase in ionic strength leads to the formation of aggregates. Gelation happens abruptly and precipitates when salt concentration exceeds 11 mM; however, with Laponite concentrations above 10 g/L salt concentration does not impact gelation time. The house-of-cards structure is obtained at lower salt concentrations or at pH values below 11 and is generated by preferential interaction between the negative charge on the basal plane and the positive charge on the edge of the particles. At higher salt concentrations band-type aggregates or stacked configurations can be generated by face-to-face interactions with cations, which can later transition into the house-of-cards structure. Other environmental changes, such as local humidity, can cause the clay to absorb or lose water, resulting in variable swelling [20]. The permeability to water and the diffusion of small molecules depend on the orientation of the clay particles within the gel. Well-oriented particles can be used as a barrier to gases and liquids, while randomly or haphazardly oriented particles can increase permeability [21]. Swelling can be prevented by the formation of interactions between polymers and Laponite, controlling in this way the slow release [22–24].

Nanosilicates are optically transparent in aqueous media. Laponite can be functionalized with fluorophores, luminescence, and paramagnetic particles [25,26]. These characteristics can be beneficial, especially in ophthalmic applications, since they enable imaging of subsurface cellular behavior, design of complex printed tissues [27], and facilitate optical coherence tomography (OCT) and magnetic resonance imaging (MRI) for monitoring, diagnosis, and treatment of pathologies [28,29].

Laponite is a rheology modifier commonly used to adjust the overall viscosity of the drug formulation and to control non-Newtonian behaviors such as shear thinning or shear thickening [30,31]. This thixotropic property of Laponite [32] facilitates injectability using small-gauge needles and improves shear-thinning behavior, which is highly desirable for injectable hydrogel devices in which encapsulated drugs such as proteins or antibodies and/or cell activity must be preserved under the high shear stress exerted by injection [33].

Biocompatibility is key for medical translation. Based on experimental and modeled data, the U.S. Environmental Protection Agency has verified that Laponite is a safe chemical of low concern. A range of studies have demonstrated the high biocompatibility of Laponite, establishing its widespread biomedical application. Laponite does not present systemic toxicity after oral, intramuscular, or ocular administration [34–40] at low concentrations (0.1–7% w/v) or with an inhibitory concentration (IC50) of 4 mg/mL [41]. In addition, after intravenous administration a nanocomposite based on Laponite exhibited no hemolytic activity in vitro and no histopathological alterations in the brain, heart, liver, or kidney tissues of mice in vivo [42]. However, prolonged oral medication is not recommended due to the risk of kidney stone formation and the elimination of enzymes and other nutritive elements. Furthermore, high concentrations of nanosilicates can reduce cell proliferation in vitro [43]. Several studies claim IC50 values of Laponite vary considerably, ranging from 0.05 to 50 mg/mL [44]. Laponite particles have been shown to naturally degrade in ~30 days on average; a hydrogel with a residence time of >30 days prevents complete Laponite particles escaping the hydrogel, thereby preventing adverse cytotoxicity [45]. Laponite, especially Laponite® XLG, is considered suitable for biomedical application due to its low heavy metal content. This hydrous nanosilicate contains elements such as magnesium, zinc, lithium, and iron that are also found in the body and in brain metabolism, and its nontoxic degradation products [Na^{+}, Mg^{2+}, $Si(OH)_4$, Li^{+}] are easily absorbed by the body [42,46]. Fig. 1.

This review examines the scientific evidence currently available on Laponite in ophthalmology. It also focuses on potential applications in the eye that can benefit from the promising opportunities offered by innovative Laponite-based biomaterials. It looks at the biomedical applications of Laponite in 1) drug delivery of antibiotics, anti-inflammatories, growth factors, other proteins, and cancer treatments; 2) bleeding prevention or treatment; and 3) tissue engineering through regenerative medicine using scaffolds.

2. Methodology

A systematic search was conducted using the Preferred Reporting Items for Systematic Reviews and Meta-Analyses (PRISMA) guidelines for structured reviews. The literature search was carried out on platforms such as Web of Science®, the Wiley database, https://www.sciencedirect.com/topics/biochemistry-genetics-and-molecular-biology/scopus®, Google Scholar®, Pubmed, PubChem, Mendeley® and the science.gov databases as at August 2023. For the literature search, different combinations of keywords, such as "clay minerals", "Laponite", "biomedical applications", "review", and "ophthalmology" were used. The identification, screening, eligibility, and inclusion of scientific evidence are shown in Table 1.

The studies identified, from general to specific, were those containing the following: the general term ["clay minerals"], which found 48 521 matches in Web of Science, 14 400 in Google Scholar, and nearly 3000 in both Pubmed and PubChem (since 1915); the specific term ["Laponite"], which found more than 2700 matches in Web of Science, more than 2200 in Google Scholar, and around 700 results in Pubmed (since 1969); and ["Laponite NM"], which returned a total of 187 results in Pubmed and 179 consolidated references in PubChem (since 2007). As can be seen in Table 1, using Boolean operators to combine the

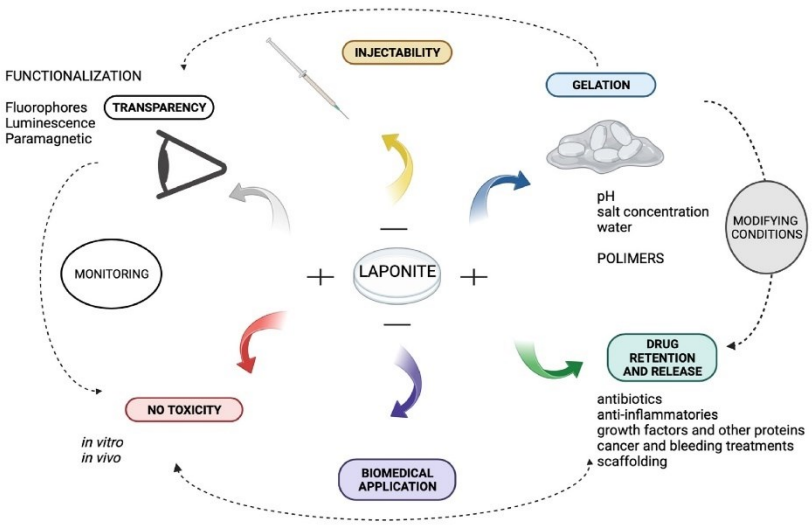

Fig. 1. Laponite properties for ophthalmological applications. Created in BioRender.com.

Table 1
Search sequence for the selection of studies considered for review. * The complete list of studies is provided in the supplementary material.

Database	"Laponite" and "review" (since 1992)	"Laponite" and "biomedical applications" (since 2009)	"Laponite" and "biomedical applications" and "review" (since 2017)	"Laponite" and "ophthalmology" (since 2018)	Screening
Google Scholar	>3000	>1000	>1000	114	**Identification**
Web of Science	155	81	16	1	
PubMed	22	45	12	5	
Google Scholar	173	126	126	7	**Eligibility**
Web of Science	26	52	10	1	
PubMed	17	39	12	4	
After eliminating repetitions	188	179	131	11	**TOTAL 242** *

selected terms ["Laponite" and "review"], ["Laponite" and "biomedical applications"], ["Laponite" and "biomedical applications" and "review"], and ["Laponite" and "ophthalmology"] to focus more specifically on the ophthalmic application of Laponite produced fewer matches, which were found in more recent scientific papers.

For the screening step, all the titles obtained from all the database searches using the Boolean operators and keywords ["Laponite" and "review"], ["Laponite" and "biomedical applications"], ["Laponite" and "biomedical applications" and "review"] and ["Laponite" and "ophthalmology"] were read. For those references that met the exclusion and inclusion criteria, respectively, the abstract was read in the eligibility step. The exclusion criteria were 1) communications, abstracts, or studies with little scientific evidence (i.e. not included in the Journal Citation Reports (JCR®) database) on mineral clays and not mentioning Laponite, 2) references focused solely on chemical properties, or 3) industrial applications, and 4) references in non-English languages. The inclusion criteria were studies or reviews focused on 1) Laponite clay in general terms, 2) clay minerals, including Laponite, for biomedical applications, and 3) the use of Laponite in the eye. If the paper was considered of special interest as regards ophthalmic translation or application, or as regards the perspective offered, the complete paper was read in detail and incorporated in this review.

For the inclusion step, the studies selected were classified based on whether they were 1) conducted in the eye or 2) not conducted in the eye but the drugs are also used in the eye, the tissue evaluated in vitro or in vivo is also present in the eye, the pathologies treated also occur in the eye, and/or the new treatments are potentially applicable in the eye. Accordingly, topics relating to drug delivery, bleeding and tissue engineering using regenerative medicine and scaffolds were discussed.

3. Results

In total, 173 publications were included in this review, around 80 % of which were published in the last 10 years (between 2013 and 2023) (Table 2 and Supplementary Table 1). Regarding studies conducted in or for the eye, we found 11 publications focusing on "Laponite" and "ophthalmology". However, only 4 of the 11 were conducted on in vivo animal eyes (on healthy rabbit eyes and on rats with induced glaucoma, and by two different routes of administration: suprachoroidal, performed surgically; and intravitreal, by minimally invasive injection). After suprachoroidal and intravitreal administration in rabbit eyes, Laponite exhibited biocompatibility since there were no significant differences in intraocular pressure, no relevant ocular complications were found after either route of administration, and no pathological changes were observed in histology. In addition, slow degradation of Laponite was observed over 14 weeks. Laponite presence in the vitreous

Table 2
Summary of studies involving Laponite conducted in or for the eye in the last 10 years (2013–2023).

PUBLICATION	STUDY	MOLECULE	ROUTE	OUTCOMES
Article	*In vitro* & *In vivo*	Brimonidine	Intravitreal administration	Brimonidine–Laponite treatment for glaucoma can be monitored non-invasively using vitreoretinal interface imaging captured with optical coherence tomography over 24 weeks of follow-up and correlated with brimonidine levels measured in rat eyes [28].
Article	*In vivo*	–	Intravitreal & suprachoroidal administration	Safety and biocompatibility of Laponite clay in rabbit eyes [40].
Article	*In vitro*	Dexamethasone	Vitreous humor models	Laponite clay can retain dexamethasone by simple physisorption and deliver it in a controlled manner in solutions used as models for the vitreous humor. It is transparent in the gel state, and the preparation method is simple [47].
Article	*In vitro* & *In vivo*	Dexamethasone	Intravitreal & suprachoroidal administration	Sustained-release delivery of dexamethasone using Laponite as a carrier after intravitreal and suprachoroidal administration in rabbit eyes over 14 weeks [48].
Article	*In vitro* & *In vivo*	Brimonidine	Intravitreal administration	A brimonidine–Laponite intravitreal formulation has an ocular hypotensive and neuroprotective effect throughout 6 months of follow-up in glaucomatous rats [49].
Review	*In vivo*	–	Suprachoroidal administration	Delivery of existing and novel therapeutic agents, such as Laponite, into the potential space between the sclera and choroid and a promising drug delivery route to the posterior segment of the eye [50].
Editorial	*In vitro* & *In vivo*	Brimonidine	Intravitreal administration	The most recent cutting-edge research in ophthalmic drug delivery, highlighting a glaucoma treatment combining a hypotensive and neuroprotective intravitreal formulation of brimonidine–Laponite that could be monitored non-invasively using optical coherence tomography [51].
Review	*In vitro* & *In vivo*	–	–	Summarizes recent findings and patents on various nanotechnology products, such as Laponite, in ocular drug delivery [52].
Review	*In vitro* & *In vivo*	–	–	Natural and synthetic clays for drug delivery and tissue engineering applications from in vitro/in vivo studies [53].
Review	*In vitro* & *In vivo*	–	–	New three-dimensional delivery strategies, including Laponite, for growth factors show promise compared to conventional methods [54].
Review	*In vitro* & *In vivo*	–	–	Applications on biological cationic mineral clay systems [55].
Review	*In vitro* & *In vivo*	–	–	Hydrogels including Laponite for drug delivery and biomedical devices among several applications [56].

was indirectly confirmed by complexometric titration taking advantage of Laponite's high magnesium ion content [40]. Thereafter, controlled in vitro delivery of dexamethasone was evaluated in solutions used as models for the vitreous humor. This study highlighted the simplicity of the preparation method, in which physisorption was modulated by changing the solvent in the adsorption process [47]. The same study group also exhibited good tolerance and sustained-release delivery of two drugs (dexamethasone and brimonidine) commonly used in ophthalmology. A dexamethasone–Laponite formulation was obtained from the interaction between the non-ionic drug and Laponite, mostly by hydrogen bonding involving hydroxyl and carbonyl groups and, after suprachoroidal and intravitreal administration in healthy rabbit eyes, was well tolerated; dexamethasone levels in the choroid–retina unit and vitreous were detected up to 24 weeks. It concluded that Laponite increased the intraocular retention time of dexamethasone when compared with conventional solutions [48]. Intravitreal injection is an administration route commonly used in ophthalmology to maintain therapeutic drug levels near the neuroretina when treating pathological conditions. In glaucomatous rat eyes, a brimonidine–Laponite formulation injected into the vitreous induced an ocular hypotensive and neuroprotective effect, corroborated over 24 weeks by electroretinography, OCT, and higher retinal ganglion cell counts using immunohistochemistry; the authors even observed delayed bilateral neuroprotection [49]. Furthermore, the brimonidine–Laponite formulation was monitored noninvasively using vitreoretinal interface imaging captured with OCT [28]. The formulation was identified as vitreous hyperreflective aggregates which correlated with brimonidine levels measured in the eye. The other publications found were studies or reviews citing the aforementioned [15,50–56]. (Fig. 2).

The following scientific studies were not conducted in the eye, but they could be potentially applicable in ophthalmology since the same drugs are used, the tissue evaluated in vitro or in vivo is also present in the eye, the pathologies treated also occur in the eye, and/or the new treatments are potentially applicable in the eye. To examine the broad spectrum of biomedical applications of Laponite in the eye, and as ophthalmology is a medical and surgical specialty, the following studies related to drug delivery (for medical issues), bleeding (for surgical issues), and tissue engineering with regenerative medicine and scaffolds (for minimally invasive repair of the eye in prospective applications) are referenced (Fig. 3 and Supplementary Table 1).

1) **Drug retention and delivery** [57,58]. Modern drug delivery technology is only 60 years old. The first generation (1950–1980) established the basis for controlled release and successfully managed delivery systems' physical–chemical properties. The second generation developed smart delivery systems but struggled with biological barriers. Today's third generation (2010–2040) comprises modulated delivery systems designed to overcome both the physical–chemical and biological barriers [59] in the eye with the objective of administering therapeutic drug levels with minimum intervention.

Drug molecules are classified as either small or large (molecular weights 12–35 kDa) or biologics [60]. The main mechanism of Laponite drug uptake is intercalation. However, some fractions can be adsorbed on the surface of the particle. The combination of high surface area and charge also results in sustained release of the loaded therapeutics [61]. Moreover, as Laponite is highly hydrophilic it can easily interact with a range of polymeric hydrogels and cryogels, inhibiting burst lease [60,62]. Recently, Laponite-loaded polymeric hydrogels received approval from the U.S. Food and Drug Administration, thereby establishing their clinical potential [63]. Laponite nanodiscs exhibit pH- and salinity-dependent drug loading and release behavior, in which higher swelling and an acidic environment lead to faster release [64]. Laponite particles naturally dissociate into their constituent ions (Li^{-}, Mg^{2+}, and $Si(OH)_4$) in environments where the local pH is less than that of the isoelectric point of Laponite (pH ~10), degrading the nanosilicate particles in about 20–50 days [65]. It is therefore useful at the low pH values that are typically observed in inflamed, ischemic, and neoplastic tissue. However, it may be not favorable where physiological pH is required for the release of the molecule. In acidic conditions, the surface of Laponite is more positive, forming very strong bonds with negative substances. In neutral or basic pH conditions, Laponite maintains a

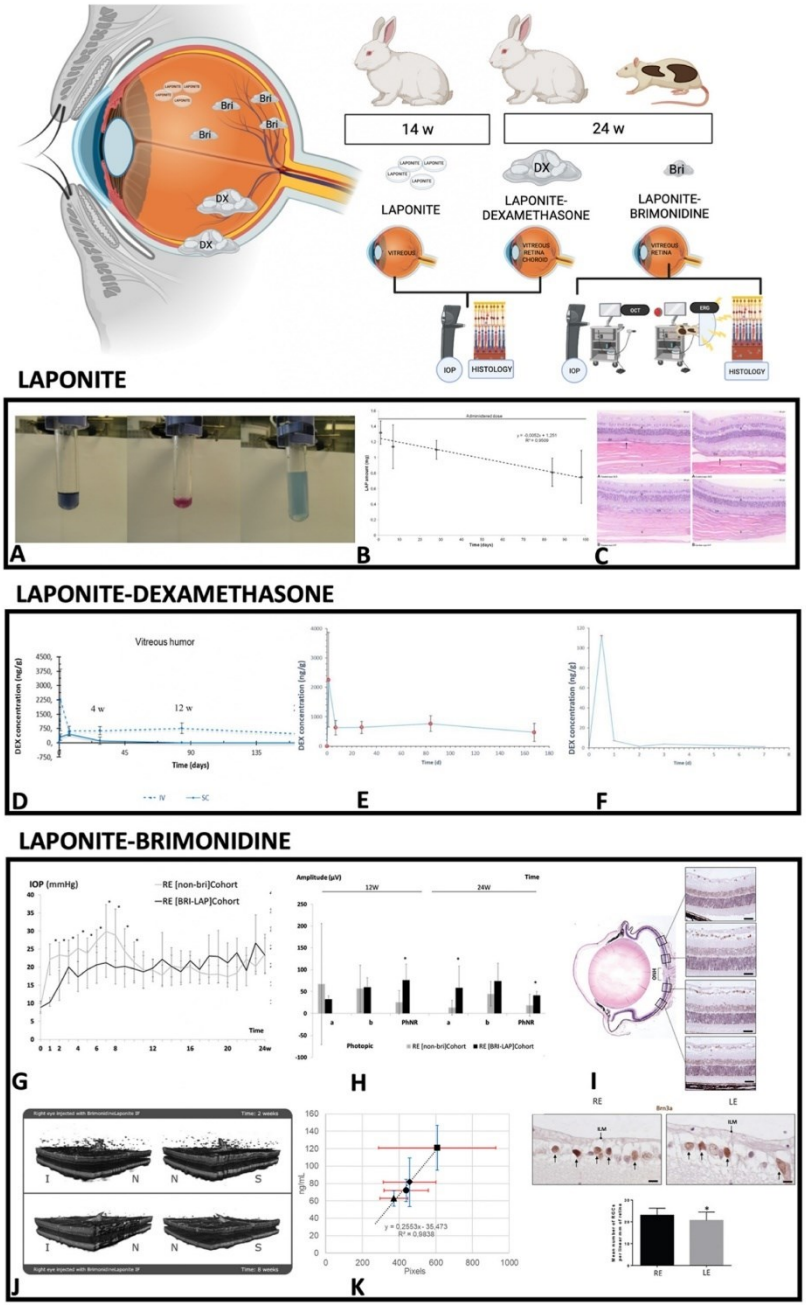

(caption on next page)

Fig. 2. Studies of Laponite conducted in the eye. Abbreviations: IOP: intraocular pressure; OCT: optical coherence tomography; ERG: electroretinography; w: weeks. Created in BioRender.com. **A**: Complexometric determination of Mg2+ in rabbit vitreous humor. Left: Eye not injected with Laponite dispersion: the blue color after addition of EBT indicates the absence of magnesium. Middle: Eye injected with Laponite dispersion: the pink color after addition of EBT indicates the presence of magnesium. Right: Color change in vitreous sample after titration with the required volume of EDTA. **B**: Laponite levels over time in the vitreous humor of intravitreous administered eyes. **C**: Representative photomicrographs showing histological sections of the retina from treated (left panel) and control eyes (right panel) at 14 weeks after injection (HE; magnification Å~ 650). Top: Suprachoroidal administration. Bottom: Intravitreal injection. All retinal layers are preserved and no differences between treated and control eyes were observed in the 20-step sections assessed. The ganglion cell layer is facing the upper side of the photograph. In suprachoroidally administered eyes, virtual spaces can be seen at the junction line between the choroid and sclera (arrows). R: retina; Ch: choroid; and S: sclera. A, B and C: Data from Ref. [40] (CC BY 4.0 license). **D**: Dexamethasone concentrations in the vitreous humor after intravitreal and suprachoroidal administration of Laponite–Dexamethasone (1:10 w w−1) suspension (10 mg mL−1). **E**: Dexamethasone concentrations in the vitreous humor after intravitreal administration of Laponite–Dexamethasone suspension. **F**: Dexamethasone concentrations in the vitreous humor after intravitreal administration of Dexamethasone solution. D, E and F: Data from Ref. [48] (CC BY 4.0 license). **G**: Intraocular pressure curves. Eye comparison between the [non-BRI] cohort (rats with ocular hypertension) and the [Bri-Lap] cohort (rats with ocular hypertension and treated with an intravitreal injection of Laponite–Brimonidine formulation). **H**: PhNR amplitude (a and PhNR waves) was statistically significantly higher in eyes treated with the Bri-Lap formulation in comparison with hypertensive and untreated eyes in the [non-Bri] cohort. Abbreviations: RE: right eye; a wave: signal from photoreceptors; b wave: signal from intermediate cells; PhNR wave: signal from retinal ganglion cells. w: week; μV: microvolts; *$p < 0.05$: statistical differences. **I**: Retinal ganglion cell analysis in glaucomatous eyes. Top: Retinal ganglion cells were counted in radial sections of the eye along 2 mm of a linear region of the retina, corresponding to four areas, two on each side of the optic nerve head. Middle: Two representative images of the ganglion cell layer marked with anti-Brn3a corresponding to a treated (RE) and non-treated eye (LE) of the same animal. Arrows mark the positive nuclei. Bottom: The mean number of retinal ganglion cells per linear mm of retina was significantly higher in hypertensive eyes injected with Laponite–Brimonidine formulation than in the untreated eyes (RE 23.00 ± 0.39 vs. LE 20.66 ± 0.98, $p = 0.040$). Abbreviations: RE: right eye; LE: left eye; ILM: internal limiting membrane. Scale bars: top: 22.72 μm; middle: 5.8 μm. G, H and I: Data from Ref. [49] (CC BY 4.0 license). **J**: 3D reconstruction of the changes in the aggregates at 2 weeks and 8 weeks of follow-up. The reconstruction is shown from two different perspectives at each point in time. Abbreviations: N: nasal; I: inferior; S: superior; IF: intravitreal formulation. **K**: Positive linear correlation between drug levels and total aggregate area. OCT data in red; brimonidine data in blue; ■: 1 week;: 4 weeks; ●: 8 weeks; ▲: 24 weeks. J and K: Data from Ref. [28] (CC BY 4.0 license).

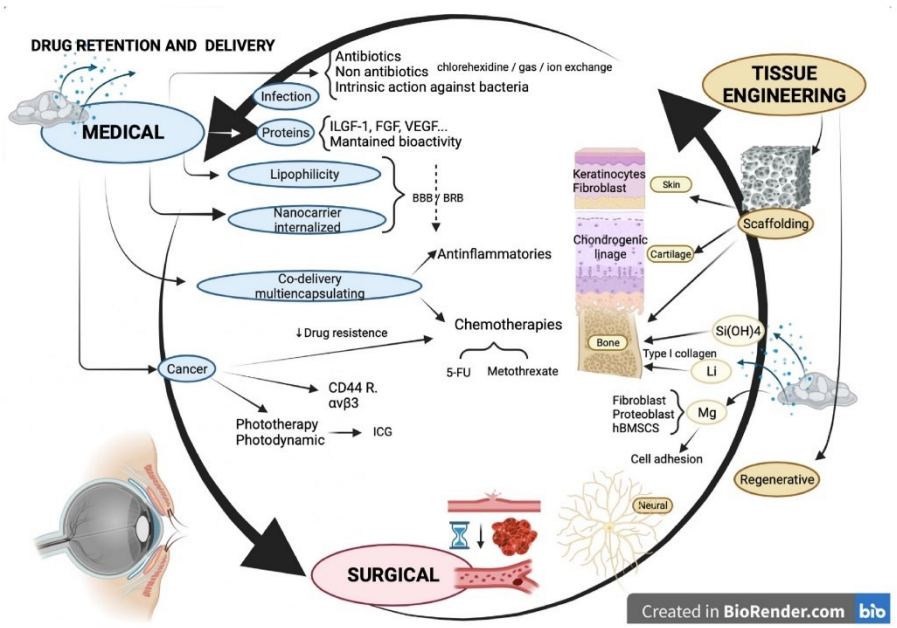

Fig. 3. Studies of Laponite not conducted in the eye, potentially applicable in ophthalmology. Abbreviations: ILGF-1: insulin-like growth factor-1; FGF: fibroblast growth factor; VEGF: vascular endothelial growth factor; BBB: blood–brain barrier; BRB: blood–retina barrier; 5-FU: 5-fluorouracil; ICG: indocyanine green; Si(OH)4: Orthosilicic acid; Li: Lithium ions; Mg: Magnesium ions. Created in BioRender.com.

negative surface by adsorptive binding. Neutral molecules may still interact with Laponite particles if their charge is anisotropically distributed [66]. This wide variety of possible bonds means Laponite has been used in a variety of studies on the delivery of both small and large molecules.

In this regard, the small molecules intercalated with Laponite for infection and inflammation prevention or treatment were antibacterial agents such as tetracycline [67], amoxicillin [68], ofloxacin, ciprofloxacin [69], vancomycin, and mafenide [70], which all exhibited extended release. Other alternatives to infection and inflammation prevention or treatment were chlorhexidine [71], gas [72], and ion exchange [73,74]. Interestingly, Laponite seems to have a specific action against Gram-negative bacteria. Anionic Laponite nanoparticles were able to effectively aggregate Gram-negative bacteria through

lipopolysaccharide binding, which decreased bacterial cells. This suggested Laponite to be beneficial in confining bacterial infection and inflammation [75]. In addition, anti-inflammatory agents such as theophylline and vitamin B12 were co-delivered [76], and dexamethasone exhibited sustained release in vitreous gel in rabbit eyes [48].

Eye and brain disorder therapy nevertheless remains challenging, partly because of the existence of the blood–retina barrier and the blood–brain barrier (BRB and BBB) [77]. In this regard, drug lipophilicity is an important parameter that determines a drug's capacity to penetrate those barriers. Laponite enhances the solubility of non-water-soluble drugs such as the antifungal itraconazole [78], the neuroprotector brimonidine (intravitreal) [28], ITH12657 (oral) [79], and donepezil (intravenous), administration of which improves delivery of either the therapeutic agent [42] or magnetic nanoparticles [80].

Regarding large molecules, the existence of hydrophilic and hydrophobic regions on the clay's surface facilitates protein molecules' interaction with the clay [81,82]. Proteins and other macromolecules can form relatively large complexes and interact with Laponite particles via face-only or edge-only interactions. Laponite–protein complex size increased with Laponite concentration due to the increase in surface area available for adsorption. Positively charged proteins (such as ribonuclease A or lysozyme) form larger complexes with Laponite and are released much more slowly than negatively charged proteins (such as bovine serum albumin). Laponite mitigated the burst release for proteins and extracellular vesicles [83,84] and allowed tunable release times. A Laponite–insulin-like growth factor-1 (ILGF-1) mimetic protein hydrogel [85] exhibited release up to 4 weeks in a rat model. As protein secondary and tertiary structure is very important for bioactivity, protein structure must be preserved following interaction and release from Laponite [60]. The maintenance of protein bioactivity was demonstrated in proteins such as albumin and lysozyme, and in growth factors such as transforming growth factor-β3 (TGF-β3), human mesenchymal stem cell-derived growth factors, fibroblast growth factor 2 (FGF2), and vascular endothelial growth factor (VEGF) [86], as well as in heparin-fibroblast growth factor 4 (FGF4) [87], human bone morphogenetic protein 2 (rhBMP2) [88], and IGF1 [85] in vitro and in vivo [31,87,89–92] —the latter focused on wounds or on spine, bone, or tendon injuries— and achieved desired physiological outcomes. However, further characterization and understanding of the Laponite–protein complex structure when used with inflammatory cytokines such as granulocyte macrophage colony-stimulating factor (GM-CSF), FMS-like tyrosine kinase-3 ligand (FlT3L), Interleukin (IL)-15, IL-2, or chemokine ligand 20 (CCL20) is necessary. At the same time, delivery of macromolecules other than proteins such as immunoglobulins, which are highly important in ophthalmology (as anti-VEGFs), presents further challenges and should be explored.

A separate point to be considered, given its significance and the evidence available, is anti-cancer therapy [93]. Nanoclays are emerging as systems offering extraordinary potential in cancer theranostics, not only as vectors for the delivery of different anti-cancer agents with intrinsic anti-tumor activity, but also in diagnosis [94,95]. Laponite can be physically triggered by temperature and magnetic/electric or light fields, which is useful in optical therapies, including photothermal therapy (PTT) and photodynamic therapy (PDT). Meanwhile, loading chemotherapeutics such as doxorubicin into the interlayer space of Laponite particle gels demonstrated the utility of this nanoclay for delivery applications [96–98], while doxorubicin exhibited higher release in the acidic environment of tumors [99]. Furthermore, Laponite served as a nanocarrier across the cellular membrane in a doxorubicin-loaded nanocomposite hydrogel versus a bolus drug dose [100]. In vivo, Laponite particles are thought to be internalized by clathrin-mediated endocytosis and subsequently degraded within the low pH environment of endosomes [101]. This internalization was also suggested after OCT visualization [28]. In addition, an antimelanoma Laponite gel formulation containing simvastatin [102], a physical crosslinking of magnetic Laponite nanoparticles with 5-fluorouracil [103]— and methotrexate, which is also used for inflammatory pathologies affecting the eye [104], exhibited antitumoral activity. Finally, benzoyl peroxide generated and sustainedly released oxygen, which chemically modified the tumor microenvironment and reversed the effects of hypoxia. Consequently, the proliferation of malignant cells decreased while the viability of healthy fibroblasts increased [105]. There are also new strategies to enhance the efficacy of chemotherapy. Co-loading or simultaneously multiencapsulating different drugs (chemotherapies) in Laponite improved their efficacy versus their effectiveness individually [97], and co-delivery with sequential release overcame tumor drug resistance [106]. In this regard, a promising cancer treatment target is CD44, a transmembrane glycoprotein overexpressed in several solid tumors such as melanoma, non-Hodgkin's lymphomas, gliomas, or meningiomas, all of them also present in the eye. Adding CD44-targeting receptors to other chemotherapies significantly enhanced antitumor activity [107]. Another example, as mentioned before, is a photothermal and photodynamic Laponite-based therapeutic agent for the treatment of cancer cells overexpressing integrin αvβ3, which involved applying a coating of polydopamine (PDA) to indocyanine green (ICG)-loaded Laponite and then conjugating polyethylene glycol-RGD (PEG-RGD) on the surface. Indocyanine green is a photothermal dye widely used in ophthalmology for choroidal pathologies [108]. ICG encapsulation efficiency was 94.1 % and the photostability of the ICG protected with Laponite and PDA was dramatically improved. This combined drug enhanced cellular uptake by cancer cells overexpressing integrin αvβ3 and caused cell death under in vitro near-infrared laser irradiation by generating reactive oxygen species [109]. Furthermore, Laponite exhibited luminescent properties, producing bright red and bright green emissions [26], or was functionalized by fluorophores [25,110], thereby suggesting its utility for imaging diagnosis.

In addition to serving as a delivery system for the molecules mentioned above, Laponite has long been known for its hemostatic ability. Studies potentially applicable to the prevention or treatment of bleeding in surgical settings are briefly referenced below.

2) Bleeding: Hematotoxicity is one of the factors limiting in vivo use of biomaterials. Hemolysis and coagulation induced by clay particles offer a possible use of these nanocomposite systems in vivo [111,112]. A shear-thinning nanocomposite hydrogel composed of synthetic silicate nanoplatelets and gelatin promoted coagulation. The combination of injectability, rapid mechanical recovery, and physiological stability resulted in a promising hemostat with which to treat incompressible wounds. It would therefore be beneficial in the case of retrobulbar bleeding, in which compression would be forbidden in an open eye so as to avoid iatrogenic optic neuropathy. The tendency of these clays to elicit a procoagulant response depends on the structural and surface properties of the clay. Magnesium aluminum hydroxide layers might limit hemorrhage via adhesion to tissues and red blood cells. As calcium and magnesium ions are required for certain enzymatic reactions in the coagulation cascade, their delivery by materials might therefore influence coagulation kinetics. Factor XII activation correlates with negative surface charge density. Laponite's ability to readily absorb water and swell upon hydration may thicken the blood and restrict blood flow. Furthermore, addition of Laponite to hydrogels used as an injectable hemostat provided enhanced physiological stability and accelerated clotting time by increasing platelet binding and therefore reducing hemostatic clot formation time from 7 min (normal physiological process) to less than 3 min. Sustained release of entrapped therapeutics (VEGF) also promoted enhanced wound healing [111,113]. The incorporation of Laponite into a gelatin hydrogel improved antithrombogenicity and hemocompatibility, and incorporation into a dextran-based hydrogel did not significantly alter hemolysis. Wang et al. found that Laponite particles presented <5 % hemolysis, which could be improved by sintering Laponite particles at high heat. Meanwhile, a mixed suspension containing Laponite and gelatin and incorporated into the polymerization of the acrylamide network resisted nonspecific protein adsorption, improved the degree of hemolysis, and eventually prolonged clotting

time [39,69,114]. Thus, hemolysis and coagulation should not be a major concern with Laponite–hydrogel composites, as demonstrated by their good blood compatibility [39,69,114].

Finally, two novel therapies with potential application in several areas of ophthalmology are presented.

3) **Tissue engineering: regenerative medicine and scaffolds**. Laponite has been used for numerous tissue engineering applications. Tissue engineering is a relatively new field where science and engineering work together to reach new frontiers in regenerative medicine. It employs scaffolds, biodegradable structures seeded with human cells and growth factors to develop new tissue while the scaffolds themselves degrade [115]. Meeting the growing demand for personalized implants and tissue scaffolds requires the advanced biomaterials and processing strategies that the fabrication of 3D structures entails. Bioprinting is a revolutionary innovation that can generate 3D scaffolds —even with time-dependent transformation of the printed construct (4D)— and achieve expanding patterns [116], mimicking the complexity of the extracellular matrix and providing excellent functional and biological cues for faster tissue regeneration. Laponite offers a promising platform for bioprinting the cells, resulting in cell-laden constructs designed to assist tissue repair and recover functionality [117–122]. In this regard, the shape of the filler has a relevant impact on the mechanical properties and printability of the scaffolds [123,124]. Laponite gels with different morphologies (droplets, rings, strings, and clay microcapsules) were able to flow through syringe needles and re-establish the gel network due to the Laponite's self-assembling property. Printed scaffolds demonstrated excellent shape fidelity up to 2 cm in height and with changed orientations of between 20° and 90° up to 3 weeks, after which their mechanical properties drastically decreased. Mechanical testing revealed that nonporous solid scaffolds had a higher compressive strain than porous ones. However, current research still lacks answers regarding the mechanisms by which nanofiller shape and morphology affect mechanical and rheological properties. Most studies suggest the formation of a house-of-cards structure; however, this effect does not generally arise at the low concentrations usually considered. Our group demonstrated that, when injected, Laponite intravitreous formed a unique clog when using dexamethasone in healthy rabbits [48] but formed multiples and microaggregates when using brimonidine in glaucomatous rats [28], confirming what in vitro studies of Laponite concentrations have previously shown [15,125]. This fact makes it evident that more research into soft-tissue engineering applications is needed [126,127].

Furthermore, appropriate bioink viscosity is critical to cell printing. Cell-laden Laponite-based nanocomposite bioinks demonstrated superior printing properties that enabled the creation of complex forms and the spreading of various encapsulated cells [128–130]. Cell-laden constructs preserved their morphological properties and exhibited good cell viability (70–75 %) for up to 3 weeks [129], although this also decreased when Laponite concentration rose to 1 % [131].

Recent literature in the field of 3D scaffold bioprinting confirms the enormous potential that use of Laponite has for skin, cartilage, and bone repair/regeneration [132]. An advantage of Laponite is that it creates regenerative microenvironments [133]. In this regard, experimental studies using next-generation sequencing technology demonstrated that nanoclays influence genetics [134]. Laponite exhibited cell viability in relation to https://www.sciencedirect.com/topics/engineering/keratinocyte [37] and fibroblast cells [135], stabilized the intrinsic triple-helical conformation of collagen [136], bridged the tissue gaps, and led differentiation towards the chondrogenic lineage when cultured in a chondrogenic-inducing medium [91,137]. However, Laponite dissolution in an aqueous environment also degraded in nontoxic products, such as $Si(OH)_4$, Li^+, and Mg^{2+}, which enhanced osteogenic cell function and promoted osteogenesis by influencing nucleation and deposition of inorganic calcium and phosphate ions in an extracellular matrix. Orthosilicic acid stimulates osteoblast differentiation and type 1 collagen synthesis [138]. Lithium ions are known to promote type 1 collagen and to initiate canonical Wnt-reactive osteogenic genes via glycogen synthase kinase-3 beta (GSK3β) inhibition [139]. It has been shown to impart osteogenic and angiogenic potential [130]. Furthermore, Laponite could enhance bovine serum albumin and VEGF release kinetics. Magnesium ions are engaged in initiating osteogenesis-governing pathways [140–142] and have been shown to promote cell adhesion to biomaterial surfaces [143] by interacting with the adhesion protein of the integrin family, the primary perpetrators of cell adhesion [144–147].

Nanosized Laponite particles can also themselves directly adhere to the cell surface [148,149] and internalize into the cells [41,150], inducing osteogenic differentiation of mesenchymal stem cells without the use of differentiating media [144–146,151–154]. Nevertheless, the mechanisms involved in clay-induced osteogenic differentiation are still poorly understood [155]. Schmidt et al. demonstrated increased cell adhesion and flat and well-spread cell morphology after increasing the Laponite content in a nanocomposite film. Laponite inclusion in PEG hydrogels at 40–70 % (wt%) improved cell adhesion and proliferation and the spreading of mouse preosteoblasts [156,157], mouse fibroblasts [158], and human bone marrow stromal cells (hBMSCs) [38] in a clay-concentration-reliant manner.

Furthermore, 3D-printable zwitterionic Laponite hydrogel demonstrated neural cell viability by growing cells with extended neurites [159].

4. Discussion

A biomaterial is a material intended to interface with biological systems to evaluate, treat, augment, or replace any tissue, organ, or function of the body and, in the case of the eye, to compensate for vision loss which may or may not be related to age. Ophthalmic biomaterials try to emulate natural materials, and important requirements must be met [160–162]. Compatibility remains a fundamental issue, as does the ability to deliver oxygen to tissue. A refractive index near that of water is also required, which means most materials to be placed in the eye must be transparent, a prerequisite unique to ophthalmic biomaterials. In addition, a combination of surface and mechanical properties that remain stable throughout the application period must also be produced. Lubrication and friction, tissue protection during surgery, tissue integration, and healing modulation are also widely considered to be important. Numerous studies have shown various biomaterials to be highly beneficial in treating ophthalmic conditions. Biomaterials, tissue engineering, and regenerative medicine are therefore becoming increasingly important to advancing ophthalmology and optometry. This review shows the benefits and the potential biomedical applicability of Laponite as an ophthalmic biomaterial. Apart from being biocompatible, easily injectable, and optically transparent, Laponite increases therapeutic delivery and uptake of several drugs used in ophthalmology, with the added advantage of encouraging intrinsic antimicrobial activity by modifying the ionic or oxygen microenvironment. In this regard, since the use of fewer antibiotics is currently supported and encouraged to avoid resistance, Laponite could also have a role in ophthalmology where eye drops based on iodine, ozone, or chlorhexidine have demonstrated their bactericidal efficacy [163]. Laponite achieves sustained release of molecules and even of extracellular vesicles [164] and when combined with other hydrogel polymers can diminish the initial burst. Sustained release has been demonstrated in small antibiotic and anti-inflammatory molecules widely used in ophthalmology, such as tetracyclines, quinolones, or corticosteroids. These drugs are widely used to treat inflammatory processes affecting the palpebral, such as blepharitis or prophylactics for cataract surgery, among others. Two drugs commonly used in medical and surgical glaucoma therapy (brimonidine and 5-fluorouracil) exhibited sustained release and efficacy. Moreover, the sustained release of macromolecules such as growth factors (e.g., mimetic protein ILGF-1) and other proteins (e.g., VEGF) while maintaining functionality has been demonstrated.

ILGF-1 could be useful likely as insulin eye drops, which have shown great effectiveness in closure of corneal ulcers [165], with the added advantages of retaining water to prevent desiccation, reducing the number of applications, and maintaining optical transparency. However, we have not been able to find any reference to the combination of Laponite with anti-VEGF antibodies, widely and repeatedly used as a therapeutic target in ocular pathologies of the posterior pole causing blindness, such as age-related macular degeneration or diabetic retinopathy. In this regard, the intravitreal and suprachoroidal tolerance and efficacy of Laponite has already been demonstrated. The added capacity of photothermal and photodynamic therapy could be another avenue to explore in relation to potential application of Laponite in choroidal pathology.

The eye is an organ in which the three embryological structures —endoderm, mesoderm, and ectoderm— are present. It is therefore composed of skin, connective tissue, bone tissue, blood vessels, muscle, and neural tissue [166]. Laponite has a regenerative role in mesenchymal (keratinocytes, fibroblasts, chondrocytes, osteoblasts) and vascular tissues, which is useful for the repair of damaged or lost tissue. As Laponite improves stimulus responsiveness, increases cell adhesion and differentiation, and improves scaffolds' mechanical properties, it could be applicable in lid and orbital surgery with tissue defects. Autografts or donor transplants are still the gold standards for replacing lost functional tissue. However, the biomaterial Laponite could facilitate the performance of minimally invasive procedures by simplifying injection and/or placement of scaffolds cultured with the patient's cells versus the complex reconstructive surgery that is currently performed [167]. Moreover, facial and lid surgery can produce bleeding that is sometimes difficult to stem. In this sense, Laponite could also facilitate the procedure by reducing bleeding time. However, no reviewed articles have evaluated Laponite in periocular and/or orbital tissue; most have focused on articular orthosis.

Regarding neural tissue, only four publications referring to Laponite were found. One tested Laponite on cultured medulloblastoma cells, another on mouse brain tissue, and the other two on rabbit and rat retinas. The studies carried out with Laponite in the eye demonstrated the absence of toxicity and even animal neuroretinal protection after suprachoroidal and intravitreal administration. Thus, Laponite would be a possible biomaterial to consider for retinal tissue bioprinting in future studies.

Laponite is also useful for imaging, cell tracking, or directing. These characteristics are potentially also used in ophthalmology. The Laponite–brimonidine intravitreal formulation was visualized and monitored using vitreous OCT imaging and even correlated with intraocular drug levels. In addition, Laponite can be functionalized with different markers or molecules to target and internalize the target cell and exert its beneficial and/or harmful effect (in the case of cancer). This theranostic advantage that Laponite offers could change the clinical practice and prognosis of ocular tumors or pathologies that are difficult or impossible to access in the orbit or optic nerve such as gliomas [168], which represent a high risk of iatrogenic blindness.

Finally, not only does Laponite meet the requirements stated by Ferrari et al. for nanotechnology for therapy [169,170], but also does so for ophthalmic purposes, as this review has shown: (1) it enables administration of lipophilic drugs, such as brimonidine, a common hypopressure and neuroprotective antiglaucoma drug; (2) it provides sustained targeted delivery of therapeutic agents to target cells or tissues; (3) it overcomes the epithelial and endothelial barriers due to drug transcytosis and its easy injectability; (4) it delivers large therapeutic agents (macromolecular structures such as growth factors, i.e., ILGF) to the intracellular sites of action; (5) it enables co-delivery of two or more therapeutic agents to produce synergistic action, obtained with anti-inflammatory or chemotherapy drugs but potentially used in other multifactorial pathologies such as neurodegenerative diseases; (6) it has a high circulation time compared to free drugs, thanks to drug retention with sustained delivery, which decreases cytotoxicity; (7) it improves the pharmacokinetic profile; (8) it enables visualization of therapeutic agent delivery sites by combining therapeutic agents with imaging techniques such as OCT or MRI; and (9) it allows in vivo real-time OCT monitoring of therapeutic efficacy.

Limitations on use of Laponite and future studies: The review conducted shows numerous advantages and potential applications of Laponite in ophthalmology. However, it also found a few, partially reversible limitations on use of Laponite in biomedicine which are discussed below. Regarding drug delivery, the electrostatic interactions between the nanosheets limit dispersion in aqueous media, although the addition of other compounds reduced such electrostatic interactions and accelerated the dispersion of the films [171]. There could also be potential toxicity at high concentrations. Laponite's bactericidal action is due to bacteria aggregation (limited to Gram-negative bacteria as Laponite did not cause flocculation of Gram-positive *Bacillus subtilis* bacteria nor did it bind to lipoteichoic acid from bacterial envelopes) [75]. Finally, regarding tissue engineering and scaffolding, although Laponite helps, the limited printability of the soft materials remains a challenge [172]. As regards intraocular administration, although no explicit references to limitations were found, intravitreal injection was reported to produce a transient IOP increase at around 3 days, similar to other hydrogels [49]. Although its luminescent property could produce light scattering and alter visual quality, no in vivo studies have evaluated this [173]. Finally, removal of the material in the case of allergy or intolerance would possibly require a challenging surgical intervention. Future studies should therefore analyze these issues. Furthermore, this review focuses solely on Laponite clay for ophthalmic application; comparing other types of clays with potential application in ophthalmology would also be beneficial.

5. Conclusion

In conclusion, this review presents the few studies carried out on application of the biomaterial Laponite in the eye and/or ocular tissue to date. However, there is extensive scientific evidence suggesting that Laponite can be used in all ocular structures and tissues, from the skin and ocular appendages to the retina and orbit. Its advantages include —in the case of ophthalmology— biocompatibility, optical transparency, nanosize thickness, and thixotropy facilitating easy injection, in addition to its capacity to retain all types of molecules, even in co-loading, and its ability to release them progressively to treat the target cell after administration in the form of topical gel or skin, intravitreal, or suprachoroidal injection, or as scaffolds. It also possesses intrinsic bactericidal and regenerative characteristics. Laponite's clinical transformation in terms of drug delivery seems more feasible, straightforward, and closer. Scaffolding, in contrast, and especially for neural tissue, seems distant, as the complex connections between retinal cell types remain a challenge. Laponite is therefore a biomaterial that merits further study in medical, surgical, and regenerative applications in future ophthalmological research.

Patents

E.G.M., J.M.F., J.A.M., and L.E.P. are inventors on a pending European patent application (No. 20 382 021.2) related to this technology. The terms of this arrangement are being managed by the Aragon Health Research Institute (IIS Aragon), Zaragoza University and the Spanish Science Research Council (CSIC) in accordance with its conflict-of-interest policies.

Funding

This study was supported by Grants M17/00213, JR22/00057, PI17/01726, PI17/01946, and PI20/00437 (Carlos III Health Institute), and by MAT2017-83858-C2-1, MAT2017-83858-C2-2, PID2020-113281 R B-C2-1, and PID2020-113281 R B-C2-2 funded by (*MCIN/AEI/*

10.13039/501 100 011 033).

TOC

This is the first review to present the biomedical applications of Laponite for ophthalmology from a medical, surgical and regenerative perspective. Very few studies have been conducted in the eye, but both the findings and new treatments resulting from previous research seem potentially applicable to ophthalmology in the future.

CRediT authorship contribution statement

Maria J. Rodrigo: Conceptualization, Funding acquisition, Supervision, Writing - original draft, Writing - review & editing. **Maria J. Cardiel:** Investigation, Methodology, Software, Validation, Writing - review & editing. **Jose M. Fraile:** Conceptualization, Funding acquisition, Investigation, Methodology, Writing - original draft, Writing - review & editing. **Jose A. Mayoral:** Conceptualization, Supervision, Validation, Writing - review & editing. **Luis E. Pablo:** Conceptualization, Funding acquisition, Project administration, Supervision, Writing - review & editing. **Elena Garcia-Martin:** Conceptualization, Formal analysis, Supervision, Writing - original draft, Writing - review & editing.

Declaration of competing interest

The authors declare the following financial interests/personal relationships which may be considered as potential competing interests: Elena Garcia-Martin reports financial support was provided by Carlos III Health Institute. Maria J Rodrigo reports financial support was provided by Carlos III Health Institute. Luis E Pablo reports financial support was provided by Spain Ministry of Science and Innovation. Maria J Rodrigo reports was provided by Spain Ministry of Science and Innovation. Maria J Cardiel reports financial support was provided by Spain Ministry of Science and Innovation. Elena Garcia-Martin has patent #No. 20 382 021.2 pending to Pending European patent application (No. 20 382 021.2) related to this technology. If there are other authors, they declare that they have no known competing financial interests or personal relationships that could have appeared to influence the work reported in this paper.

Data availability

Data will be made available on request.

Appendix A. Supplementary data

Supplementary data to this article can be found online at https://doi.org/10.1016/j.mtbio.2023.100935.

References

[1] K.S. Katti, H. Jasuja, S.V. Jaswandkar, S. Mohanty, D.R. Katti, Nanoclays in medicine: a new frontier of an ancient medical practice, Mater Adv 3 (2022) 7484–7500, https://doi.org/10.1039/D2MA00528J.

[2] Ebers Papyrus | The National Archives, (n.d.). https://discovery.nationalarchives.gov.uk/details/r/58a9bba9-1312-487a-9a6f-829ccd091d21 (accessed August 14, 2023).

[3] E. Strouhal, B. Vachala, H. Vymazalová, S.M. Miller, The medicine of the ancient Egyptians, The Medicine of the Ancient Egyptians. American Univ. in Cairo Press. Pag 1 240 (n.d.). https://books.google.com/books/about/Medicine_of_the_Ancient_Egyptians.html?hl=es&id=im9IzQEACAAJ (accessed August 15, 2023).

[4] L. Pauling, The structure of the micas and related minerals, Proc. Natl. Acad. Sci. U. S. A. 16 (1930) 123–129, https://doi.org/10.1073/PNAS.16.2.123.

[5] T. Hu, Z. Gu, G.R. Williams, M. Strimaite, J. Zha, Z. Zhou, X. Zhang, C. Tan, R. Liang, Layered double hydroxide-based nanomaterials for biomedical applications, Chem. Soc. Rev. 51 (2022) 6126–6176, https://doi.org/10.1039/D2CS00236A.

[6] Q. Weng, X. Wang, X. Wang, Y. Bando, D. Golberg, Functionalized hexagonal boron nitride nanomaterials: emerging properties and applications, Chem. Soc. Rev. 45 (2016) 3989–4012, https://doi.org/10.1039/C5CS00869G.

[7] K. Zhang, Y. Zhuang, W. Zhang, Y. Guo, X. Liu, Functionalized MoS2-nanoparticles for transdermal drug delivery of atenolol, Drug Deliv. 27 (2020) 909–916, https://doi.org/10.1080/10717544.2020.1778815.

[8] K. Shafran, C. Jeans, S.J. Kemp, K. Murphy, Dr Barbara S. Neumann: clay scientist and industrial pioneer; creator of Laponite®, Clay Miner. 55 (2020) 256–260, https://doi.org/10.1180/CLM.2020.35.

[9] B.S. Neumann, Behaviour of a synthetic clay in pigment dispersions, Rheol. Acta 4 (1965) 250–255, https://doi.org/10.1007/BF01973660/METRICS.

[10] B.S. Neumann, Synthetic hectorite-type clay minerals 401 (1967) 107.

[11] Taylor: Nature of synthetic swelling clays and their... - Google Académico, (n.d.). Page 777-780. https://scholar.google.com/scholar_lookup?title=Nature+of+synthetic+swelling+clays+and+their+use+in+emulsion+paint&author=Taylor+J.&author=Neumann+B.S.&publication+year=1968&journal=Journal+of+the+Oil+and+Colour+Chemists%E2%80%99+Association&volume=51&pages=232-253 (accessed December 9, 2023)..

[12] D. Ss, N. None, H. K, S. S, H. A, F. A, T. M, Laponite-based nanomaterials for biomedical applications: a review, Curr. Pharmaceut. Des. 25 (2019) 424–443, https://doi.org/10.2174/1381612825666190402165845.

[13] H. Tomás, C.S. Alves, J. Rodrigues, Laponite®, A key nanoplatform for biomedical applications? Nanomedicine 14 (2018) 2407–2420, https://doi.org/10.1016/j.nano.2017.04.016.

[14] O. Samoylenko, O. Korotych, M. Manilo, Y. Samchenko, V. Shlyakhovenko, N. Lebovka, Biomedical applications of laponite® based nanomaterials and formulations, Springer Proc. Phys. 266 (2022) 385–452, https://doi.org/10.1007/978-3-030-80924-9_15/COVER.

[15] G. Kiaee, N. Dimitrakakis, S. Sharifzadeh, H.J. Kim, R.K. Avery, K. M. Moghaddam, R. Haghniaz, E.P. Yalcintas, N.R. de Barros, S. Karamikamkar, A. Libanori, A. Khademhosseini, P. Khoshakhlagh, Laponite-based nanomaterials for drug delivery, Adv. Healthcare Mater. 11 (2022), https://doi.org/10.1002/ADHM.202102054.

[16] C. Wang, S. Min, Y. Tian, Injectable and cell-laden hydrogel in the contained bone defect animal model: a systematic review, Tissue Engineering and Regenerative Medicine 2023 (2023) 1–9, https://doi.org/10.1007/S13770-023-00569-2.

[17] A.K. Gaharwar, L.M. Cross, C.W. Peak, K. Gold, J.K. Carrow, A. Brokesh, K. A. Singh, 2D nanoclay for biomedical applications: regenerative medicine, therapeutic delivery, and additive manufacturing, Adv. Mater. 31 (2019), https://doi.org/10.1002/ADMA.201900332.

[18] H.H. Murray, Overview — clay mineral applications, Appl. Clay Sci. 5 (1991) 379–395, https://doi.org/10.1016/0169-1317(91)90014-Z.

[19] R.E. Grim, Clay Mineralogy: the clay mineral composition of soils and clays is providing an understanding of their properties, Science 135 (1962) 890–898, https://doi.org/10.1126/SCIENCE.135.3507.890.

[20] F. Uddin, Clays, nanoclays, and montmorillonite minerals, Metall Mater Trans A Phys Metall Mater Sci 39 (2008) 2804–2814, https://doi.org/10.1007/S11661-008-9603-5/METRICS.

[21] C.J. Wu, A.K. Gaharwar, P.J. Schexnailder, G. Schmidt, Development of biomedical polymer-silicate nanocomposites: a materials science perspective, Materials 3 (2010) 2986–3005, https://doi.org/10.3390/MA3052986, 2010, Vol. 3, Pages 2986-3005.

[22] H. Takeno, Y. Kimura, W. Nakamura, O.H. Campanella, D. Díaz Díaz, Mechanical, swelling, and structural properties of mechanically tough clay-sodium polyacrylate blend hydrogels, Gels 3 (2017) 10, https://doi.org/10.3390/GELS3010010, 2017, Vol. 3, Page 10.

[23] C. Tipa, M.T. Cidade, J.P. Borges, L.C. Costa, J.C. Silva, P.I.P. Soares, Clay-based nanocomposite hydrogels for biomedical applications: a review, Nanomaterials 12 (2022) 3308, https://doi.org/10.3390/NANO12193308, 2022, Vol. 12, Page 3308.

[24] H. Yadav, R. Agrawal, A. Panday, J. Patel, S. Maiti, Polysaccharide-silicate composite hydrogels: review on synthesis and drug delivery credentials, J. Drug Deliv. Sci. Technol. 74 (2022), 103573, https://doi.org/10.1016/J.JDDST.2022.103573.

[25] T. Wang, X. Hu, S. Zheng, X. Liu, C. Wang, Z. Tong, Adsorption of fluorophores and N-isopropylacrylamide on laponite, Appl. Clay Sci. 58 (2012) 102–107, https://doi.org/10.1016/J.CLAY.2012.01.021.

[26] H. Li, M. Li, Y. Wang, W. Zhang, Luminescent hybrid materials based on laponite clay, Chem. Eur J. 20 (2014) 10392–10396, https://doi.org/10.1002/CHEM.201402794.

[27] B. Ruzicka, E. Zaccarelli, L. Zulian, R. Angelini, M. Sztucki, A. Moussaïd, T. Narayanan, F. Sciortino, Observation of empty liquids and equilibrium gels in a colloidal clay, Nat. Mater. 10 (2011) 56–60, https://doi.org/10.1038/NMAT2921.

[28] M.J. Rodrigo, A.P. Del Palomar, A. Montolío, S. Mendez-Martinez, M. Subias, M. J. Cardiel, T. Martinez-Rincon, J. Cegoñino, J.M. Fraile, E. Vispe, J.A. Mayoral, V. Polo, E. Garcia-Martin, Monitoring new long-lasting intravitreal formulation for glaucoma with vitreous images using optical coherence tomography, Pharmaceutics 13 (2021) 217, https://doi.org/10.3390/PHARMACEUTICS13020217, 2021, Vol. 13, Page 217.

[29] Y.P. Yew, K. Shameli, M. Miyake, N.B.B. Ahmad Khairudin, S.E.B. Mohamad, T. Naiki, K.X. Lee, Green biosynthesis of superparamagnetic magnetite Fe3O4 nanoparticles and biomedical applications in targeted anticancer drug delivery system: a review, Arab. J. Chem. 13 (2020) 2287–2308, https://doi.org/10.1016/J.ARABJC.2018.04.013.

[30] X. Liu, S.R. Bhatia, Laponite® and Laponite®-PEO hydrogels with enhanced elasticity in phosphate-buffered saline, Polym. Adv. Technol. 26 (2015) 874–879, https://doi.org/10.1002/PAT.3514.
[31] B. Liu, J. Li, X. Lei, S. Miao, S. Zhang, P. Cheng, Y. Song, H. Wu, Y. Gao, L. Bi, G. Pei, Cell-loaded injectable gelatin/alginate/LAPONITE® nanocomposite hydrogel promotes bone healing in a critical-size rat calvarial defect model, RSC Adv. 10 (2020) 25652–25661, https://doi.org/10.1039/D0RA03040F.
[32] H.A. Barnes, Thixotropy—a review, J Nonnewton Fluid Mech 70 (1997) 1–33, https://doi.org/10.1016/S0377-0257(97)00004-9.
[33] S.S. Gharaie, S.M.H. Dabiri, M. Akbari, Smart shear-thinning hydrogels as injectable drug delivery systems, Polymers 10 (2018) 1317, https://doi.org/10.3390/POLYM10121317, 2018, Vol. 10, Page 1317.
[34] J.H. Lee, W.J. Han, H.S. Jang, H.J. Choi, Highly tough, biocompatible, and magneto-responsive Fe3O4/laponite/PDMAAm nanocomposite hydrogels, Sci. Rep. 9 (2019), https://doi.org/10.1038/S41598-019-51555-5.
[35] L. Zhang, G. He, Y. Yu, Y. Zhang, X. Li, S. Wang, Design of biocompatible chitosan/polyaniline/laponite hydrogel with photothermal conversion capability, Biomolecules 12 (2022) 1089, https://doi.org/10.3390/BIOM12081089, 2022, Vol. 12, Page 1089.
[36] F. Topuz, M. Bartneck, Y. Pan, F. Tacke, One-step fabrication of biocompatible multifaceted nanocomposite gels and nanolayers, Biomacromolecules 18 (2017) 386–397, https://doi.org/10.1021/ACS.BIOMAC.6B01483.
[37] R.R. Domeneguetti, V.Y. Sakai, G.F. Perotti, I.C. Silva, A. Tercjak, H.S. Barud, F. Pavan, V.R.L. Constantino, S.J. Ribeiro, Structural and morphological properties of in situ biosynthesis of biocompatible bacterial cellulose/Laponite nanocomposites, Appl. Clay Sci. 234 (2023), 106851, https://doi.org/10.1016/j.clay.2023.106851.
[38] A.K. Gaharwar, V. Kishore, C. Rivera, W. Bullock, C.J. Wu, O. Akkus, G. Schmidt, Physically crosslinked nanocomposites from silicate crosslinked PEO: mechanical properties and osteogenic differentiation of human mesenchymal stem cells, Macromol. Biosci. 12 (2012) 779–793, https://doi.org/10.1002/MABI.201100508.
[39] C. Wang, S. Wang, K. Li, Y. Ju, J. Li, Y. Zhang, J. Li, X. Liu, X. Shi, Q. Zhao, Preparation of laponite bioceramics for potential bone tissue engineering applications, PLoS One 9 (2014), e99585, https://doi.org/10.1371/JOURNAL.PONE.0099585.
[40] E. Prieto, E. Vispe, A. De Martino, M. Idoipe, M.J. Rodrigo, E. Garcia-Martin, J. M. Fraile, V. Polo-Llorens, J.A. Mayoral, Safety study of intravitreal and suprachoroidal Laponite clay in rabbit eyes, Graefe's Arch. Clin. Exp. Ophthalmol. 256 (2018) 535–546, https://doi.org/10.1007/S00417-017-3893-5/METRICS.
[41] A.K. Gaharwar, S.M. Mihaila, A. Swami, A. Patel, S. Sant, R.L. Reis, A.P. Marques, M.E. Gomes, A. Khademhosseini, Bioactive silicate nanoplatelets for osteogenic differentiation of human mesenchymal stem cells, Adv. Mater. 25 (2013) 3329–3336, https://doi.org/10.1002/ADMA.201300584.
[42] A.K. Singh, S.K. Mishra, G. Mishra, A. Maurya, R. Awasthi, M.K. Yadav, N. Atri, P. K. Pandey, S.K. Singh, Inorganic clay nanocomposite system for improved cholinesterase inhibition and brain pharmacokinetics of donepezil, Drug Dev. Ind. Pharm. 46 (2020) 8–19, https://doi.org/10.1080/03639045.2019.1698594.
[43] S. Maisanaba, S. Pichardo, M. Puerto, D. Gutiérrez-Praena, A.M. Cameán, A. Jos, Toxicological evaluation of clay minerals and derived nanocomposites: a review, Environ. Res. 138 (2015) 233–254, https://doi.org/10.1016/J.ENVRES.2014.12.024.
[44] I. Veernala, J. Giri, A. Pradhan, P. Polley, R. Singh, S.K. Yadava, Effect of fluoride doping in laponite nanoplatelets on osteogenic differentiation of human dental follicle stem cells (hDFSCs), Sci. Rep. 9 (2019), https://doi.org/10.1038/S41598-018-37327-7.
[45] A.M. Brokesh, L.M. Cross, A.L. Kersey, A. Murali, C. Richter, C.A. Gregory, I. Singh, A.K. Gaharwar, Dissociation of nanosilicates induces downstream endochondral differentiation gene expression program, Sci. Adv. 8 (2022) 9404, https://doi.org/10.1126/SCIADV.ABL9404/SUPPL_FILE/SCIADV.ABL9404_DATA FILES S1 TO S6.ZIP.
[46] D.W. Thompson, J.T. Butterworth, The nature of laponite and its aqueous dispersions, J. Colloid Interface Sci. 151 (1992) 236–243, https://doi.org/10.1016/0021-9797(92)90254-J.
[47] J.M. Fraile, E. Garcia-Martin, C. Gil, J.A. Mayoral, L.E. Pablo, V. Polo, E. Prieto, E. Vispe, Laponite as carrier for controlled in vitro delivery of dexamethasone in vitreous humor models, Eur. J. Pharm. Biopharm. 108 (2016) 83–90, https://doi.org/10.1016/j.ejpb.2016.08.015.
[48] E. Prieto, M.J. Cardiel, E. Vispe, M. Idoipe, E. Garcia-Martin, J.M. Fraile, V. Polo, J.A. Mayoral, L.E. Pablo, M.J. Rodrigo, Dexamethasone delivery to the ocular posterior segment by sustained release Laponite formulation, Biomed. Mater. 15 (2020), https://doi.org/10.1088/1748-605X/ABA445.
[49] M.J. Rodrigo, M.J. Cardiel, J.M. Fraile, S. Mendez-Martinez, T. Martinez-Rincon, M. Subias, V. Polo, J. Ruberte, T. Ramirez, E. Vispe, C. Luna, J.A. Mayoral, E. Garcia-Martin, Brimonidine-LAPONITE® intravitreal formulation has an ocular hypotensive and neuroprotective effect throughout 6 months of follow-up in a glaucoma animal model, Biomater. Sci. 8 (2020) 6246–6260, https://doi.org/10.1039/d0bm01013h.
[50] C.R. Wan, L. Muya, V. Kansara, T.A. Ciulla, Suprachoroidal delivery of small molecules, nanoparticles, gene and cell therapies for ocular diseases, Pharmaceutics 13 (2021) 288, https://doi.org/10.3390/PHARMACEUTICS13020288, 2021, Vol. 13, Page 288.
[51] A. Chauhan, L. Fitzhenry, A.P. Serro, Recent advances in ophthalmic drug delivery, Pharmaceutics 14 (2022), https://doi.org/10.3390/PHARMACEUTICS14102075.
[52] N. Gupta, S. Goel, H. Gupta, Patent review on nanotechnology in ocular drug delivery, Recent Pat. Nanomed. 3 (2013) 37–46, https://doi.org/10.2174/1877912311202990004.
[53] C. Nomicisio, M. Ruggeri, E. Bianchi, B. Vigani, C. Valentino, C. Aguzzi, C. Viseras, S. Rossi, G. Sandri, Natural and synthetic clay minerals in the pharmaceutical and biomedical fields, Pharmaceutics 15 (2023) 1368, https://doi.org/10.3390/PHARMACEUTICS15051368, 2023, Vol. 15, Page 1368.
[54] L.M. Caballero Aguilar, S.M. Silva, S.E. Moulton, Growth factor delivery: defining the next generation platforms for tissue engineering, J. Contr. Release 306 (2019) 40–58, https://doi.org/10.1016/J.JCONREL.2019.05.028.
[55] M. Ghadiri, W. Chrzanowski, R. Rohanizadeh, Biomedical applications of cationic clay minerals, RSC Adv. 5 (2015) 29467–29481, https://doi.org/10.1039/c4ra16945j.
[56] C.W. Peak, J.J. Wilker, G. Schmidt, A review on tough and sticky hydrogels, Colloid Polym. Sci. 291 (2013) 2031–2047, https://doi.org/10.1007/S00396-013 3021 Y, 2013 291:9.
[57] J. Dong, Z. Cheng, S. Tan, Q. Zhu, Clay nanoparticles as pharmaceutical carriers in drug delivery systems, Expet Opin. Drug Deliv. 18 (2021) 695–714, https://doi.org/10.1080/17425247.2021.1862792.
[58] C. Viseras, P. Cerezo, R. Sanchez, I. Salcedo, C. Aguzzi, Current challenges in clay minerals for drug delivery, Appl. Clay Sci. 48 (2010) 291–295, https://doi.org/10.1016/J.CLAY.2010.01.007.
[59] Y.H. Yun, B.K. Lee, K. Park, Controlled drug delivery: historical perspective for the next generation, J. Contr. Release 219 (2015) 2, https://doi.org/10.1016/J.JCONREL.2015.10.005. –7.
[60] S.T. Koshy, D.K.Y. Zhang, J.M. Grolman, A.G. Stafford, D.J. Mooney, Injectable nanocomposite cryogels for versatile protein drug delivery, Acta Biomater. 65 (2018) 36–43, https://doi.org/10.1016/J.ACTBIO.2017.11.024.
[61] R. Davis, R.A. Urbanowski, A.K. Gaharwar, 2D layered nanomaterials for therapeutics delivery, Curr Opin Biomed Eng 20 (2021), 100319, https://doi.org/10.1016/j.cobme.2021.100319.
[62] I.A. Podaru, P.O. Stănescu, R. Ginghină, Ş. Stoleriu, B. Trică, R. Şomoghi, M. Teodorescu, Poly(N-vinylpyrrolidone)–Laponite XLG nanocomposite hydrogels: characterization, properties and comparison with divinyl monomer-crosslinked hydrogels, Polymers 14 (2022) 4216, https://doi.org/10.3390/POLYM14194216/S1.
[63] K213385-Janice Hogan, (n.d.). https://www.fda.gov/medical- (accessed August 15, 2023)..
[64] M. Roozbahani, M. Kharaziha, R. Emadi, pH sensitive dexamethasone encapsulated laponite nanoplatelets: release mechanism and cytotoxicity, Int. J. Pharm. 518 (2017) 312–319, https://doi.org/10.1016/J.IJPHARM.2017.01.001.
[65] R.P. Mohanty, Y.M. Joshi, Chemical stability phase diagram of aqueous Laponite dispersions, Appl. Clay Sci. 119 (2016) 243–248, https://doi.org/10.1016/J.CLAY.2015.10.021.
[66] K. Das, K. Rawat, H.B. Bohidar, Surface patch binding induced interaction of anisotropic nanoclays with globular plasma proteins, RSC Adv. 6 (2016) 104117–104125, https://doi.org/10.1039/C6RA11669H.
[67] M. Ghadiri, H. Hau, W. Chrzanowski, H. Agus, R. Rohanizadeh, Laponite clay as a carrier for in situ delivery of tetracycline, RSC Adv. 3 (2013) 20193–20201, https://doi.org/10.1039/C3RA43217C.
[68] S. Wang, F. Zheng, Y. Huang, Y. Fang, M. Shen, M. Zhu, X. Shi, Encapsulation of amoxicillin within laponite-doped poly(lactic-co-glycolic acid) nanofibers: preparation, characterization, and antibacterial activity, ACS Appl. Mater. Interfaces 4 (2012) 6393–6401, https://doi.org/10.1021/AM302130B.
[69] J. Luo, Z. Ma, F. Yang, T. Wu, S. Wen, J. Zhang, L. Huang, S. Deng, S. Tan, Fabrication of laponite-reinforced dextran-based hydrogels for NIR-responsive controlled drug release, ACS Biomater. Sci. Eng. 8 (2022) 1554–1565, https://doi.org/10.1021/acsbiomaterials.1c01389.
[70] M. Ghadiri, W. Chrzanowski, R. Rohanizadeh, Antibiotic eluting clay mineral (Laponite®) for wound healing application: an in vitro study, J. Mater. Sci. Mater. Med. 25 (2014) 2513–2526, https://doi.org/10.1007/S10856-014-5272-7.
[71] G.R. Peraro, E.H. Donzelli, P.F. Oliveira, D.C. Tavares, C.H. Gomes Martins, E. F. Molina, E.H. de Faria, Aminofunctionalized LAPONITE® as a versatile hybrid material for chlorhexidine digluconate incorporation: cytotoxicity and antimicrobial activities, Appl. Clay Sci. 195 (2020), 105733, https://doi.org/10.1016/J.CLAY.2020.105733.
[72] K. Park, J.I. Dawson, R.O.C. Oreffo, Y.H. Kim, J. Hong, Nanoclay-polyamine composite hydrogel for topical delivery of nitric oxide gas via innate gelation characteristics of laponite, Biomacromolecules 21 (2020) 2096–2103, https://doi.org/10.1021/ACS.BIOMAC.0C00086/SUPPL_FILE/BM0C00086_SI_001.PDF.
[73] X. Tang, J. Dai, H. Sun, S. Nabanita, S. Petr, L. Tang, Q. Cheng, D. Wang, J. Wei, Copper doped nano laponite coating on poly(butylene succinate) scaffold with antibacterial properties and cytocompatibility for biomedical application, J. Nanomater. 2018 (2018), https://doi.org/10.1155/2018/5470814.
[74] N. Li, L. Yu, Z. Xiao, C. Jiang, B. Gao, Z. Wang, Biofouling mitigation effect of thin film nanocomposite membranes immobilized with laponite mediated metal ions, Desalination 473 (2020), 114162, https://doi.org/10.1016/J.DESAL.2019.114162.
[75] S. Malekkhaiat Häffner, L. Nyström, K.L. Browning, H. Mörck Nielsen, A. A. Strömstedt, M.J.A. Van Der Plas, A. Schmidtchen, M. Malmsten, Interaction of laponite with membrane components-consequences for bacterial aggregation and infection confinement, ACS Appl. Mater. Interfaces 11 (2019) 15389–15400, https://doi.org/10.1021/ACSAMI.9B03527.
[76] U. Nandi, V. Trivedi, D. Douroumis, A.P. Mendham, N.J. Coleman, Layered silicate-alginate composite particles for the pH-mediated release of theophylline, Pharmaceuticals 13 (2020) 1–13, https://doi.org/10.3390/PH13080182.

[77] F. Persano, S. Batasheva, G. Fakhrullina, G. Gigli, S. Leporatti, R. Fakhrullin, Recent advances in the design of inorganic and nano-clay particles for the treatment of brain disorders, J. Mater. Chem. B 9 (2021) 2756–2784, https://doi.org/10.1039/D0TB02957B.

[78] H. Jung, H.M. Kim, Y. Bin Choy, S.J. Hwang, J.H. Choy, Itraconazole–Laponite: kinetics and mechanism of drug release, Appl. Clay Sci. 40 (2008) 99–107, https://doi.org/10.1016/J.CLAY.2007.09.002.

[79] I. Bravo, L. Viejo, C. de los Ríos, E.M. García-Frutos, M. Darder, Cellulose/pectin-based materials incorporating Laponite indole derivative hybrid for oral administration and controlled delivery of the neuroprotective drug, Int. J. Biol. Macromol. 234 (2023), 123765, https://doi.org/10.1016/J.IJBIOMAC.2023.123765.

[80] A.S. Aguiar, L. Michels, F.G. da Silva, C. Kern, G. Gomide, C.M. Ferreira, J. Depeyrot, R. Aquino, G.J. da Silva, The use of a laponite dispersion to increase the hydrophilicity of cobalt-ferrite magnetic nanoparticles, Appl. Clay Sci. 193 (2020), 105663, https://doi.org/10.1016/J.CLAY.2020.105663.

[81] M. Fernandes De Oliveira, C.T. Johnston, G.S. Premachandra, B.J. Teppen, H. Li, D.A. Laird, D. Zhu, S.A. Boyd, Spectroscopic study of carbaryl sorption on smectite from aqueous suspension, Environ. Sci. Technol. 39 (2005) 9123–9129, https://doi.org/10.1021/ES048108S.

[82] A.T.T. Tran, B.J. James, A study the interaction forces between the bovine serum albumin protein and montmorillonite surface, Colloids Surf. A Physicochem. Eng. Asp. 414 (2012) 104–114, https://doi.org/10.1016/J.COLSURFA.2012.08.066.

[83] K. Mau, I.A. Barroso, M.Y. Brunet, B. Peacock, A.S. Federici, D.A. Hoey, S.C. Cox, Controlled release of epigenetically enhanced extracellular vesicles from a GelMA/nanoclay composite hydrogel to promote bone repair, Int. J. Mol. Sci. 23 (2022) 832, https://doi.org/10.3390/IJMS23020832/S1.

[84] H. Hu, L. Dong, Z. Bu, Y. Shen, J. Luo, H. Zhang, S. Zhao, F. Lv, Z. Liu, miR-23a-3p abundant small extracellular vesicles released from Gelma/nanoclay hydrogel for cartilage regeneration, J. Extracell. Vesicles 9 (2020), 1778883, https://doi.org/10.1080/20013078.2020.1778883.

[85] J. Li, E. Weber, S. Guth-Gundel, M. Schuleit, A. Kuttler, C. Halleux, N. Accart, A. Doelemeyer, A. Basler, B. Tigani, K. Wuersch, M. Fornaro, M. Kneissel, A. Stafford, B.R. Freedman, D.J. Mooney, Tough composite hydrogels with high loading and local release of biological drugs, Adv. Healthcare Mater. 7 (2018), https://doi.org/10.1002/ADHM.201701393.

[86] D.J. Page, C.E. Clarkin, R. Mani, N.A. Khan, J.I. Dawson, N.D. Evans, Injectable nanoclay gels for angiogenesis, Acta Biomater. 100 (2019) 378–387, https://doi.org/10.1016/J.ACTBIO.2019.09.023.

[87] C. Wang, Z. Gong, X. Huang, J. Wang, K. Xia, L. Ying, J. Shu, C. Yu, X. Zhou, F. Li, C. Liang, Q. Chen, An injectable heparin-Laponite hydrogel bridge FGF4 for spinal cord injury by stabilizing microtubule and improving mitochondrial function, Theranostics 9 (2019) 7016–7032, https://doi.org/10.7150/THNO.37601.

[88] Y.H. Kim, X. Yang, L. Shi, S.A. Lanham, J. Hilborn, R.O.C. Oreffo, D. Ossipov, J. I. Dawson, Bisphosphonate nanoclay edge-site interactions facilitate hydrogel self assembly and sustained growth factor localization, Nat. Commun. 11 (2020), https://doi.org/10.1038/S41467-020-15152-9.

[89] L.M. Cross, J.K. Carrow, X. Ding, K.A. Singh, A.K. Gaharwar, Sustained and prolonged delivery of protein therapeutics from two dimensional nanosilicates, ACS Appl. Mater. Interfaces 11 (2019) 6741–6750, https://doi.org/10.1021/ACSAMI.8B17733/ASSET/IMAGES/MEDIUM/AM-2018-17733N_0007.GIF.

[90] R. Waters, S. Pacelli, R. Maloney, I. Medhi, R.P.H. Ahmed, A. Paul, Stem cell secretome-rich nanoclay hydrogel: a dual action therapy for cardiovascular regeneration, Nanoscale 8 (2016) 7371–7376, https://doi.org/10.1039/C5NR07806G.

[91] J.I. Dawson, J.M. Kanczler, X.B. Yang, G.S. Attard, R.O.C. Oreffo, Clay gels for the delivery of regenerative microenvironments, Adv. Mater. 23 (2011) 3304–3308, https://doi.org/10.1002/ADMA.201100968.

[92] D.M.R. Gibbs, C.R.M. Black, G. Hulsart Billstrom, P. Shi, E. Scarpa, R.O.C. Oreffo, J.I. Dawson, Bone induction at physiological doses of BMP through localization by clay nanoparticle gels, Biomaterials 99 (2016) 16–23, https://doi.org/10.1016/j.biomaterials.2016.05.010.

[93] D. Peixoto, I. Pereira, M. Pereira-Silva, F. Veiga, M.R. Hamblin, Y. Lvov, M. Liu, A. C. Paiva-Santos, Emerging role of nanoclays in cancer research, diagnosis, and therapy, Coord. Chem. Rev. 440 (2021), 213956, https://doi.org/10.1016/j.ccr.2021.213956.

[94] D.-K. Ji, C. Ménard-Moyon, A. Bianco, Physically-triggered nanosystems based on two dimensional materials for cancer theranostics, Adv. Drug Deliv. Rev. 138 (2019) 211–232, https://doi.org/10.1016/j.addr.2018.08.010.

[95] L. Zhou, M. Zou, Y. Xu, P. Lin, C. Lei, X. Xia, Nano drug delivery system for tumor immunotherapy: next-generation therapeutics, Front. Oncol. 12 (2022), https://doi.org/10.3389/FONC.2022.864301.

[96] S. Tang, J. Chen, J. Cannon, M. Chekuri, M. Farazuddin, J.R. Baker, S.H. Wang, Delicate hybrid laponite–cyclic poly(ethylene glycol) nanoparticles as a potential drug delivery system, Pharmaceutics 15 (2023) 1998, https://doi.org/10.3390/PHARMACEUTICS15071998/S1.

[97] T.B. Becher, M.C.P. Mendonça, M.A. De Farias, R.V. Portugal, M.B. De Jesus, C. Ornelas, Soft nanohydrogels based on laponite nanodiscs: a versatile drug delivery platform for theranostics and drug cocktails, ACS Appl. Mater. Interfaces 10 (2018) 21891–21900, https://doi.org/10.1021/ACSAMI.8B06149.

[98] S. Wang, Y. Wu, R. Guo, Y. Huang, S. Wen, M. Shen, J. Wang, X. Shi, Laponite nanodisks as an efficient platform for Doxorubicin delivery to cancer cells, Langmuir 29 (2013) 5030–5036, https://doi.org/10.1021/LA4001363.

[99] S. Xiao, R. Castro, D. Maciel, M. Gonçalves, X. Shi, J. Rodrigues, H. Tomás, Fine tuning of the pH-sensitivity of laponite-doxorubicin nanohybrids by polyelectrolyte multilayer coating, Mater. Sci. Eng., C 60 (2016) 348–356, https://doi.org/10.1016/J.MSEC.2015.11.051.

[100] M. Gonçalves, P. Figueira, D. Maciel, J. Rodrigues, X. Qu, C. Liu, H. Tomás, Y. Li, pH-sensitive Laponite(®)/doxorubicin/alginate nanohybrids with improved anticancer efficacy, Acta Biomater. 10 (2014) 300–307, https://doi.org/10.1016/J.ACTBIO.2013.09.013.

[101] N. Iturrioz-Rodríguez, R. Martín Rodríguez, C. Renero-Lecuna, F. Aguado, L. González-Legarreta, J. González, M.L. Fanarraga, A.C. Perdigón, Free-labeled nanoclay intracellular uptake tracking by confocal Raman imaging, Appl. Surf. Sci. 537 (2021), 147870, https://doi.org/10.1016/j.apsusc.2020.147870.

[102] N. Suterio, G.C. Bazzo, G.S. Rauber, A.H. Silva, T. Caon, A.L. Parize, T. B. Creczynski-Pasa, H.K. Stulzer, Laponite® gel formulation containing sinvastatin for melanoma treatment, Appl. Clay Sci. 228 (2022), 106651, https://doi.org/10.1016/J.CLAY.2022.106651.

[103] O. Goncharuk, Y. Samchenko, L. Kernosenko, O. Korotych, T. Poltoratska, N. Pasmurtseva, O. Oranska, D. Sternik, I. Mamyshev, Thermoresponsive hydrogels physically crosslinked with magnetically modified LAPONITE® nanoparticles, Soft Matter 16 (2020) 5689–5701, https://doi.org/10.1039/D0SM00929F.

[104] R.J. Stawell, Methotrexate in inflammatory eye disease, Ocul. Immunol. Inflamm. 11 (2003) 79–82, https://doi.org/10.1076/OCII.11.2.79.15918.

[105] A. Motealleh, N.S. Kehr, Injectable oxygen generating nanocomposite hydrogels with prolonged oxygen delivery for enhanced cell proliferation under hypoxic and normoxic conditions, J. Mater. Chem. B 8 (2020) 4195–4201, https://doi.org/10.1039/D0TB00885K.

[106] L. Zheng, B. Zhou, X. Qiu, X. Xu, G. Li, W.Y.W. Lee, J. Jiang, Y. Li, Direct assembly of anticancer drugs to form Laponite-based nanocomplexes for therapeutic co-delivery, Mater. Sci. Eng., C 99 (2019) 1407–1414, https://doi.org/10.1016/J.MSEC.2019.02.083.

[107] T. Jiang, G. Chen, X. Shi, R. Guo, Hyaluronic acid-decorated Laponite® nanocomposites for targeted anticancer drug delivery, Polymers 11 (2019) 137, https://doi.org/10.3390/POLYM11010137, 2019, Vol. 11, Page 137.

[108] T. Bacci, D.J. Oh, M. Singer, S.V. Sadda, K.B. Freund, Ultra-widefield indocyanine green angiography reveals patterns of choroidal venous insufficiency influencing pachychoroid disease, Invest. Ophthalmol. Vis. Sci. 63 (2022), https://doi.org/10.1167/IOVS.63.1.17.

[109] F. Xu, M. Liu, X. Li, Z. Xiong, X. Cao, X. Shi, R. Guo, Loading of indocyanine green within polydopamine-coated laponite nanodisks for targeted cancer photothermal and photodynamic therapy, Nanomaterials 8 (2018), https://doi.org/10.3390/NANO8050347 (Basel).

[110] F. López Arbeloa, V. Martínez Martínez, T. Arbeloa, I. López Arbeloa, Photoresponse and anisotropy of rhodamine dye intercalated in ordered clay layered films, J. Photochem. Photobiol. C Photochem. Rev. 8 (2007) 85–108, https://doi.org/10.1016/J.JPHOTOCHEMREV.2007.03.003.

[111] A.K. Gaharwar, R.K. Avery, A. Assmann, A. Paul, G.H. McKinley, A. Khademhosseini, B.D. Olsen, Shear-thinning nanocomposite hydrogels for the treatment of hemorrhage, ACS Nano 8 (2014) 9833–9842, https://doi.org/10.1021/NN503719N/SUPPL_FILE/NN503719N_SI_001.PDF.

[112] S.E. Baker, A.M. Sawvel, N. Zheng, G.D. Stucky, Controlling bioprocesses with inorganic surfaces: layered clay hemostatic agents, Chem. Mater. 19 (2007) 4390–4392, https://doi.org/10.1021/CM071457B/SUPPL_FILE/CM071457B-FILE001.PDF.

[113] G. Lokhande, J.K. Carrow, T. Thakur, J.R. Xavier, M. Parani, K.J. Bayless, A. K. Gaharwar, Nanoengineered injectable hydrogels for wound healing application, Acta Biomater. 70 (2018) 35–47, https://doi.org/10.1016/J.ACTBIO.2018.01.045.

[114] C. Li, C. Mu, W. Lin, T. Ngai, Gelatin effects on the physicochemical and hemocompatible properties of gelatin/PAAm/laponite nanocomposite hydrogels, ACS Appl. Mater. Interfaces 7 (2015) 18732–18741, https://doi.org/10.1021/ACSAMI.5B05287/ASSET/IMAGES/MEDIUM/AM-2015-052878_0007.GIF.

[115] J.L. Dávila, M.A. d'Ávila, Rheological evaluation of Laponite/alginate inks for 3D extrusion based printing, Int. J. Adv. Manuf. Technol. 101 (2019) 675–686, https://doi.org/10.1007/S00170-018-2876-Y/METRICS.

[116] J. Guo, R. Zhang, L. Zhang, X. Cao, 4D printing of robust hydrogels consisted of agarose nanofibers and polyacrylamide, ACS Macro Lett. 7 (2018) 442–446, https://doi.org/10.1021/ACSMACROLETT.7B00957/SUPPL_FILE/MZ7B00957_SI_002.MPG.

[117] N. Zandi, E.S. Sani, E. Mostafavi, D.M. Ibrahim, B. Salch, M.A. Shokrgozar, E. Tamjid, P.S. Weiss, A. Simchi, N. Annabi, Nanoengineered shear-thinning and bioprintable hydrogel as a versatile platform for biomedical applications, Biomaterials 267 (2021), 120476, https://doi.org/10.1016/J.BIOMATERIALS.2020.120476.

[118] E. Munoz-Perez, A. Perez-Valle, M. Igartua, E. Santos-Vizcaino, R.M. Hernandez, High resolution and fidelity 3D printing of Laponite and alginate ink hydrogels for tunable biomedical applications, Biomater. Adv. 149 (2023), 213414, https://doi.org/10.1016/J.BIOADV.2023.213414.

[119] C. Qin, C. Wu, Inorganic biomaterials-based bioinks for three-dimensional bioprinting of regenerative scaffolds, View 3 (2022), 20210018, https://doi.org/10.1002/VIW.20210018.

[120] V.A. Kasyanov, J. Hodde, M.C. Hiles, C. Eisenberg, L. Eisenberg, L.E.F. De Castro, I. Ozolanta, M. Murovska, R.A. Draughn, G.D. Prestwich, R.R. Markwald, V. Mironov, Rapid biofabrication of tubular tissue constructs by centrifugal casting in a decellularized natural scaffold with laser-machined micropores, J. Mater. Sci. Mater. Med. 20 (2009) 329–337, https://doi.org/10.1007/S10856-008-3590-3.

[121] Y. Jin, C. Liu, W. Chai, A. Compaan, Y. Huang, Self-supporting nanoclay as internal scaffold material for direct printing of soft hydrogel composite structures in air, ACS Appl. Mater. Interfaces 9 (2017) 17456–17465, https://doi.org/10.1021/ACSAMI.7B03613.
[122] N.A. Sears, D.R. Seshadri, P.S. Dhavalikar, E. Cosgriff-Hernandez, A review of three-dimensional printing in tissue engineering, Tissue Eng., Part B 22 (2016) 298–310, https://doi.org/10.1089/TEN.TEB.2015.0464.
[123] H. Li, C. Tan, L. Li, Review of 3D printable hydrogels and constructs, Mater. Des. 159 (2018) 20–38, https://doi.org/10.1016/J.MATDES.2018.08.023.
[124] T. Xia, W. Liu, L. Yang, A review of gradient stiffness hydrogels used in tissue engineering and regenerative medicine, J. Biomed. Mater. Res. 105 (2017) 1799–1812, https://doi.org/10.1002/JBM.A.36034.
[125] B. Ruzicka, E. Zaccarelli, A fresh look at the Laponite phase diagram, Soft Matter 7 (2011) 1268–1286, https://doi.org/10.1039/C0SM00590H.
[126] K. Haraguchi, Development of soft nanocomposite materials and their applications in cell culture and tissue engineering, J. Stem Cells Regen. Med. 8 (2012) 2, https://doi.org/10.46582/JSRM.0801002.
[127] L.Y. Zhou, J. Fu, Y. He, A review of 3D printing technologies for soft polymer materials, Adv. Funct. Mater. 30 (2020), 2000187, https://doi.org/10.1002/ADFM.202000187.
[128] A. Nadernezhad, O.S. Caliskan, F. Topuz, F. Afghah, B. Erman, B. Koc, Nanocomposite bioinks based on agarose and 2D nanosilicates with tunable flow properties and bioactivity for 3D bioprinting, ACS Appl. Bio Mater. 2 (2019) 796–806, https://doi.org/10.1021/acsabm.8b00665.
[129] T. Ahlfeld, G. Cidonio, D. Kilian, S. Duin, A.R. Akkineni, J.I. Dawson, S. Yang, A. Lode, R.O.C. Oreffo, M. Gelinsky, Development of a clay based bioink for 3D cell printing for skeletal application, Biofabrication 9 (2017), 034103, https://doi.org/10.1088/1758-5090/AA7E96.
[130] G. Cidonio, C.R. Alcala Orozco, K.S. Lim, M. Glinka, I. Mutreja, Y.H. Kim, J. I. Dawson, T.B.F. Woodfield, R.O.C. Oreffo, Osteogenic and angiogenic tissue formation in high fidelity nanocomposite Laponite-gelatin bioinks, Biofabrication 11 (2019), https://doi.org/10.1088/1758-5090/AB19FD.
[131] D. Kharaghani, E. Kaffashsaei, M.K. Haider, I.S. Kim, The effect of polymeric nanofibers used for 3D-printed scaffolds on cellular activity in tissue engineering: a review, Int. J. Mol. Sci. 24 (2023) 9464, https://doi.org/10.3390/IJMS24119464, 2023, Vol. 24, Page 9464.
[132] S. Heid, A.R. Boccaccini, Advancing bioinks for 3D bioprinting using reactive fillers: a review, Acta Biomater. 113 (2020) 1–22, https://doi.org/10.1016/J.ACTBIO.2020.06.040.
[133] K. Nagahama, N. Oyama, K. Ono, A. Hotta, K. Kawauchi, T. Nishikata, Nanocomposite injectable gels capable of self-replenishing regenerative extracellular microenvironments for in vivo tissue engineering, Biomater. Sci. 6 (2018) 550–561, https://doi.org/10.1039/C7BM01167A.
[134] J.K. Carrow, L.M. Cross, R.W. Reese, M.K. Jaiswal, C.A. Gregory, R. Kaunas, I. Singh, A.K. Gaharwar, Widespread changes in transcriptome profile of human mesenchymal stem cells induced by two-dimensional nanosilicates, Proc. Natl. Acad. Sci. U. S. A. 115 (2018) E3905–E3913, https://doi.org/10.1073/PNAS.1716164115.
[135] V. de A.M. Gonzaga, A.L. Poli, J.S. Gabriel, D.Y. Tezuka, T.A. Valdes, A. Leitão, C. F. Rodero, T.M. Bauab, M. Chorilli, C.C. Schmitt, Chitosan-laponite nanocomposite scaffolds for wound dressing application, J. Biomed. Mater. Res. B Appl. Biomater. 108 (2020) 1388–1397, https://doi.org/10.1002/JBM.B.34487.
[136] J. Shi, R. Zhang, N. Yang, Y. Zhang, B.W. Mansel, S. Prabakar, J. Ma, Hierarchical incorporation of surface-functionalized laponite clay nanoplatelets with type i collagen matrix, Biomacromolecules 22 (2021) 504–513, https://doi.org/10.1021/ACS.BIOMAC.0C01391/SUPPL_FILE/BM0C01391_SI_001.PDF.
[137] E. Saygili, P. Saglam-Metiner, B. Caknak, E. Alarcin, G. Beceren, P. Tulum, Y.-W. Kim, K. Gunes, G.G. Eren-Ozcan, D. Akakin, J. Y. Sun, O. Yesil-Celiktas, Bilayered laponite/alginate poly(acrylamide) composite hydrogel for osteochondral injuries enhances macrophage polarization: an in vivo study, Biomater. Adv. 134 (2022), 112721, https://doi.org/10.1016/j.msec.2022.112721.
[138] D.M. Reffitt, N. Ogston, R. Jugdaohsingh, H.F.J. Cheung, B.A.J. Evans, R.P. H. Thompson, J.J. Powell, G.N. Hampson, Orthosilicic acid stimulates collagen type 1 synthesis and osteoblastic differentiation in human osteoblast-like cells in vitro, Bone 32 (2003) 127–135, https://doi.org/10.1016/S8756-3282(02)00950-X.
[139] C.M. Hedgepeth, L.J. Conrad, J. Zhang, H.C. Huang, V.M.Y. Lee, P.S. Klein, Activation of the Wnt signaling pathway: a molecular mechanism for lithium action, Dev. Biol. 185 (1997) 82–91, https://doi.org/10.1006/DBIO.1997.8552.
[140] P. Cheng, P. Han, C. Zhao, S. Zhang, H. Wu, J. Ni, P. Hou, Y. Zhang, J. Liu, H. Xu, S. Liu, X. Zhang, Y. Zheng, Y. Chai, High-purity magnesium interference screws promote fibrocartilaginous entheses regeneration in the anterior cruciate ligament reconstruction rabbit model via accumulation of BMP-2 and VEGF, Biomaterials 81 (2016) 14–26, https://doi.org/10.1016/J.BIOMATERIALS.2015.12.005.
[141] S. Yoshizawa, A. Brown, A. Barchowsky, C. Sfeir, Magnesium ion stimulation of bone marrow stromal cells enhances osteogenic activity, simulating the effect of magnesium alloy degradation, Acta Biomater. 10 (2014) 2834–2842, https://doi.org/10.1016/J.ACTBIO.2014.02.002.
[142] S. Jatav, Y.M. Joshi, Chemical stability of Laponite in aqueous media, Appl. Clay Sci. 97–98 (2014) 72–77, https://doi.org/10.1016/J.CLAY.2014.06.004.
[143] H. Zreiqat, C.R. Howlett, A. Zannettino, P. Evans, G. Schulze-Tanzil, C. Knabe, M. Shakibaei, Mechanisms of magnesium-stimulated adhesion of osteoblastic cells to commonly used orthopaedic implants, J. Biomed. Mater. Res. 62 (2002) 175–184, https://doi.org/10.1002/JBM.10270.
[144] Z. Martín-Moldes, D. López Barreiro, M.J. Buehler, D.L. Kaplan, Effect of the silica nanoparticle size on the osteoinduction of biomineralized silk-silica nanocomposites, Acta Biomater. 120 (2021) 203–212, https://doi.org/10.1016/J.ACTBIO.2020.10.043.
[145] K. Kundu, A. Afshar, D.R. Katti, M. Edirisinghe, K.S. Katti, Composite nanoclay-hydroxyapatite-polymer fiber scaffolds for bone tissue engineering manufactured using pressurized gyration, Compos. Sci. Technol. 202 (2021), 108598, https://doi.org/10.1016/j.compscitech.2020.108598.
[146] K. Kundu, D.R. Katti, K.S. Katti, Tissue-engineered interlocking scaffold blocks for the regeneration of bone, JOM 72 (2020) 1443–1457, https://doi.org/10.1007/S11837-020-04027-5/METRICS.
[147] N. Dinjaski, D. Ebrahimi, S. Ling, S. Shah, M.J. Buehler, D.L. Kaplan, Integrated modeling and experimental approaches to control silica modification of design silk-based biomaterials, ACS Biomater. Sci. Eng. 3 (2017) 2877–2888, https://doi.org/10.1021/acsbiomaterials.6b00236.
[148] S. Miao, J. Zhou, B. Liu, X. Lei, T. Wang, X. Hao, P. Cheng, H. Wu, Y. Song, G. Pei, L. Bi, A 3D bioprinted nano-laponite hydrogel construct promotes osteogenesis by activating PI3K/AKT signaling pathway, Mater Today Bio 16 (2022), https://doi.org/10.1016/J.MTBIO.2022.100342.
[149] S. Wang, R. Castro, X. An, C. Song, Y. Luo, M. Shen, H. Tomás, M. Zhu, X. Shi, Electrospun laponite-doped poly(lactic-co-glycolic acid) nanofibers for osteogenic differentiation of human mesenchymal stem cells, J. Mater. Chem. 22 (2012) 23357–23367, https://doi.org/10.1039/C2JM34249A.
[150] S.M. Mihaila, A.K. Gaharwar, R.L. Reis, A. Khademhosseini, A.P. Marques, M. E. Gomes, The osteogenic differentiation of SSEA-4 sub-population of human adipose derived stem cells using silicate nanoplatelets, Biomaterials 35 (2014) 9087–9099, https://doi.org/10.1016/J.BIOMATERIALS.2014.07.052.
[151] A.H. Ambre, D.R. Katti, K.S. Katti, Nanoclays mediate stem cell differentiation and mineralized ECM formation on biopolymer scaffolds, J. Biomed. Mater. Res. 101 (2013) 2644–2660, https://doi.org/10.1002/JBM.A.34561.
[152] M. Mousa, J.A. Milan, O. Kelly, J. Doyle, N.D. Evans, R.O.C. Oreffo, J.I. Dawson, The role of lithium in the osteogenic bioactivity of clay nanoparticles, Biomater. Sci. 9 (2021) 3150–3161, https://doi.org/10.1039/D0BM01444C.
[153] D. Choi, J. Heo, J. Aviles Milan, R.O.C. Oreffo, J.I. Dawson, J. Hong, Y.H. Kim, Structured nanofilms comprising Laponite® and bone extracellular matrix for osteogenic differentiation of skeletal progenitor cells, Mater. Sci. Eng., C 118 (2021), https://doi.org/10.1016/J.MSEC.2020.111440.
[154] Y. Chen, Y. Chen, T. Han, Z. Xie, Y. Yang, S. Chen, C. Wang, Enhanced osteogenic and antibacterial properties of polyetheretherketone by ultraviolet-initiated grafting polymerization of a gelatin methacryloyl/epsilon-poly-L-lysine/laponite hydrogel coating, J. Biomed. Mater. Res. (2023), https://doi.org/10.1002/JBM.A.37589.
[155] M. Mousa, N.D. Evans, R.O.C. Oreffo, J.I. Dawson, Clay nanoparticles for regenerative medicine and biomaterial design: a review of clay bioactivity, Biomaterials 159 (2018) 204–214, https://doi.org/10.1016/J.BIOMATERIALS.2017.12.024.
[156] A.K. Gaharwar, P.J. Schexnailder, B.P. Kline, G. Schmidt, Assessment of using laponite cross-linked poly(ethylene oxide) for controlled cell adhesion and mineralization, Acta Biomater. 7 (2011) 568–577, https://doi.org/10.1016/J.ACTBIO.2010.09.015.
[157] C.W. Peak, J.K. Carrow, A. Thakur, A. Singh, A.K. Gaharwar, Elastomeric cell-laden nanocomposite microfibers for engineering complex tissues, Cell. Mol. Bioeng. 8 (2015) 404–415, https://doi.org/10.1007/S12195-015-0406-7/METRICS.
[158] P.J. Schexnailder, A.K. Gaharwar, R.L. Bartlett, B.L. Seal, G. Schmidt, Tuning cell adhesion by incorporation of charged silicate nanoparticles as cross-linkers to polyethylene oxide, Macromol. Biosci. 10 (2010) 1416–1423, https://doi.org/10.1002/MABI.201000053.
[159] N. Sällström, A. Capel, M.P. Lewis, D.S. Engström, S. Martin, 3D printable zwitterionic nano-composite hydrogel system for biomedical applications, J. Tissue Eng. 11 (2020), https://doi.org/10.1177/2041731420967294/ASSET/IMAGES/LARGE/10.1177_2041731420967294-FIG7.JPEG.
[160] Biomaterials and Regenerative Medicine in Ophthalmology - first ed., (n.d.). https://shop.elsevier.com/books/biomaterials-and-regenerative-medicine-in-ophthalmology/chirila/978-1-84569-443-2 (accessed December 4, 2023).
[161] T. Chirila, D. Harkin, 18.4 Choice of materials for repair, Biomaterials and Regenerative Medicine in Ophthalmology (2009) 477.
[162] M.P. Ferraz, Biomaterials for ophthalmic applications, Appl. Sci. 12 (2022) 5886, https://doi.org/10.3390/APP12125886, 2022, Vol. 12, Page 5886.
[163] D. Tognetto, M.R. Pastore, G.M. Guerin, G. Decorti, M. Franzin, C. Lagatolla, G. Cirigliano, Bactericidal activity of three different antiseptic ophthalmic preparations as surgical prophylaxis, Graefes Arch. Clin. Exp. Ophthalmol. 260 (2022) 289–293, https://doi.org/10.1007/S00417-021-05361-3.
[164] Y. Ju, Y. Hu, P. Yang, X. Xie, B. Fang, Extracellular vesicle-loaded hydrogels for tissue repair and regeneration, Mater Today Bio 18 (2023), 100522, https://doi.org/10.1016/J.MTBIO.2022.100522.
[165] D. Diaz-Valle, B. Burgos-Blasco, D. Rego-Lorca, V. Puebla-Garcia, P. Perez-Garcia, J.M. Benitez-del-Castillo, R. Herrero-Vanrell, M. Vicario-de-la-Torre, J. A. Gegundez Fernandez, Comparison of the efficacy of topical insulin with autologous serum eye drops in persistent epithelial defects of the cornea, Acta Ophthalmol. 100 (2022) e912–e919, https://doi.org/10.1111/AOS.14997.
[166] J.B. Miesfeld, N.L. Brown, Eye organogenesis: a hierarchical view of ocular development, Curr. Top. Dev. Biol. 132 (2019) 351–393, https://doi.org/10.1016/BS.CTDB.2018.12.008.

[167] M. Mukit, F. Anbar, K. Dadireddy, P. Konofaos, Eyelid reconstruction: an algorithm based on defect location, J. Craniofac. Surg. 33 (2022) 821–826, https://doi.org/10.1097/SCS.0000000000008433.
[168] M.K. Farazdaghi, W.R. Katowitz, R.A. Avery, Current treatment of optic nerve gliomas, Curr. Opin. Ophthalmol. 30 (2019) 356, https://doi.org/10.1097/ICU.0000000000000587.
[169] M. Ferrari, Cancer nanotechnology: opportunities and challenges, Nat. Rev. Cancer 5 (2005) 161–171, https://doi.org/10.1038/nrc1566, 2005 5:3.
[170] S. Siddique, J.C.L. Chow, Application of nanomaterials in biomedical imaging and cancer therapy, Nanomaterials 10 (2020) 1700, https://doi.org/10.3390/NANO10091700, 2020, Vol. 10, Page 1700.
[171] X. Liu, X. Niu, Z. Fu, L. Liu, S. Bai, J. Wang, L. Li, Y. Wang, X. Guo, A facile approach to obtain highly tough and stretchable LAPONITE®-based nanocomposite hydrogels, Soft Matter 16 (2020) 8394–8399, https://doi.org/10.1039/D0SM01132K.
[172] C.A. Rickert, S. Mansi, D. Fan, P. Mela, O. Lieleg, A mucin-based bio-ink for 3D printing of objects with anti-biofouling properties, Macromol. Biosci. 23 (2023), https://doi.org/10.1002/MABI.202300198.
[173] M.C. Grüner, K.P.S. Zanoni, C.F. Borgognoni, C.C. Melo, V. Zucolotto, A.S.S. De Camargo, Reaching biocompatibility with nanoclays: eliminating the cytotoxicity of Ir(III) complexes, ACS Appl. Mater. Interfaces 10 (2018) 26830–26834, https://doi.org/10.1021/ACSAMI.8B10842.

DISCUSIÓN

El uso de biomateriales en general y de biomateriales oftálmicos en particular está en continuo crecimiento, integrando conocimientos, ideas y avances de múltiples disciplinas, como la medicina, la biología, la química, la física, y la ingeniería, lo cual permite un número ilimitado de posibilidades para explorar. Con la llegada de las nuevas generaciones, los biomateriales han conseguido reducir las complicaciones y toxicidades, así como mejorar la biocompatibilidad. Además, con la introducción de los hidrogeles sintéticos, es decir, polímeros capaces de dirigir y retener agua sin disolverse en un medio acuoso, la gama de biomateriales oftálmicos ha aumentado considerablemente. El envejecimiento progresivo de la población ha propiciado que los problemas oculares sean cada vez más frecuentes, y, en este sentido, los biomateriales han contribuido en los últimos años a mejorar o restaurar la visión, repercutiendo de manera positiva en la calidad de vida de muchos pacientes. De hecho, el ojo es el primer órgano en el que se implantó un material extraño para cumplir la función de lo que hoy se denomina biomaterial. Las enfermedades del segmento posterior del ojo son difíciles de tratar por la poca permeabilidad de los tejidos, las barreras anatómicas y fisiológicas propias del ojo y la baja biodisponibilidad del fármaco en el tejido diana. Las medidas disponibles actualmente, en muchos casos, son insuficientes para mantener niveles terapéuticos adecuados del fármaco en la región posterior del ojo. Se trata, por tanto, de un campo donde urge seguir explorando e investigando nuevas estrategias terapéuticas. En los últimos años se han llevado a cabo investigaciones enfocadas en los sistemas de nanopartículas como biomateriales capaces de liberar fármacos de forma sostenida, lo que permite de forma simultánea reducir la dosis y mantener la administración de forma prolongada a nivel del tejido diana. Entre los diversos nanomateriales que se están explorando, la Laponita, un silicato estratificado coloidal sintético, destaca como un biomaterial especialmente prometedor y emergente.

La **Laponita** como biomaterial oftalmológico reúne una serie de características fisicoquímicas y biológicas que la hacen especialmente atractiva para su aplicación ocular, siendo destacable el hecho de ser un nanomaterial biocompatible, fácilmente inyectable y ópticamente transparente, con cualidades como la tixotropía, que facilita su inyección, y la capacidad para retener todo tipo de moléculas, así como para liberarlas de manera progresiva. Nuestro grupo realizó estudios previos con la Laponita, tanto a nivel *in vitro* como *in vivo*. En el primero de ellos se creó y caracterizó, *in vitro*, una nueva formulación de dexametasona utilizando una matriz de Laponita como base (formulación DEX/LAP), la cual mostró una liberación inicial de dexametasona de menos del 40% seguida de una liberación sostenida durante 24 semanas (Fraile et al., 2016). Se testó sobre soluciones que emulaban el humor vítreo. Este estudio puso de relieve la sencillez del método de preparación, en el que la fisisorción se modulaba cambiando el disolvente en el proceso de adsorción. Un estudio en paralelo demostró que la administración de Laponita en ojos sanos de conejo es segura y biocompatible, con persistencia intraocular tras inyección intravítrea y supracoroidea (Prieto et al., 2018). No hubo diferencias significativas en la presión intraocular, no se observaron complicaciones oculares relevantes, ni cambios patológicos en el estudio histológico. Además, se observó una lenta degradación de Laponita durante 14 semanas. La presencia de Laponita en el vítreo se confirmó indirectamente mediante valoración complexométrica aprovechando el alto contenido de iones de magnesio de ésta.

Continuando esta misma línea de investigación, la presente Tesis Doctoral se ha focalizado en evaluar *in vivo* la biocompatibilidad y eficacia de Laponita como portador de

varios agentes farmacológicos de diferentes características, concretamente un antiinflamatorio esteroideo de amplísima aplicación en patología oftalmológica como la dexametasona y un agente de baja solubilidad como la brimonidina. Se han comparado dos vías distintas de administración (supracoroidea, realizada quirúrgicamente; e intravítrea, mediante inyección mínimamente invasiva) y se ha trabajado con modelos animales tanto sanos como enfermos (Figura 11). Además, se ha monitorizado de manera mínimamente invasiva la formulación intravítrea mediante escaneos del gel vitreo mediante tomografía de coherencia óptica.

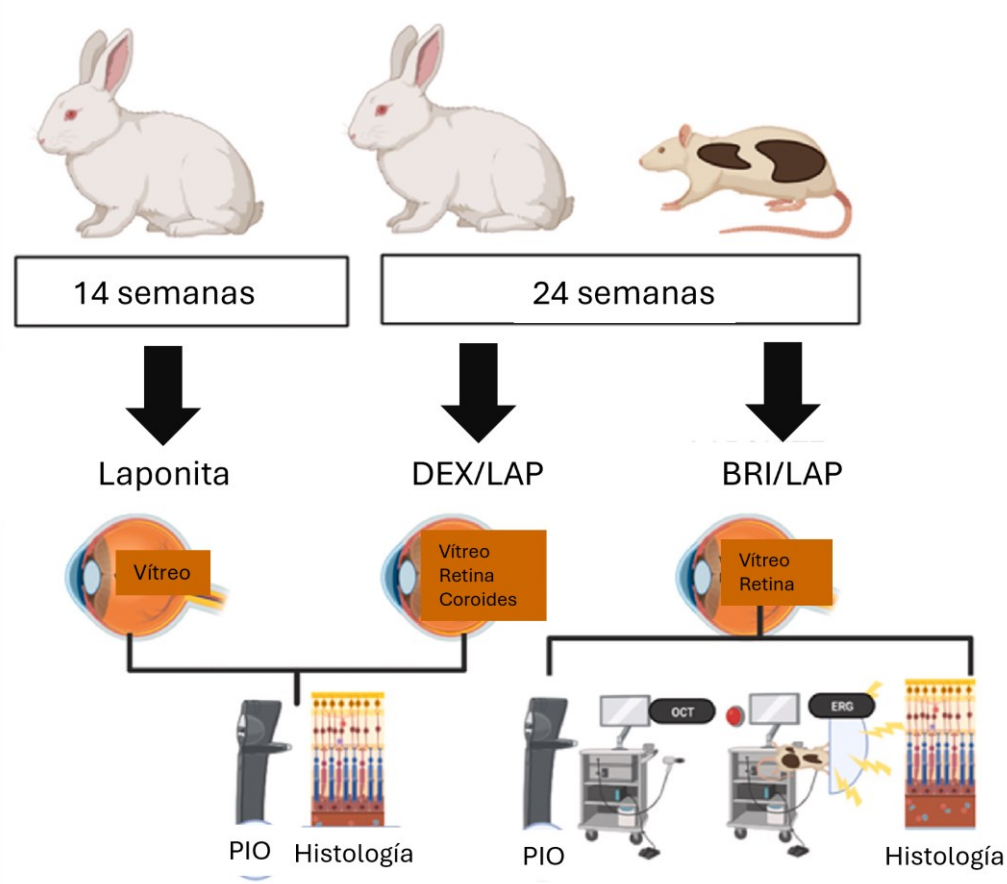

Figura 11. Estudios *in vivo* llevados a cabo con Laponita. Abreviaturas: DEX/LAP: dexametasona/Laponita; BRI/LAP: brimonidina/Laponita; PIO: presión intraocular; OCT: tomografía de coherencia óptica; ERG; electrorretinografía.

El primero de los trabajos que constituyen la presente Tesis Doctoral se centró en evaluar el **perfil farmacocinético y la seguridad ocular de la nueva formulación DEX/LAP**. Para llevarlo a cabo, se administró sobre ojos sanos de conejo, tras haber quedado demostrada la idoneidad de este modelo animal para los estudios farmacocinéticos por la buena correlación entre el humor vítreo de los conejos y el de los humanos (del Amo & Urtti, 2015). La elección de la dexametasona como fármaco obedece al hecho concomitante de su gran uso en el tratamiento de la patología del segmento posterior y de su alta hidrosolubilidad, lo que supone que para administrarla por vía intravítrea o supracoroidea se requiere utilizar sistemas que permitan una liberación sostenida del fármaco.

Actualmente en la práctica clínica se dispone de glucocorticoides que pueden administrarse por vía intravítrea en suspensión o en implantes biodegradables y no biodegradables. Tras la administración IV, su cinética ocular muestra un pico inicial a nivel del vítreo, para luego disminuir progresivamente y variable hasta estabilizar los niveles, tras lo cual descienden hasta volverse no detectables, dependiendo del periodo de actividad del tipo de mecanismo de liberación. En nuestro caso, la **administración IV** de 0,1 mg de dexametasona en forma de suspensión (10 mg ml^{-1}) de DEX/LAP, además de presentar la ventaja de administrarse como un nanogel suave inyectado con una aguja de 25 G (Soni et al., 2016), produjo un pico de liberación de dexametasona breve y precoz el primer día, seguido de un descenso en la primera semana y unos niveles posteriores en meseta hasta los 6 meses. Además, la dosis de dexametasona administrada fue inferior a la que incluye el implante IV biodegradable de PLGA, Ozurdex® (0,1 frente a 0,7 mg).

En cuanto a la **administración supracoroidea**, presenta varias ventajas sobre la administración intravítrea, entre ellas un menor riesgo de hemorragia en la pars plana, el hecho de no producir opacidad en el eje visual (cataratas o cuerpos flotantes), mayor biodisponibilidad en el tejido diana y menor respuesta inmunitaria. Este gran potencial se manifiesta en el creciente número de patentes y de publicaciones al respecto en los últimos años (Gilger et al., 2014). En nuestro estudio, la dosis de 0,05 mg de dexametasona en forma de suspensión (10 mg ml^{-1}) de DEX/LAP a nivel del espacio supracoroideo, mostró un pico durante la semana 1, seguido por un descenso progresivo hasta la semana 12 y manteniéndose hasta la semana 24. En este caso, se pudo demostrar que la administración supracoroidea de DEX/LAP aumentó la disponibilidad de dexametasona en la unidad retina-coroides en comparación con la inyección intravítrea de Ozurdex® y también se mantuvo de forma más constante y prolongada hasta el final del del estudio. Esto podría evitar la sobredosificación, fluctuaciones y efectos secundarios, ya que ningún animal del estudio mostró aumentos de la PIO, cataratas o infecciones tras la administración supracoroidea de DEX/LAP. Hasta donde sabemos, sólo se ha realizado un estudio de administración de dexametasona en el espacio supracoroideo (Barbosa Saliba et al., 2016). Este estudio demostró la seguridad y eficacia del control de la inflamación en ratas con uveítis tras la colocación quirúrgica de un implante de poliuretano/- dexametasona de degradación lenta, pero utilizó dosis mucho más altas de dexametasona que en nuestro estudio.

Comparando los resultados en ambas vías de administración, las dos fueron seguras. Nuestros resultados sugieren un mayor beneficio de la vía supracoroidea de DEX/LAP en comparación con la vía intravítrea, aunque la vía supracoroidea provocó una mayor hiperemia y defectos epiteliales sobre la superficie ocular, que se atribuyeron a la intervención quirúrgica del proceso de canulación y tuvieron carácter reversible y temporal, y podrían minimizarse con el uso de inyecciones como Clearside®. Sin embargo, la iatrogenia por inyección intravítrea tuvo carácter permanente (catarata) y generó la visión de un cuerpo flotante hasta el final del estudio. Además, la vía supracoroidea mantuvo niveles sostenidos de dexametasona en los tejidos oculares con una menor cantidad de fármaco inyectado en el ojo (0,1 mg intravítrea frente a 0,05 mg supracoroidea). La vía intravítrea mostró mayor dilución y pico inicial, por lo que se necesitó más dosis de dexametasona, con el consiguiente mayor riesgo de efectos secundarios, como la hipertensión ocular. No obstante, la amplia experiencia obtenida con las inyecciones intravítreas en la práctica clínica hace que esta vía pueda ser más adecuada en contextos clínicos donde se requiere mayor dosis inicial de ataque. Las principales **limitaciones** atribuibles a este estudio vienen

determinadas por: (1) La imposibilidad de detectar niveles de dexametasona en el tejido diana para comparar ambas vías de administración y, a su vez, con otras formulaciones ya existentes. (2) La no realización de pruebas sanguíneas para determinar los niveles de dexametasona en sangre. (3) La ausencia de estudios histológicos que confirmaran la correcta ubicación de la formulación DEX/LAP. (4) Trabajar solo sobre modelos animales sanos, desconociendo el comportamiento farmacocinético del agente terapéutico en modelos de enfermedad. En conclusión, con este trabajo quedó demostrado que la liberación de dexametasona a partir de Laponita se mantiene hasta 6 meses en el cuerpo vítreo de ojos de conejo sanos de forma segura.

A partir de ahí, continuando con el proceso de investigación basado en la Laponita y su aplicación oftalmológica, al no existir ningún tratamiento intravítreo enfocado al control de la neuropatía glaucomatosa, se decidió introducir tres cambios importantes. (1) Uso de brimonidina, un fármaco hipotensor ocular de baja solubilidad, para demostrar el carácter generalizable del método de liberación. (2) Aplicar en un modelo de enfermedad (glaucoma crónico) para confirmar la ausencia de efectos secundarios y el efecto terapéutico mantenido durante un período prolongado. (3) Pruebas en otro animal (ratas), como requerimiento previo a los ensayos traslacionales. Este segundo estudio de la presente Tesis Doctoral es el primer estudio *in vivo* que muestra que un sistema de liberación sostenida de brimonidina (única inyección intravítrea de **formulación BRI/LAP**), produjo la mayor reducción mantenida de la PIO (Chiang, Kim, et al., 2016) (Pek et al., 2016) y un efecto neuroprotector durante al menos 6 meses, incluso en un modelo de enfermedad en el que se supone que la neurodegeneración se produce más rápidamente. La formulación BRI-LAP produjo un efecto hipotensor neto (disminución de aproximadamente 9 mmHg) en ojos con hipertensión ocular durante 8 semanas, que es el doble del tiempo descrito al utilizar nanoesponjas intravítreas (Lambert et al., 2015). El mayor efecto hipotensor se observó en las fases tempranas coincidiendo con la mayor liberación de brimonidina (aproximadamente 120-80 ng ml^{-1}) y desapareció en fases tardías, cuando la liberación de brimonidina se estabilizó (aproximadamente 60 ng ml^{-1}). Curiosamente, el inicio del tratamiento con la formulación BRI/LAP en un ojo también pudo controlar la PIO en el ojo contralateral, aunque los niveles de brimonidina estuvieran por debajo del límite de detección. Es probable que a los 6 meses la mayor parte de la brimonidina analizada esté asociada a Laponita. La cantidad mínima (desconocida) de brimonidina no asociada no podría controlar eficazmente la PIO en las fases finales del estudio. Esta observación coincide con otros autores, que muestran un efecto de hipopresión ocular inicialmente superior (Lambert et al., 2015) que disminuye posteriormente (hasta 4 semanas) (Chiang, Kim, et al., 2016). La brimonidina tiene una vida media corta (12 horas) y una eliminación rápida en el ojo (Walters, 1996). Al administrarse por vía intravítrea, esta formulación garantizaría el cumplimiento del tratamiento y un control satisfactorio de la enfermedad durante largos periodos de tiempo, siendo necesaria su administración quizá dos veces al año.

Los exámenes neurorretinianos mediante tecnología OCT mostraron que la formulación BRI-LAP mejoró la protección estructural axonal (hasta la semana 6) y se mantuvo en las células ganglionares hasta las fases intermedias (semanas 6 y 8) y tardías (semanas 12 y 24). Estos resultados corroboran los anteriores, en los que el mayor efecto hipotensor observado en las primeras fases del estudio protegió a los axones del daño dependiente de la PIO, mientras que las concentraciones de brimonidina inferiores (del orden de nanogramos) detectadas en la fase de meseta proporcionaron posteriormente

protección neurorretiniana al interactuar con los receptores adrenérgicos de la retina (Woldemussie et al., 2007) (Kalapesi et al., 2005). Además, mostró un efecto neurorpotector en el ojo contralateral (también hipertenso, pero no tratado), que pueden haber sido consecuencia de la diseminación contralateral retrógrada y anterógrada de la sustancia a través de la vía visual (Davis et al., 2016) (Lawlor et al., 2018) (Evangelho et al., 2019) y de la mejora del transporte axonal por la brimonidina (Lambert et al., 2011). Por otro lado, también mostró un efecto funcional protector, a través del protocolo de respuesta negativa fotópica de la ERG, aplicable principalmente a las CGRs (mayor amplitud en la semana 12) y los axones (latencia mantenida), que se corroboró en los estudios histológicos con un mayor recuento de CGRs utilizando un anticuerpo específico Brn3a. Kim et al (Kim et al., 2015) también informaron de un efecto neuroprotector tras la inyección intravítrea de nanopartículas cargadas de brimonidina que mejoraron la supervivencia de las CGR en un modelo de aplastamiento del nervio óptico, aunque no duró más de 14 días. La formulación intravítrea de BRI/LAP tuvo un efecto protector estructural y funcional en la retina que se mantuvo en los fotorreceptores bajo estimulación fotópica (pero no bajo estimulación escotópica) en las etapas posteriores (semana 24), y puede deberse al tiempo necesario para que la formulación atraviese las diferentes capas de la retina. De hecho, desde las primeras semanas se observó la formulación en el vítreo mediante OCT, pero no fue hasta la semana 12 cuando se observó intrarretina.

Este estudio demuestra que el uso de Laponita como portador de fármacos para la administración intraocular presenta varias ventajas. (1) Desde una perspectiva química, la formulación de BRI/LAP es fácil y sencilla de preparar y la liberación del fármaco no está asociada a la degradación del portador, a diferencia de otros sistemas de administración de fármacos (Sun et al., 2017). (2) Desde una perspectiva clínica, la formulación de gel transparente, tixotrópico y a nanoescala permite inyectarlo en el cuerpo vítreo a través de agujas de menor calibre, a diferencia de BrimoDDS® -que requiere aplicadores - u otros dispositivos e implantes (Deokule et al., 2012). Como **limitaciones**, se produjo un nivel sorprendente e inesperado de muerte precoz de ratas. Esto pudo deberse tanto a la repetición de la anestesia intraperitoneal con dexmedetomidina como a los efectos depresores de la brimonidina sobre el sistema nervioso central. Es por ello por lo que sería aconsejable realizar análisis de sangre y futuros estudios de ajuste y escalado farmacodinámico o de inserción de manera simultánea con diferentes agentes en el soporte de arcilla (Arranz-Romera et al., 2019), antes de explorar la posible transferibilidad a la práctica clínica.

Los estudios realizados mediante OCT aportaron información no solo de la estructura y grosor neurorretinianos, sino también de la interfase vitreorretiniana, donde se observó la formulación en forma de agregados hiperreflectantes. A partir de estos hallazgos se realizó el siguiente trabajo de esta Tesis Doctoral con el fin de **monitorizar la formulación BRI/LAP** mediante una caracterización cualitativa y cuantitativa de dichos agregados en función de los cambios en la intensidad de la señal vítrea observada, respecto a la intensidad del epitelio pigmentario de la retina, expresado como ratio VIT/EPR. Los agregados vítreos hiperreflectantes tendieron a asentarse en la superficie retiniana y alcanzaron el espacio intrarretiniano, posiblemente por difusión debido al pequeño tamaño de las plaquetas de LAP (1 nm de alto, 30 nm de diámetro) capaces de atravesar los poros de la membrana limitante interna y a la lipofilia de la brimonidina. La **OCT** fue fundamental para demostrar la degradación *in vivo* de la cantidad de BRI/LAP inyectada (basada en el área total de

agregados) y la agregación morfológica y dinámica de las moléculas de LAP (basada en el área media de agregados). La intensidad relativa y el tamaño de los agregados disminuyeron progresivamente durante 24 semanas en los ojos de las ratas tratadas según se degradaba la FI BRI/LAP. E interesantemente, la intensidad relativa VIT/EPR y el área total de agregados se correlacionaron con los niveles de brimonidina medidos en el ojo.

Los resultados *in vivo* coincidieron con los *in vitro.* (1) La mayor tasa de degradación de BRI/LAP coincidió con liberación de brimonidina y se produjo en las primeras etapas, y entre la mitad y final del estudio la degradación se produjo muy lentamente. (2) La mayor agregación de las primeras fases coincidió con el inicio del daño inducido por la hipertensión ocular y por tanto con un aumento de la acidosis, y en fases posteriores los agregados se empequeñecieron, lo que sugiere una menor acidosis y muerte celular debida al efecto neuroprotector. (3) Además, en la semana 3 los ojos tratados presentaron un pico hipertensivo. La LAP se hincha en medio acuoso, por lo que nuestra hipótesis era que un aumento del tamaño del agregado era responsable del aumento de la PIO. Mediante OCT se constató un aumento del tamaño de la FI BRI/LAP en las primeras fases (2-3 semanas), lo que confirmó nuestra hipótesis.

Por otro lado, la OCT es una tecnología no invasiva que ha demostrado poder ofrecer imágenes casi histológicas según la luz transmitida o reflejada al atravesar la luz distintas estructuras con densidades diferentes. El aumento de señal que ofrece la FI BRI/LAP puede ser consecuencia de la lipofilia de la brimonidina y de los componentes de silicio y magnesio de la LAP. Dado que la OCT es una técnica de obtención de imágenes por dispersión de la luz, una mayor intensidad relativa VIT/EPR indicaría una mayor dispersión de la luz, con riesgo de percepción de moscas volantes. A este respecto, el tamaño de los agregados era del orden de micras (de 850 a 760 micras), mucho menor que el implante Ozurdex® o Brimo DDS®. En la mayoría de los agregados no se detectó ninguna sombra, lo que sugiere que la percepción potencial de cuerpos flotantes sería mínima o inexistente. Esto se traduciría en menor disconfort para los pacientes, incluyendo el menor grosor de la aguja.

En resumen, el análisis mediante OCT del vítreo muestra que la intensidad relativa VIT/EPR es (1) significativamente mayor en los ojos tratados con la FI BRI/LAP que en los no tratados; (2) que los valores de intensidad disminuyen con el tiempo; (3) que los agregados pueden calcularse con un alto grado de reproducibilidad y (4) que el área total agregada se correlaciona con la cantidad de brimonidina en todas las fases del estudio y muestra una curva de degradación similar. Por lo tanto, la intensidad relativa de VIT/EPR parece ser un marcador útil y objetivo para la monitorización no invasiva de la formulación BRI/LAP, postulándose como un novedoso método de medición no invasivo.

En cuanto a las **limitaciones**, hay que tener en cuenta varios aspectos. (1) La profundidad del vítreo analizada mediante OCT es parcial y se limita a un máximo de 1,9 mm. No obstante, el análisis realizado en la interfase vitreorretiniana mediante un protocolo de seguimiento (que consiste en estudiar exactamente el mismo lugar en exploraciones seriadas) presenta una muestra representativa del gel vítreo completo, como han mostrado otros investigadores (Chu et al., 2013) (Korot et al., 2016). La alta correlación mostrada en los resultados (intensidad de la señal OCT frente a concentración de brimonidina en el ojo) demuestra la aplicabilidad en ratas y, presentada como escala logarítmica, sugiere que no sería necesario el estudio de todo el cuerpo vítreo. Sin embargo, estos animales tienen un cristalino enorme y, por tanto, un volumen vítreo muy pequeño en comparación con los

humanos. En estudios posteriores se recomendaría el análisis completo del cuerpo vítreo para corroborar la aplicabilidad de este seguimiento en animales con una estructura organizativa similar a la humana, como los cerdos o los perros. También sería deseable llevar a cabo estudios solo con Laponita, dado que esta técnica es adecuada para formulaciones hiperreflectantes, rasgo que en nuestro estudio puede haber sido atribuible a la brimonidina. (2) Algunos de los puntos hiperreflectantes se pudieran deber a la inflamación latente (Keane et al., 2014) secundaria a la inducción del glaucoma, con la consiguiente alteración o aumento de la intensidad de la señal. (3) Por último, considerando la traslación a entornos clínicos, las opacidades vítreas presentes en los individuos de edad avanzada y que son la población objetivo principal de esta formulación, serían una cuestión para considerar. Sin embargo, en general, las opacidades flotantes suelen mantenerse en un rango estable y el método de monitorización presentado en este estudio se realiza con una señal relativa (VIT/EPR).

Finalmente, en el último trabajo de esta Tesis Doctoral se realizó una **revisión** de los estudios realizados con Laponita en el ojo en los últimos 10 años, y de los estudios que no se realizaron en el ojo, pero que podrían ser potencialmente aplicables en oftalmología ya que se utilizan los mismos fármacos, el tejido evaluado *in vitro* o *in vivo* también está presente en el ojo, las patologías tratadas también se dan en el ojo y/o los nuevos tratamientos son potencialmente aplicables en el ojo. Para examinar el amplio espectro de aplicaciones biomédicas de Laponita en el ojo, y dado que la oftalmología es una especialidad médica y quirúrgica, se hizo referencia a estudios relacionados con la administración de fármacos (para cuestiones médicas), hemorragias (para cuestiones quirúrgicas) e ingeniería de tejidos con medicina regenerativa y andamiajes (para la reparación mínimamente invasiva del ojo en aplicaciones prospectivas).

La revisión mostró las numerosas evidencias científicas que sugieren que la Laponita puede utilizarse en todas las estructuras y tejidos oculares, desde la piel y los apéndices oculares hasta la retina y la órbita, a pesar de los pocos estudios realizados hasta la fecha sobre la aplicación del biomaterial Laponita en el ojo y/o tejido ocular. Entre sus ventajas destacan -en el caso de la oftalmología- la biocompatibilidad, la transparencia óptica, el grosor nanométrico y la tixotropía que facilita la inyección, además de su capacidad para retener todo tipo de moléculas, incluso en co-carga, y su habilidad para liberarlas progresivamente para tratar la célula diana tras su administración en forma de gel tópico o inyección cutánea, intravítrea o supracoroidea, o como andamiaje. También posee características bactericidas y regenerativas intrínsecas. La transformación clínica de la Laponita en términos de administración de fármacos parece más factible, sencilla y cercana. El andamiaje, en cambio, y especialmente para el tejido neural, parece lejano, ya que las complejas conexiones entre los tipos celulares de la retina siguen siendo un reto. Se concluyó con la idea de que la Laponita parece ser un biomaterial que merece un estudio más profundo en aplicaciones médicas, quirúrgicas y regenerativas en futuras investigaciones oftalmológicas.

Resultado de todo lo anteriormente expuesto y con vistas a una futura traslación, el grupo de investigación protegió el uso de Laponita para aplicación oftalmológica mediante una solicitud de **patente** europea registrada (#No. 20 382 021.2) por la Universidad de Zaragoza.

CONCLUSIONES

1. La **formulación de dexametasona - Laponita** (DEX/LAP) administrada mediante inyección intravítrea mínimamente invasiva y mediante administración supracoroidea resultó **segura y biocompatible** en ojos sanos de conejo.

2. Una **única administración intravítrea o supracoroidea** de la formulación DEX/LAP produjo la liberación progresiva de dexametasona y prolongó el tiempo de permanencia en el humor vítreo y la unidad coroides-retina **hasta 6 meses** en comparación con las formulaciones convencionales.

3. La administración mediante inyección intravítrea de la **formulación de brimonidina - Laponita** (BRI/LAP) tuvo un **efecto hipotensor y neuroprotector** funcional y estructural en ratas con glaucoma inducido.

4. Una **única inyección intravítrea** de la formulación BRI/LAP produjo una liberación sostenida de brimonidina y fue capaz de mantener dicho efecto hipotensor y neuroprotector durante **al menos 6 meses**.

5. La formulación intravítrea BRI/LAP pudo ser visualizada y monitorizada mediante los cambios en la intensidad de la señal vítrea respecto a la intensidad del epitelio pigmentario de la retina, utilizando la tecnología de imagen no invasiva de **tomografía de coherencia óptica** (OCT).

6. Este novedoso sistema de medición objetiva por OCT permitió la **monitorización** de la formulación intravítrea BRI/LAP, y mostró una correlación adecuada con los niveles del fármaco brimonidina en el ojo constituyéndose como un potencial biomarcador para su uso en la monitorización terapéutica en ensayos clínicos.

7. La revisión sistemática de la bibliografía reveló una **escasez de estudios llevados a cabo** hasta la fecha sobre el biomaterial Laponita en el ojo, pero con evidencia científica de biocompatibilidad y potencial aplicación en el ojo.

8. La translación a la práctica clínica del biomaterial Laponita como **sistema de administración de fármacos** parece un hecho factible, sencillo y próximo. Sin embargo, su aplicación en el campo de la medicina regenerativa parece todavía lejano.

BIBLIOGRAFÍA

AGUZZI, C., CEREZO, P., VISERAS, C., & CARAMELLA, C. (2007). Use of clays as drug delivery systems: Possibilities and limitations. *Applied Clay Science*, *36*(1–3), 22–36. https://doi.org/10.1016/j.clay.2006.06.015

Ahmad, I., Teotia, P., Erickson, H., & Xia, X. (2020). Recapitulating developmental mechanisms for retinal regeneration. *Progress in Retinal and Eye Research*, *76*, 100824. https://doi.org/10.1016/j.preteyeres.2019.100824

Ahn, S. J., Hong, H. K., Na, Y. M., Park, S. J., Ahn, J., Oh, J., Chung, J. Y., Park, K. H., & Woo, S. J. (2016). Use of Rabbit Eyes in Pharmacokinetic Studies of Intraocular Drugs. *Journal of Visualized Experiments*, *113*. https://doi.org/10.3791/53878

Almasieh, M., Wilson, A. M., Morquette, B., Cueva Vargas, J. L., & Di Polo, A. (2012). The molecular basis of retinal ganglion cell death in glaucoma. *Progress in Retinal and Eye Research*, *31*(2), 152–181. https://doi.org/10.1016/j.preteyeres.2011.11.002

Arranz-Romera, A., Esteban-Pérez, S., Garcia-Herranz, D., Aragón-Navas, A., Bravo-Osuna, I., & Herrero-Vanrell, R. (2019). Combination therapy and co-delivery strategies to optimize treatment of posterior segment neurodegenerative diseases. *Drug Discovery Today*, *24*(8), 1644–1653. https://doi.org/10.1016/j.drudis.2019.03.022

Awwad, S., Mohamed Ahmed, A. H. A., Sharma, G., Heng, J. S., Khaw, P. T., Brocchini, S., & Lockwood, A. (2017). Principles of pharmacology in the eye. *British Journal of Pharmacology*, *174*(23), 4205–4223. https://doi.org/10.1111/bph.14024

Barar, J., Javadzadeh, A. R., & Omidi, Y. (n.d.). Ocular novel drug delivery: impacts of membranes and barriers. *Expert Opin Drug Deliv*, *5*, 567–581.

Barbosa Saliba, J., Vieira, L., Fernandes-Cunha, G. M., Rodrigues Da Silva, G., Ligório Fialho, S., Silva-Cunha, A., Bousquet, E., Naud, M.-C., Ayres, E., Oréfice, R. L., Tekaya, M., Kowalczuk, L., Zhao, M., & Behar-Cohen, F. (2016). Anti-Inflammatory Effect of Dexamethasone Controlled Released From Anterior Suprachoroidal Polyurethane Implants on Endotoxin-Induced Uveitis in Rats. *Investigative Ophthalmology & Visual Science*, *57*(4), 1671–1679. https://doi.org/10.1167/iovs.15-18127

Barnes, H. A. (1997). Thixotropy—a review. *Journal of Non-Newtonian Fluid Mechanics*, *70*(1–2), 1–33. https://doi.org/10.1016/S0377-0257(97)00004-9

Bear, M. F., Paradiso Michael A, & Connors, B. W. (2002). *Neurociencia explorando el futuro* (Masson, Ed.).

Bisht, R., Mandal, A., Jaiswal, J. K., & Rupenthal, I. D. (2018). Nanocarrier mediated retinal drug delivery: overcoming ocular barriers to treat posterior eye diseases. *WIREs Nanomedicine and Nanobiotechnology*, *10*(2). https://doi.org/10.1002/wnan.1473

Brokesh, A. M., Cross, L. M., Kersey, A. L., Murali, A., Richter, C., Gregory, C. A., Singh, I., & Gaharwar, A. K. (2022). Dissociation of nanosilicates induces downstream endochondral differentiation gene expression program. *Science Advances*, *8*(17). https://doi.org/10.1126/sciadv.abl9404

Calvo, P., Abadia, B., Ferreras, A., Ruiz-Moreno, O., Verdes, G., & Pablo, L. E. (2015). Diabetic Macular Edema: Options for Adjunct Therapy. *Drugs*, *75*(13), 1461–1469. https://doi.org/10.1007/s40265-015-0447-1

Caplan, A., Fett, N., Rosenbach, M., Werth, V. P., & Micheletti, R. G. (2017). Prevention and management of glucocorticoid-induced side effects: A comprehensive review: Ocular, cardiovascular, muscular, and psychiatric side effects and issues unique to pediatric patients. *Journal of the American Academy of Dermatology*, *76*(2), 201–207. https://doi.org/10.1016/j.jaad.2016.02.1241

Chen, M., Li, X., Liu, J., Han, Y., & Cheng, L. (2015). Safety and pharmacodynamics of suprachoroidal injection of triamcinolone acetonide as a controlled ocular drug release model. *Journal of Controlled Release*, *203*, 109–117. https://doi.org/10.1016/j.jconrel.2015.02.021

Chennamaneni, S. R., Mamalis, C., Archer, B., Oakey, Z., & Ambati, B. K. (2013). Development of a novel bioerodible dexamethasone implant for uveitis and postoperative cataract inflammation. *Journal of Controlled Release : Official Journal of the Controlled Release Society*, *167*(1), 53–59. https://doi.org/10.1016/j.jconrel.2013.01.007

Chiang, B., Jung, J. H., & Prausnitz, M. R. (2018). The suprachoroidal space as a route of administration to the posterior segment of the eye. *Advanced Drug Delivery Reviews*, *126*, 58–66. https://doi.org/10.1016/j.addr.2018.03.001

Chiang, B., Kim, Y. C., Doty, A. C., Grossniklaus, H. E., Schwendeman, S. P., & Prausnitz, M. R. (2016). Sustained reduction of intraocular pressure by supraciliary delivery of brimonidine-loaded poly(lactic acid) microspheres for the treatment of glaucoma. *Journal of Controlled Release : Official Journal of the Controlled Release Society*, *228*, 48–57. https://doi.org/10.1016/j.jconrel.2016.02.041

Chiang, B., Venugopal, N., Edelhauser, H. F., & Prausnitz, M. R. (2016). Distribution of particles, small molecules and polymeric formulation excipients in the suprachoroidal space after microneedle injection. *Experimental Eye Research*, *153*, 101–109. https://doi.org/10.1016/j.exer.2016.10.011

Chiang, B., Venugopal, N., Grossniklaus, H. E., Jung, J. H., Edelhauser, H. F., & Prausnitz, M. R. (2017). Thickness and Closure Kinetics of the Suprachoroidal Space Following Microneedle Injection of Liquid Formulations. *Investigative Opthalmology & Visual Science*, *58*(1), 555. https://doi.org/10.1167/iovs.16-20377

Chu, C. J., Herrmann, P., Carvalho, L. S., Liyanage, S. E., Bainbridge, J. W. B., Ali, R. R., Dick, A. D., & Luhmann, U. F. O. (2013). Assessment and in vivo scoring of murine experimental autoimmune uveoretinitis using optical coherence tomography. *PloS One*, *8*(5), e63002. https://doi.org/10.1371/journal.pone.0063002

Ciulla, T. A., Harris, A., McIntyre, N., & Jonescu-Cuypers, C. (2014). Treatment of diabetic macular edema with sustained-release glucocorticoids: intravitreal triamcinolone acetonide, dexamethasone implant, and fluocinolone acetonide implant. *Expert Opinion on Pharmacotherapy*, *15*(7), 953–959. https://doi.org/10.1517/14656566.2014.896899

Cuenca, N., Pinilla, I., Fernández-Sánchez, L., Salinas-Navarro, M., Alarcón-Martínez, L., Avilés-Trigueros, M., de la Villa, P., Miralles de Imperial, J., Villegas-Pérez, M. P., & Vidal-Sanz, M. (2010). Changes in the inner and outer retinal layers after acute increase of the intraocular

pressure in adult albino Swiss mice. *Experimental Eye Research*, *91*(2), 273–285. https://doi.org/10.1016/j.exer.2010.05.020

Das, S. S., Neelam, Hussain, K., Singh, S., Hussain, A., Faruk, A., & Tebyetekerwa, M. (2019). Laponite-based Nanomaterials for Biomedical Applications: A Review. *Current Pharmaceutical Design*, *25*(4), 424–443. https://doi.org/10.2174/1381612825666190402165845

Davis, B. M., Crawley, L., Pahlitzsch, M., Javaid, F., & Cordeiro, M. F. (2016). Glaucoma: the retina and beyond. *Acta Neuropathologica*, *132*(6), 807–826. https://doi.org/10.1007/s00401-016-1609-2

del Amo, E. M., Rimpelä, A.-K., Heikkinen, E., Kari, O. K., Ramsay, E., Lajunen, T., Schmitt, M., Pelkonen, L., Bhattacharya, M., Richardson, D., Subrizi, A., Turunen, T., Reinisalo, M., Itkonen, J., Toropainen, E., Casteleijn, M., Kidron, H., Antopolsky, M., Vellonen, K.-S., … Urtti, A. (2017). Pharmacokinetic aspects of retinal drug delivery. *Progress in Retinal and Eye Research*, *57*, 134–185. https://doi.org/10.1016/j.preteyeres.2016.12.001

del Amo, E. M., & Urtti, A. (2015). Rabbit as an animal model for intravitreal pharmacokinetics: Clinical predictability and quality of the published data. *Experimental Eye Research*, *137*, 111–124. https://doi.org/10.1016/j.exer.2015.05.003

Deokule, S. P., Baffi, J. Z., Guo, H., Nazzaro, M., & Kaneko, H. (2012). Evaluation of extended release brimonidine intravitreal device in normotensive rabbit eyes. *Acta Ophthalmologica*, *90*(5), e344-8. https://doi.org/10.1111/j.1755-3768.2012.02418.x

Ding, C., Wang, P., & Tian, N. (2011). Effect of general anesthetics on IOP in elevated IOP mouse model. *Experimental Eye Research*, *92*(6), 512–520. https://doi.org/10.1016/j.exer.2011.03.016

Domeneguetti, R., Sakai, V., Perotti, G., Silva, I., Tercjak, A., Barud, H., Pavan, F., Constantino, V., & Ribeiro, S. (2023). Structural and morphological properties of in-situ biosynthesis of biocompatible bacterial cellulose/Laponite nanocomposites. *Appl. Clay Sci*, *234*, 106851.

Dossarps, D., Bron, A. M., Koehrer, P., Aho-Glélé, L. S., Creuzot-Garcher, C., Berthon, L., Maftouhi, Q.-E., Bakhti, A., Conrath, J., Le Mer, Y., Ramahefasolo, C. B., Coscas, F., Français, C., Grenet, T., Cohen, S. Y., Uzzan, J., Razavi, S., Saleh, M., Delbosc, B., … Pisella, P.-J. (2015). Endophthalmitis After Intravitreal Injections: Incidence, Presentation, Management, and Visual Outcome. *American Journal of Ophthalmology*, *160*(1), 17-25.e1. https://doi.org/10.1016/j.ajo.2015.04.013

Emami-Naeini, P., & Yiu, G. (2019). Medical and Surgical Applications for the Suprachoroidal Space. *International Ophthalmology Clinics*, *59*(1), 195–207. https://doi.org/10.1097/IIO.0000000000000251

Ethier, C. R., Johnson, M., & Ruberti, J. (2004). Ocular biomechanics and biotransport. *Annual Review of Biomedical Engineering*, *6*, 249–273. https://doi.org/10.1146/annurev.bioeng.6.040803.140055

Evangelho, K., Mogilevskaya, M., Losada-Barragan, M., & Vargas-Sanchez, J. K. (2019). Pathophysiology of primary open-angle glaucoma from a neuroinflammatory and neurotoxicity perspective: a review of the literature. *International Ophthalmology*, *39*(1), 259–271. https://doi.org/10.1007/s10792-017-0795-9

Ferraz, M. P. (2022). Biomaterials for Ophthalmic Applications. *Applied Sciences*, *12*(12), 5886. https://doi.org/10.3390/app12125886

Fraile, J. M., Garcia-Martin, E., Gil, C., Mayoral, J. A., Pablo, L. E., Polo, V., Prieto, E., & Vispe, E. (2016). Laponite as carrier for controlled in vitro delivery of dexamethasone in vitreous humor models. *European Journal of Pharmaceutics and Biopharmaceutics : Official Journal of Arbeitsgemeinschaft Fur Pharmazeutische Verfahrenstechnik e.V*, *108*, 83–90. https://doi.org/10.1016/j.ejpb.2016.08.015

Gaharwar, A. K., Cross, L. M., Peak, C. W., Gold, K., Carrow, J. K., Brokesh, A., & Singh, K. A. (2019). 2D Nanoclay for Biomedical Applications: Regenerative Medicine, Therapeutic Delivery, and Additive Manufacturing. *Advanced Materials (Deerfield Beach, Fla.)*, *31*(23), e1900332. https://doi.org/10.1002/adma.201900332

Gaharwar, A. K., Kishore, V., Rivera, C., Bullock, W., Wu, C.-J., Akkus, O., & Schmidt, G. (2012). Physically crosslinked nanocomposites from silicate-crosslinked PEO: mechanical properties and osteogenic differentiation of human mesenchymal stem cells. *Macromolecular Bioscience*, *12*(6), 779–793. https://doi.org/10.1002/mabi.201100508

Ganapathy, P. S., Lowder, C. Y., Arepalli, S., Baynes, K., Li, M., Bena, J., & Srivastava, S. K. (2018). Treatment Duration and Side Effect Profile of Long-Term Use of Intravitreal Preservative-Free Triamcinolone Acetonide in Uveitis. *American Journal of Ophthalmology*, *194*, 63–71. https://doi.org/10.1016/j.ajo.2018.07.003

Garcia-Valenzuela, E., Shareef, S., Walsh, J., & Sharma, S. C. (1995). Programmed cell death of retinal ganglion cells during experimental glaucoma. *Experimental Eye Research*, *61*(1), 33–44. https://doi.org/10.1016/s0014-4835(95)80056-5

Gaudana, R., Ananthula, H. K., Parenky, A., & Mitra, A. K. (2010). Ocular drug delivery. *The AAPS Journal*, *12*(3), 348–360. https://doi.org/10.1208/s12248-010-9183-3

Gilger, B. C., Mandal, A., Shah, S., & Mitra, A. K. (2014). Episcleral, intrascleral, and suprachoroidal routes of ocular drug delivery - recent research advances and patents. *Recent Patents on Drug Delivery & Formulation*, *8*(2), 81–91. https://doi.org/10.2174/1872211308021407070935O9

Gu, B., Liu, J., Li, X., Ma, Q., Shen, M., & Cheng, L. (2015). Real-Time Monitoring of Suprachoroidal Space (SCS) Following SCS Injection Using Ultra-High Resolution Optical Coherence Tomography in Guinea Pig Eyes. *Investigative Ophthalmology & Visual Science*, *56*(6), 3623–3634. https://doi.org/10.1167/iovs.15-16597

Habot-Wilner, Z., Noronha, G., & Wykoff, C. C. (2019). Suprachoroidally injected pharmacological agents for the treatment of chorio-retinal diseases: a targeted approach. *Acta Ophthalmologica*, *97*(5), 460–472. https://doi.org/10.1111/aos.14042

Haller, J. A., Bandello, F., Belfort, R., Blumenkranz, M. S., Gillies, M., Heier, J., Loewenstein, A., Yoon, Y. H., Jiao, J., Li, X.-Y., Whitcup, S. M., Ozurdex GENEVA Study Group, & Li, J. (2011). Dexamethasone intravitreal implant in patients with macular edema related to branch or central retinal vein occlusion twelve-month study results. *Ophthalmology*, *118*(12), 2453–2460. https://doi.org/10.1016/j.ophtha.2011.05.014

Hartman, R. R., & Kompella, U. B. (2018). Intravitreal, Subretinal, and Suprachoroidal Injections: Evolution of Microneedles for Drug Delivery. *Journal of Ocular Pharmacology and Therapeutics : The Official Journal of the Association for Ocular Pharmacology and Therapeutics*, *34*(1–2), 141–153. https://doi.org/10.1089/jop.2017.0121

Holekamp, N. M. (2010). The vitreous gel: more than meets the eye. *American Journal of Ophthalmology*, *149*(1), 32–36. https://doi.org/10.1016/j.ajo.2009.07.036

Jindal, V. (2015). Interconnection between brain and retinal neurodegenerations. *Molecular Neurobiology*, *51*(3), 885–892. https://doi.org/10.1007/s12035-014-8733-6

Jonas, J. B., Aung, T., Bourne, R. R., Bron, A. M., Ritch, R., & Panda-Jonas, S. (2017). Glaucoma. *Lancet (London, England)*, *390*(10108), 2183–2193. https://doi.org/10.1016/S0140-6736(17)31469-1

Jung, J. H., Chae, J. J., & Prausnitz, M. R. (2019). Targeting drug delivery within the suprachoroidal space. *Drug Discovery Today*, *24*(8), 1654–1659. https://doi.org/10.1016/j.drudis.2019.03.027

Jung, J. H., Chiang, B., Grossniklaus, H. E., & Prausnitz, M. R. (2018). Ocular drug delivery targeted by iontophoresis in the suprachoroidal space using a microneedle. *Journal of Controlled Release : Official Journal of the Controlled Release Society*, *277*, 14–22. https://doi.org/10.1016/j.jconrel.2018.03.001

Kalapesi, F. B., Coroneo, M. T., & Hill, M. A. (2005). Human ganglion cells express the alpha-2 adrenergic receptor: relevance to neuroprotection. *The British Journal of Ophthalmology*, *89*(6), 758–763. https://doi.org/10.1136/bjo.2004.053025

Keane, P. A., Karampelas, M., Sim, D. A., Sadda, S. R., Tufail, A., Sen, H. N., Nussenblatt, R. B., Dick, A. D., Lee, R. W., Murray, P. I., Pavesio, C. E., & Denniston, A. K. (2014). Objective measurement of vitreous inflammation using optical coherence tomography. *Ophthalmology*, *121*(9), 1706–1714. https://doi.org/10.1016/j.ophtha.2014.03.006

Kersey, J. P., & Broadway, D. C. (2006). Corticosteroid-induced glaucoma: a review of the literature. *Eye (London, England)*, *20*(4), 407–416. https://doi.org/10.1038/sj.eye.6701895

Kiaee, G., Dimitrakakis, N., Sharifzadeh, S., Kim, H.-J., Avery, R. K., Moghaddam, K. M., Haghniaz, R., Yalcintas, E. P., Barros, N. R. de, Karamikamkar, S., Libanori, A., Khademhosseini, A., & Khoshakhlagh, P. (2022). Laponite-Based Nanomaterials for Drug Delivery. *Advanced Healthcare Materials*, *11*(7), e2102054. https://doi.org/10.1002/adhm.202102054

Kim, K. E., Jang, I., Moon, H., Kim, Y. J., Jeoung, J. W., Park, K. H., & Kim, H. (2015). Neuroprotective Effects of Human Serum Albumin Nanoparticles Loaded With Brimonidine on Retinal Ganglion Cells in Optic Nerve Crush Model. *Investigative Ophthalmology & Visual Science*, *56*(9), 5641–5649. https://doi.org/10.1167/iovs.15-16538

Kim, S. H., Lutz, R. J., Wang, N. S., & Robinson, M. R. (2007). Transport barriers in transscleral drug delivery for retinal diseases. *Ophthalmic Research*, *39*(5), 244–254. https://doi.org/10.1159/000108117

Korot, E., Comer, G., Steffens, T., & Antonetti, D. A. (2016). Algorithm for the Measure of Vitreous Hyperreflective Foci in Optical Coherence Tomographic Scans of Patients With Diabetic Macular Edema. *JAMA Ophthalmology*, *134*(1), 15–20. https://doi.org/10.1001/jamaophthalmol.2015.3949

Kumar, A., Sehra, S. V., Thirumalesh, M. B., & Gogia, V. (2012). Secondary rhegmatogenous retinal detachment following intravitreal bevacizumab in patients with vitreous hemorrhage or tractional retinal detachment secondary to Eales' disease. *Graefe's Archive for Clinical and Experimental Ophthalmology = Albrecht von Graefes Archiv Fur Klinische Und Experimentelle Ophthalmologie*, *250*(5), 685–690. https://doi.org/10.1007/s00417-011-1890-7

Kwak, H. W., & D'Amico, D. J. (1992). Evaluation of the retinal toxicity and pharmacokinetics of dexamethasone after intravitreal injection. *Archives of Ophthalmology (Chicago, Ill. : 1960)*, *110*(2), 259–266. https://doi.org/10.1001/archopht.1992.01080140115038

Lambert, W. S., Carlson, B. J., van der Ende, A. E., Shih, G., Dobish, J. N., Calkins, D. J., & Harth, E. (2015). Nanosponge-Mediated Drug Delivery Lowers Intraocular Pressure. *Translational Vision Science & Technology*, *4*(1), 1. https://doi.org/10.1167/tvst.4.1.1

Lambert, W. S., Ruiz, L., Crish, S. D., Wheeler, L. A., & Calkins, D. J. (2011). Brimonidine prevents axonal and somatic degeneration of retinal ganglion cell neurons. *Molecular Neurodegeneration*, *6*(1), 4. https://doi.org/10.1186/1750-1326-6-4

Lapasin, R., Abrami, M., Grassi, M., & Šebenik, U. (2017). Rheology of Laponite-scleroglucan hydrogels. *Carbohydrate Polymers*, *168*, 290–300. https://doi.org/10.1016/j.carbpol.2017.03.068

Lawlor, M., Danesh-Meyer, H., Levin, L. A., Davagnanam, I., De Vita, E., & Plant, G. T. (2018). Glaucoma and the brain: Trans-synaptic degeneration, structural change, and implications for neuroprotection. *Survey of Ophthalmology*, *63*(3), 296–306. https://doi.org/10.1016/j.survophthal.2017.09.010

Lee, J. H., Han, W. J., Jang, H. S., & Choi, H. J. (2019). Highly Tough, Biocompatible, and Magneto-Responsive Fe3O4/Laponite/PDMAAm Nanocomposite Hydrogels. *Scientific Reports*, *9*(1), 15024. https://doi.org/10.1038/s41598-019-51555-5

Levkovitch-Verbin, H., Quigley, H. A., Martin, K. R. G., Valenta, D., Baumrind, L. A., & Pease, M. E. (2002). Translimbal laser photocoagulation to the trabecular meshwork as a model of glaucoma in rats. *Investigative Ophthalmology & Visual Science*, *43*(2), 402–410.

Liu, B., Li, J., Lei, X., Miao, S., Zhang, S., Cheng, P., Song, Y., Wu, H., Gao, Y., Bi, L., & Pei, G. (2020). Cell-loaded injectable gelatin/alginate/LAPONITE® nanocomposite hydrogel promotes bone healing in a critical-size rat calvarial defect model. *RSC Advances*, *10*(43), 25652–25661. https://doi.org/10.1039/d0ra03040f

Liu, X., & Bhatia, S. R. (2015). Laponite® and Laponite®-PEO hydrogels with enhanced elasticity in phosphate-buffered saline. *Polymers for Advanced Technologies*, *26*(7), 874–879. https://doi.org/10.1002/pat.3514

Lowder, C., Belfort, R., Lightman, S., Foster, C. S., Robinson, M. R., Schiffman, R. M., Li, X.-Y., Cui, H., Whitcup, S. M., & Ozurdex HURON Study Group. (2011). Dexamethasone intravitreal implant for noninfectious intermediate or posterior uveitis. *Archives of Ophthalmology (Chicago, Ill. : 1960)*, *129*(5), 545–553. https://doi.org/10.1001/archophthalmol.2010.339

Maisanaba, S., Pichardo, S., Puerto, M., Gutiérrez-Praena, D., Cameán, A. M., & Jos, A. (2015). Toxicological evaluation of clay minerals and derived nanocomposites: a review. *Environmental Research*, *138*, 233–254. https://doi.org/10.1016/j.envres.2014.12.024

Miller, N. R., Newman, N. J., Miller, N. R., & Newman, N. J. (Eds.). (n.d.). Embryology, anatomy,and physiology of the afferent visual pathway. In *Walsh & Hoyt's Clinical Neuro-Ophthalmology* (6th edn, Vol. 1, pp. 3–82). Wilkins.

Morrison, J. C., Cepurna, W. O., & Johnson, E. C. (2015). Modeling glaucoma in rats by sclerosing aqueous outflow pathways to elevate intraocular pressure. *Experimental Eye Research*, *141*, 23–32. https://doi.org/10.1016/j.exer.2015.05.012

Morrison, J. C., Moore, C. G., Deppmeier, L. M., Gold, B. G., Meshul, C. K., & Johnson, E. C. (1997). A rat model of chronic pressure-induced optic nerve damage. *Experimental Eye Research*, *64*(1), 85–96. https://doi.org/10.1006/exer.1996.0184

Murray, H. H. (1991). Overview — clay mineral applications. *Applied Clay Science*, *5*(5–6), 379–395. https://doi.org/10.1016/0169-1317(91)90014-Z

Nelson, R., & Connaughton, V. (1995). *Bipolar Cell Pathways in the Vertebrate Retina*.

Neumann, B. (1965). Behaviour of a synthetic clay in pigment dispersions. *Rheol. Acta* , *4*, 250–255.

Olsen, T. W., Feng, X., Wabner, K., Csaky, K., Pambuccian, S., & Cameron, J. D. (2011). Pharmacokinetics of pars plana intravitreal injections versus microcannula suprachoroidal injections of bevacizumab in a porcine model. *Investigative Ophthalmology & Visual Science*, *52*(7), 4749–4756. https://doi.org/10.1167/iovs.10-6291

Oray, M., Abu Samra, K., Ebrahimiadib, N., Meese, H., & Foster, C. S. (2016). Long-term side effects of glucocorticoids. *Expert Opinion on Drug Safety*, *15*(4), 457–465. https://doi.org/10.1517/14740338.2016.1140743

Patel, S. R., Lin, A. S. P., Edelhauser, H. F., & Prausnitz, M. R. (2011). Suprachoroidal drug delivery to the back of the eye using hollow microneedles. *Pharmaceutical Research*, *28*(1), 166–176. https://doi.org/10.1007/s11095-010-0271-y

Pauling, L. (1930). The Structure of the Micas and Related Minerals. *Proceedings of the National Academy of Sciences of the United States of America*, *16*(2), 123–129. https://doi.org/10.1073/pnas.16.2.123

Pek, Y. S., Wu, H., Mohamed, S. T., & Ying, J. Y. (2016). Long-Term Subconjunctival Delivery of Brimonidine Tartrate for Glaucoma Treatment Using a Microspheres/Carrier System. *Advanced Healthcare Materials*, *5*(21), 2823–2831. https://doi.org/10.1002/adhm.201600780

Pershing, S., Bakri, S. J., & Moshfeghi, D. M. (2013). Ocular hypertension and intraocular pressure asymmetry after intravitreal injection of anti-vascular endothelial growth factor agents. *Ophthalmic Surgery, Lasers & Imaging Retina*, *44*(5), 460–464. https://doi.org/10.3928/23258160-20130909-07

Prieto, E., Vispe, E., De Martino, A., Idoipe, M., Rodrigo, M. J., Garcia-Martin, E., Fraile, J. M., Polo-Llorens, V., & Mayoral, J. A. (2018). Safety study of intravitreal and suprachoroidal Laponite clay in rabbit eyes. *Graefe's Archive for Clinical and Experimental Ophthalmology = Albrecht von Graefes Archiv Fur Klinische Und Experimentelle Ophthalmologie*, *256*(3), 535–546. https://doi.org/10.1007/s00417-017-3893-5

Prieto, E., Vispe, E., Otín-Mallada, S., Garcia-Martin, E., Polo-Llorens, V., Fraile, J. M., Pablo, L. E., & Mayoral, J. A. (2017). Determination of Three Corticosteroids in the Biologic Matrix of Vitreous Humor by HPLC-tandem Mass Spectrometry: Method Development and Validation. *Current Eye Research*, *42*(2), 244–251. https://doi.org/10.1080/02713683.2016.1183795

Rai, U. D. J. P., Young, S. A., Thrimawithana, T. R., Abdelkader, H., Alani, A. W. G., Pierscionek, B., & Alany, R. G. (2015). The suprachoroidal pathway: a new drug delivery route to the back of the eye. *Drug Discovery Today*, *20*(4), 491–495. https://doi.org/10.1016/j.drudis.2014.10.010

Reffitt, D. M., Ogston, N., Jugdaohsingh, R., Cheung, H. F. J., Evans, B. A. J., Thompson, R. P. H., Powell, J. J., & Hampson, G. N. (2003). Orthosilicic acid stimulates collagen type 1 synthesis and osteoblastic differentiation in human osteoblast-like cells in vitro. *Bone*, *32*(2), 127–135. https://doi.org/10.1016/s8756-3282(02)00950-x

Rodrigues, L. A. de S., Figueiras, A., Veiga, F., de Freitas, R. M., Nunes, L. C. C., da Silva Filho, E. C., & da Silva Leite, C. M. (2013). The systems containing clays and clay minerals from modified drug release: a review. *Colloids and Surfaces. B, Biointerfaces*, *103*, 642–651. https://doi.org/10.1016/j.colsurfb.2012.10.068

Romani, A. M. P. (2011). Cellular magnesium homeostasis. *Archives of Biochemistry and Biophysics*, *512*(1), 1–23. https://doi.org/10.1016/j.abb.2011.05.010

Ruberte, J., Carretero, A., & Navarro, M. (2017). *Morphological Mouse Phenotyping: Anatomy, Histology and Imaging*. Elsevier Science. https://books.google.es/books?id=4jqpDQAAQBAJ

Samimi Gharaie, S., Dabiri, S. M. H., & Akbari, M. (2018). Smart Shear-Thinning Hydrogels as Injectable Drug Delivery Systems. *Polymers*, *10*(12). https://doi.org/10.3390/polym10121317

Samoylenko, O., Korotych, O., Manilo, M., Samchenko, Y., Shlyakhovenko, V., & Lebovka, N. (2022). Biomedical Applications of Laponite®-Based Nanomaterials and Formulations. In L. Bulavin & N. Lebovka (Eds.), *Soft Matter Systems for Biomedical Applications* (pp. 385–452). Springer International Publishing.

Samsel, P. A., Kisiswa, L., Erichsen, J. T., Cross, S. D., & Morgan, J. E. (2011). A novel method for the induction of experimental glaucoma using magnetic microspheres. *Investigative Ophthalmology & Visual Science*, *52*(3), 1671–1675. https://doi.org/10.1167/iovs.09-3921

Shafran, K., Jeans, C., Kemp, S. J., & Murphy, K. (2020). Dr Barbara S. Neumann: clay scientist and industrial pioneer; creator of Laponite®. *Clay Minerals*, *55*(3), 256–260. https://doi.org/10.1180/clm.2020.35

Singh, A. K., Mishra, S. K., Mishra, G., Maurya, A., Awasthi, R., Yadav, M. K., Atri, N., Pandey, P. K., & Singh, S. K. (2020). Inorganic clay nanocomposite system for improved cholinesterase inhibition and brain pharmacokinetics of donepezil. *Drug Development and Industrial Pharmacy*, *46*(1), 8–19. https://doi.org/10.1080/03639045.2019.1698594

Soni, K. S., Desale, S. S., & Bronich, T. K. (2016). Nanogels: An overview of properties, biomedical applications and obstacles to clinical translation. *Journal of Controlled Release : Official Journal of the Controlled Release Society*, *240*, 109–126. https://doi.org/10.1016/j.jconrel.2015.11.009

Sreekantam, S., Macdonald, T., Keane, P. A., Sim, D. A., Murray, P. I., & Denniston, A. K. (2017). Quantitative analysis of vitreous inflammation using optical coherence tomography in patients receiving sub-Tenon's triamcinolone acetonide for uveitic cystoid macular oedema. *The British Journal of Ophthalmology*, *101*(2), 175–179. https://doi.org/10.1136/bjophthalmol-2015-308008

Staniford, M. C., Lezhnina, M. M., Gruener, M., Stegemann, L., Kuczius, R., Bleicher, V., Strassert, C. A., & Kynast, U. H. (2015). Photophysical efficiency-boost of aqueous aluminium

phthalocyanine by hybrid formation with nano-clays. *Chemical Communications (Cambridge, England)*, *51*(70), 13534–13537. https://doi.org/10.1039/c5cc05352h

Sun, J., Lei, Y., Dai, Z., Liu, X., Huang, T., Wu, J., Xu, Z. P., & Sun, X. (2017). Sustained Release of Brimonidine from a New Composite Drug Delivery System for Treatment of Glaucoma. *ACS Applied Materials & Interfaces*, *9*(9), 7990–7999. https://doi.org/10.1021/acsami.6b16509

Takeno, H., Kimura, Y., & Nakamura, W. (2017). Mechanical, Swelling, and Structural Properties of Mechanically Tough Clay-Sodium Polyacrylate Blend Hydrogels. *Gels (Basel, Switzerland)*, *3*(1). https://doi.org/10.3390/gels3010010

Thakur, A., Kadam, R. S., & Kompella, U. B. (2011). Influence of drug solubility and lipophilicity on transscleral retinal delivery of six corticosteroids. *Drug Metabolism and Disposition: The Biological Fate of Chemicals*, *39*(5), 771–781. https://doi.org/10.1124/dmd.110.037408

Thompson, D., & Butterworth, J. (1992). The nature of laponite and its aqueous dispersions. *Journal of Colloid and Interface Science*, *151*, 236–243.

Tipa, C., Cidade, M. T., Borges, J. P., Costa, L. C., Silva, J. C., & Soares, P. I. P. (2022). Clay-Based Nanocomposite Hydrogels for Biomedical Applications: A Review. *Nanomaterials (Basel, Switzerland)*, *12*(19). https://doi.org/10.3390/nano12193308

Tomás, H., Alves, C. S., & Rodrigues, J. (2018). Laponite®: A key nanoplatform for biomedical applications? *Nanomedicine : Nanotechnology, Biology, and Medicine*, *14*(7), 2407–2420. https://doi.org/10.1016/j.nano.2017.04.016

Touchard, E., Berdugo, M., Bigey, P., El Sanharawi, M., Savoldelli, M., Naud, M.-C., Jeanny, J.-C., & Behar-Cohen, F. (2012). Suprachoroidal electrotransfer: a nonviral gene delivery method to transfect the choroid and the retina without detaching the retina. *Molecular Therapy : The Journal of the American Society of Gene Therapy*, *20*(8), 1559–1570. https://doi.org/10.1038/mt.2011.304

Tyagi, P., Kadam, R. S., & Kompella, U. B. (2012). Comparison of suprachoroidal drug delivery with subconjunctival and intravitreal routes using noninvasive fluorophotometry. *PloS One*, *7*(10), e48188. https://doi.org/10.1371/journal.pone.0048188

Uji, A., & Yoshimura, N. (2016). Microarchitecture of the Vitreous Body: A High-Resolution Optical Coherence Tomography Study. *American Journal of Ophthalmology*, *168*, 24–30. https://doi.org/10.1016/j.ajo.2016.04.021

Urcola, J. H., Hernández, M., & Vecino, E. (2006). Three experimental glaucoma models in rats: comparison of the effects of intraocular pressure elevation on retinal ganglion cell size and death. *Experimental Eye Research*, *83*(2), 429–437. https://doi.org/10.1016/j.exer.2006.01.025

Urtti, A. (n.d.). Challenges and obstacles of ocular pharmacokinetics and drug delivery. *Adv Drug Deliv Rev*, *58*, 1131–1135.

Urtti, A. (2006). Challenges and obstacles of ocular pharmacokinetics and drug delivery. *Advanced Drug Delivery Reviews*, *58*(11), 1131–1135. https://doi.org/10.1016/j.addr.2006.07.027

Vecino, E., & Sharma, S. (2011). *Glaucoma animal models*.

Veernala, I., Giri, J., Pradhan, A., Polley, P., Singh, R., & Yadava, S. K. (2019). Effect of Fluoride Doping in Laponite Nanoplatelets on Osteogenic Differentiation of Human Dental Follicle Stem Cells (hDFSCs). *Scientific Reports*, *9*(1), 915. https://doi.org/10.1038/s41598-018-37327-7

Vidal-Sanz, M., Salinas-Navarro, M., Nadal-Nicolás, F. M., Alarcón-Martínez, L., Valiente-Soriano, F. J., de Imperial, J. M., Avilés-Trigueros, M., Agudo-Barriuso, M., & Villegas-Pérez, M. P. (2012). Understanding glaucomatous damage: anatomical and functional data from ocular hypertensive rodent retinas. *Progress in Retinal and Eye Research*, *31*(1), 1–27. https://doi.org/10.1016/j.preteyeres.2011.08.001

Walters, T. R. (1996). Development and use of brimonidine in treating acute and chronic elevations of intraocular pressure: a review of safety, efficacy, dose response, and dosing studies. *Survey of Ophthalmology*, *41 Suppl 1*, S19-26. https://doi.org/10.1016/s0039-6257(96)82028-5

Wang, C., Min, S., & Tian, Y. (2023). Injectable and Cell-Laden Hydrogel in the Contained Bone Defect Animal Model: A Systematic Review. *Tissue Engineering and Regenerative Medicine*, *20*(6), 829–837. https://doi.org/10.1007/s13770-023-00569-2

Wang, G., Maciel, D., Wu, Y., Rodrigues, J., Shi, X., Yuan, Y., Liu, C., Tomás, H., & Li, Y. (2014). Amphiphilic polymer-mediated formation of laponite-based nanohybrids with robust stability and pH sensitivity for anticancer drug delivery. *ACS Applied Materials & Interfaces*, *6*(19), 16687–16695. https://doi.org/10.1021/am5032874

Wang, J., Wang, G., Sun, Y., Wang, Y., Yang, Y., Yuan, Y., Li, Y., & Liu, C. (2016). In Situ formation of pH-/thermo-sensitive nanohybrids via friendly-assembly of poly(N-vinylpyrrolidone) onto LAPONITE®. *RSC Advances*, *6*(38), 31816–31823. https://doi.org/10.1039/C5RA25628C

Wang, L., Zhou, M. Ben, & Zhang, H. (2021). The Emerging Role of Topical Ocular Drugs to Target the Posterior Eye. *Ophthalmology and Therapy*, *10*(3), 465–494. https://doi.org/10.1007/s40123-021-00365-y

Weinreb, R. N., Aung, T., & Medeiros, F. A. (2014). The pathophysiology and treatment of glaucoma: a review. *JAMA*, *311*(18), 1901–1911. https://doi.org/10.1001/jama.2014.3192

Williams, R., Ryves, W. J., Dalton, E. C., Eickholt, B., Shaltiel, G., Agam, G., & Harwood, A. J. (2004). A molecular cell biology of lithium. *Biochemical Society Transactions*, *32*(Pt 5), 799–802. https://doi.org/10.1042/BST0320799

WoldeMussie, E., Ruiz, G., Wijono, M., & Wheeler, L. A. (2001). Neuroprotection of retinal ganglion cells by brimonidine in rats with laser-induced chronic ocular hypertension. *Investigative Ophthalmology & Visual Science*, *42*(12), 2849–2855.

Woldemussie, E., Wijono, M., & Pow, D. (2007). Localization of alpha 2 receptors in ocular tissues. *Visual Neuroscience*, *24*(5), 745–756. https://doi.org/10.1017/S0952523807070605

Wu, C.-J., Gaharwar, A. K., Schexnailder, P. J., & Schmidt, G. (2010). Development of Biomedical Polymer-Silicate Nanocomposites: A Materials Science Perspective. *Materials*, *3*(5), 2986–3005. https://doi.org/10.3390/ma3052986

Xiao, S., Castro, R., Maciel, D., Gonçalves, M., Shi, X., Rodrigues, J., & Tomás, H. (2016). Fine tuning of the pH-sensitivity of laponite-doxorubicin nanohybrids by polyelectrolyte multilayer coating. *Materials Science & Engineering. C, Materials for Biological Applications*, *60*, 348–356. https://doi.org/10.1016/j.msec.2015.11.051

Yadav, H., Agrawal, R., Panday, A., Patel, J., & Maiti, S. (2022). Polysaccharide-silicate composite hydrogels: Review on synthesis and drug delivery credentials. *Journal of Drug Delivery Science and Technology*, *74*, 103573. https://doi.org/10.1016/J.JDDST.2022.103573

Yun, Y. H., Lee, B. K., & Park, K. (2015). Controlled Drug Delivery: Historical perspective for the next generation. *Journal of Controlled Release : Official Journal of the Controlled Release Society*, *219*, 2–7. https://doi.org/10.1016/j.jconrel.2015.10.005

Zhang, L., He, G., Yu, Y., Zhang, Y., Li, X., & Wang, S. (2022). Design of Biocompatible Chitosan/Polyaniline/Laponite Hydrogel with Photothermal Conversion Capability. *Biomolecules*, *12*(8). https://doi.org/10.3390/biom12081089

Zhang, Y., Bazzazi, H., Lima E Silva, R., Pandey, N. B., Green, J. J., Campochiaro, P. A., & Popel, A. S. (2018). Three-Dimensional Transport Model for Intravitreal and Suprachoroidal Drug Injection. *Investigative Ophthalmology & Visual Science*, *59*(12), 5266–5276. https://doi.org/10.1167/iovs.17-23632

Zhao, L. Z., Zhou, C. H., Wang, J., Tong, D. S., Yu, W. H., & Wang, H. (2015). Recent advances in clay mineral-containing nanocomposite hydrogels. *Soft Matter*, *11*(48), 9229–9246. https://doi.org/10.1039/c5sm01277e

APÉNDICE

1. Factor de impacto de las revistas, áreas temáticas y contribución del doctorando

“Dexamethasone delivery to the ocular posterior segment by sustained-release Laponite formulation”.

Autores: Prieto E, **Cardiel MJ**, Vispe E, Idoipe M, Garcia-Martin E, Fraile JM, Polo V, Mayoral JA, Pablo LE, Rodrigo MJ.

Revista: Biomed Mater. 2020 Nov 21;15(6):065021.

DOI: 10.1088/1748-605X/aba445.

PMID: 32647098.

JCR-Q2. Factor de impacto (JCR 2019): 3,174.

ISSN: 1748-6041.

Área temática: ENGINEERING, BIOMEDICAL 31/87.

Contribución del doctorando: investigación, metodología, redacción, revisión y edición.

“Brimonidine-LAPONITE® intravitreal formulation has an ocular hypotensive and neuroprotective effect throughout 6 months of follow-up in a glaucoma animal model”.

Autores: Rodrigo MJ, **Cardiel MJ**, Fraile JM, Mendez-Martinez S, Martinez-Rincon T, Subias M, Polo V, Ruberte J, Ramirez T, Vispe E, Luna C, Mayoral JA, Garcia-Martin E.

Revista: Biomater Sci. 2020 Nov 21;8(22):6246-6260.

DOI: 10.1039/d0bm01013h.

PMID: 33016285.

JCR-Q1. Factor de impacto (JCR 2019): 6,183.

ISSN: 2047-4849.

Área temática: MATERIALS SCIENCE, BIOMATERIALS 6/38.

Contribución del doctorando: metodología, redacción, revisión.

“Monitoring new long-lasting intravitreal formulation for glaucoma with vitreous images using optical coherence tomography”.

Autores: Rodrigo MJ, Perez del Palomar A, Montolio A, Mendez-Martinez S, Subias M, Cardiel MJ, Martinez-Rincon T, Cegoñino J, Fraile JM, Vispe E, Mayoral JA, Polo V, Garcia-Martin E.

Revista: Pharmaceutics 2021 Feb 5;13(2):217.

DOI: 10.3390/pharmaceutics13020217.

PMID: 33562488.

JCR-Q1. Factor de impacto (JCR 2020): 6,321.

ISSN: 1999-4923.

Área temática: PHARMACOLOGY & PHARMACY 29/276.

Contribución del doctorando: metodología.

“Laponite for biomedical applications: An ophthalmological perspective”.

Autores: Rodrigo MJ, Cardiel MJ, Fraile JM, Mayoral JA, Pablo LE, Garcia-Martin E.

Revista: Mater Today Bio. 2023 Dec 28;24:100935. Erratum in: Mater Today Bio. 2024 Jan 27;25:100964.

DOI: 10.1016/j.mtbio.2023.100935 .

PMID: 38239894.

JCR-Q1. Factor de impacto (JCR 2022): 8,2.

ISSN: 2590-0064.

Área temática: ENGINEERING, BIOMEDICAL 13/96.

Contribución del doctorando: investigación, metodología, software, validación, redacción, revisión y edición.

2. Renuncia de los coautores no doctores

Escuela de Doctorado
Universidad Zaragoza

RENUNCIA DE LOS COAUTORES DE LOS TRABAJOS PRESENTADOS COMO PARTE DE UNA TESIS DOCTORAL EN LA MODALIDAD DE COMPENDIO DE PUBLICACIONES

1.- Datos personales del coautor		
Apellidos: VISPE PALACÍN	Nombre: EUGENIO	
DNI/Pasaporte/NIE: 18032420Y	Teléfono 876553290	Correo electrónico [redacted]

2.- Tesis Doctoral
Título: LAPONITA PARA APLICACIÓN OFTALMOLÓGICA. EVALUACIÓN EN MODELOS ANIMALES
Autor: MARÍA JOSÉ CARDIEL GARCÍA
Programa de doctorado: MEDICINA

3.- Publicaciones que formarán parte de la tesis y de las que el firmante es coautor

Rodrigo MJ, Cardiel MJ, Fraile JM, Mendez-Martinez S, Martinez-Rincon T, Subias M, Polo V, Ruberte J, Ramirez T, Vispe E, Luna C, Mayoral JA, Garcia-Martin E. Brimonidine-LAPONITE® intravitreal formulation has an ocular hypotensive and neuroprotective effect throughout 6 months of follow-up in a glaucoma animal model. Biomater Sci. 2020 Nov 21;8(22):6246-6260. doi: 10.1039/d0bm01013h. Epub 2020 Oct 5. PMID: 33016285.

Prieto E, Cardiel MJ, Vispe E, Idoipe M, Garcia-Martin E, Fraile JM, Polo V, Mayoral JA, Pablo LE, Rodrigo MJ. Dexamethasone delivery to the ocular posterior segment by sustained-release Laponite formulation. Biomed Mater. 2020 Nov 21;15(6):065021. doi: 10.1088/1748-605X/aba445. PMID: 32647098.

Rodrigo MJ, Palomar APD, Montolío A, Mendez-Martinez S, Subias M, Cardiel MJ, Martinez-Rincon T, Cegonino J, Fraile JM, Vispe E, Mayoral JA, Polo V, Garcia-Martin E. Monitoring New Long-Lasting Intravitreal Formulation for Glaucoma with Vitreous Images Using Optical Coherence Tomography. Pharmaceutics. 2021 Feb 5;13(2):217. doi: 10.3390/pharmaceutics13020217. PMID: 33562488; PMCID: PMC7915309

RENUNCIA:

Renuncio a que las publicaciones anteriores puedan ser presentadas como parte de otra tesis doctoral en la modalidad de compendio de publicaciones.

<lugar>,<fecha>

Firma: VISPE PALACIN EUGENIO - DNI 18032420Y [redacted]

Conforme a lo dispuesto en la legislación vigente (Reglamento (UE) 2016/679, de 27 de abril), de protección de datos de carácter personal, le informamos que sus datos pasarán a ser tratados por la Universidad de Zaragoza con la finalidad de gestionar la gestión académica y administrativa de sus estudiantes, así como su participación en actividades y servicios universitarios. Puede ejercer sus derechos de acceso, rectificación, limitación, oposición y portabilidad ante el Gerente de la UZ

Escuela de Doctorado
Universidad Zaragoza

RENUNCIA DE LOS COAUTORES DE LOS TRABAJOS PRESENTADOS COMO PARTE DE UNA TESIS DOCTORAL EN LA MODALIDAD DE COMPENDIO DE PUBLICACIONES

1.- Datos personales del coautor		
Apellidos: VISPE PALACÍN	Nombre: EUGENIO	
DNI/Pasaporte/NIE: 18032420Y	Teléfono 876553290	Correo electrónico [redacted]

2.- Tesis Doctoral
Título: LAPONITA PARA APLICACIÓN OFTALMOLÓGICA. EVALUACIÓN EN MODELOS ANIMALES
Autor: MARÍA JOSÉ CARDIEL GARCÍA
Programa de doctorado: MEDICINA

3.- Publicaciones que formarán parte de la tesis y de las que el firmante es coautor

Rodrigo MJ, Cardiel MJ, Fraile JM, Mendez-Martinez S, Martinez-Rincon T, Subias M, Polo V, Ruberte J, Ramirez T, Vispe E, Luna C, Mayoral JA, Garcia-Martin E. Brimonidine-LAPONITE® intravitreal formulation has an ocular hypotensive and neuroprotective effect throughout 6 months of follow-up in a glaucoma animal model. Biomater Sci. 2020 Nov 21;8(22):6246-6260. doi: 10.1039/d0bm01013h. Epub 2020 Oct 5. PMID: 33016285.

Prieto E, Cardiel MJ, Vispe E, Idoipe M, Garcia-Martin E, Fraile JM, Polo V, Mayoral JA, Pablo LE, Rodrigo MJ. Dexamethasone delivery to the ocular posterior segment by sustained-release Laponite formulation. Biomed Mater. 2020 Nov 21;15(6):065021. doi: 10.1088/1748-605X/aba445. PMID: 32647098.

Rodrigo MJ, Palomar APD, Montolío A, Mendez-Martinez S, Subias M, Cardiel MJ, Martinez-Rincon T, Cegonino J, Fraile JM, Vispe E, Mayoral JA, Polo V, Garcia-Martin E. Monitoring New Long-Lasting Intravitreal Formulation for Glaucoma with Vitreous Images Using Optical Coherence Tomography. Pharmaceutics. 2021 Feb 5;13(2):217. doi: 10.3390/pharmaceutics13020217. PMID: 33562488; PMCID: PMC7915309

RENUNCIA:

Renuncio a que las publicaciones anteriores puedan ser presentadas como parte de otra tesis doctoral en la modalidad de compendio de publicaciones.

<lugar>,<fecha>

Firma: VISPE PALACIN EUGENIO - DNI 18032420Y [redacted]

Conforme a lo dispuesto en la legislación vigente (Reglamento (UE) 2016/679, de 27 de abril), de protección de datos de carácter personal, le informamos que sus datos pasarán a ser tratados por la Universidad de Zaragoza con la finalidad de gestionar la gestión académica y administrativa de sus estudiantes, así como su participación en actividades y servicios universitarios. Puede ejercer sus derechos de acceso, rectificación, limitación, oposición y portabilidad ante el Gerente de la UZ

Escuela de Doctorado
Universidad Zaragoza

RENUNCIA DE LOS COAUTORES DE LOS TRABAJOS PRESENTADOS COMO PARTE DE UNA TESIS DOCTORAL EN LA MODALIDAD DE COMPENDIO DE PUBLICACIONES

1.- Datos personales del coautor		
Apellidos: SUBÍAS PERIÉ	Nombre: MANUEL	
DNI/Pasaporte/NIE: 18055956J	Teléfono 615048562	Correo electrónico [redacted]

2.- Tesis Doctoral
Título: LAPONITA PARA APLICACIÓN OFTALMOLÓGICA. EVALUACIÓN EN MODELOS ANIMALES
Autor: MARÍA JOSÉ CARDIEL GARCÍA
Programa de doctorado: MEDICINA

3.- Publicaciones que formarán parte de la tesis y de las que el firmante es coautor

Rodrigo MJ, Cardiel MJ, Fraile JM, Mendez-Martinez S, Martinez-Rincon T, Subias M, Polo V, Ruberte J, Ramirez T, Vispe E, Luna C, Mayoral JA, Garcia-Martin E. Brimonidine-LAPONITE® intravitreal formulation has an ocular hypotensive and neuroprotective effect throughout 6 months of follow-up in a glaucoma animal model. Biomater Sci. 2020 Nov 21;8(22):6246-6260. doi: 10.1039/d0bm01013h. Epub 2020 Oct 5. PMID: 33016285.

Rodrigo MJ, Palomar APD, Montolío A, Mendez-Martinez S, Subias M, Cardiel MJ, Martinez-Rincon T, Cegoñino J, Fraile JM, Vispe E, Mayoral JA, Polo V, Garcia-Martin E. Monitoring New Long-Lasting Intravitreal Formulation for Glaucoma with Vitreous Images Using Optical Coherence Tomography. Pharmaceutics. 2021 Feb 5;13(2):217. doi: 10.3390/pharmaceutics13020217. PMID: 33562488; PMCID: PMC7915309

RENUNCIA:

Renuncio a que las publicaciones anteriores puedan ser presentadas como parte de otra tesis doctoral en la modalidad de compendio de publicaciones.

<lugar>,<fecha>

Zaragoza 16 de abril de 2024

Firma: SUBIAS PERIE MANUEL - 18055956J [redacted]

Conforme a lo dispuesto en la legislación vigente (Reglamento (UE) 2016/679, de 27 de abril), de protección de datos de carácter personal, le informamos que sus datos pasarán a ser tratados por la Universidad de Zaragoza con la finalidad de gestionar la gestión académica y administrativa de sus estudiantes, así como su participación en actividades y servicios universitarios. Puede ejercer sus derechos de acceso, rectificación, limitación, oposición y portabilidad ante el Gerente de la UZ

Proyecto PID2020-113281RB-C22 financiado por MICIU/AEI /10.13039/501100011033